REFINING THE GENETICS OF MUSCULAR DYSTROPHIES WITH DEFECTIVE GLYCOSYLATION OF DYSTROGLYCAN

Caroline Godfrey

Thesis presented in partial fulfilment of the degree of Doctor of Philosophy at the Institute of Child Health, University College London.

2010

I, Caroline Godfrey confirm that the work presented in this thesis is my own. Where information has been derived from other sources, I confirm that this has been indicated in the thesis.

ABSTRACT

The aberrant glycosylation of α-dystroglycan is associated with a subset of clinically heterogeneous muscular dystrophies collectively referred to as dystroglycanopathies. Mutations in seven genes are currently known to result in these autosomal recessive disorders. To define the mutation frequency and clinical phenotypes associated with mutations in five of these genes, I analysed a large cohort of patients. This study redefined the clinical spectrum associated with mutations in *POMT1*, *POMT2*, *POMGNT1*, *FKTN* and *LARGE*. Mutations in these genes were detected in approximately a third of all cases indicating that, after the exclusion of *FKRP* involvement, the majority of patients with a dystroglycanopathy harbour mutations in novel genes. In order to identify novel genes in these disorders I applied a candidate gene approach to the whole genome. Genes known to be causative in dystroglycanopathy animal models and those predicted to function within the pathway of dystroglycan glycosylation were investigated. Mutation screening indicated that defects in *GYLTL1B*, *β3GNT1*, *WWP1*, *GYG1*, *GYG2*, *MGAT5B* and *DAG1* are not frequent causes of human dystroglycanopathy. In order to evaluate the function of a subset of candidate genes, I optimised a cell culture model of dystroglycanopathy. Using a ribonucleotide interference based strategy, the expression of candidate genes were modulated in a mouse myogenic cell line. The down regulation of *β3gnt1* induced a marked reduction in the glyco-epitope present on α-dystroglycan. This finding confirms *β3gnt1* as a key enzyme functioning in the pathway of α-dystroglycan glycosylation. In addition, I combined the use of high density single nucleotide polymorphism genotyping platforms, expression microarrays and sequencing data to investigate the cause of disease in a small consanguineous pedigree. In summary, this data set has refined genotype-phenotype correlations of known causative genes as well as investigated the involvement of novel loci in muscular dystrophies with defective glycosylation of dystroglycan.

PUBLICATIONS PERTAINING TO THE WORK WITHIN THIS THESIS

Godfrey C, Clement E, Mein R, Brockington M, Smith J, Talim B, *et al.* Refining genotype phenotype correlations in muscular dystrophies with defective glycosylation of dystroglycan. Brain 2007; 130: 2725-35.

Godfrey C, Escolar D, Brockington M, Clement EM, Mein R, Jimenez-Mallebrera C, *et al.* Fukutin gene mutations in steroid-responsive limb girdle muscular dystrophy. Ann Neurol 2006; 60: 603-10.

Clement EM, **Godfrey C**, Tan J, Brockington M, Torelli S, Feng L, *et al.* Mild POMGNT1 mutations underlie a novel limb-girdle muscular dystrophy variant. Arch Neurol 2008; 65: 137-41.

Clement E, Mercuri E, **Godfrey C**, Smith J, Robb S, Kinali M, *et al.* Brain involvement in muscular dystrophies with defective dystroglycan glycosylation. Ann Neurol 2008; 64: 573-82

Muntoni F, Brockington M, **Godfrey C**, Ackroyd M, Robb S, Manzur A, *et al.* Muscular dystrophies due to defective glycosylation of dystroglycan. Acta Myol 2007; 26: 129-35.

Jimenez-Mallebrera C, Torelli S, Feng L, Kim J, **Godfrey C**, Clement E, *et al.* A Comparative Study of alpha-Dystroglycan Glycosylation in Dystroglycanopathies Suggests that the Hypoglycosylation of alpha-Dystroglycan Does Not Consistently Correlate with Clinical Severity. Brain Pathol 2008; 19: 596-611.

COLLABORATORS

Clinical evaluations were carried out by Professor F Muntoni and Dr E Clement at the Dubowitz Neuromuscular Centre, Institute of Child Health, University College London.

The evaluation of muscle pathology was performed by Professor C Sewry, Dr L Feng and Dr C Jimenez-Mallebrera at the Dubowitz Neuromuscular Centre, Institute of Child Health, University College London.

Mutation screening was carried out by me in collaboration with Dr S Abbs and Mrs R Mein at Guy's DNA laboratory, GSTS Pathology, Guy's Hospital, London.

POMGNT1 enzymatic profiling was performed by Dr H Schachter, Dr J Vajsar and Dr J Tan at the Department of Structural Biology and Biochemistry, University of Toronto, Canada.

Where indicated within the text, the functional analysis of sequence variants was performed by Professor K Campbell, Dr T Willer and Dr Y Hara in the Howard Hughes Medical Institute, University of Iowa, USA.

The zebrafish morphant described in this thesis was generated by Dr D Stemple and Dr Y Lin at the Wellcome Trust Sanger Institute, Cambridge University.

Single nucleotide polymorphism (SNP) genotyping and gene expression profiling were performed by the University College London Genomics facility in collaboration with Dr M Hubank. The analysis of SNP data was performed by Professor R Kleta and Dr H Stanescu at the department of Internal Medicine, UCL.

ACKNOWLEDGEMENTS

Firstly I would like to acknowledge my supervisor Professor F Muntoni (Dubowitz Neuromuscular Centre, Institute of Child Health, University College London) for his guidance and support throughout this project. I owe thanks to Dr L Game (Genomics Laboratory, MRC Clinical Sciences Centre, University College London) who supervised my research during the first half of my studies. In addition I would like to express thanks to Dr P Stanier (Neural Development, Institute of Child Health, University College London) for his assistance throughout the latter stages of this project and in particular during the writing of this thesis.

I would like to acknowledge members of the Dubowitz Neuromuscular Centre for creating an enjoyable and stimulating atmosphere in which to work. In particular I would like to thank Dr S Torelli and Mr M Brockington for taking time to impart their experimental expertise and Dr E Clement for her invaluable assistance with the clinical aspects of this project.

I am incredibly grateful for the continued support from Dr S Abbs and members of the DNA Laboratory at Guy's Hospital, with special mention to Dr M Yau, Mrs R Mein, Miss J Pagan and Mr T Cullup. I would also like to express my gratitude to both Professor R Kleta and Dr H Stanescu at the department of Internal Medicine, UCL and to Dr D Kelberman at the Institute of Child Health, UCL for their invaluable assistance.

I would like to thank the Muscular Dystrophy Campaign for funding this project and the patients and their families who consented to research within this field.

Finally this section would be incomplete without thanking my family, in particular Mr AD Godfrey. I would also like to make special mention of Mr K Yates for his unfaltering support and encouragement.

TABLE OF CONTENTS

LIST OF FIGURES

LIST OF TABLES

ABBREVIATIONS

AD	Autosomal dominant
AR	Autosomal recessive
Bp	Base pair
BSA	Bovine serum albumin
CDG	Congenital disorders of glycosylation
CMD	Congenital muscular dystrophy
CMD-CRB	CMD with cerebellum involvement
CMD-MR	CMD with mental retardation
CMD-no MR	CMD with no mental retardation
DAG	Dystrophin-associated glycoproteins
DAP	Dystrophin-associated proteins
DbSNP	Single Nucleotide Polymorphism database
DGC	Dystrophin glycoprotein complex
DMD	Duchenne muscular dystrophy
DMEM	Dulbecco's Modified Eagle Medium
DNA	Deoxyribonucleic acid
dNTP	Deoxyribonucleotide triphosphate
Dol-P-Man	Dolichol-phosphate-mannose
DTT	Dithiothreitol
ECACC	European Collection of Cell Cultures
ECL	Electrochemiluminescence
EDTA	Ethylenediaminetetraacetic acid
ER	Endoplasmic reticulum
FCMD	Fukuyama CMD
GalNAc	*N*-acetylgalactosamine
GlcNAc	*N*-acetylglucosamine
HCl	Hydrochloric acid
HGVS	Human Genome Variation Society
HRP	Horseradish peroxidise
kb	Kilobase
kDa	Kilodalton

LB	Luria-Bertani
LCMV	Lymphocytic choriomeningitis virus
LGMD	Limb girdle muscular dystrophy
LGMD-MR	LGMD with mental retardation
LGMD-no MR	LGMD with no mental retardation
MDC1C	Muscular dystrophy congenital type 1C
MDC1D	Muscular dystrophy congenital type 1D
MEB	Muscle eye brain disease
mRNA	Messenger RNA
MOPS	3-(N-morpholino) propane sulfonic acid
OMIM	Online Mendelian Inheritance in Man
PBS	Phosphate buffered saline
PCR	Polymerase chain reaction
RNA	Ribonucleic acid
RNAi	Ribonucleotide interference
RPMI	Roswell Park Memorial Institute
SDS	Sodium dodecyl sulphate
SEM	Standard error of the mean
siRNA	Short interfering RNA
SNP	Single nucleotide polymorphism
TBST	Tris Buffered Saline with tween 20
TAE	Tris-acetate-EDTA
Tris	Tris(hydroxymethyl)aminomethane
UDP	Uridine 5’-diphosphate
WWS	Walker-Warburg syndrome

AIMS OF THIS THESIS

Prior to the commencement of work for this thesis, muscular dystrophies caused by defective glycosylation of dystroglycan were ill defined. Individual studies assessing the mutation frequency and clinical spectrum associated with each causative gene were only carried out on a small number of families and individuals. The underlying genetic defect in a large number of patients had yet to be established.

The aims of this thesis were therefore to:

1) Refine genotype-phenotype correlations within the dystroglycanopathies.

2) Apply the candidate gene approach to dystroglycanopathy cases with no molecular diagnosis.

3) Further analyse a consanguineous pedigree previously reported to be linked to 1q42.

The following chapters reflect the approximate chronological sequence of work performed for this thesis. The refinement of genotype-phenotype correlations described in results chapter 3 formed the basis of the candidate gene approach in results chapter 4. Results chapter 5 describes further analysis of a family previously studied in the Dubowitz Neuromuscular Centre. An overall introduction, description of methods and discussion comprise chapters 1, 2 and 6 respectively.

CHAPTER 1. INTRODUCTION

1 INTRODUCTION

1.1 MUSCULAR DYSTROPHY

The term muscular dystrophy encompasses a large group of hereditary diseases characterised by progressive weakness and degeneration of skeletal muscle. Distinct muscular dystrophies demonstrate varied patterns of muscular involvement which can include differential weakness of the limbs, respiratory impairment, cardiac involvement, as well as including damage to the nerves controlling the muscle itself. Diseases vary widely in their clinical severity ranging from neonatal presentation associated with early death to late onset adult forms of relatively mild muscular dystrophy. In all cases progressive muscle weakness follows the progression of muscle damage which can lead to loss of ambulation and premature death if respiratory and/or cardiac muscles are significantly compromised. A variety of different inheritance patterns exist within this group of clinically and genetically heterogeneous diseases (Guglieri et al., 2008; Mercuri et al., 2002).

Originally, defects in structural proteins were identified in muscular dystrophies. More recently it has been recognised that underlying pathological mechanisms not only involve defective structural proteins but include the disruption of proteins functioning in a variety of cellular systems. These proteins reside in a number of discrete subcellular components of skeletal myofibres and include the nucleus, Golgi apparatus, endoplasmic reticulum (ER), sarcomere, extracellular matrix and sarcolemma (Figure 1) (Davies and Nowak, 2006).

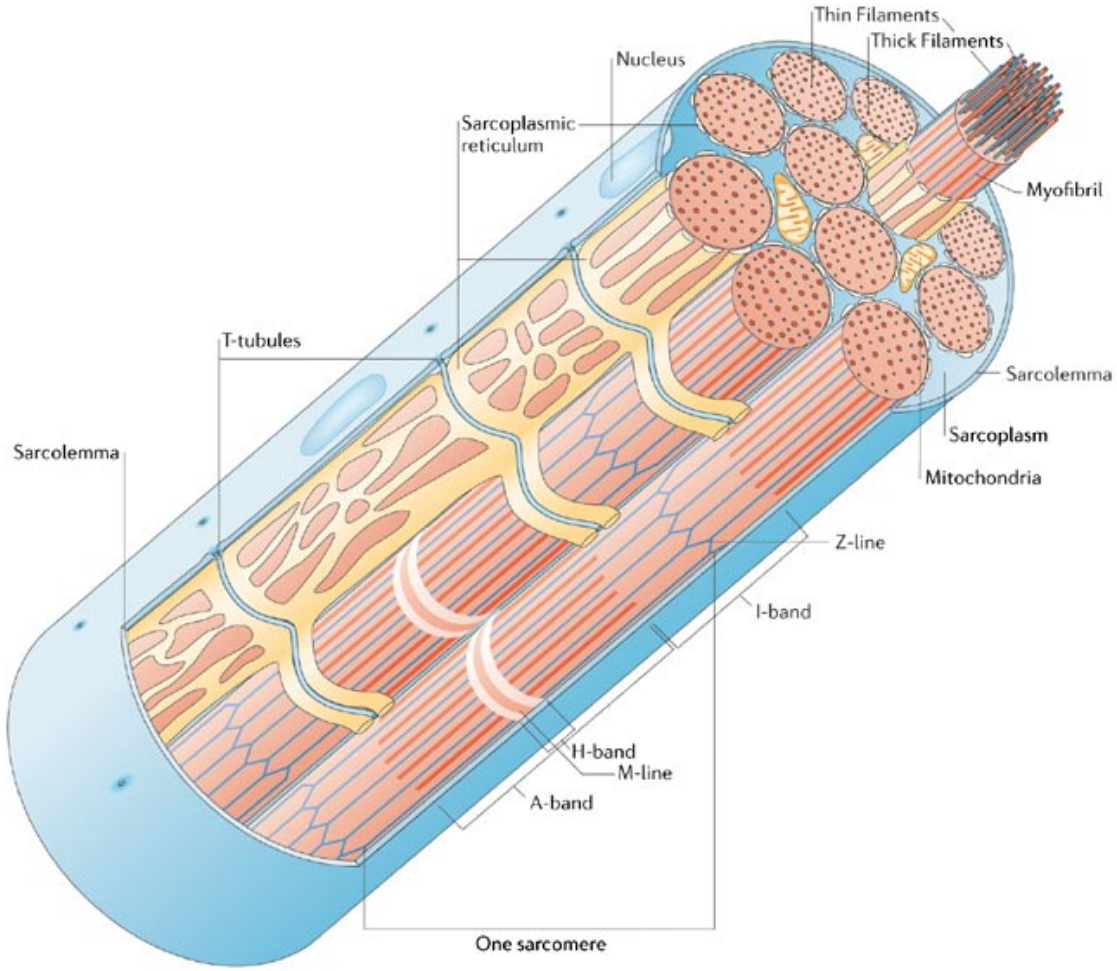

Figure 1. The structure of a single muscle fibre.

An individual skeletal muscle consists of hundreds of thousands of muscle fibres. Fibres are long multinucleated cylindrical cells formed by the fusion of developmental myoblasts. The muscle's contractile units lying within each fibre are known as myofibrils. Each myofibre is composed of regularly aligning myofilaments organised into units known as sarcomeres. They are enveloped by a plasma membrane known as the sarcolemma and an overlying basal lamina. The sarcolemma acts as a physical barrier separating the fibre from the surrounding extracellular environment as well as mediating interactions between the synactia and extracellular matrix. Figure modified from Davies *et al.* (Davies and Nowak, 2006). Permission to reproduce this figure has been granted by Nature Publishing Group.

Historically, forms of muscular dystrophy have been recognised according to their distinct clinical manifestations, for example: Duchenne muscular dystrophy, Becker muscular dystrophy, muscle eye brain disease (MEB) and Walker-Warburg syndrome (WWS). As the molecular basis of these conditions is uncovered, common pathogenic mechanisms have been identified. This has lead to the grouping of different forms of muscular dystrophy; Duchenne muscular dystrophy and Becker muscular dystrophy, both caused by defects in dystrophin, are now collectively referred to as 'dystrophinopathies' This nomenclature has been further complicated by allele heterogeneity which underlies extreme clinical diversity.

This may be best exemplified by the laminopathies where defects in lamin A and C (encoded by *LMNA*) cause a variety of human diseases (Gruenbaum et al., 2005). Autosomal dominant (AD) *LMNA* mutations were initially associated with Emery-Dreifuss muscular dystrophy yet are also associated with familial partial lipodystrophy, dilated cardiomyopathy and Hutch-Gilford progeria syndrome. Autosomal recessive (AR) *LMNA* mutations are associated with Charcot Marie Tooth and Mandibuloacral muscular dystrophy as well as rare cases of Emery-Dreifuss muscular dystrophy. Autosomal dominant and AR mutations in emerin, another component of the nuclear envelope, also cause Emery-Dreifuss muscular dystrophy (Brown et al., 2008). Lamin A and C participate in the LINC complex that, along with nesprin, link the nucleoskeleton with the cytoskeleton (Crisp et al., 2006). Mutations in the genes encoding the nuclear envelope proteins nesprin-1 and -2 (encoded by *SYNE1* and *SYNE2* respectively) have recently been described in patients with features of Emery-Dreifuss muscular dystrophy (Zhang et al., 2007). Recessive mutations in *SYNE1* have also been linked to Arthrogryposis multiplex congenita and adult onset cerebellar ataxia (Attali et al., 2009; Gros-Louis et al., 2007). This example clearly illustrates how delineating the underlying aetiology of muscular dystrophy is a complex task.

To date, over 30 different genes are implicated in muscular dystrophy whose encoded proteins now include enzymes, signalling molecules, RNA binding proteins and protein kinases (Davies and Nowak, 2006). There is currently no reliable data on the prevalence or incidence of the majority of muscular dystrophies, or indeed these diseases as a whole. The most common type of muscular dystrophy in the United Kingdom is the severe Duchenne Muscular Dystrophy (DMD) which affects 1 in 3500 newborn boys.

DMD is caused by an absence of the protein dystrophin and is characterised by progressive muscular dystrophy, cardiomyopathy and respiratory failure. The majority of patients are diagnosed before 6 years of age, become wheelchair bound in their early teens and rarely live beyond 30 years of age (Manzur et al., 2008). The *DMD* gene is the longest human gene spanning 2.4 megabases of the X chromosome and encoding a 3684 amino acid dystrophin protein (Davies et al., 1983; Koenig et al., 1988). *DMD* was the first gene to be associated with muscular dystrophy. Its discovery in turn led to the identification of a number of structural muscle proteins in rapid succession (Ervasti et al., 1990; Koenig et al., 1988).

A skeletal muscle biopsy often plays an integral role in the diagnosis of muscular dystrophy. In the Dubowitz Neuromuscular Centre, open, or commonly, needle biopsies are typically taken from the quadriceps (Dubowitz and Sewry, 2006). Key dystrophic features are observed by histological staining of transverse sections of skeletal muscle. The overall morphology of the muscle fibres in relation to non contractile elements such as nuclei, connective tissue and blood vessels can be observed using the histological stain haematoxylin and eosin (Figure 2) (Dubowitz and Sewry, 2006).

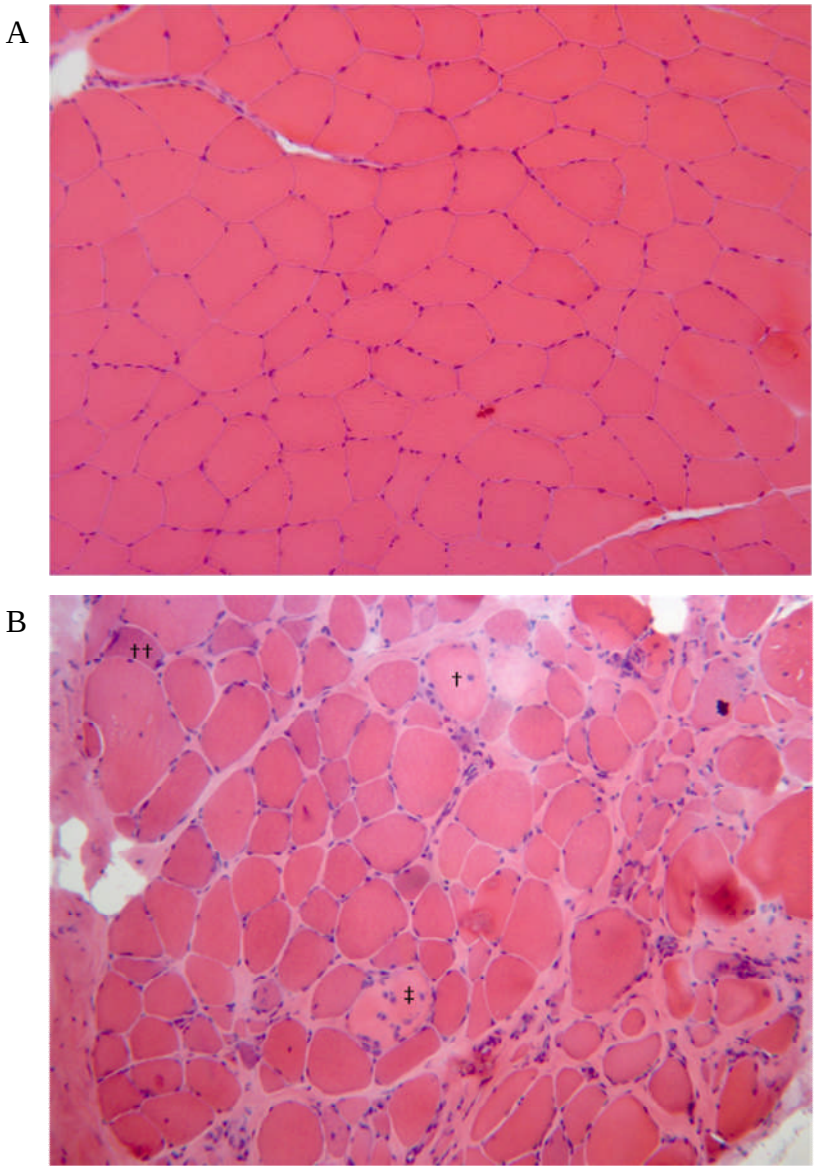

Figure 2. Dystrophic skeletal muscle.

Muscle histology is often used to confirm that the muscle has dystrophic changes. Dystrophic changes are detected on transverse sections of skeletal muscle biopsies. Haematoxylin and eosin staining of normal muscle (A) and dystrophic muscle (B). Normal myofibres are approximately equal in diameter with nuclei located around the periphery (A). Dystrophic muscle is characterised by an accumulation of fat and connective tissue between fibres, increased variability in fibre size, a rounded morphology of cells, the presence of central nuclei (†), necrotic fibres (††) and the presence of regenerating fibres (basophilic fibre‡) (Dubowitz and Sewry, 2006). Images from Dr Lucy Feng, Dubowitz Neuromuscular Centre, Institute of Child Health, UCL.

1.1.1 Dystrophin Glycoprotein Complex

The dystrophin glycoprotein complex (DGC) is an oligomeric assemblage of proteins. This macromolecular structure can be purified from plasma membranes solubilised with detergent (Ervasti et al., 1990; Yoshida and Ozawa, 1990). Initially components of this complex were designated as either dystrophin-associated proteins (DAP) or dystrophin-associated glycoproteins (DAG) (Ervasti et al., 1990). Proteins were referred to as 156DAG, 59DAP, 50DAG, 43DAG, 35DAG and 25DAP reflecting their approximate molecular weights. A subsequent report describing this complex referred to proteins as A0, A1, A2, A3a/A3b, A4 and A5 and divided them into two sub-complexes; the dystrophin and sarcoglycan complexes (Yoshida and Ozawa, 1990). The DGC is present along the sarcolemma of skeletal muscle fibres and contains an array of cytoplasmic, transmembrane and extracellular matrix proteins. Components of the DGC include: the cytoplasmic proteins dystrophin and syntrophins (α and β), the transmembrane protein sarcospan, the glycoproteins dystroglycan (α and β) and sarcoglycans (α, β, γ, and δ) (Figure 3) (Ervasti and Campbell, 1991).

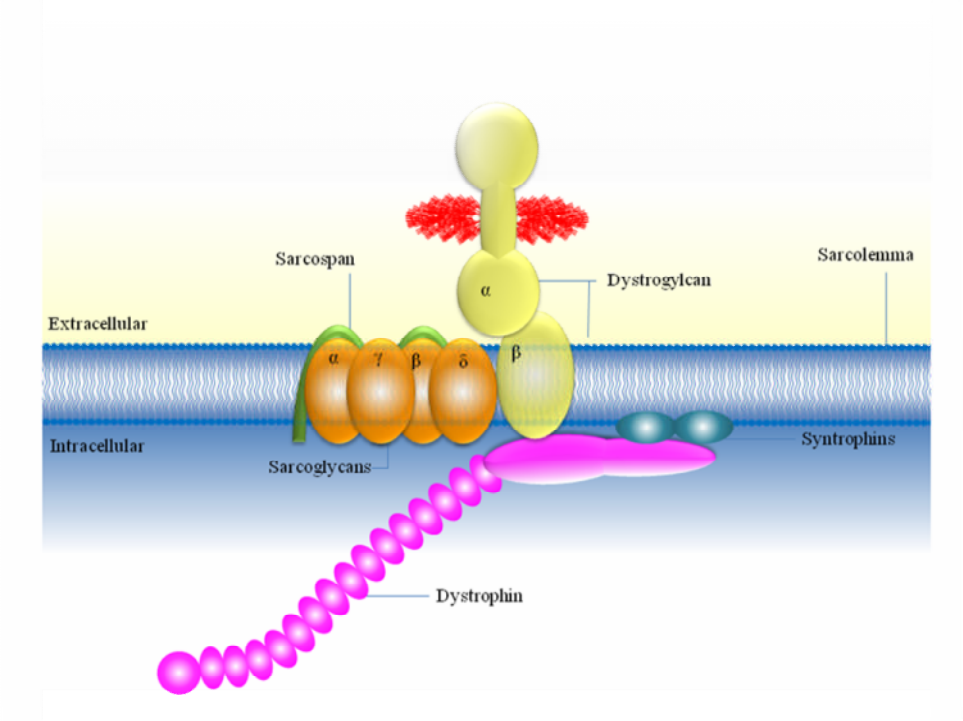

Figure 3. Integral components of the dystrophin glycoprotein complex.

The dystrophin glycoprotein complex forms a crucial connection between the intracellular cytoskeleton and the extracellular matrix. Alpha-dystroglycan has a dumbbell like appearance. Attached *O*-linked glycans are depicted in red and occur in the central mucin like region of α-dystroglycan. These glycans facilitate the attachment of extracellular matrix ligands. Figure based on that from Davies *et al.* (Davies and Nowak, 2006).

Although the exact function of this complex has yet to be fully elucidated, it is thought these proteins confer structural stability to the sarcolemma during cyclic contraction and relaxation (Petrof et al., 1993). Defects in protein members of the DGC are thought to render muscle fibres more venerable to damage. Various forms of muscular dystrophy have now been linked to mutations in genes encoding components of the DGC (Table 1).

*	**Protein (*encoding gene*)** **	**Gene ID** †	**Function**	**Associated muscular dystrophy** ‡
Transmembrane	Dystroglycan; α- and β- (*DAG1*)	1605	Connects the extracellular matrix with the intracellular cytoskeleton.	A range of muscular dystrophies are associated with hypoglycosylation of α-dystroglycan. Walker-Warburg syndrome [OMIM_236670], Muscle eye brain disease [OMIM_253280], Fukuyama congenital muscular dystrophy [OMIM_253800], MDC1C [OMIM_606612], MDC1D [OMIM_608840], LGMD2I [OMIM_607155], LGMD2K [OMIM_609308], CDG1O [OMIM_612937].
	Sarcospan (*SSPN*)	8082	Uncharacterised structural role	No mutations detected in muscular dystrophy patients to date.
	Sarcoglycans; α- (*SGCA*), β- (*SGCB*), γ- (*SGCG*), and δ- (*SGCD*)	6442, 6443, 6445, 6444	Structural and signalling role.	LGMD2D [OMIM_608099], LGMD2E [OMIM_604286], LGMD2F [OMIM_601287] and LGMD2C [OMIM_253700] respectively.
Cytoplasmic	Dystrophin (*DMD*)	1756	Anchoring the cytoskeleton to the sarcolemma	Duchenne [OMIM_310200] and Becker muscular Dystrophy [OMIM_300376].
	Syntrophins; α- (*SNTA1*) and β- (*SNTB1*)	6640, 6641	Connects dystrophin to nNOS	No mutations detected in muscular dystrophy patients to date.

Table 1. Muscular dystrophies caused by defective components of the DGC.

New nomenclature for genetic loci is based on the age of onset and mode of inheritance (LGMD1 for autosomal forms and LGMD2 for dominant forms of late onset muscular dystrophy, CMD for congenital forms of muscular dystrophy, all of which are recessive). Within each category a numerical suffix indicates the chronological order of their discovery (Bushby and Beckmann, 1995). * Skeletal myofiber subcellular localisation. ** Gene symbols and names as per HUGO nomenclature (www.genomes.org). † Entrez Gene Identifier in the NCBI database (http://www.ncbi.nlm.nih.gov/). ‡ Muscular dystrophy caused by mutations in the respective gene (reviewed in (Davies and Nowak, 2006)) followed by the Online Mendelian Inheritance in Man reference (http://www.ncbi.nlm.nih.gov/OMIM). ECM; extra-cellular matrix.

Dystroglycan is an integral membrane protein linking the intracellular cytoskeleton to proteins within the extracellular matrix. Dystroglycan was originally isolated from skeletal muscle through its interaction with dystrophin. Research has primarily focussed on its role in skeletal muscle and its function within the DGC has been extensively studied. Dystroglycan is also expressed in numerous developing and adult tissues and is typically found in cells facing basement membranes. Novel roles have continued to emerge and dystroglycan has been found to function in a diverse range of cellular processes including development, signalling and adhesion (Barresi and Campbell, 2006; Smalheiser and Schwartz, 1987).

1.2 DYSTROGLYCAN

The gene encoding dystroglycan, *DAG1*, was initially cloned in 1992 and subsequently mapped to 3p21 in 1993 (Ibraghimov-Beskrovnaya et al., 1992; Ibraghimov-Beskrovnaya et al., 1993). The primary structure of dystroglycan is highly conserved across mammalian species and displays a high degree of homology throughout lower invertebrates. Mammalian *DAG1* consists of two coding exons and encodes a single mRNA species which is translated into a pro-peptide of 895 amino acids (Holt et al., 2000). An N-terminal signal peptide directs insertion of dystroglycan into the ER membrane. The pro-peptide is post-translationally cleaved at Ser654 yielding two non-covalently associated subunits known as α and β (Figure 4) (Ibraghimov-Beskrovnaya et al., 1992). Alpha-dystroglycan is a peripheral membrane glycoprotein and binds to components of the extracellular matrix. Beta-dystroglycan is a transmembrane protein that binds via its cytoplasmic domain to components of the cell cytoskeleton (Yoshida and Ozawa, 1990).

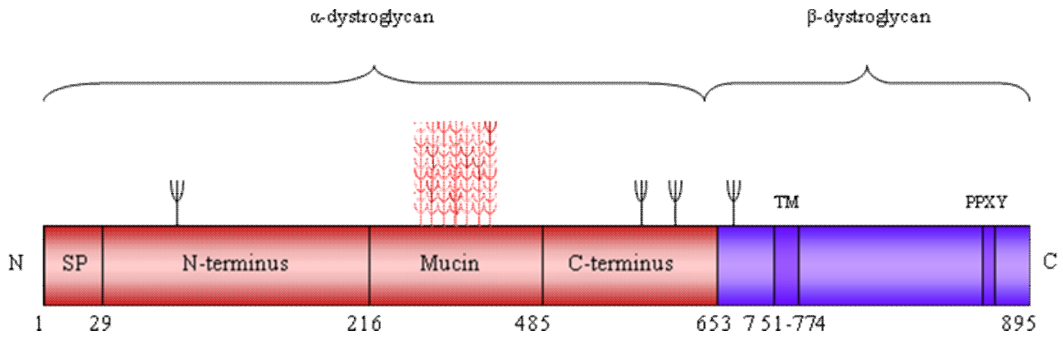

Figure 4. The structure of dystroglycan encoded by *DAG1*.

Black branches indicate *N*-linked sugar chains. Red branches indicate *O*-linked sugar chains. SP; signal peptide, TM; transmembrane domain, PPXY; dystrophin-binding site, C; C-terminus, N; N-terminus ends. Numbers indicate amino acids within each domain. Figure based on that from Michele *et al.* (Michele et al., 2002).

The molecular mechanism underlying the dystroglycan pro-peptide cleavage into its α and β subunits remains largely undefined. Cleavage occurs within a full sea urchin, enterokinase, agrin module suggesting an autoproteolysis mechanism (Akhavan et al., 2008). The pro-peptide is cleaved in an early processing event within the ER and proceeds glycosylation (Smalheiser and Kim, 1995). The functional significance is not yet fully understood particularly because the peptide is not cleaved into subunits in *Drosophila melanogaster* (Patnaik and Stanley, 2005). Despite this, studies have indicated that this event is crucial for normal muscle development in mammals. Jayasinha *et al.* demonstrated that the overexpression of an uncleaved dystroglycan precursor in transgenic mice induced muscular dystrophy along with disorders in the proliferation and differentiation of neurons (Jayasinha et al., 2003).

In the context of the DGC, transmembrane β-dystroglycan binds intracellularly to members of the dystrophin family, which in turn bind to the actin associated cytoskeleton. In tissues other than skeletal muscle, dystroglycan binds to various alternative splice forms of dystrophin or one of its autosomal orthologs, utrophin (Chung and Campanelli, 1999). The carboxy terminal 15 amino acids of β-dystroglycan contains a PPXY motif facilitating binding to the C-terminal cysteine-rich regions of dystrophin (or utrophin) which in turn comprise of a WW-like domain, an EF hand domain and a ZZ domain. WW domains are named after two highly conserved tryptophan residues, in this case 21 amino acids apart and are widely conserved among structural, regulatory and signalling proteins (Sudol et al., 1995). The EF hand region stabilises the WW domain, which is in turn stabilised and strengthened by the ZZ domain. A more distantly related paralog of dystrophin lacking a WW domain, yet containing an EF hand domain; α-dystrobrevin, also binds to β-dystroglycan (Chung and Campanelli, 1999). A WW-like domain in Caveolin-3 also recognises the PPXY domain of β-dystroglycan. It has been demonstrated that Caveolin-3 can effectively block the interaction of dystrophin with β-dystroglycan *in vitro* and may therefore competitively regulate the recruitment of dystrophin to the sarcolemma *in vivo* (Sotgia et al., 2000).

Beta-dystroglycan also interacts with rapsyn, a postsynaptic protein involved in clustering of acetylcholine receptors and the signalling adapter molecule Grb2 (Cartaud et al., 1998; Yang et al., 1995). The biological significance of these interactions has

remained elusive. The cytoplasmic tail of β-dystroglycan also binds to components of the ERK-MAP kinase cascade including MEK and ERK (Spence et al., 2004). These interactions implicate β-dystroglycan in signal transduction pathways and in the formation of neuromuscular junctions (Henry and Campbell, 1999).

Alpha-dystroglycan is heavily glycosylated. Electron microscopy of α-dystroglycan by Brancaccio *et al.* showed a dumbbell like appearance with a globular N-domain, a long stalk like region in the mucin domain and a globular C-domain (Brancaccio et al., 1995). This subunit is retained at the cell surface and binds to extracellular matrix ligands (Brancaccio et al., 1995; Brancaccio et al., 1997). Primary sequence analysis of *α*-dystroglycan predicts its molecular mass to be approximately 70 kDa although it migrates in a heterogeneous pattern on sodium dodecyl sulphate gels (Ibraghimov-Beskrovnaya et al., 1992). Its molecular mass is increased to 156 kDa in mammalian skeletal and cardiac muscle due to its extensive glycosylation. Alpha-dystroglycan migrates at 140 kDa and 120 kDa in brain and peripheral nerve respectively, reflecting tissue specific modifications (Ibraghimov-Beskrovnaya et al., 1993; Leschziner et al., 2000; Yamada et al., 1994). In addition, the varied molecular weight of human and chick skeletal muscle *α*-dystroglycan during different developmental stages reflects developmentally regulated modifications (Brown et al., 2004; Leschziner et al., 2000). The structural characterisation of the mucin rich portion of α-dystroglycan has so far remained unsuccessful due to its extensive glycosylation (Chiba et al., 1997).

Alpha-dystroglycan establishes a network of interactions with components of the extracellular matrix such as laminin 1 and 2, agrin, perlecan, neurexin and biglycan (Henry and Campbell, 1999). The binding of biglycan, an extracellular proteoglycan, binds to the C-terminal domain of α-dystroglycan. This interaction is dependent on the chondroitin sulphate side chains present on biglycan (Bowe et al., 2000). In contrast to biglycan, the binding of laminins, agrin, perlecan and neurexin is strictly dependent on the glycosylation status of *α*-dystroglycan (Michele et al., 2002; Michele and Campbell, 2003). Each of these ligands contain a laminin G domain mediating their high affinity Ca2+ -dependent binding to *α*-dystroglycan (Hohenester et al., 1999; Talts et al., 1999; Tisi et al., 2000). Laminins are composed of three distinct chains termed α, β, and γ. To date five α, four β, and three γ chains have been identified that can combine to form 15 different isoforms. Dystroglycan binds with high affinity to the laminin G domains of

laminin 1 (α1β1γ1) and laminin 2 (α2β1γ1) α chains (Talts et al., 1999). Laminin α2 forms a crucial link between *α*-dystroglycan and the basal lamina (Henry and Campbell, 1999).

The sarcoglycans form an integral subcomplex within the DGC. These four single span transmembrane subunits (α, β, γ and δ) are tightly associated with sarcospan. Evidence has indicated that these proteins serve to stabilise dystroglycan. Although a mechanism for this is unknown, evidence suggests that δ-sarcoglycan is in close molecular proximity to dystroglycan (Chan et al., 1998). Recently a novel function of the sarcoglycan complex has been demonstrated in whole body glucose homeostasis and skeletal muscle metabolism (Groh et al., 2009). The transmembrane integrin subunits are associated with members of the laminin family and have been found to co-localise with dystroglycan in certain cell types. Despite this there is no evidence of direct binding between the two proteins.

1.2.1 Glycosylation

The glycosylation of proteins enables immense functional diversity and the importance of the glycome in a vast range of biological processes is only just beginning to emerge. Between 1-2% of the human genome encodes enzymes involved in glycan formation. Glycans serve a variety of structural and functional roles and are synthesised by several biochemical pathways (Varki, 2008). Inherited pathological mutations occur in all major glycan families. Defects in the human glycome have been associated with over 30 different genetic diseases. These rare human diseases are biochemically and clinically heterogeneous and usually affect multiple organ systems (Freeze, 2006).

Major glycan groups are classified according to their glycan-peptide linkage regions. *N*-linked glycans describe the attachment of an oligosaccharide to the amide group of an asparagine residue via an aspartylglycosylamine link. The largest number of known glycosylation disorders affect *N*-glycosylation and are referred to as congenital disorders of glycosylation (referred to as CDGs).

Congenital disorders of glycosylation are classified according to their defects and are subdivided into two types; I and II. Type I CDGs are caused by defects in the assembly

of lipid linked oligosaccharides in the ER resulting in the production of incomplete glycan structures. A complete loss of *N*-glycosylation is lethal therefore viable mutations create hypomorphic alleles where insufficient or incomplete glycan precursors are produced that are inefficiently transferred to proteins. Type II CDGs are caused by defects in altered processing of protein bound sugar chains and describe a more diverse aetiology with mutations occurring in glycosyltransferases, nucleotide sugar transporters and cytoplasmic proteins that traffic into and within the Golgi apparatus.

Accurate diagnosis is often problematic due to the variability of clinical features as well as their overlap with other multisystemic metabolic disorders (Freeze, 2006). To overcome this, a diagnostic assay has been developed on the basis that the majority of patients demonstrate an under sialylation of serum glycoproteins detected by the analysis of serum transferrin. Transferrin has two *N*-glycosylation sites with a typical desialylated biantennary glycan on each side. Isoelectric focusing using ion-exchange chromatography is used to identify the glycoforms present on transferrin.

Both α-dystroglycan and β-dystroglycan also contain *N*-linked glycans, yet enzymatic removal of these glycans only alters α-dystroglycan's molecular weight by approximately 4 kDa (Ervasti and Campbell, 1991). However full chemical deglycosylation results in the complete loss of ligand binding activity (Ervasti and Campbell, 1993). The remainder of α-dystroglycan glycosylation is thought to reside in the serine/threonine rich 'mucin' domain. The mucin domain contains fifty-five potential sites for glycosylation of serine or threonine residues in the middle third of the molecule.

O-linked glycans describe the attachment of a reducing terminal *N*-acetylgalactosamine (GalNAc) to the hydroxyl group of serine/threonine residues. Several unique types of *O*-glycosylation have also been identified such as *O*-linked fucose, glucose, *N*-acetylglucosamine (GlcNAc) and mannose. *O*-mannosylation describes the attachment of an oligosaccharide to the hydroxyl group of a serine or threonine residue via mannose. *O*-mannosylation is well characterised in yeast and is essential for viability affecting cell wall integrity and rigidity. Subsequently mammalian *O*-mannosylation was found to reside on dystroglycan (Endo, 1999). Alpha-dystroglycan glycan

sequencing studies have been performed on three different tissues from three different species: bovine peripheral nerve; rabbit skeletal muscle and sheep brain (Matsumura et al., 1997; Smalheiser and Schwartz, 1987; Toda et al., 2003). In all these studies the following glycan was identified NeuAcα2,3Galβ1,4GlcNAcβ1,2Manα-*O*-Ser/Thr. Alpha-dystroglycan is the only identified carrier of this glycan. Phosphorimaging of a recombinant dystroglycan containing only the mucin-like domain has suggested that phosphorylation occurs on the *O*-linked mannose residue (Yoshida-Moriguchi et al., 2010). A significant amount of Galβ1,3GalNAcα-*O* was also identified, suggesting that multiple *O*-linked structures exist. In addition to the structures found in peripheral nerve and skeletal muscle the *O*-mannosyl-linked LewisX antigen Galβ1,4(Fucα1,3)GlcNAcβ1,2Manα-*O* was detected in the brain. Analysis of whole rat brain revealed *O*-mannose based glycans account for one third of all *O*-linked glycans in the brain. As well as those structures previously reported by α-dystroglycan glycan sequencing studies, 1,6 substituted Manα-*O* structures have also been found in *O*-linked brain glycans including;
NeuAcα2,3Galβ1,4GlcNAcβ1,2[NeuAcα2,3Galβ1,4GlcNAcβ1,6]Manα-*O* (Chai et al., 1999). It has not yet been shown if this structure resides on dystroglycan or other *O*-linked glycans in the brain (Figure 5).

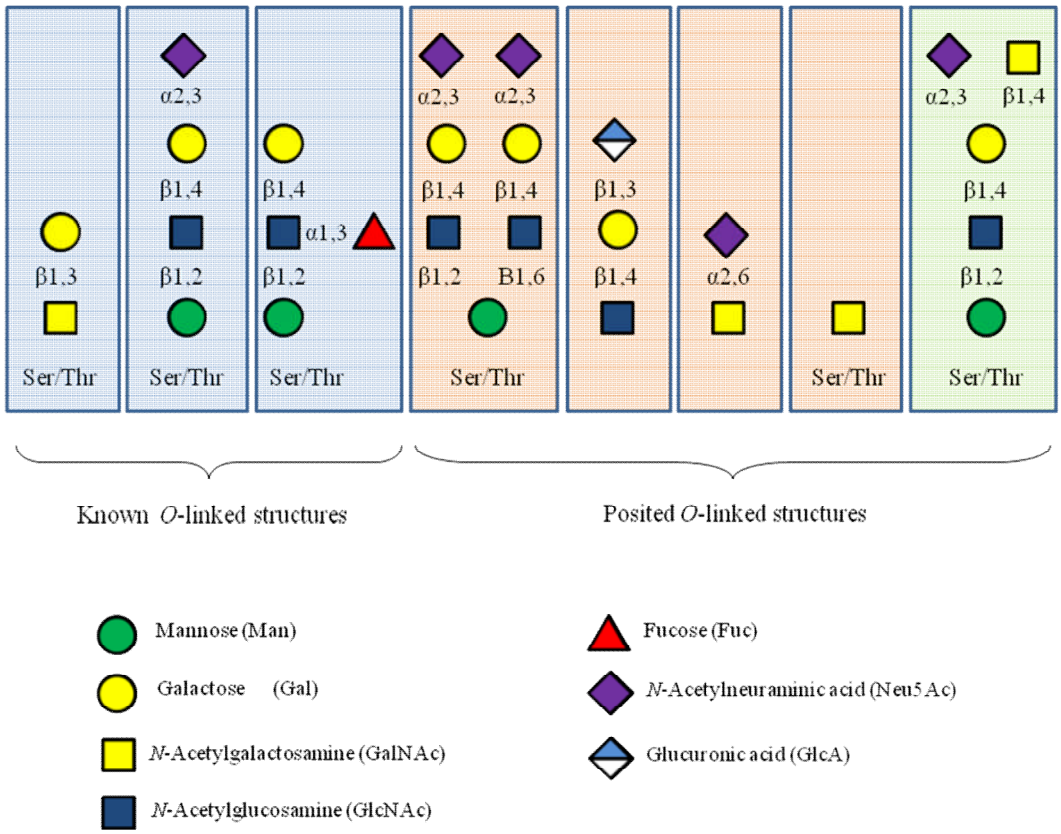

Figure 5. Glycan structures and dystroglycan.

The three glycan structures identified on α-dystroglycan by glycan sequencing studies are shown in the blue shaded boxes. Glycan sequences shown in the orange boxes represent those posited to be present on α-dystroglycan based on lectin and antibody binding analyses. The *O*-linked branched mannose structure shown in the green shaded box has been included due to its presence in brain tissue although it has not yet been established if this exists on α-dystroglycan (Martin, 2003). Symbolic representation of monosaccharides follows the nomenclature proposed by the Consortium for Functional Glycomics (www.functionalglycomics.org).

It is worth noting that all studies to date have all been performed using dystroglycan purified by carbohydrate binding lectins (e.g. wheat germ agglutinin). Due to the use of this enriched form of dystroglycan, these structures may only represent a subset of glycans present on this glycoprotein (Martin, 2003). Further studies are needed to clarify the heterogeneity and distribution of *O*-mannosyl glycans in various tissues both during development and under pathological conditions.

1.2.2 Aberrant Post-Translational Modifications in Disease

More recently it has emerged that perturbation of extensive post-translational processing of dystroglycan plays a role in human disease. Defects in a number of proteins that glycosylate dystroglycan, or are thought to do so, have been shown to cause muscular dystrophy (Michele et al., 2002; Muntoni et al., 2008). The processing of dystroglycan also affects its function as a cellular receptor for human pathogens and has implications in the progression of cancer (Cao et al., 1998; Rambukkana et al., 1998; Singh et al., 2004).

Abnormalities in the structure and function of basement membranes are hallmarks of metastatic disease. Disruption of the interaction between cancer cells and the extracellular matrix is believed to provide a mechanism by which tumours can invade surrounding tissues and metastasise. The expression of dystroglycan at the interface between the basal lamina and the plasma membrane, as well as its function in cell adhesion suggests a possible role in this process. Multiple post-translational modifications of dystroglycan have been identified in carcinoma cells, which are thought to modulate the composition and function of dystroglycan. The glycosylation of dystroglycan is altered in invasive carcinoma cells causing a complete loss of its laminin binding properties (Singh 2004). Low or absent dystroglycan has been correlated with a higher tumour stage, high proliferation index, and lower overall survival in these cells. Beta-dystroglycan expression is preserved in cancer cell lines although a truncated β-dystroglycan is observed and expressed as a 31 kDa protein. Singh et al also described the loss of α-dystroglycan caused by protease-dependent shedding from the cell surface (Singh et al., 2004). These studies indicate that abnormalities in dystroglycan processing can be a common feature in carcinogenesis

and may contribute to the progression of metastatic disease (Henry et al., 2001; Muschler et al., 2002).

Glycosylation of α-dystroglycan has also been implicated in the binding of human pathogens. The first cellular receptor for Old World arenaviruses was identified as dystroglycan. Arenaviruses represent a genus of virus and are subdivided into two major groups; the Old World arenaviruses found in Europe and Africa and the New World arenaviruses, endemic in the Americas. Each arenavirus species has a natural reservoir in one or a limited number of closely related rodent species. The virus is maintained in the asymptomatic natural rodent host as a persistent infection. Viral transmission to humans via contact with infected rodents can cause severe disease. The attachment of the virus to its cellular receptor represents an important determinant for cellular tropism, host range and disease potential. Alpha-dystroglycan is the primary receptor for the Old World lymphocytic choriomeningitis virus (LCMV), the Lassa virus, the related African arenaviruses Mopeia and Mobala, as well as the Clade C New World arenaviruses Latino and Oliveros.

The COOH-terminal region of *α*-dystroglycan's first globular domain and the NH_2-terminal end of the mucin-like domain form the binding site for LCMV. LCMV and laminin-1 use, in part, an overlapping binding site on *α*-dystroglycan and the ability of an LCMV isolate to compete with laminin-1 for receptor binding is determined by its binding affinity to α-dystroglycan (Kunz et al., 2001). The construction of deletion constructs has indicated that β-dystroglycan does not act as a cofactor with α-dystroglycan for arenavirus binding and entry (Kunz et al., 2003). Post-translational modifications of α-dystroglycan are crucial for its function as a cellular receptor for the Lassa virus, the LCMV, African arenaviruses Mopeia and Clade C New World arenaviruses (Imperiali et al., 2005; Kunz et al., 2005).

1.3 DYSTROGLYCANOPATHIES

Post-translational modifications of dystroglycan are associated with a number of autosomal recessive muscular dystrophies. The aberrant glycosylation of α-dystroglycan, yet not β-dystroglycan, is the primary pathological mechanism in a range

of disorders characterised by muscular dystrophy with variable brain and ocular abnormalities (Michele et al., 2002).

Phenotypic severity in patients is extremely variable. At the most severe end of the clinical spectrum are WWS, MEB and Fukuyama congenital muscular dystrophy (FCMD) (Beltran-Valero de Bernabe et al., 2002; Kobayashi et al., 1998; Yoshida et al., 2001). These conditions are characterised by congenital muscular dystrophy (CMD) with severe structural brain and eye abnormalities, which in WWS results in early infantile death (van Reeuwijk et al., 2005a). Conversely, individuals at the mildest end of the clinical spectrum may present in adult life with limb girdle muscular dystrophy (LGMD) with no associated brain or eye involvement (Brockington et al., 2001b). A number of intermediate phenotypes between these extremes have also been described including: congenital muscular dystrophy type 1D, with subtle brain involvement and mental retardation (Longman et al., 2003); congenital muscular dystrophy type 1C (MDC1C), a CMD variant in which the brain can be entirely normal and LGMD2K, a variant with microcephaly and mental retardation but a relatively mild LGMD–like phenotype (Balci et al., 2005; Brockington et al., 2001a). Recently the term 'dystroglycanopathy' has been adopted to encompass this clinically and genetically heterogeneous collection of disorders (Godfrey et al., 2007).

Common to all these disorders is the pathological feature of reduced glycosylation (*hypo*glycosylation) of α-dystroglycan (Michele et al., 2002). The finding that *α*-dystroglycan glycosylation is perturbed is based on loss of immunoreactivity to one or both monoclonal antibodies IIH6 and VIA4-1 which are specific for glycoepitopes present on *α*-dystroglycan. The glycan structures recognised by the antibodies IIH6 and VIA4-1 are as yet uncharacterised.

Immunofluorescence is evaluated in parallel with β-dystroglycan labelling and routinely performed on transverse sections of skeletal muscle. A reduction or complete absence of binding using the carbohydrate dependent antibodies IIH6 and/or VIA4-1, in conjunction with the retention of β-dystroglycan labelling is now used as a routine diagnostic tool (Figure 6) (Jimenez-Mallebrera et al., 2003). The extent of hypoglycosylation is variable between patients and ranges from a virtual absence of epitope in muscle to a minimal reduction in some fibres (Jimenez-Mallebrera et al.,

2008). The evalutation of immunoreactivity to IIH6 and β-dystroglycan labelling on western blot is a powerful technique yet is often only performed on a research basis due to the shortage of material available for analysis. A secondary reduction in laminin α-2 labelling is also observed and reflects the reduced capacity of hypoglycosylated α-dystroglycan to bind its extracellular matrix ligands.

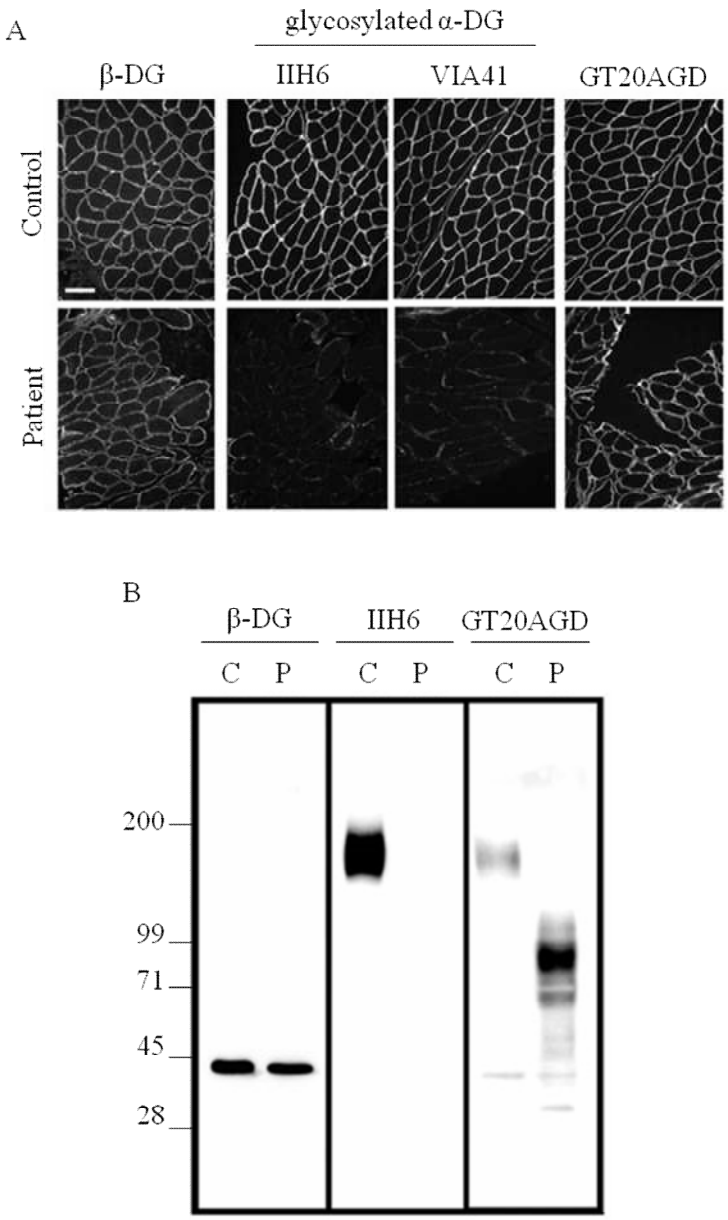

Figure 6. Hypoglycosylation of α-dystroglycan as detected on skeletal muscle biopsy. Diagnostic features of dystroglycanopathy skeletal muscle using antibodies against β-dystroglycan; β-DG, carbohydrate moieties present on α-dystroglycan; IIH6 and VIA4-1 and core α-dystroglycan; GT20ADG. A) Immunohistochemical analysis of transverse sections of skeletal muscle from a dystroglycanopathy patient and a control normal muscle. The hallmark of dystroglycanopathy muscle is a specific reduction of immunoreactivity to either IIH6 or V1A-4 yet the retention of immunoreactivity to β-dystroglycan and GT20ADG. B) Immunoblot analysis of WGA-enriched total muscle from control normal muscle (C) and a dystroglycanopathy patient (P). The molecular

weight of β-dystroglycan is unchanged on western blot analysis yet a dramatic reduction in molecular weight of α-dystroglycan is seen using the GT20ADG antibody due to hypoglycosylation. Primary sequence analysis of α-dystroglycan predicts a molecular mass of 72 kDa however α-dystroglycan in skeletal muscle migrates to 156 kDa. Figure modified from Michele *et al.* (Michele et al., 2002). Permission to reproduce this figure has been granted by Nature Publishing Group.

1.3.1 Molecular Defects

Proteins residing within the Golgi apparatus and the ER mediate post-translational processing such as the attachment and modification of carbohydrate molecules to form glycoproteins. Whereas genetic defects in *DAG1* itself have not yet been identified in human disease, defects in four proteins of the Golgi apparatus and three proteins of the ER have been shown to cause a dystroglycanopathy phenotype (Table 2). The detection of mutations in genes encoding these putative or demonstrated glycosyltransferases and accessory glycosyltransferase proteins uncovers a novel pathogenic mechanism causing muscular dystrophy (Muntoni et al., 2002).

Functional analysis of the glycosyltransferases *POMT1*, *POMT2* and *POMGNT1* has demonstrated their pathway specific function in the production of *O*-mannose linked glycans (Figure 7). The function of *FKTN*, *FKRP* and *LARGE* have yet to be fully characterised (Brockington et al., 2001a; Kobayashi et al., 1998; Longman et al., 2003). Very recently a somewhat unexpected report described mutations in *DPM3* giving rise to a dystroglycanopathy-like phenotype (Lefeber et al., 2009).

Protein (*encoding gene*) *	**Gene ID ****	**location †**	**Molecular function ††**	**Subcellular localisation ‡**	**Initial phenotypic description ‡‡**	**OMIM reference ±**
Fukutin (*FKTN*)	607440	9q31-q33	Molecular function unclassified	Golgi apparatus	Fukuyama congenital muscular dystrophy (FCMD) (Kobayashi et al., 1998)	OMIM_253800
Fukutin related protein (*FKRP*)	606596	19q13.3	Molecular function unclassified	Golgi apparatus ≠	Congenital muscular dystrophy 1C (MDC1C) (Brockington et al., 2001a)	OMIM_606612
Protein-*O*-linked mannose beta 1,2-*N*-acetylglucosaminyltransferase (*POMGNT1*)	606822	1p34.1	Glycosyltransferase	Golgi apparatus	Muscle eye brain disease (MEB) (Yoshida et al., 2001)	OMIM_253280
Protein-*O*-mannosyltransferase 1 (*POMT1*)	607423	9q34.1	Glycosyltransferase	Endoplasmic reticulum	Walker-Warburg syndrome (WWS) (Beltran-Valero de Bernabe et al., 2002)	OMIM_236670
Like-glycosyltransferase (*LARGE*)	603590	22q12.3	Glycosyltransferase	Golgi apparatus	Congenital muscular dystrophy 1D (MDC1D) (Longman et al., 2003)	OMIM_608840
Protein-*O*-mannosyltransferase 2 (*POMT2*)	607439	14q24	Glycosyltransferase	Endoplasmic reticulum	Walker-Warburg syndrome (WWS) (van Reeuwijk et al., 2005b)	OMIM_236670
Dolichyl-phosphate mannosyltransferase polypeptide 3 (*DPM3*)	605951	1q22	Molecular function unclassified	Endoplasmic reticulum	Mild muscular dystrophy with dilated cardiomyopathy (CDG type I) (Lefeber et al., 2009)	OMIM_612937 ±±

Table 2. An overview of causative dystroglycanopathy genes.

* Gene symbols and names as per HUGO nomenclature (www.genenames.org/). ** Entrez Gene Identifier from the NCBI database (http://www.ncbi.nlm.nih.gov/). † Denotes chromosomal location. †† Molecular function as classified by the PANTHER (Protein ANalysis THrough Evolutionary Relationships) Classification System (http://www.pantherdb.org/). ‡ Subcellular localisation as annotated via the Universal Protein Resource Knowledge Base (UniProtKB) (www.uniprot.org). ≠ The subcellular localisation of *FKRP* is controversial with reports using tagged recombinant proteins differing from those using antibodies to endogenous *FKRP* protein (Beedle et al., 2007; Esapa et al., 2002; Keramaris-Vrantsis et al., 2007; Matsumoto et al., 2004; Torelli et al., 2005). ‡‡ Initial phenotype associated with mutations in the respective gene. ± Online Mendelian Inheritance in Man reference (http://www.ncbi.nlm.nih.gov/OMIM). ±± To date mutations in *DPM3* have only been detected in a single patient.

Fukutin; FKTN

Fukuyama congenital muscular dystrophy (FCMD) [OMIM 253800] was described within the Japanese population where it is the second most common form of muscular dystrophy after Duchenne muscular dystrophy (Kobayashi et al., 1998). The high incidence of FCMD in Japan is related to a founder mutation in the gene *Fukutin (FKTN)* occurring over 2000 years ago (Colombo et al., 2000). A 3 kb retrotransposon is present in the 3' untranslated region and is present in the homozygous state in approximately 90% of all Japanese FCMD patients (Kobayashi et al., 1998). With a carrier frequency of this mutation of 1 in 188, FCMD is the most common autosomal recessive disease in Japan (Watanabe et al., 2005). The 3 kb insertion is thought to render the transcript unstable and globally down regulate the *FKTN* transcript. This mutation was the first report of a human disease caused by an ancient retrotransposal integration (Kobayashi et al., 1998). Dystroglycan glycosylation was subsequently shown to be perturbed in FCMD (Hayashi et al., 2001).

The *FKTN* gene encodes a 461-amino acid protein showing similarities to a family of proteins involved in modifying cell surface molecules such as glycoproteins and glycolipids (Aravind and Koonin, 1999). The protein has a putative glycosyltransferase domain (DxD) yet despite this, enzymatic activity is yet to be demonstrated and the function of fukutin remains largely unknown (Breton and Imberty, 1999).

Knockout mice generated for *Fktn* are embryonically lethal (Kurahashi et al., 2005). To overcome the embryonic lethality of these mice, chimeric knockout mice were generated. Mice composed of less than 50% *Fktn* null cells demonstrate compromised survival, typical muscular dystrophy and associated brain and ocular abnormalities (Takeda et al., 2003).

Fukutin related protein; *FKRP*

Patients with a severe form of congenital muscular dystrophy were reported to harbour mutations in a homologue of *FKTN*; *Fukutin Related Protein*; *FKRP* (Brockington et al., 2001a) (referred to as MDC1C [OMIM 606612]. These reports were immediately followed by the identification of mutations in patients with a mild form of limb girdle

muscular dystrophy; LGMD2I [OMIM 607155) (Brockington et al., 2001a; Brockington et al., 2001b). The incidence of LGMD2I is particularly high in northern European Caucasian populations due to the prevalence of a single mutation: c.826C>A; Leu276Ile. The occurrence of this mutation on a common core haplotype suggests that Leu276Ile is a founder mutation that is dispersed among populations of European origin (Frosk et al., 2005).

FKRP encodes a 495 amino acid protein predicted to contain a hydrophobic transmembrane spanning region followed by a stem region and a putative catalytic domain. Despite the presence of a DxD domain no transferase activity has been identified (Brockington et al., 2001a). The downregulation of *FKRP* in zebrafish embryos causes alterations in somatic structure and muscle fibre organisation as well as defects in developing neuronal structures and eye morphology (Thornhill et al., 2008). An *FKRP* murine knockdown model exists where the inclusion of a *Neo* cassette causes a reduction in mRNA causing mild muscular involvement yet severe neuronal abnormalities and mice die soon after birth (Ackroyd et al., 2009).

Protein-O-linked mannose beta 1,2-N-acetylglucosaminyltransferase; POMGNT1

Muscle eye brain disease [OMIM 253280] is particularly prevalent in the Finnish population. Linkage analysis revealed a founder splice site mutation in Protein-*O*-linked mannose beta 1,2-*N*-acetylglucosaminyltransferase (*POMGNT1*) (Diesen et al., 2004). This type II membrane protein, similar to other Golgi glycosyltransferases, catalyses the addition of an *N*-acetylglucosamine (GlcNAc) residue through Beta1,2 linkage to the mannose group using uridine 5'-diphosphate (UDP)-GlcNAc as a donor substrate. *POMGNT1* encodes a 660 amino acid protein containing an N-terminal cytoplasmic tail, a transmembrane domain, a stem domain and a C-terminal catalytic domain (Yoshida et al., 2001; Zhang et al., 2002). *POMGNT1* has been shown to directly interact with *FKTN* in the Golgi apparatus. The formation of this complex is thought to modulate *POMGNT1* enzymatic activity (Xiong et al., 2006). The abolition of *Pomgnt1* expression in mice causes multiple developmental defects in muscle, eye, and brain, similar to the phenotypes observed in human MEB (Liu et al., 2006).

Protein-O-mannosyltransferase 1; POMT1

The gene encoding glycosyltransferase Protein-*O*-mannosyltransferase 1 (*POMT1*) was cloned in 1999 and was the first *O*-mannosyl-transferase detected in humans. It was suggested as a promising candidate for dystroglycanopathy phenotypes as it was predicted to function as *O*-mannosyl glycan GlcNAc transferase and catalyse the first step in the assembly of the *O*-mannose-linked glycan moiety of *α*-dystroglycan (Jurado et al., 1999). Mutations were subsequently identified in patients with WWS; the most severe end of the clinical spectrum of dystroglycanopathies [OMIM 236670] (Beltran-Valero de Bernabe et al., 2002). *POMT1* encodes a 747 amino acid protein that is localised to the Golgi apparatus. RNA interference (RNAi) knockdown experiments in *Drosophila melanogaster* caused a rotation of the abdomen by 30-60° demonstrating its requirement for normal muscle development in the fly (Ichimiya et al., 2004). As with *Fktn* null mice, *Pomt1* ablation is early embryonically lethal (Willer et al., 2004).

Like-glycosyltransferase; LARGE

The transgenic enervated (*enr*) mouse and the myodystrophy mouse ($Large^{myd}$) present with pathological features similar to congenital muscular dystrophy patients and were later shown to have hypoglycosylated α-dystroglycan (Grewal et al., 2001; Holzfeind et al., 2002; Levedakou et al., 2005). Both mice harbour part gene deletions in the gene *Large*, thus named due to its extensive genomic span. Candidate gene analysis of the human ortholog in a cohort of dystroglycanopathy patients revealed a mutation in a congenial muscular dystrophy patient with mental retardation; MDC1D [OMIM 608840] (Longman et al., 2003).

LARGE was originally named due to its extensive genomic coverage of approximately 650 kb despite a coding region of only 2268 base pairs (bp). The 756 amino acid protein contains an N-terminal transmembrane domain, a coiled-coil domain and three conserved DxD motifs located in two predicted catalytic domains suggesting the possibility of a bifunctional enzyme (Brockington et al., 2005). The exact activity of *LARGE* is unknown and enzymes related to *LARGE* catalyse modifications unrelated to *O*-mannosylation (Patnaik and Stanley, 2005). The protein resides in the Golgi apparatus and appears to recognise an aminoterminal region of *α*-dystroglycan defining an enzyme-substrate recognition motif necessary to initiate functional glycosylation.

Molecular recognition of *α*-dystroglycan by *LARGE* is required for the biosynthesis of a functional dystroglycan and to prevent muscle degeneration (Kanagawa et al., 2004). A recent report from Yoshida-Moriguchi *et al.* described the treatment of wheat germ agglutinin enriched glycoproteins from skeletal muscle with cold aqueous hydrofluoric acid which specifically cleaves phosphodiester linkages. This led to a reduction in the molecular weight of α-dystroglycan along with a loss of IIH6 immunoreactivity and laminin binding function (Yoshida-Moriguchi et al., 2010). Using patient cell lines, the authors speculate that *LARGE* participates in post-phosphoryl modification of the *O*-mannosyl glycan.

Protein-O-mannosyltransferase 2; POMT2

Protein-*O*-mannosyltransferase (*POMT2*) was the second eukaryotic *O*-mannosyltransferase gene to be described showing high identity to its paralog *POMT1* (Willer et al., 2002). Candidate gene screening in combination with homozygosity mapping detected mutations in *POMT2* in a cohort of WWS patients [OMIM 236670] (van Reeuwijk et al., 2005b). The coexpression of *POMT1* and *POMT2* is necessary for enzymatic activity (Manya et al., 2004). *POMT1* and *POMT2* reside in the ER and transfer a mannosyl residue from dolichol-phosphate-mannose (Dol-P-Man) to serine or threonine residues (Manya et al., 2004).

A clockwise helical rotation of the body is caused by mutation of the *Pomt* homologs in *Drosophila melanogaster*. The *rotated abdomen* (*rt*) and *twisted* (*tw*) phenotypes are thought to be due to insufficient torque in muscle architecture needed during segmental development (Lyalin et al., 2006; Martin-Blanco and Garcia-Bellido, 1996).

Dolichyl-phosphate mannosyltransferase polypeptide 3; DPM3

In July 2009 Lefber *et al.* reported a patient presenting with mild muscular dystrophy, dilated cardiomyopathy and stroke like episodes with no associated brain or eye involvement with an intriguing molecular defect [OMIM 612937]. A reduction in immunoreactivity to IIH6 was seen on immunohistochemistry from a skeletal muscle biopsy. Due to the patient's unusual clinical presentation transferrin isoelectric focusing of the patient's blood serum was performed. The assay revealed an abnormal transferrin

profile suggesting a CDG type I pattern consistent with a disorder in *N*-glycosylation and a defect in the ER. Further to this, analysis of the patient's fibroblasts revealed a reduction in Dol-P-Man synthase activity (Lefeber et al., 2009).

Dol-P-Man is the glycol donor for all mannosylation reactions taking place on the luminal side of the ER. The donation of mannose is required for four different pathways of glycosylation; *N*-glycosylation, *C*-mannosylation, *O*-mannosylation and GPI-anchor formation. In higher eukaryotes the Dol-P-Man synthase complex is composed of three subunits. The catalytic subunit *DPM1* is located in the cytoplasm and transfers mannose from the nucleotide sugar GDP-Mannose to membrane embedded dolichol-phosphate resulting in the formation of Dol-P-Man. *DPM3* anchors this catalytic subunit to the ER via its coiled-coil domain. *DPM2* is located in the ER membrane and is required for stabilisation of the complex. Mutation analysis performed on the DPM subunits identified a homozygous missense mutation in *DMP3*. This sequence alteration was confirmed as pathogenic by co-transfection experiments in Chinese hamster ovary cells showing a reduced binding capacity of *DMP3* that tethers catalytic *DPM1* to the ER membrane. Although the mild defect in Dol-P-Man would be expected to affect all four glycosylation pathways, *O*-mannosylation was found to be more sensitive to this reduction and considered to be the cause of clinical features (Lefeber et al., 2009).

Prior to this report CDGs and dystroglycanopathies had been regarded as two separate groups of glycosylation disorders. Although children with CDGs are profoundly hypotonic, skeletal muscle is not a primary target. This patient has a clinical presentation of dystroglycanopathy with hypoglycosylation of α-dystroglycan, yet the biochemical features of a CDG, therefore bridging the gap between these two glycosylation disorders.

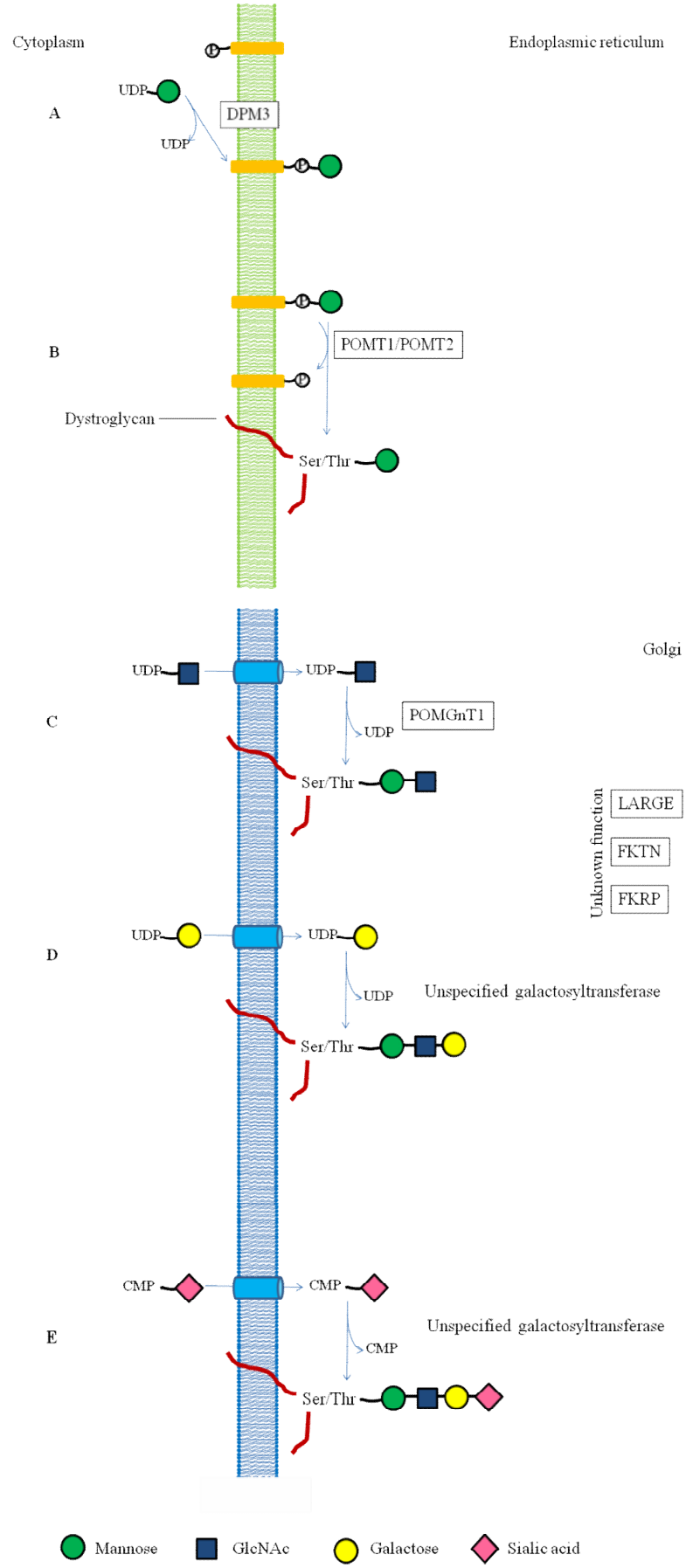

Figure 7. *O*-mannose biosynthetic pathway.

A diagrammatic representation of *O*-mannose linked glycan assembly beginning in the ER and completed in the Golgi apparatus. The Dol-P-Man synthase complex (comprising of *DMP1*, *DMP2* and *DMP3*) transfers mannose from GDP-mannose to dolichol-phosphate resulting in dolichol-phosphate mannose (A). The heterodimeric enzyme protein-*O*-mannosyltransferase (*POMT1*/*POMT2*) then adds mannose in α1-*O* linkage to Serine (Ser) / Threonine (Thr) residues located in the central portion of α-dystroglycan's mucin domain (B). In the Golgi apparatus (C-E) a pathway specific protein *O*-mannose β1,2GlcNAc transferase (*POMGNT1*) uses UDP-GlcNAc to add a β1,2GlcNAc residue to the mannose creating a disaccharide (C). The *O*-mannose structure is completed by the addition of a β1,4-galactose and 2,3-sialic acid residues added by unspecified transferases (D-E). The functions of *LARGE*, *FKRP* and *FKTN* remain uncharacterised. Those enzymes depicted in boxes are known to cause a dystroglycanopathy phenotype when mutated. Diagram based on those from Freeze *et al.* (Freeze, 2006; Varki, 2008).

1.3.2 Mechanisms of Pathogenesis

To further understand the role of dystroglycan a variety of knockout and conditional knockout mouse models have been developed. Global abolition of *Dag1* expression results in embryonic lethality around day 5.5 due to structural and functional perturbations of the Reichert's membrane; a thick, early forming basement membrane that surrounds the rodent embryo separating it from the maternal circulation (Williamson et al., 1997). However, another basement membrane forming between the visceral endoderm and ectoderm appears to persist in *Dag1* null embryos arguing against a general role for dystroglycan in basement membrane assembly (Henry et al., 1998). In contrast, the abolition of dystroglycan expression in lower species such as zebrafish does not impair embryonic development although adult fish display a severe form of dystrophy (Parsons et al., 2002).

Work is underway to better understand the underlying mechanisms and functional consequences underlying dystroglycanopathy phenotypes specifically. A number of both naturally occurring and targeted animal models defective in genes implicated in the pathway of glycosylation have also been studied. As with *Dag1* null mice, *Pomt1* ablation is early embryonically lethal, both strains of mice fail to synthesise the Reichert's membrane, a basement membrane that surrounds the blastocyst (Willer et al., 2004).

Chimeric dystroglycan knockout mice developed a form of muscular dystrophy (Cote et al., 1999). Conditional knockout mice with the specific ablation of dystroglycan in skeletal muscle resulted in the loss of the dystrophin glycoprotein complex and demonstrated that dystroglycan has a central role in maintenance of muscle fibre integrity (Cohn et al., 2002).

<u>Skeletal muscle dystrophy</u>

The glycosylated moiety of α-dystroglycan is crucial for binding with extracellular matrix ligands in skeletal muscle which connect the sarcolemma with the extracellular matrix. Abnormal dystroglycan-ligand interactions underlie a major pathological

hallmark of disease (Figure 8). A secondary reduction in laminin was first described in FCMD patients (Hayashi et al., 1993). Alpha-dystroglycan glycosylation is required for the clustering of agrin and laminin 1 (Campanelli et al., 1994; Cohen et al., 1997).

The monoclonal antibody IH6 is known to bind to a carbohydrate moiety that mediates and functionally blocks the interaction between α-dystroglycan and laminin α-2 (Brown et al., 1999). Antibody blocking studies using the monoclonal antibody IIH6 in primary muscle cultures results in myotubes that are decreased in size, show myofibril disorganisation and a loss of spontaneous contractile activity compared to controls (Brown et al., 1999).

The perturbation of basement membranes in muscle has been described in both patients with WWS and FCMD and is thought to represent an important pathogenic event. Electron microscopy of skeletal muscle fibres in all patients studied with FCMD had a thin and disrupted appearance of the basement membrane (Ishii et al., 1997). Studies in a patient with WWS caused by mutations in *POMT1* showed alterations in non necrotic fibres in two distinct subcellular compartments; the basal lamina and nucleus (Sabatelli et al., 2003).

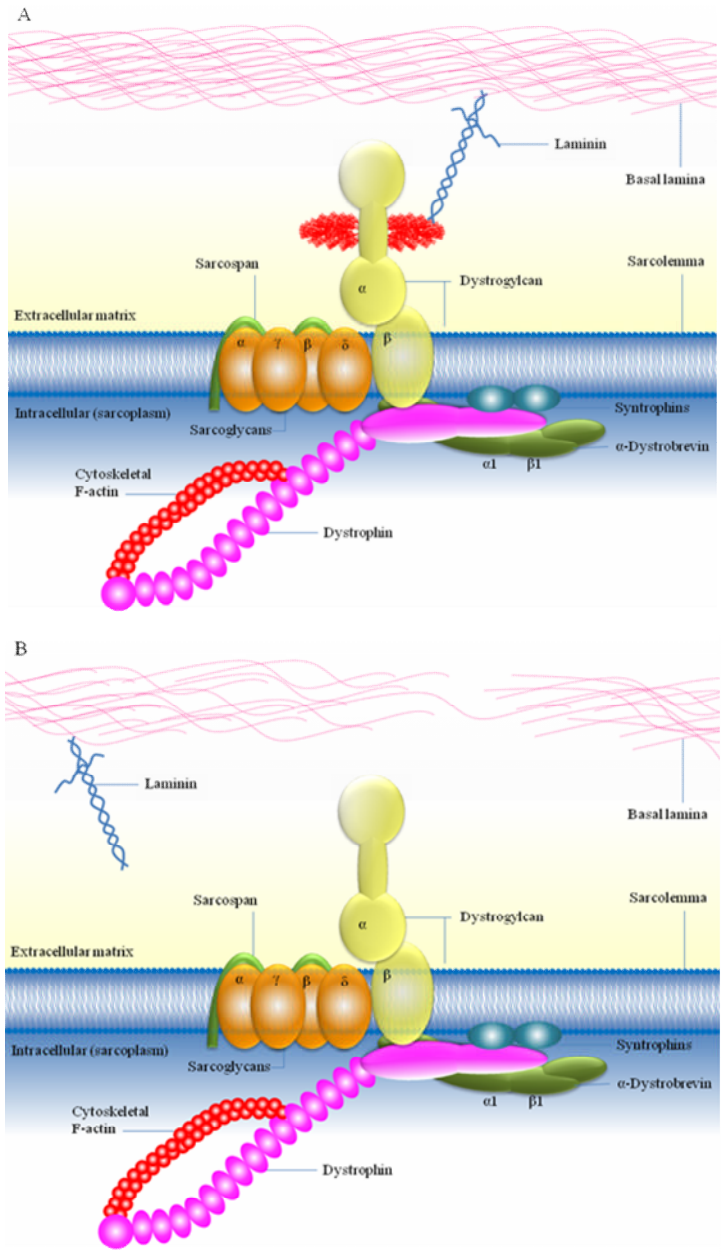

Figure 8. Hypoglycosylation of dystroglycan within the DGC.

The basement membrane of skeletal muscle fibres consists of layers of extracellular matrix material. The inner layer, referred to as the basal lamina, is directly linked to the plasma membrane (sarcolemma). The glycosylated moiety of α-dystroglycan is crucial for binding with extracellular matrix ligands such as laminin (A). Abnormal ligand-matrix interactions and altered basal lamina composition and organisation are thought to underlie the pathological mechanisms in skeletal muscle from dystroglycanopathy patients (B). Figure based on that from Barresi *et al.* (Barresi et al., 2004).

Aberrant neuronal migration during cortical development

Brain involvement is a frequent yet not constant feature in patients with a dystroglycanopathy. Patients vary from normal cognitive development and normal brain magnetic resonance imaging to severe structural brain abnormalities in patients with associated learning difficulties. A hierarchical pattern of changes is observed from isolated cerebellar cysts, to structural involvement affecting brainstems and pons, polymicrogyria and cobblestone lissencephalic changes, ventricular dilation and white matter abnormalities (Clement et al., 2008a).

Disruptions in neuronal migration and development of the cerebral wall are observed at the most severe end of the clinical spectrum of dystroglycanopathy patients. Lissencephaly describes the smooth appearance of the cortex and is caused by defective neuronal migration during development of the cerebral cortex. Whereas mutations in regulators of the microtubule cytoskeleton have been identified in classic lissencephaly, mutations in the basal lamina of the central nervous system underlie cobblestone lissencephaly (also referred to as type II lissencephaly) (Olson and Walsh, 2002).

The human cerebral cortex is a highly folded sheet of six neuronal layers each with characteristic histological and functional properties. These layers are established during embryonic development by the radial migration of postmitotic neurons from the middle of the brain to the developing cortical layers near the surface. Neurons are generated in specialised proliferative zones along ventricular cavities called ventricular zones. Neurons migrate along specialised elongated cells known as radial glial cells. These span the entire cortical wall from the ventricular zone and are attached to the basal lamina via specialised radial end feet. Neurons then migrate along radial glial cells from the proliferative zone, through the fibre rich intermediate zone and into the developing cortical plate immediately beneath the marginal zone. The neuronal layers are laid in an inside out pattern with early generated neurons occupying deep layers and those later migrating cells located in superficial layers (Figure 9) (Olson and Walsh, 2002).

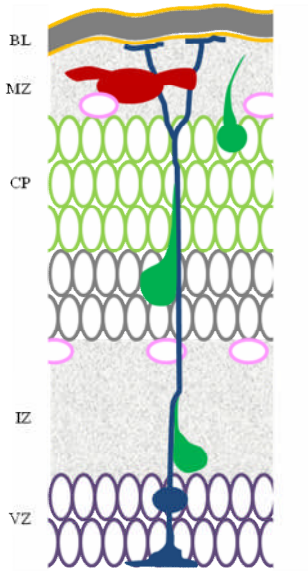

Figure 9. Neuronal migration during cortical development.

Neurons (solid green cells) migrate on specialised elongated cells; radial glial cells (solid blue cell) which span the whole cortical wall from the ventricular zone (VZ) to the basal lamina (BL) of the pial surface, where the specialised glial endfeet terminate. Neurons migrate from the proliferative ventricular zone through the fibre-rich intermediate zone (IZ) into the developing cortical plate (CP). Neurons arrest migration at the top of the cortical plate (CP), immediately beneath the marginal zone (MZ). Figure based on that from Olson *et al.* (Olson and Walsh, 2002).

The correct formation of the basement membrane is essential for neuronal migration. Disordered cortical layering and clusters of neurons and glial beyond the pial basement membrane have been identified in patients with FCMD, MEB and WWS. The migration of neurons or neuronal precursors, out of the developing brain through breaches in the superficial neural basal lamina, produces bumpy neuronal cobblestones (ectopia) (Figure 10). Glycosylated α-dystroglycan is highly expressed in both the pial membranes and neurons themselves although its exact role remains unknown (Saito et al., 2006).

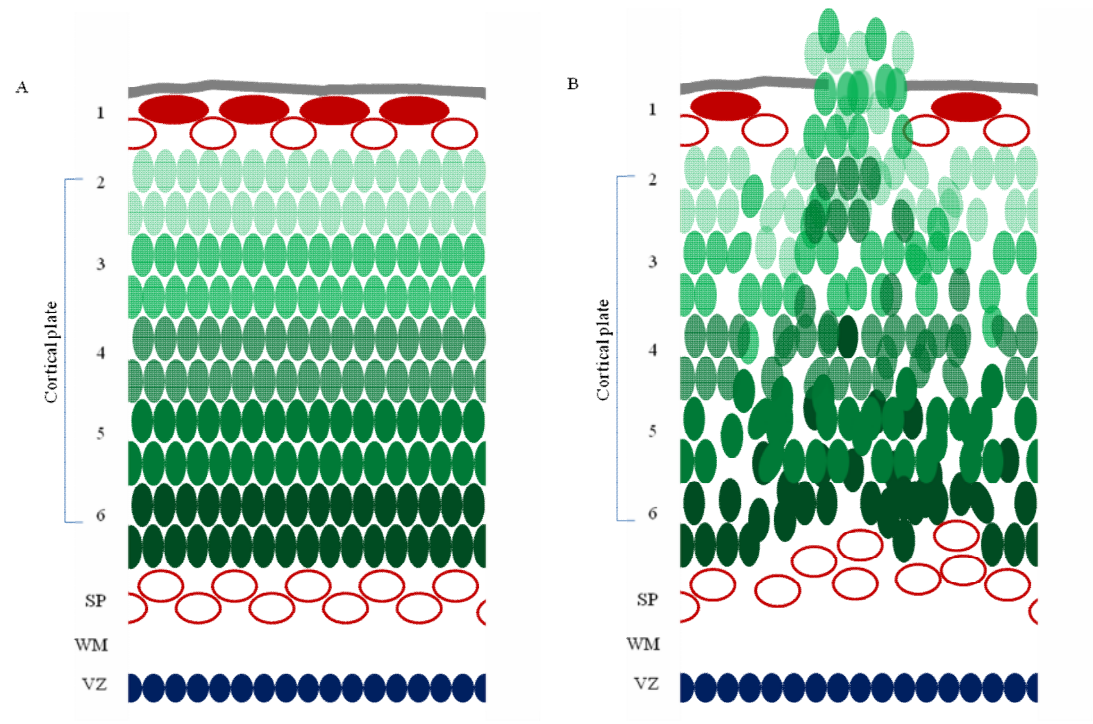

Figure 10. Neuronal migration defects and cobblestone lissencephaly.

A) The normal mammalian neocortex is comprised of six cellular layers overlying a band of white matter (WM). The cortical plate (green cells, layers 2-6) is sandwiched between layer 1 (upper red cells) and the subplate (SP; lower red cells). B) Description of cobblestone lissencephaly showing characteristic features. The basal lamina is fragmented and neurons migrate through the breach to form ectopic bumps on the surface of the brain. Figure based on that from Olson *et al.* (Olson and Walsh, 2002).

Whereas the neocortex has deep grooves (sulci) and wrinkles (gyri) in primates, rodents have a smooth cortical appearance therefore cannot display lissencephaly as such. Mutant mice with cortical migration defects do show deficiencies in basal lamina integrity as well as superficial bumps of neurons analogous to the cobblestone cortex observed in humans. Both the *Fkrp-Neo*^{Try307Asn} knockdown and *Pomgnt1* knockout mice brains display pial basement membrane breaches during rapid cerebral cortical expansion at embryonic day 13.5 with radial end feet growing out of the neural boundary. Basement membrane breaches are also found in chimeric mice of *Fktn* KO and the *Large*^{myd} mice. Brain specific ablation of mouse dystroglycan causes structural defects with discontinuities in the pial surface basal lamina (glia limitans) (Moore et al., 2002).

Ocular abnormalities

Ocular abnormalities can be a frequent feature in patients with a dystroglycanopathy. Eye abnormalities including congenital cataracts and microphthalmia are common findings in patients with WWS. Congenital glaucoma, progressive myopathy, retinal atrophy and juvenile cataracts are observed in patients with MEB disease. Little is known of the pathogenic mechanisms operating in these patients.

Ocular abnormalities are observed in mouse models of dystroglycanopathies. The *Fkrp-Neo*^{Try307Asn}, *Fktn* chimera, *Pomgnt1* null and *Large*^{myd} mice all show eye involvement. The inner limiting membrane is a basement membrane that separates the retina from the vitreous body. The mechanical strength of the inner limiting membrane is known to be essential for normal eye development. *Fkrp-Neo*^{Try307Asn} newborn mice show a marked disorganisation of the inner limiting membrane and an invasion of cells into the vitreous body. Ectopic nuclei were present outside the inner limiting vitreous body (Ackroyd et al., 2009). A disorganisation of the retinal lamina, retinal detachment and lens opacification are present in *Fktn* chimeric mice (Takeda et al., 2003). Thinner inner and outer neuroblastic layers are also present in *Pomgnt1* null mice and *Large*^{myd} mice (Holzfeind et al., 2002; Liu et al., 2006).

1.4 PERSPECTIVES

Recent years have seen an explosion in our understanding of aberrant glycosylation in muscular dystrophies. Emphasis has moved away from identifying structural proteins of skeletal muscle towards the discovery of enzymes and proteins involved in modifying these components. Since its original description in 2002, hypoglycosylation of α-dystroglycan has been identified in several forms of muscular dystrophy. Defects have been identified in putative and demonstrated glycosyltransferases and accessory glycosyltransferase proteins implicated in the formation of characterised and uncharacterised glycans. The correct glycosylation of α-dystroglycan seems to be crucial for muscle function and in more severe clinical presentations, brain and eye formation. The molecular characterisation of many of these patients remains to be performed and with the recent promise of therapeutic strategies for these disorders, these fundamental issues are ever more pressing.

CHAPTER 2: PATIENTS AND METHODS

2 PATIENTS AND METHODS

2.1 PATIENTS

2.1.1 Patient cohorts

Three different patient cohorts (A, B and C) were studied, the inclusion criteria for each is detailed below. Research pertaining to patient cohorts A, B and C is detailed in chapters 3, 4 and 5 respectively. Clinical data was analysed by Professor F Muntoni and Dr E Clement. Muscle pathology was evaluated by Professor C Sewry, Dr L Feng and Dr C Jimenez-Mallebrera. This work was performed via the Dubowitz Neuromuscular Centre which provides a national specialist diagnostic and assessment service for Congenital Muscular Dystrophies and Congenital Myopathies (National Commissioning Group service). This study was approved by Hammersmith Hospital Ethics Committee REC reference number: 2000/5802.

Patient cohort A

Patient cohort A consisted of 92 unrelated individuals (Patients A1-A92). This included a large group of patients from Australia (27 patients) and Turkey (16 patients). The majority of the remaining patients were recruited via the Hammersmith Hospital National Commissioning Group service and included DNA from individuals referred from across the UK and Europe with a few samples from further afield. Mutations in *FKRP* had previously been excluded in all cases (Brockington et al., 2001a).

The inclusion criterion was specified as hypoglycosylation of α-dystroglycan at the sarcolemma by immunolabeling of skeletal muscle sections (Brown et al., 2004; Dubowitz and Sewry, 2007). Eighty patients met this criterion whilst in the remaining 12 cases there was no muscle available to perform α-dystroglycan studies. This later group of patients were included due to their clinical phenotype being highly suggestive of a dystroglycanopathy and consisted of children with CMD, elevated serum creatine kinase and brain MRI evocative of a cobblestone lissencephaly. All the patients who had had a muscle biopsy were studied by standard immunocytochemical and/or Western

blotting analysis in order to rule out dystrophinopathy, LGMDs such as sarcoglycanopathies, calpainopathy and dysferlinopathy, merosin deficient CMD and collagen VI deficiency (Dubowitz and Sewry, 2007). Clinical data was collated and patients were divided into phenotypic categories.

Patient cohort B

Patient cohort B consisted of 40 unrelated individuals (Patients B1-B40). The majority of the patients were recruited via the Dubowitz Neuromuscular Centre. In addition to meeting the inclusion criteria stipulated for cohort A, mutations in *POMT1*, *POMT2*, *POMGNT1*, *LARGE*, *FKTN* and *FKRP* had previously been excluded in each patient by uni-directional sequencing. In eleven of the forty patients, no muscle was available for immunocytochemical study.

Patient cohort C

A consanguineous family was studied for linkage analysis and is referred to throughout this thesis as pedigree 1. The proband (patient C1-1) had previously been included in cohort A and therefore screened for mutations in *POMT1*, *POMT2*, *POMGNT1*, *LARGE*, *FKTN* and *FKRP*.

Pedigree 1 has previously been described in Brockington *et al*. and Muntoni *et al*. The parents of the four affected children are first cousins of United Arab origin (Brockington et al., 2000; Muntoni et al., 1998). Early motor milestones were delayed in the four affected children; they were able to walk but could not run, and they rose from the floor with the use of a Gower manoeuvre. Facial weakness, generalized muscle hypertrophy, and wasting of the sternocleidomastoids and pectoralis muscle were consistent features. For over nine years, there was no significant progression of the muscle weakness; however, the two oldest girls died of respiratory complications, one at 4 years of age and the other at 7 years of age. The two remaining children, aged 8 and 5 years old, were found to be hypoventilating at night. They have been ventilated by use of nocturnal ventilation via a biphasic positive airway pressure machine with excellent results. Intellect was normal. Investigations revealed grossly elevated creatine kinase levels in all the children (range 2,270–7,650 IU/litre; normal values <190 IU/litre).

Ethnically matched control cohort

Control samples were from a cohort of parental bloods of White European ethnicity following ethical approval by the Hammersmith and Queen Charlotte's and Chelsea Trust Research Ethics Committee (2001/6029).

2.2 METHODS

Unless otherwise stated, all water was purified using an Elix system (Millipore) combining reverse osmosis and electro-deionisation.

2.2.1 Genomic DNA Manipulation

Genomic DNA extraction

Unless otherwise stated genomic DNA was extracted in the referring centre's laboratory using standard protocols. DNA was stored at 4°C for short-term storage or -20°C for long-term storage.

DNA from lymphoblastoid cells (Patients C1-1, Table 4) was extracted using the DNeasy Blood and Tissue Kit (Qiagen) following the manufacturer's protocol. The DNeasy procedure combines the selective binding properties of a silica-based membrane with centrifugation. DNA adsorbs to the DNeasy membrane in the presence of high concentrations of chaotropic salt, which removes hydrated molecules in solution. Cells are first lysed using proteinase K. Lysate is added to the spin column and DNA is selectively bound to the DNeasy membrane during centrifugation. Contaminants are removed during a series of wash steps and the DNA is eluted in 200 µl of H_20.

Whole genome amplification

The availability of patient samples is frequently a limitation in downstream analysis. In order to preserve precious genetic material, methods of whole genome amplification

have been developed. This allows the amplification of the entire genome from limited initial quantities of high molecular weight DNA ensuring those samples are not exhausted during mutation screening. Recently a technique known as Multiple Displacement Amplification has been developed and involves the binding of random hexamers to denatured DNA. The enzyme φ29 DNA polymerase carries out strand displacement synthesis under isothermic conditions. Subsequent additional priming events occur on displaced strands leading to a network of hyper branched DNA structures (Figure 11). The high fidelity φ29 enzyme does not disassociate from the genomic DNA template facilitating the generation of fragments of up to 100 kb (average product length being more than 10 kb) (Dean et al., 2002). The enzyme's 3' to 5' exonuclease proofreading ability means that error rates are 100 times lower than Taq polymerase therefore maintaining high fidelity during replication (Hosono et al., 2003). The enzyme's ability to resolve secondary structures reduces amplification bias to less than 3 fold in contrast to 4-6 orders of magnitude for polymerase chain reaction (PCR) based whole genome amplification methods (Dean et al., 2002).

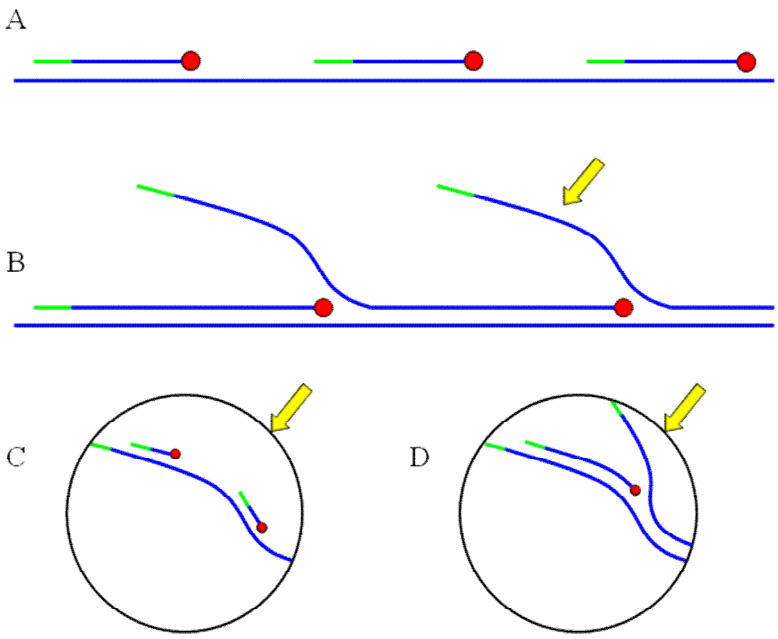

Figure 11. Sequential representation of the branched structures created during multiple displacement amplification.

A) Random hexamers (green) are hybridised to linear DNA (blue) and extension is carried out by φ29 DNA polymerase (red). B) As the front of the extending complementary strand of DNA encounters a double-stranded section of DNA, the advancing new strand displaces the old one from the template. C) and D) hexamers subsequently hybridise with these displaced strands creating an extensive series of branched structures.

Multiple displacement amplification reactions were performed on purified genomic DNA using the Repli-g UltraFast Mini kit (Qiagen) and the Repli-g Midi kit (Qiagen) following the manufacturer's recommended protocol. In brief, the sample material is lysed and the DNA is denatured by adding a denaturation buffer. After denaturation has been stopped by the addition of a neutralisation buffer, a master mix, containing a reaction buffer and REPLI-g UltraFast DNA Polymerase is added. The isothermal reaction proceeds for 1.5 hours at 30°C. Amplified DNA was stored at 4°C for short-term storage or -20°C for long-term storage. A 1:12.5 dilution was used for downstream PCR amplification.

Whole genome amplification from the remainder of patient C1-1's skeletal muscle biopsy was carried out using the REPLI-g Midi kit according to a user-developed protocol available from Qiagen. This protocol had been optimised for WGA from flash-frozen tissue sections as follows; the remainder of the skeletal muscle biopsy from patient C1-1 was placed in a microcentrifuge containing 10 µl of Tris(hydroxymethyl)aminomethane (Tris)-acetate buffer and incubated at room temperature (15-25°C) for 10 minutes with occasional vortexing. 10 µl of buffer D2 (containing 1 M DTT and Reconstituted Buffer DLB) was added, vortexed briefly and placed on ice for 30 minutes. 10 µl of Stop Solution was then added to the lysed tissue and mixed briefly by vortexing. The tissue debris and lysed tissue cells were then separated by pulse centrifugation. 40 µl of master mix containing REPLI-g Midi Reaction Buffer, REPLI-g Midi DNA Polymerase and Nuclease-free H_20 was added to 10 µl of lysed tissue cells and mixed by vortexing and brief centrifugation. The mixture was incubated at 30°C for 16 hours followed by heat inactivation at 65°C for 3 minutes.

Purification of multiple displacement amplification

The QIAamp DNA Micro Kit was used to clean up multiple displacement amplified samples prior to submission for whole genome single nucleotide polymorphism (SNP) analysis following the manufacturer's recommended protocol. This protocol removes enzymes, unused primers and nucleotides and results in a pure DNA in aqueous solution.

A total of 10 µl of amplified product was bound to a silica membrane using the Buffers AW1 and AW2. Contaminants are removed with a single wash step with Buffer AW2. DNA is eluted from the column in a volume of 20 µl of Buffer AE.

Genomic DNA quantification and concentration

Genomic DNA concentration was determined using the NanoDrop ND-1000 Spectrophotometer according to manufacturer's instructions. Genomic DNA samples were concentrated to >50 ng/µl prior to submission to the UCL Genomics facility using the RC10.10 vacuum centrifuge (Jouan) at 50°C for approximately 20 minutes.

DNA agarose gel electrophoresis

Agarose gels of 1-2% (w/v) in 1 x Tris-acetate-EDTA (TAE) buffer were routinely used to analyse PCR products, whole genome amplification products and genomic DNA quality. Gels were prepared by heating the agarose-TAE suspension in a microwave until dissolved. After the solution had cooled, ethidium bromide was added to a concentration of 0.1 mg/ml and the solution was poured into an appropriate gel tray. Once set, the gel was submerged in 1 x TAE running buffer. One volume of gel loading buffer was added to 5 volumes of sample and loaded into the wells. Electrophoresis was carried out at 70 volts (V), until DNA fragments were resolved. DNA was visualised under ultra-violet light using the ImageMaster VDS (Pharmacia Biotech). The size of DNA fragments was estimated by comparison to DNA markers run simultaneously with the samples. One hundred bps and 1 kilo base (kb) ladders (Invitrogen) were routinely used.

Single nucleotide polymorphism array

Genotypes from patient cohort C were generated with the use of SNP genotyping platforms (GeneChip Human Mapping 500K Nsp array, Affymetrix) by the UCL Genomics facility (www.genomics.ucl.ac.uk/).

Genotypes were examined by Professor R Kleta and Dr H Stanescu in the UCL School of Life and Medical Sciences. Multipoint linkage analysis and haplotype reconstruction

was performed with Simwalk (version 2.91) and Allegro (version 2.0) for an autosomal recessive model with complete penetrance. The data was formatted with Mega2 (version 4.0) through ALOHOMORA (version 0.30, Win32). Mendelian inconsistencies were checked with the use of PedCheck (version 1.1) and Graphical Representation of Relationship Errors. Unlikely genotypes were filtered with the use of Merlin (version 1.1, alpha 3). Haplotype output files were visualised with HaploPainter.

2.2.2 RNA Manipulation

RNA extraction

RNA from tissue and cells was extracted using the RNeasy mini kit (Qiagen) following the manufacturer's protocol. The RNeasy procedure combines the selective binding properties of a silica-based membrane with centrifugation. A specialised high-salt buffer system allows up to 100 μg of RNA longer than 200 bases to bind to the RNeasy silica membrane thus providing enrichment for mRNA. Samples are first lysed and homogenized in the presence of a highly denaturing guanidine-thiocyanate-containing buffer which immediately inactivates RNases to ensure purification of intact RNA.

Initially solid tissue samples were disrupted by grinding to a fine powder under liquid nitrogen. The ground sample was then transferred to a liquid nitrogen cooled 1.5 ml tube and 350 μl lysis buffer added. When extracting RNA from pre-cut 10-12 μm muscle sections, 350 μl of Lysis buffer was added directly to the sample without the need for tissue disruption. Extraction of RNA from patient lymphoblastoid cell lines and C2C12 cells was initiated by the addition of 350 μl of lysis buffer and dislodged from the surface of the tissue culture plastic by agitation with a cell scraper. Following the manufacturer's recommended protocol the disrupted cell and tissue lysates were subsequently homogenised by passing through a QIAshredder spin column. Ethanol is subsequently added to the homogenate to provide appropriate binding conditions and transferred to an RNeasy Mini Spin Column. On column digestion of DNA during RNA purification was performed using the RNase-Free DNase Set. Contaminants are washed away and the RNA is eluted in 30 μl of H_20.

RNA quantification

Total RNA concentration was determined using the NanoDrop ND-1000 Spectrophotometer according to manufacturer's instructions.

Synthesis of first-strand complementary DNA

The Superscript III First–Strand Synthesis System for Reverse Transcription PCR (RT-PCR) was used in the synthesis of first-strand complementary DNA (cDNA). RT reactions were performed by initially mixing 1-2 µl of RNA (typically between 150 - 300 ng/µl), 0.5 µg (1 µl) random primer and 1 µl 10 mM deoxyribonucleotide triphosphate (dNTP) mix and nuclease free H_20 to a total of 10 µl, denatured at 65°C for 5 minutes and chilled on ice for 1 minute. The following components were then added; 2 µl of 5 x reaction buffer, 4 µl 25 mM $MgCl_2$, 2 µl 0.1 M Dithiothreitol (DTT), 200 U (1 µl) RNase OUT and 200 U (1 µl) SuperScript III RT enzyme. The reaction was then annealed at 20°C for 20 minutes and cDNA synthesised at 50°C for 50 minutes. The reaction was terminated at 85°C for 5 minutes. 200 U (1 µl) of RNase H was subsequently added and incubated at 37°C for 20 minutes to facilitate the removal of RNA-DNA hybrids. Products were then stored at -20 for future use. cDNA used in Real Time PCR reactions was created using random hexamers (please refer to section 2.2.2).

Relative quantification Real Time PCR

Relative Quantification Real Time PCR was performed in triplicate using the Taqman System (Applied Biosystems). A sample volume of 25 µl in each well was prepared with 12.5 µl of Real Time PCR master mix (2 x) (Applied Biosystems), 11.25 µl of H_20 and cDNA and 1.25 µl of the appropriate probe. cDNA was amplified using the 9600 Emulation mode; reactions were initially heated at 50°C for 2 minutes and 95°C for 10 minutes, followed by 40 cycles of segments of 95°C for 15 seconds and 60°C for 1 minute in a 7500 Applied Biosystems Sequence Detection System. The housekeeping gene *β-actin (Actb)* was used for normalisation. Data acquisition and analysis was performed using the Applied Biosystems 7500 Fast System. Relative Quantification was calculated by the Comparative Ct method. The following TaqMan Gene Expression Assays were used: *mβ3gnt1*, Mm00723578_m1; *mActb*, Mm00607939_s1; mMgat5b,

Mm00556891_m1; *mPomt1*, Mm00520170_m1; *mGyg*, Mm00516516_m1; *mGyltl1b*, Mm00554376_m1; *mWwp1*, Mm01214107_m1.

Expression arrays

RNA was used for expression analysis from patients C1-1 and C1-4 and three unaffected controls (see Table 4). Samples were submitted to the UCL Genomics facility for analysis using the GeneChip(R) Human Gene 1.0 ST Arrays (Affymetrix). Microarray analysis was performed by the UCL Genomics facility with a two-way empirical Bayes ANOVA approach.

2.2.3 Mutation Screening

The mutation screening of *POMT1*, *POMT2*, *POMGNT1*, *LARGE* and *FKTN* was carried out by myself at the DNA laboratory, GSTS Pathology at Guy's Hospital, London prior to the start of this thesis by a combination of uni-directional sequencing and heteroduplex analysis as previously described (Godfrey et al., 2007; Godfrey et al., 2006). Candidate gene mutation screening was performed using a combination of bi-directional and uni-directional sequencing. High throughput automated sequencing was performed at the DNA laboratory, GSTS Pathology at Guy's Hospital, London by myself. Low throughput mutation screening was performed manually at the Dubowitz Neuromuscular Centre, Institute of Child Health.

Mutation screening was typically carried out using uni-directional sequencing of multiple displacement amplified DNA. Bi-directional sequencing was performed on problematic templates. Sequence alterations detected with multiple displacement amplified DNA were confirmed with bi-directional sequencing from unamplified genomic DNA.

Products were detected using an ABI3730xl automated genetic analyser (Applied Biosystems). Analysis of uni-directional and bidirectional sequence traces was performed using Mutation Surveyor software version 2.61 (Soft Genetics). Sequence variants were investigated using the Alamut software (Interactive Biosoftware).

Mutation nomenclature was based on the following GenBank Accession numbers; *β3GNT1*; NM_006876.2, *DAG1*; NM_004393.2, *GYG1*; NM_004130.2, *GYG2*; NM_001079855.1, *GYLTL1B*; NM_152312.3, *FKTN*; NM_006731.1, *KCNK1*; NM_002245.3, *LARGE*; NM_133642.2, *LBR*; NM_002296.2, *MGAT5B*; NM_144677.2, *NRXN1*; NM_004801.4 and NM_138735.2, *POMGNT1*; NM_017739.1, *POMT1*; NM_007171.2, *POMT2*; NM_013382.3, *PSEN2*; NM_000447.2, *TCAP*; NM_003673.3, *TTC13*; NM_024525.3, *WWP1*; NM_007013.3 with nucleotide number 1 corresponding to the first base of the translation initiation codon. Gene names and sequence variations are in accordance with guidelines stipulated by the Human Genome Variation Society (HGVS).

Primer design

Genomic sequences were obtained via the ensembl genome browser (www.ensembl.org). A combination of automated primer design via Primer3 (http://www2.eur.nl/fgg/kgen/primer/), the PCR Suite (http://www-fgg.eur.nl/kgen/primer/) and manual design was incorporated. Genomic DNA primers were designed to amplify the entire coding region and were located a minimum of 50 base pairs from each intron/exon boundary.

SNPs were avoided within the primer binding sites to prevent allele specific non amplification. SNPs within the primer binding sites were avoided using the Diagnostic SNP Check software available online from the National Genetics Reference Laboratory (www.ngrl.man.ac.uk/SNPCheck).

To facilitate a stream line sequencing approach a non fluorescent 24 nucleotide sequence tag was attached to the 5’ end of both the forward and reverse primers. This system enabled all amplified fragments to be sequenced with a universal primer.

Primer tags (5’ to 3’)

Forward	GTCTCAGTTCAGGTGTCCTTCCTG
Reverse	AGACGTCTTGTGTCGTGGCTACTG

Universal sequencing primers (5’ to 3’)

Forward	CAGTTCAGGTGTCCTTCCT
Reverse	GTCTTGTGTCGTGGCTACT

Primers were supplied by Sigma and Operon. Primer stocks were stored at -20 ˚C at a concentration of 250 pmol/µl. Working primer dilutions were stored at 4 ˚C at a variety of concentrations.

Polymerase chain reaction

The amplification efficiency of genomic primer pairs was initially assessed in 10 µl reactions and processed manually. Four different PCR protocols (PCR protocols A, B, C and D) were tested sequentially until the reaction, analysed by gel electrophoresis, resulted in a suitable product for downstream analysis. The PCR conditions for each are detailed below;

PCR protocol A; 5 µl of 2x QIAGEN Multiplex PCR Buffer, 3 µl of primer mix (containing forward and reverse primers) at 1 pmol/µl and 2 µl of control genomic DNA (25 pmol/µl). Cycling conditions were 95°C for 15 minutes; 32 cycles of 95°C for 1 minute, 56°C for 1 minute 30 seconds, 72°C for 1 minute 30 seconds, followed by 72°C for 5 minutes and 60°C for 30 minutes.

PCR protocol B; this protocol was identical to that described above yet with a higher annealing temperature of 62°C.

PCR protocol C; this protocol contains identical PCR components yet incorporates a series of reduced extension temperatures to allow the amplification of AT rich regions modified from Su *et al.* (Su et al., 1996). Cycling conditions were 95°C for 15 minutes; 32 cycles of 95°C for 30 seconds, 55°C for 1 minute 30 seconds, 50°C for 30 seconds, 60°C for 1 minute 30 seconds, followed by 60°C for 5 minutes.

PCR protocol D; 5 µl of 2x QIAGEN Multiplex PCR Buffer, 1 µl of primer mix (containing forward and reverse primers) at 2.5 pmol/µl, 2 µl of 7-deaza dGTP (Roche), 1 µl of DMSO (Sigma) and 1 µl of control genomic DNA (25 pmol/µl). Cycling conditions were 95°C for 15 minutes; 32 cycles of 95°C for 1 minute, 56°C for 1 minute

30 seconds, 72°C for 1 minute 30 seconds, followed by 72°C for 5 minutes and 60°C for 30 minutes.

Appendices Tables 2-14 detail specific amplicon primer sequences and amplification conditions. A negative PCR control containing all the reaction components except template was included for the amplification of each fragment.

Automated mutation screening

To increase sample throughput and facilitate the screening of both a large number of amplicons and patient DNA samples, each stage of mutation screening was fully automated in 384 well plates using a combination of three liquid handling platforms; MultiPROBE II Liquid Handling System (PerkinElmer, Life Sciences), the Biomek NXP liquid handling robot (Beckman Coulter) and the Nanodrop II Liquid Handler (Innovadyne). Protocols used routinely in Guy's DNA laboratory for high throughput processing were followed and are summarised below.

PCRs were automated on the MultiPROBE II Liquid Handling System (PerkinElmer, Life Sciences). The MultiPROBE II system is controlled by WinPREP applications software facilitating the set up of complex protocols created in Excel and transferred as comma separated variable files. A variable number of patient DNA samples and amplicons were set up on each plate.

PCR volumes were typically scaled down to 5 µl for automation. A volume of 2 µl of primer mix (1 pmol/µl forward and reverse primer mix) was initially dispensed into each well of a 384 well plate and dried down on a heating block at 55 ˚C for 45 minutes. 3 µl of Qiagen MultiMix and 2 µl of DNA (approximately 25 ng/µl) was then pipetted into each well and the appropriate PCR program performed on a DNA Engine Dyad thermal cycler (Bio-Rad formerly MJ Research).

The removal of unincorporated dNTPs, primers and salts was fully automated using the Ampure system (Agencourt) on the Biomek NXP liquid handling robot (Beckman Coulter). This was performed in accordance to manufacturer's instructions and DNA laboratory, GSTS Pathology at Guy's Hospital standard protocols. Initially AMPure

beads are added to the PCR reaction and the PCR amplicon is bound to magnetic beads. Upon transfer of the PCR plate to a magnetic plate the bound PCR amplicons are separated from contaminants by washing with ethanol. The amplicons are then eluted from the magnetic beads in 30 µl of H_20.

The set up of cycle sequencing was fully automated on the Nanodrop II Liquid Handler (Innovadyne). 2 µl of universal sequencing mix was added to 1 µl of AMPure purified PCR product. Sequencing mix consisted of 0.15 µl of BigDye version 3.1 (Applied Biosystems), 0.45 µl of Big Dye Buffer (Applied Biosystems), 0.6 µl of Q solution (Qiagen), 0.3 µl of universal primer (5 pmol/µl) to a total volume of 2 µl with H_20. Cycle sequencing conditions were 30 cycles of; 96°C for 30 seconds (ramped to 96°C at 1 per second), 50°C for 15 seconds (ramped to 50°C at 1 per second), 60°C for 1 minute (ramped to 60°C at 1 per second).

The dye-terminator removal process was fully automated using the Agencourt CleanSEQ paramagnetic bead system on the Nanodrop II Liquid Handler (Innovadyne) and the Biomek NXP liquid handling robot (Beckman Coulter). Initially ethanol and CleanSEQ (Agencourt) reagent is added to the sequencing reaction. Sequencing products are subsequently bound to magnetic beads. Contaminants are then separated from sequencing products via the application of a magnetic field and washed with ethanol. Sequencing products are then eluted from the magnetic particles in 0.1 mM ethylenediaminetetraacetic acid (EDTA).

Manual mutation screening

When processing fewer than 20 amplicons, samples were processed manually using the conditions described in the Polymerase Chain Reaction section above. Successful amplification was verified by running 3 µl of PCR product on an agarose gel. The removal of excess dNTPs and primers from the PCR product was performed using a combination of two hydrolytic enzymes together with a buffer. Exonuclease I (*Escherichia coli*) removes residual single-stranded primers and any extraneous single-stranded DNA produced in the PCR. Shrimp alkaline phosphatase removes the remaining dNTPs from the PCR mixture. 1.5 µl of shrimp alkaline phosphatase (USB Corporation) and 0.5 µl of exonuclease I (Biolabs) was added directly to 5 µl of PCR

product and incubated at 37°C for 15 minutes. After treatment the reaction is inactivated by heating to 80°C for 15 minutes. Purified PCR products were typically submitted either to The Wolfson Institute for Biomedical Research, UCL sequencing service or the MRC CSC Genomics Laboratory DNA sequencing service at Imperial College London.

2.2.4 Plasmid Manipulation

Preparation of vectors and inserts

The coding sequence of *POMGNT1* (NM_017739) had previously been cloned into the high copy number pcDNA3.1/V5-His TOPO expression vector (Invitrogen) from reverse transcribed total human brain RNA (ClonTech). This vector directs the synthesis of a fusion protein tagged at its C-terminal end with the V5 epitope (GKPIPNPLLGLDST).

Site-directed mutagenesis

The mutagenesis of *POMGNT1* was achieved with a PCR reaction containing a proof reading polymerase with a low amplification cycle number to maintain a high fidelity PCR yield. Overlapping primers contained the desired base change (c.1666G>A detected in patient A20) necessary to alter the amino acid sequence in the resulting *POMGNT1* protein (p.Asp556Asn). Oligonucleotides were designed with the substitution located in the centre and flanked by twelve complementary oligonucleotides. Primers used to mutate the cloned *POMGNT1* are shown below with mismatched primers indicated in red.

Forward primer (3' to 5') GCTGAGGTTCTG**A**ACCACAGCAAGA
Reverse primer (3' to 5') TCTTGCTGTGGT**T**CAGAACCTCAGC

The PCR conditions were as follows; 2 µl (1U) of ProofStart DNA Polymerase (Qiagen), 1 µl of forward and reverse primer (50 pmol/µl), 1 µl of 10 mM dNTP, 10 µl of Q solution (Qiagen), 5 µl of buffer (Qiagen), 250 ng of plasmid DNA to a total of 50 µl with H_20.

PCR products were purified using Qiagen Quick columns following the manufacturer's recommended protocol. This system utilises the selective binding properties of a silica membrane to facilitate the absorption of DNA in the presence of high concentrations of salt whilst contaminants pass through the membrane. Excess primers, enzymes and unincorporated nucleotides do not bind to the silica membrane but flow through the spin column. Finally salts are washed away by both ethanol and buffers. 17 µl of cleaned PCR product was subsequently treated with 1 µl of restriction enzyme *Dpn*I (10 U) and 2 µl of buffer for 1 hour at 37°C to remove contaminating parental plasmid DNA. The methylated template DNA is selectively digested leaving newly synthesised unmethylated DNA undigested.

Plasmid DNA was transformed into chemically competent bacteria cells (please refer to section 2.2.5). Cells grown on Luria-Bertani (LB) agar (Invitrogen) were selected by ampicillin resistance and plasmids from candidate colonies were isolated from LB broth (Invitrogen) by Qiagen Mini-prep or Qiagen Midi-prep kits. Plasmid DNA was sequenced to confirm the presence of the desired mutation. The entirety of the plasmid was subsequently sequenced to exclude the acquisition of mutations during multiple rounds of replication.

2.2.5 Bacterial Manipulation

Storage of bacteria

The One Shot TOP10 Chemically Competent *Escherichia coli* (Invitrogen) cells were used for the propagation of plasmid DNA. All plasmids used in this thesis carried the ampicillin resistance gene. Antibiotic selection using ampicillin was applied at all stages of growth. Bacterial transformants were grown in LB broth (Invitrogen) or on LB agar (Invitrogen) containing 100 µg/ml ampicillin (SIGMA). Inoculated bacteria were stored in 50% (v/v) glycerol (SIGMA) in LB broth with ampicillin at -80°C.

Transformation of competent bacteria by heat shock

Competent cells were thawed on ice in 50 µl aliquots. A total of 4 µl PCR product was added and left on ice for a further 30 minutes, cells were then heat shocked at 42°C for

30 seconds and then returned to ice for a further 2 minutes. The heat shocked cells were then added to 250 µl of Super Optimal Broth medium (Invitrogen) and incubated at 37°C for 1 hour with 200 rotations per minute. Finally cells were spread on LB agar plates containing 100 µl/ml ampicillin, left for 30 minutes at room temperature for the suspension to become absorbed into the L-agar. Plates were then inverted and incubated at 37°C over night.

Growth of inoculated bacterial cultures

Single colonies selected from a freshly streaked selective LB agar plate were used to inoculate 5 ml of LB medium containing 100 µg/ml ampicillin. The propagation of a desired clone was also performed by adding 25 µl of glycerol stock to 5 ml LB medium containing 100 µg/ml ampicillin. Cultures were incubated for 12-16 hours at 37°C with vigorous shaking at 180 rpm. Bacteria cells grown in LB broth were lysed and plasmid DNA selectively isolated using Qiagen Mini-prep and Midi-prep systems.

Isolation of plasmid DNA

The QIAprep Spin Miniprep Kit DNA purification system (Qiagen) was routinely used to prepare up to 20 µg of high copy plasmid DNA. The Qiagen HiSpeed Plasmid Midi Kit purification system (Qiagen) was routinely used to prepare up to 100 µg of high copy plasmid DNA. Plasmid DNA was isolated from bacterial cultures according to the manufacturer's recommended protocol.

The QIAprep Miniprep procedure is based on alkaline lysis of bacterial cells followed by the adsorption of DNA onto silica in the presence of high salt. The silica membrane allows the selective absorption of plasmid DNA in high salt conditions and elution in low salt buffers. Contaminants such as endonucleases, salts, RNA, cellular proteins and metabolites are not retained on the membrane.

The Qiagen Midiprep DNA purification system is based on a modified alkaline lysis procedure, followed by the binding of plasmid DNA to Qiagen Anion-Exchange Resin under appropriate low salt and pH conditions. Contaminants are removed by a medium

salt wash and plasmid DNA is eluted in a high-salt buffer. The DNA is subsequently concentrated and desalted by isopropanol precipitation.

2.2.6 Cell Culture

C2C12 cells are routinely used as a model of myogenic differentiation. Myoblasts can be induced to fuse into myotubes upon confluence and lowering of serum medium concentrations. These cells were originally obtained by Yaffe and Saxel through selective serial passage of myoblasts cultured from the thigh muscle of C3H mice 70 hours after a crush injury (Yaffe and Saxel, 1977).

Fibroblast cell cultures for patient A20 had previously been derived from a skin biopsy and processed by the biopsy team at the Dubowitz Neuromuscular Centre.

Peripheral blood lymphocytes from patient C1-1 and C1-4 had previously been submitted to the European Collection of Cell Cultures (Health Protection Agency) for transformation with the EBV virus. Subsequent lymphoblastoid cells were stored in the Health Protection Agency's Human Genetic Collection. Table 4 details those cell lines used from both affected and unaffected individuals.

	Individual	ECACC cell line ID	ECACC Collection	Age at sampling	Gender	Ethnic origin
Pedigree 1	Patient C1-4 (pedigree 1)	FG0012	Human Genetic Collection	08.05	Male	Arabic
	Patient C1-1 (pedigree 1)	FG0013	Human Genetic Collection	11.05	Female	Arabic
Unrelated controls	Unaffected	C0106	Human Random Collection	24	Male	UK Caucasian
	Unaffected	C0126	Human Random Collection	24	Female	UK Caucasian
	Unaffected sibling of CB0409 (condition; Psoriasis)	CB0411	Human Genetic Collection	13.02	Female	UK Caucasian

Table 3. Lymphoblastoid cell lines sourced from the European Collection of Cell Cultures (ECACC).

Growth conditions

C2C12 and fibroblast cell lines were routinely grown in a monolayer in 75 cm^2 tissue culture flasks at 37°C in a humid atmosphere maintained at 5% (v/v) CO_2. Cells were cultured in growth medium; Dulbecco's modified Eagle's medium (DMEM) (SIGMA) supplemented with 20% (v/v) Fetal Bovine Serum Gold (PAA) and 2 mM L-glutamine (SIGMA). Cells were typically seeded at 1/10 dilutions and passaged once a week as follows; the medium was removed from the flask and the cells were washed with 5 ml of DMEM. 2 ml of trypsin-EDTA solution was added to the flask and cells were returned to the incubator for 2-5 minutes. The majority of cells disassociate from the plastic during this time and any remaining adherent cells were dislodged by gentle tapping. 5 ml of growth medium was added to neutralise the trypsin. The cell suspension was subsequently aerated by vigorous pipetting. A suitable dilution was made by adding part of the suspension to 10 ml of growth medium and incubated as normal. C2C12 cells were differentiated with fusion medium upon confluence; DMEM supplemented with 2% Horse Serum (PAA) and 2 mM L-glutamine (SIGMA).

Lymphoblastoid cells were grown in suspension in Roswell Park Memorial Institute (RPMI) growth medium at 37°C in a humid atmosphere maintained at 5% (v/v) $C0_2$. The ampoule of frozen cells was added to 10 ml of RPMI in a 25 cm^2 tissue culture flask and cultured over night. A further 10 ml of RPMI was added the following day. On day three the cells were seeded at ¼ in 75 cm^2 tissue culture flasks and harvested 24 hours later.

Freezing and thawing cells

C2C12 and fibroblasts cells were treated with trypsin-EDTA, as described above, and counted in a hemocytometer. C2C12, fibroblasts and lymphoblastoid cell suspensions were centrifuged at 1500 rpm for 5 minutes and pellets re-suspended in freezing medium (90% Fetal Bovine Serum (PAA), 10% DMSO (Sigma)). Approximately one million cells were frozen per 1 ml of freezing medium. The cells were frozen in a cryogenic chamber (surrounded by isopropanol) at -80°C overnight and transferred to liquid nitrogen storage the following day.

When thawing cells, vials were removed from liquid nitrogen storage and thawed rapidly at 37°C in the incubator. Cells were re-suspended slowly in 10 ml growth medium and transferred to a flask. Once C2C12 and fibroblasts cells had adhered to the plastic the culture medium was replaced with fresh growth medium.

2.2.7 Transient Transfections

Transient transfections were performed using the lipid based transfection reagents Gene Juice (Novagen) and Lipofectamine 2000 (Invitrogen) allowing efficient delivery of nucleic acids ranging from small RNAs to large plasmids. All transfection experiments were performed at least 3 times.

Short interfering RNA

Short interfering RNA (siRNA) oligonucleotides specific for mouse *Pomt1, Gyg* and *β3gnt1* were obtained from Ambion. A list of siRNA oligonucleotides used is shown in Table 4. A total of 100,000 cells were plated in 6 well culture dishes containing cover slips and cultured overnight in 2 ml of supplemented DMEM to reach 70% confluence the following day. Cells were transiently transfected using Lipofectamine 2000 reagent (Invitrogen) in serum-free media (Opti-MEM, Invitrogen) using the following protocol; both 100 μM of RNAi and 5 μl Lipofectamine 2000 reagent were diluted in 500 μl Opti-MEM and incubated separately for 5 minutes. The diluted RNAi and Lipofectamine were then combined. All incubations were performed at room temperature. Culture medium was removed from the cells and the cells were washed with Opti-MEM prior to the addition of the mixture. Cells were transfected 24 hours after plating and then re-transfected 72 hours after plating. Cells were harvested 96 hours after plating in the appropriate buffer for western blotting or Real Time PCR analysis.

Protein (encoding gene) *	**Silencer(R) Select Pre-designed siRNA**		
	siRNA ID **	**Sense**	**Antisense**
Protein-*O*-mannosyltransferase 1 (*Pomt1*)	s97376	CGUGGAAUCUGAUCGGAGAtt	UCUCCGAUCAGAUUCCACGcg
	s97374	CCCUGGUUGUAGCAUGGUAtt	UACCAUGCUACAACCAGGGca
Glycogenin 1 (*Gyg1*)	s77650	CCCUCCAUUGAAACGUAUAtt	UAUACGUUUCAAUGGAGGGtt
	s77652	GGACAGUGGUGAUUCUGCUtt	AGCAGAAUCACCACUGUCCaa
UDP-GlcNAc:betaGal beta-1,3-*N*-acetylglucosaminyltransferase 1 (*β3gnt1*)	s99324	CCAGCGCAAUAAGAUCCUUtt	AAGGAUCUUAUUGCGCUGGtt
	s99323	GAAUGCCGAUGAACAAGAAtt	UUCUUGUUCAUCGGCAUUCgg

Table 4. siRNA oligonucleotides.

Probes for specific knockdown of mouse *Pomt1*, *Gyg1* and *β3gnt1*. * Gene symbols and names as per HUGO nomenclature (www.genenames.org/). ** siRNA identification code (ID) (www.ambion.com).

Plasmid transfection

Cells were plated in 6 well dishes on round glass coverslips (10 mm diameter) and incubated in growth medium to reach 70% confluence. Cells were transiently transfected using Gene Juice (Novagen) in Opti-MEM using the following protocol; 3 µl of Gene Juice was diluted in 20 µl of Opti-MEM and incubated for 5 minutes at room temperature. 0.5 µg of plasmid was then added to the above mix and incubated for 15 minutes at room temperature. Culture medium was removed from the cells and the cells were washed with Opti-MEM prior to the addition of the mixture. Cells were transfected for 24 hours before transferring to growth medium. After four days cells were harvested in the appropriate buffer for western blotting or fixed in 2% paraformaldehyde for immunohistochemical analysis.

2.2.8 Protein Manipulation

Preparation of cell homogenates

Fibroblast cell homogenates were sent to Harry Schatner's laboratory in the Department of Structural Biology and Biochemistry in Toronto, Canada to assay patient A20's *POMGNT1* function (please refer to section 3.2.3). A total of four 175 cm^2 flasks were grown as described above. Once confluent, cells were washed with Phosphate Buffered Saline (PBS) before being scraped and transferred to a 50 ml centrifuge tube. Cells were subsequently washed with PBS to ensure the removal of serum media. The cells were then divided into 1.5 ml microcentrifuge tubes and centrifuged at 1500 rpm for 5 minutes to form pellets. Pellets were stored at -80°C and transported on dry ice.

Protein extraction from cultured cells

To inhibit contaminating proteases, cellular proteins were extracted in lysis buffer consisting of 75 mM Tris-HCl, 1% sodium dodecyl sulphate (SDS) plus Complete Protease Inhibitor Cocktail (Roche). One complete Mini tablet was dissolved in 750 µl H_20, 50 µl aliquots were stored at -20 for a maximum of 12 weeks. A total of 35 µl of protease inhibitor cocktail solution was added to a 500 µl aliquot of sample buffer. Cells were dislodged from the plastic with protease inhibitor and a plastic cell scraper (30 µl

or 70 µl of protease inhibitor was used for a 75 cm^2 or 175 cm^2 culture flask respectively). The cells were then boiled for 3 minutes in a 1.5 screw top tube followed by centrifugation (14,000 rpm) for 3 minutes at 4°C. The supernatant was transferred to a new tube and treated with 1 U of DNaseI for 20 minutes at room temperature. Protein extractions were then stored at -80°C.

SDS poly-acrylamide gel electrophoresis

Proteins were resolved using the NuPAGE Bis-Tris system in conjunction with the XCell SureLock™ Mini-Cell system (Invitrogen Life Sciences) according to the manufacturer's protocol.

Corresponding amounts of sample (typically 21.25 µl) and 4X NuPAGE LDS sample buffer were mixed to give a volume of 30 µl. 5 µl of NuPAGE reducing agent was added to each sample (0.5M DTT) immediately prior to heating. Samples were then boiled for 3 minutes and a total of 35 µl loaded into each well. The migration of proteins was estimated by comparison to markers run simultaneously alongside samples; 10 µl of SeeBlue Plus2 Pre-Stained Standard was routinely used.

The pre-cast NuPAGE Bis-Tris-HCl buffered (pH 6.4) 4-12% polyacrylamide gels were removed from their pouches and rinsed with H_20. The tape and comb were gently removed and sample wells rinsed repeatedly with 1X NuPAGE SDS Running Buffer. Once the gel cassette and buffer core were assembled in the Mini-Cell the upper chamber was filled with 200 ml NuPAGE MOPS SDS Running Buffer. 500 µl of NuPAGE antioxidant was added to the running buffer in the upper chamber to ensure that samples did not re-oxidise during electrophoresis. The lower chamber was filled with 600 ml NuPAGE MOPS SDS Running Buffer. Denaturing electrophoresis was carried out at 200 V at 4°C until the Myoglobin Red (19 kDa) had migrated to the bottom of the gel (Figure 12). The cassette was subsequently removed from the Mini-Cell system, the plates separated and the gel removed for processing.

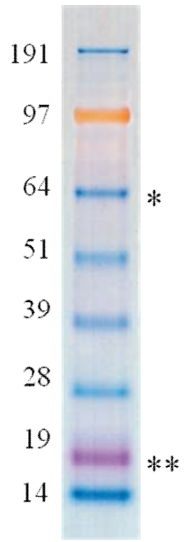

Figure 12. Migration of bands in the SeeBlue Plus2 Pre-Stained Standard (NuPAGE MOPS system).

The apparent molecular weights in kDa are illustrated on the left. * The membrane was cut horizontally at the 64 kDa protein band to allow the staining of both α and β-dystroglycan within a single lane. ** Electrophoresis was performed until the 19 kDa protein band had migrated to the bottom of the gel. Image adapted from Invitrogen.com.

Western transfer

Proteins were transferred to a nitrocellulose membrane using the NuPAGE XCell II™ blotting apparatus. Blotting pads, filter paper and Hybond-Electrochemiluminescence (ECL) nitrocellulose membrane (Amersham Biosciences) were soaked in 1X NuPAGE Transfer buffer (with the addition of methanol as per manufacturer's protocol). The gel was transferred from the cassette to a piece of filter paper and the pre-soaked membrane placed over the gel. The gel and membrane were sandwiched between filter paper and blotting pads in the correct orientation to ensure the gel is closest to the cathode core. The blot module was then held closely together and placed in the lower buffer chamber with the gel tension wedge locked into place. The blot module was filled with 1x NuPAGE Transfer Buffer until the gel / membrane assembly was covered. The outer chamber was filled with H_20 and the transfer performed at 30 V for 2 hours 30 minutes at 4°C. The membrane was then inspected for the presence of the SeeBlue Plus2 Pre-Stained Standard to confirm the transfer of proteins.

Immunoblotting

Where appropriate, the nitrocellulose membrane was cut vertically to allow staining with a number of different antibodies. In addition the membrane was typically cut horizontally at approximately 64 kDa to permit the staining of α and β-dystroglycan within the same well (Figure 12). Nitrocellulose strips were blocked overnight at 4°C. The membrane was sequentially probed with the appropriate antibodies and buffers at room temperature for 1 hour. After each antibody incubation period the nitrocellulose membrane was washed in buffer alone for 3 x 10 minutes at room temperature. All blocking, washing and incubations were carried out with gentle shaking.

For glycosylated α-dystroglycan detection the nitrocellulose membrane strips were blocked in 3% bovine serum albumin (BSA) (v/w) (IgG- and protease-free, Jackson Laboratories) IIH6 buffer (20 mM Tris 0.1 NaCl, pH 7.4). The primary antibody, IIH6 (Millipore; 1/2000) was diluted in 3% BSA (w/v) IIH6 buffer. The secondary antibody, Polyclonal Rabbit anti-mouse IgM (Dako; 1:2000) and tertiary antibody Streptavidin horseradish peroxidise (HRP) (Dako; 1:10,000) were incubated in IIH6 buffer only.

For β-dystroglycan detection the nitrocellulose membrane strips were blocked in 10% skimmed milk powder (w/v) (Fluka) Tris-buffered saline with 0.5% Tween 20 (TBST) (v/v). The primary antibody, 43DAG/8D5 (Vector Laboratories; 1:150) was incubated in 5% skimmed milk powder (w/v) TBST. The secondary antibody, anti-mouse Ig biotinylated species specific whole antibody (Amersham; 1:2000) and tertiary antibody HRP-Streptavidin (DAKO; 1:10,000) were incubated in TBST only.

For V5 recombinant fusion protein detection the nitrocellulose membrane strips were blocked in 3% BSA (w/v) TBST. The primary antibody Anti-V5 (Invitrogen; 1:10,000) was incubated in 3% BSA (v/w) TBST. The secondary antibody anti-rabbit HRP (DAKO; 1:50,000) was incubated in TBST only.

For myogenin detection the nitrocellulose membrane strips were blocked in 10% skimmed milk powder (w/v) TBST. The primary antibody F5D (Developmental Studies Hybridoma Bank; 1:500) was incubated in 5% skimmed milk powder (w/v) TBST. The secondary antibody anti-mouse Ig biotinylated species specific whole antibody (Amersham; 1:2000) and tertiary antibody HRP-Streptavidin (DAKO; 1:1000) were incubated in TBSB only.

After washing, membranes were visualized using chemiluminescence (ECL+Plus, Amersham), according to manufacturer's instructions. Film was typically processed in a Xograph Compact X4 film processor (Xograph Imaging Systems).

Stripping and re-probing western blot membrane

Membrane stripping describes the complete removal of bound reagents such as ECL solution, antibodies and blocking solution from the WB nitrocellulose membrane. The membrane was submerged in stripping buffer (100 mM 2-mercaptoethanol, 2% SDS, 62.5 mM Tris-HCl pH 6.7) and incubated at 50°C for 30 minutes with occasional agitation in a fume hood. The membrane was then washed for 2 x 10 minutes in large volumes of TBST or IIH6 buffer (as appropriate) at room temperature. Subsequent blocking and immunodetection was then carried out as outlined above.

Immunohistochemistry

C2C12 cells grown on coverslips were transfected with wild-type and mutant pcDNA3.1/V5-His TOPO expression vectors (as described above). Cells were washed in PBS before being fixed in 2% paraformaldehyde (dissolved in PBS+NaOH adjusted to pH 7.4 with HCl) for 10 minutes, followed by washing twice in PBS for 10 minutes. Fixed cells could then be stored at 4°C in PBS for a few days if necessary. After fixation the cells were permeabilized in PBS with 0.05% Triton X-100 (v/v) (Sigma) for 5 minutes. For double labelling, cells were first incubated for 1 hour with monoclonal anti-GM130 (BD Biosciences; 1:500), a Golgi apparatus marker, followed by an anti-mouse conjugated to Alexa 594 (Molecular Probes; 1:500) for 30 minutes. After washing, fluorescein isothiocyanate-conjugated goat anti-V5-His (Bethyl Lab; 1:50) was applied for 1 hour. Cell nuclei were counterstained with Hoechst 33342 (Molecular Probes; 1:2000). All dilutions and washings were made in phosphate-buffered saline, and incubations were performed at room temperature. Coverslips were mounted in aqueous mountant and viewed with epifluorescence using a Leica Diaphot microscope and digitally captured using Metamorph (Universal Imaging).

Antibodies

The monoclonal mouse anti-IIH6 antibody is specific to an unknown carbohydrate epitope present on α-dystroglycan was originally obtained from female BALB/c mice immunized with purified rabbit skeletal muscle sarcolemma membranes and boosted with dystrophin-glycoprotein complex (Ervasti and Campbell, 1991). For western blotting IIH6 was purchased from Millipore whereas for immunocytochemical analysis the antibody was a kind gift from Kevin Campbell.

The monoclonal mouse anti-β-dystroglycan antibody (Vector laboratories clone 43DAG/8D5) is a synthetic peptide containing 15 of the last 16 amino acids at the end of the C-terminal region of the human dystroglycan molecule (PKNMTPYRSPPPYVP).

The polyclonal rabbit anti-V5 antibody (Invitrogen) allows the detection of recombinant fusion protein by recognising the V5 tag (IPNPLLGLD).

The monoclonal mouse anti GM130 (BD Bioscience) antibody allows the detection of Golgi apparatus matrix protein (130 kDa). GM130 recognises a protein isolated from the Triton™ X-100-insoluble Golgi matrix and peripherally associated with the cis-compartment, as demonstrated by co-localization with syntaxin5.

2.2.9 Statistical Analysis

Where specified, experiments were performed in triplicate and expressed as the mean ± the standard error of the mean (SEM) of three independent samples. For each Real Time PCR experiment, individual sample values represent the average of three samples. Analyses were interpreted with the use of unpaired Student's t-test comparing the effect against appropriate controls. A P value of less than 0.05 was considered to indicate statistical significance. Statistical analyses were performed via excel.

2.2.10 Bioinformatics

The following bioinformatics packages were used in addition to those described above; Genomic sequences were acquired from the Ensembl Genome Server (http://www.ensembl.org/index.html) and from the databases at NCBI (http://ncbi.nlm.nih.gov). Protein homology plots were produced by multiple alignments using ClustalW (www.ebi.ac.uk/clustalw/) within the BioEdit platform (www.mbio.ncsu.edu/BioEdit/bioedit.htm). Figures depicting linkage regions were manipulated using the UCSC Genome Browser (genome.ucsc.edu/). Features assigned within linkage regions were displayed using 'Custom Tracks' and the 'RefSeq Genes' track. Phylogenetic trees were constructed with TreeFam (www.TreeFam.org) (Li et al., 2006; Ruan et al., 2008). Endeavour bioinformatics software was used to prioritise candidate genes (www.esat.kuleuven.be/endeavour) (Aerts et al., 2006). The following data sources were used for ranking; Annotation (EnsemblEst, GeneOntology, Interpro, Kegg, and Swissprot); Blast; CisRegModule; Expression (SonEtAl and SuEtAl); Interaction (Bind, BioGrid, Hprd, InNetDb, Intact and Mint); Motif; Precalculated Ouzounis and Prospectr and literature. Candidate genes were classified by their biological function using the Panther data analysis tool (http://www.panther.org) (Thomas et al., 2003). Subcellular localisations were annotated via the Universal Protein Resource Knowledge Base (UniProtKB) (www.uniprot.org). Protein domains

were predicted by the Eukaryotic Linear Motif (ELM) server (http://elm.eu.org) (Puntervoll et al., 2003).

CHAPTER 3: REFINING GENOTYPE-PHENOTYPE CORRELATIONS

3 REFINING GENOTYPE-PHENOTYPE CORRELATIONS

3.1 INTRODUCTION

Muscular dystrophy syndromes associated with the hypoglycosylation of α-dystroglycan vary extensively in phenotypic severity. Historically, subsets of patients with a particular clinical presentation in specific geographical regions were studied to uncover their underlying molecular defects. As mutations were detected, specific genes became associated with discrete clinical phenotypes. This is best represented by the research performed on patients with FCMD and MEB. FCMD was described within the Japanese population where, in the majority of cases, it is caused by a homozygous 3 kb insertion mutation in the 3' UTR of the gene *FKTN* (Kobayashi et al., 1998). MEB was originally described within the Finnish population in association with mutations in *POMGNT1* (Yoshida et al., 2001). WWS was however described worldwide and originally found to be associated with mutations in *POMT1* and *POMT2* (Beltran-Valero de Bernabe et al., 2002; Currier et al., 2005; van Reeuwijk et al., 2005b). In addition, MDC1C and MDC1D are two rare congenital dystroglycanopathy syndromes, secondary to mutations in *FKRP* and *LARGE* respectively (Brockington et al., 2001a; Longman et al., 2003).

The increased availability of mutation analysis in patients with a dystroglycanopathy has subsequently led to a widening of the clinical spectrum observed for several of these genes. This is best exemplified by the range of phenotypes resulting from mutations in *FKRP*. Following the initial description of its involvement in MDC1C (Brockington et al., 2001a), it was subsequently shown to cause a very common and relatively mild variant, LGMD2I (Brockington et al., 2001b), and more recently CMD variants with associated mild structural brain (MDC1C and cerebellar cysts (Mercuri et al., 2006; Topaloglu et al., 2003)) or severe brain and eye involvement resembling WWS and MEB (Beltran-Valero de Bernabe et al., 2004; Mercuri et al., 2006).

It has also been documented that genes other than *FKRP* are involved in both milder and more severe phenotypes than originally reported. This includes the finding of *FKTN* mutations in two families with WWS as well as the involvement of *POMT1* in patients

with LGMD2K (LGMD with associated microcephaly and mental retardation) (Balci et al., 2005; de Bernabe et al., 2003).

All previous studies have been conducted on a small number of families or individuals. This causes inevitable difficulties in applying mutation frequencies to the general population. In addition, such reports make it problematic to establish: 1) whether the described clinical spectrum is truly representative of the phenotypic variability and 2) how common the originally described core phenotypes are for each of these genes.

In order to address these points, we have systematically analysed a large population of patients with a dystroglycanopathy phenotype for mutations in the associated genes. As the spectrum of phenotypes secondary to *FKRP* involvement had been extensively reported previously, 92 patients were studied in whom involvement of this gene had been excluded before proceeding with analysis of *POMT1*, *POMT2*, *POMGNT1*, *FKTN* and *LARGE*.

3.2 RESULTS

3.2.1 Clinical Findings

Patient cohort A comprised of 92 probands (patients A1-A92) from a range of ethnicities, the inclusion criteria of which is detailed in section 2.1.1. As previously stated, clinical data was analysed by Professor F Muntoni and Dr E Clement and muscle pathology was evaluated by Professor C Sewry, Dr L Feng and Dr C Jimenez-Mallebrera.

Patients were classified as having either a CMD or LGMD phenotype and further subdivided according to the degree of structural and functional brain involvement. CMD was defined as onset of weakness prenatally or within the first 6 months of life. LGMD was defined by later onset weakness, specifically after having acquired ambulation. The cohort consisted of 64 patients with CMD, 25 patients with LGMD and included a total of 59 patients with brain involvement. In three cases the clinical information available was insufficient to determine phenotypic classification. Patients were divided into 1 of 7 broad phenotypic categories described below:

1) **WWS (and WWS-like):** Onset is prenatal or at birth. Patients assigned to this category had severe structural brain abnormalities including complete agyria or severe lissencephaly with only rudimentary cortical folding, marked hydrocephalus, severe cerebellar involvement and complete or partial absence of the corpus callosum (Figure 13). Eye abnormalities including congenital cataracts, microphthalmia and buphthalmos were common. When MRI evidence was not available, death before 1 year of age was taken as suggestive of this category if other clinical findings were supportive (Cormand et al., 2001). Motor development was typically absent in these patients. Five patients were assigned to this group.

2) **MEB/FCMD-like:** These categories were merged due to the overlapping phenotypic features. Included in this group were CMD with structural brain defects less severe than that seen with WWS. MRI findings include pachygyria with preferential frontoparietal involvement, polymicrogyria, cerebellar hypoplasia, cerebellar dysplasia and frequent flattening of the pons and brainstem (Figure 13). Eye abnormalities were often present in this group and include congenital glaucoma, progressive myopia, retinal atrophy and juvenile cataracts. Individuals may, rarely, acquire the ability to walk although this is delayed. Rarely patients manage to learn a few spoken words. Thirty patients were assigned to this group, including one in whom the clinical information was limited.

A B

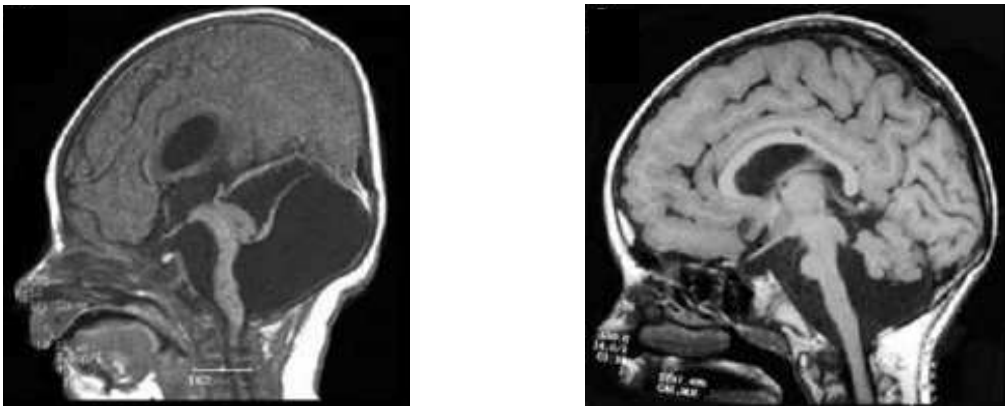

Figure 13. Brain MRI scans from patients with a severe dystroglycanopathy.
A) The brain MRI of a patient with WWS showing complete agyria. B) The brain MRI of a patient with MEB showing simplified gyral patterning with shallow sulci in the posterior temporal and parietal regions. Images from Beltran *et al.* (Beltran-Valero de Bernabe et al., 2004). Permission to reproduce this figure has been granted by BMJ Publishing Group Ltd.

3) **CMD-CRB (CMD with cerebellar involvement):** This category included CMD with mental retardation and cerebellar involvement on MRI scan as the only structural abnormality. Cerebellar abnormalities may include cysts, which are described relatively frequently in individuals with *FKRP* gene defects or cerebellar hypoplasia or dysplasia (Mercuri et al., 2006). Four patients were assigned to this group.

4) **CMD-MR (CMD with mental retardation):** CMD with mental retardation and a structurally normal brain. Patients with isolated microcephaly or minor white matter changes on MRI are included in this group. Fifteen patients were assigned to this group, including two with limited clinical information.

5) **CMD-no MR (CMD with no mental retardation):** Several patients within this group have had no neuroimaging but had entirely normal intellectual function. Ten patients were assigned to this group, one with limited information.

6) **LGMD-MR (LGMD with mental retardation):** LGMD with mental retardation and a structurally normal brain. Patients with minor white matter abnormalities and microcephaly were included in this group. This category includes patients with a phenotype resembling LGMD2K (Balci et al., 2005). Five patients were assigned to this group.

7) **LGMD-no MR (LGMD with no mental retardation):** LGMD with no mental retardation. This category includes the LGMD phenotypes resembling LGMD2I and 2L (Brockington et al., 2001b; Godfrey et al., 2006). Twenty patients were assigned to this group, six with limited clinical information.

The division of phenotypes within the cohort is shown in Table 8. Detailed clinical information for those patients in whom pathogenic mutations were detected is contained in Table 5.

Patient	α-dystroglycan epitope staining	Phenotype [a]	Age at onset [b]	CK	Motor ability [c]	Contractures [d]	Hypertrophy [e]	Spine [f]	Eyes [g]	Weakness [h]	IQ [i]	Microcephaly [j]	MRI [k]	Other [l]
1	LOW	WWS	P	4000	NS	Y	Y	Sc, RS	Poor visual attention	LL>UL	L	Y	H, CHy, WM, Lis	Gastrostomy
2	LOW	MEB-FCMD	P	3500	N/A	Y	N/A	N/A	CG	N/A	L	Y	H, BS,WM,CC,CHy	N/A
3	LOW	LGMD-MR	I	2000	W	N/A	Y	U	N/A	N/A	L	Y	Normal	N/A
4	LOW	CMD-MR	I	7800	NW 2yr	N/A	N/A	U	U	N/A	L	N/A	WM	N/A
5	LOW	LGMD-MR	I	4000	W	N	Y	U	U	N/A	L	Y	Normal	N/A
6	LOW	LGMD-MR	3Yr	8000	W		Y	N/A	U	N/A	L	Y	WM- minimal	N/A
7	LOW	CMD-MR	I	3600	St	N	Y	U	U	N/A	L	Y	Normal	N/A
8	LOW	CMD-MR	4m	18000	W	N/A	Y	RS	N/A	N/A	L	Y	WM- minimal	Choreic Movement disorder
9	LOW	MEB-FCMD	N	5500	S	Y	Y	RS, Sc	N/A	N/A	L	Y	WM, BS	N/A
10	LOW	MEB-FCMD	4Yr	5200	NW	N	Y	U		N/A	L	Y	Encephalocele	N/A
11	LOW	MEB-FCMD	7m	N/A	NS	Y	N	U	Hm	N/A		N/A	H, WM,CC,	N/A

Patient	α-dystroglycan epitope staining	Phenotype [a]	Age at onset [b]	CK	Motor ability [c]	Contractures [d]	Hypertrophy [e]	Spine [f]	Eyes [g]	Weakness [h]	IQ [i]	Microcephaly [j]	MRI [k]	Other [l]
12	LOW	MEB-FCMD	N	3100	NS	Y	N/A	RS		UL>LL	L	Y	WM	N/A
13	N/A	MEB-FCMD	8m		W	N/A	Y	U	My	UL>LL	L	N	WM , CDys, CC,PMG	N/A
14	LOW	MEB-FCMD	N	6000	S	Y	Y	Sc	CC	N/A	L	Y	BS,H,WM	SE, RIP age 11yr
15a	N/A	CMD-CRB	I	4700	W	Y	Y	N/A	N/A	UL>LL	L	Y	N/A	N/A
15b	N/A	CMD-CRB	I	5200	S	N/A	N/A	N/A	N/A	N/A	L	N/A	CHy	Micropenis and cryptorchidism
16	LOW	LGMD-MR	18m	1900	W	N	Y	U	N/A	N/A	L	N/A	NO MRI	RBBB on ECHO
17	LOW	MEB-FCMD	N	2000	NS	Y	Y	N/A	My	UL,LL	L	Y	CHy, H	Macroglossia, **
18	LOW	MEB-FCMD	I	780	NW	N	N	N/A	CG	N/A	L	N/A	BS,CC,WM,H	N/A
19	LOW	MEB-FCMD	P	1000	W	Y	Y	U	OA, My	N/A	L	N	WM,CC	SE, feeding difficulties
20	LOW	LGMD-no MR	12 Yr	12000	R	N	Y	U	My	LL>UL	NI	N		N/A
21	LOW	MEB-FCMD	N	1200	NONE	N	N	U	RD	N/A	L	N/A	H,WM,CC	SE, feeding difficulties.

Patient	α-dystroglycan epitope staining	Phenotype [a]	Age at onset [b]	CK	Motor ability [c]	Contractures [d]	Hypertrophy [e]	Spine [f]	Eyes [g]	Weakness [h]	IQ [i]	Microcephaly [j]	MRI [k]	Other [l]
22	LOW	MEB-FCMD	12m	2800	R	N	N/A	U	Pt, RA	N/A	L	N/A	CHy, CC, WM,H	Dyspraxia, feeding difficulties, SE
23	LOW	MEB-FCMD	N/A	N/A	N/A	N/A	N/A	N/A	N/A	N/A	N/A	N/A	H,CC,WM	N/A
24	N/A	WWS	N	1300	NS	N/A	N/A	U	N/A	N/A	L	N/A	CC,CHy, WM, H,Lis	N/A
25	LOW	WWS	P	5700	NONE	Y			RDy		L		H,WM,CHy, Lis	Feeding difficulties, RIP 8 weeks
26	LOW	CMD-no MR	3Yr	3200	S	N	N	U	U	G	NI	N/A	WM-MILD	Hypothyroid
27	N/A	MEB-FCMD	I	4000	S	N	Y	U	U	N/A	L	N/A	CC,WM,H	
28	LOW	WWS	N	7000	N/A	Y	Y	U	RD,Mo	N/A		N/A	WM,CHy, BS, H	Dysmorphic
29a	LOW	LGMD-no MR	4m	10000	W	N	Y	N/A	N/A	UL>LL	NI	N	N/A	Steroid responsive
29b	LOW	LGMD-no MR	4m	13000	W	N	Y	U	U	LL>UL	NI	N	Normal	Steroid responsive
30	LOW	LGMD-no MR	10m	60000	W	N	Y	U	U	LL>UL	NI	N	H-MILD	Steroid responsive
31a	LOW	LGMD-no MR	4yr	9000	R	Y	N/A	U	N/A	N/A	NI	N/A	N/A	N/A

Table 5. Clinical characteristics of 33 individuals from 31 families in whom mutations were detected.

[a] WWS; Walker-Warburg syndrome, MEB/FCMD; muscle-eye-brain/Fukuyama congenital muscular dystrophy, CMD-MR; congenital muscular dystrophy with mental retardation, CMD-no MR; congenital muscular dystrophy with no mental retardation, CMD-CRB; congenital muscular dystrophy with cerebellar involvement, LGMD-MR; limb girdle muscular dystrophy with mental retardation, LGMD-no MR; limb girdle muscular dystrophy with no mental retardation. [b] P; prenatal onset, N; neonatal onset, I; infant onset, Yr; years, m; months. [c] W; walk, S; sit, St; stand, R; run, Prefix N; never. [d-e] Y; yes, N; no. [f] RS; rigid spine, Sc; scoliosis, U; unaffected. [g] CG; congenital glaucoma, RD; retinal detachment, RA; Retinal Atrophy, CC; Congenital cataracts, OA; optic atrophy, My; myopia, Mo; microphthalmia, Pt; ptosis, U; unaffected, Hm; hypermetropia, RDy; retinal dysplasia. [h] UL; Upper limbs, LL; lower limbs, G; generalised, [i] NI; normal intelligence, L; low, [j] Y; yes, N; no, [k] H; Hydrocephalus, CC; cerebellar cysts, BS; brainstem involvement, WM; white matter abnormality, CHy; cerebellar hypoplasia, Lis; lissencephaly, CDys; cerebellar dysplasia. [l] SE; seizures, CDH; congenital dislocation of hip, RBBB; Right bundle branch block.

3.2.2 Mutation Analysis

I originally initiated the mutation screening of the *POMT1*, *POMT2*, *POMGNT1*, *LARGE* and *FKTN* in the ninety two patients described here as part of my Pre-registration clinical scientist training at Guy's DNA Laboratory prior to undertaking my PhD at University College London. The completion, characterisation and interpretation of these data, however, constituted a large proportion of my PhD studies and have therefore been included within this thesis.

A brief description of the mutation screening protocol has been included below for clarity: Genomic DNA was extracted in the referring centre's laboratory using standard methods. The complete coding regions, including intron/exon boundaries of *POMT1*, *POMT2*, *POMGNT1*, *FKTN* and *LARGE* were amplified by PCR. Amplicons were screened for mutations using a combination of uni-directional sequencing (standard dideoxynucleotide methodology) and heteroduplex analysis (methods described in (Clement et al., 2008b; Godfrey et al., 2007; Godfrey et al., 2006)). Where available, parental DNA was studied once a sequence alteration was identified in the proband. In two families, further segregation analysis was carried out to investigate the potential pathogenicity of unclassified variants. In families where a *de novo* mutation was suspected, paternity was confirmed using 11 STR markers (data not shown). Mutation nomenclature is based on the following GenBank Accession numbers; *POMT1*; NM_007171.2, *POMT2*; NM_013382.3, *POMGNT1*; NM_017739.1, *FKTN*; NM_006731.1 and *LARGE*; NM_133642.2, with nucleotide number 1 corresponding to the first base of the translation initiation codon.

Mutation screening of *POMT1*, *POMT2*, *POMGNT1*, *FKTN* and *LARGE* was performed on 92 probands in whom *FKRP* mutations had been previously excluded. Homozygous and compound heterozygous mutations were detected in a total of 31 probands (34 individuals from 31 families). Thirty seven different mutations were identified, 32 of which had not been previously reported. Pathogenic mutations are summarized in Table 6 and the comparative mutation frequencies between genes are represented in Table 8 and are represented schematically in Figure 14.

For the purposes of this study, I classified all insertions and deletions, splice site and nonsense mutations as well as previously published mutations as pathogenic. Both exonic and intronic sequence alterations were categorized as polymorphisms if they were present on The Single Nucleotide Polymorphism database (dbSNP) (http://www.ncbi.nlm.nih.gov), the Leiden database (http://www.dmd.nl) or present as an additional change in a patient with two proven pathogenic mutations (polymorphisms are shown in appendix Table 1). Amino acid substitutions were classified as pathogenic if they were detected in conjunction with a clearly pathogenic mutation or if they have been shown to segregate with disease in a large pedigree (Patients A15 and A20). In addition, two patients with homozygous missense mutations and one patient with compound heterozygous missense mutations have been included in Table 5 as they are non-conservative amino acid changes that affected an evolutionary conserved amino acid residue (patient A16, patient A18 and patient A27) (Figure 15). Patients in whom only a single sequence alteration was detected are summarised in Table 7. We have been unable to determine whether these are rare polymorphisms or pathogenic alterations in patients who harbour a second undetectable mutation. These six patients have not been included in the 34% of patients detected with mutations. Patient A25 has been included in Table 5, Table 6 and Table 8 despite the absence of a second detectable mutation due to the presence of a nonsense mutation.

Patient	Gene	Exon/intron	Nucleotide change	Predicted amino acid change	Mutation type	References
1	*POMT1*	20	c.2179_2180delTC	p.Ser727fs	Frameshift	Novel
	POMT1	20	c.2179_2180delTC	p.Ser727fs	Frameshift	Novel
2	*POMT1*	20	c.2179_2180delTC	p.Ser727fs	Frameshift	Novel
	POMT1	20	c.2179_2180delTC	p.Ser727fs	Frameshift	Novel
3	*POMT1*	7	c.598G>C	p.Ala200Pro	Missense	Leiden database
	POMT1	7	c.598G>C	p.Ala200Pro	Missense	Leiden database
4	*POMT1*	18	c.1847_1849delGGT	p.Trp616del	Deletion	Novel
	POMT1	3	c.193G>A	p.Gly65Arg	Missense	Leiden database
5	*POMT1*	11	c.1081C>T	p.Gln361X	Nonsense	Novel
	POMT1	19	c.2005G>A	p.Ala669Thr	Missense	Novel
6	*POMT1*	6	c.517_523delTTCTTCAinsG	p.Phe173_Asn175delinsAsp	Insertion/deletion	Novel
	POMT1	18	c.1868G>C	p.Arg623Thr	Missense	Novel
7	*POMT1*	7	c.598G>C	p.Ala200Pro	Missense	Leiden database
	POMT1	7	c.598G>C	p.Ala200Pro	Missense	Leiden database
8 ‡	*POMT1*	5	c.427G>T	p.Glu143X	Nonsense	Novel
	POMT1	7	c.598G>C	p.Ala200Pro	Missense	Leiden database
9 ‡	*POMT2*	21	c.2150T>C	p.Phe717Ser	Missense	Novel (*de novo*)
	POMT2	21	c.2177G>A	p.Gly726Glu	Missense	Leiden database
10	*POMT2*	19	c.1997A>G	p.Tyr666Cys	Missense	Novel
	POMT2	19	c.1997A>G	p.Tyr666Cys	Missense	Novel
11	*POMT2*	19	c.1997A>G	p.Tyr666Cys	Missense	Novel
	POMT2	11	c.1238G>C	p.Arg413Pro	Missense	Novel

Patient	Gene	Exon/intron	Nucleotide change	Predicted amino acid change	Mutation type	References
12 ‡	*POMT2*	20	c.2047A>C	p.Thr683Pro	Missense	Novel
	POMT2	9	c.1051delG	p.Ala351fs	Frameshift	Novel
13	*POMT2*	5	c.593T>A	p.Ile198Asn	Missense	Novel
	POMT2	19	c.1997A>G	p.Tyr666Cys	Missense	Novel
14	*POMT2*	10	c.1117G>T	p.Val373Phe	Missense	Novel
	POMT2	5	c.593T>A	p.Ile198Asn	Missense	Novel
15a, 15b *	*POMT2*	19	c.1997A>G	p.Tyr666Cys	Missense	Novel
	POMT2	19	c.1997A>G	p.Tyr666Cys	Missense	Novel
16	*POMT2*	5	c.551C>T	p.Thr184Met	Missense	Novel
	POMT2	21	c.2243G>C	p.Trp748Ser	Missense	Novel
17	*POMT2*	9	c.1057G>A	p.Gly353Ser	Missense	Novel [1]
	POMT2	21	c.2177G>A	p.Gly726Glu	Missense	Novel [1]
18	*POMGNT1*	6	c.526A>C	p.Thr176Pro	Missense	Novel
	POMGNT1	6	c.526A>C	p.Thr176Pro	Missense	Novel
19	*POMGNT1*	7	c.652+1G>A	Donor splice site	Splice site	Novel
	POMGNT1	17	c.1469G>A	p.Cys490Tyr	Missense	Leiden database
20 *†	*POMGNT1*	20	c.1666G>A	p.Asp556Asn	Missense	Novel [2]
	POMGNT1	20	c.1666G>A	p.Asp556Asn	Missense	Novel [2]
21	*POMGNT1*	17	c.1539+1G>A	Donor splice site	Splice site	Leiden database
	POMGNT1	17	c.1539+1G>A	Donor splice site	Splice site	Leiden database
22	*POMGNT1*	12	c.1100G>A	p.Arg367His	Missense	Novel
	POMGNT1	17	c.1539+1G>A	Donor splice site	Splice site	Leiden database

Patient	Gene	Exon/intron	Nucleotide change	Predicted amino acid change	Mutation type	References
23	*POMGNT1*	20	c.1785+2T>G	Donor splice site	Splice site	Novel
	POMGNT1	20	c.1785+2T>G	Donor splice site	Splice site	Novel
24	*POMGNT1*	17	c.1425G>A	p.Trp475X	Nonsense	Novel
	POMGNT1	17	c.1425G>A	p.Trp475X	Nonsense	Novel
25	*LARGE*	13	c.1548C>G	p.Trp516X	Nonsense	Novel
26	*FKTN*	8	c.920G>A	p.Arg307Gln	Missense	Leiden database
	FKTN	8	c.920G>A	p.Arg307Gln	Missense	Leiden database
27	*FKTN*	8	c.915G>A	p.Trp305Cys	Missense	Novel
	FKTN	8	c.915G>A	p.Trp305Cys	Missense	Novel
28	*FKTN*	8	c.919C>T	p.Arg307X	Nonsense	Novel
	FKTN	8	c.919C>T	p.Arg307X	Nonsense	Novel
29a, 29b †	*FKTN*	8	c.920G>A	p.Arg307Gln	Missense	Novel [3]
	FKTN	9	c.1167dupA	p.Phe390fs	Frameshift	Leiden database [3]
30 ‡†	*FKTN*	9	c.1167dupA	p.Phe390fs	Frameshift	Leiden database [3]
	FKTN	10	c.1363delG	p.Asp455fs	Frameshift	Novel [3]
31a, 31b	*FKTN*	4	c.340G>A	p.Ala114Thr	Missense	Novel
	FKTN	7	c.859delA	p.Thr286fs	Frameshift	Novel

Table 6. A summary of pathogenic mutations detected in this study.

Probands are numbered. Affected siblings are indicated with letters. * Family studies carried out to investigate segregation of the variant through the pedigree. † Functional characterisation described in section 3.2.3. ‡ Functional characterisation described in section 3.2.4. † Functional characterisation described in section 3.3.1. The following patients have been reported individually; [1] Patients previously described in Mercuri *et al.* 2006. [2] Patients previously described in Clement *et al.* 2007. [3] Patients previously described in Godfrey *et al.* 2006.

Patient	Gene	Exon/intron	Nucleotide change	Predicted amino acid change	Mutation type	References
32	*POMT1*	9	c.905T>G	p.Phe302Cys	missense	Novel
33	*POMT1*	20	c.2203C>T	p.Arg735Cys	missense	Novel
34	*POMT1* *POMT1*	20 20	c.2248+5A>G c.2248+5A>G	intronic intronic	intronic intronic	Novel Novel
35	*POMT1*	20	c.2246G>A	synonymous	synonymous	Novel
36	*LARGE*	4	c.309C>A	synonymous	synonymous	Novel
37	*LARGE*	12	c.1431C>T	synonymous	synonymous	Novel
38	*LARGE*	13	c.1640G>A	p.Arg547His	missense	Novel
39, 40	*LARGE*	14	c.1827A>T	synonymous	synonymous	Novel

Table 7. Summary of unclassified variants.

	WWS	MEB/FCMD	CMD-CRB	CMD-MR	CMD-no MR	LGMD-MR	LGMD-no MR	Total
POMT1	1	1	-	3	-	3	-	8
POMT2	-	6	2	-	-	1	-	9
POMGNT1	-	6	-	-	-	-	1	7
FKTN	1	1	-	-	1	-	3	6
LARGE	1	-	-	-	-	-	-	1
Mutation detected	3 (60%)	14 (47%)	2 (50%)	3 (20%)	1 (10%)	4 (80%)	4 (20%)	31 (34%)
Patient total	5	30	4	15	10	5	20	92 *

Table 8. The phenotypic distribution of patients within the cohort, the frequency of mutations in each of the five glycosyltransferase genes analysed and the comparative mutation frequencies for individual clinical categories.

WWS; Walker-Warburg syndrome, MEB/FCMD; muscle eye brain syndrome/ Fukuyama congenital muscular dystrophy, CMD-CRB; congenital muscular dystrophy with cerebellar involvement, CMD-MR; congenital muscular dystrophy with mental retardation, CMD-no MR; congenital muscular dystrophy with no mental retardation, LGMD-MR; limb girdle muscular dystrophy with mental retardation, LGMD-no MR; limb girdle muscular dystrophy with no mental retardation. * Includes three patients not assigned a clinical classification due to insufficient clinical information.

A variety of mutation types were identified; 37 missense mutations; 7 nonsense mutations; 9 frameshift mutations; 1 insertion/deletion mutation; 1 deletion and 6 splice site mutations. No mutation hotspots were identified in any of these five genes (Figure 14). From a total of 37 different mutations, eight were found to be recurrent within the cohort. The p.Ala200Pro mutation in *POMT1*, previously described as prevalent within the Turkish population, was detected in three patients, two of Turkish origin and one of Greek decent (patients A3, A7 and A8 respectively) (Balci et al., 2005). The *POMGNT1* donor splice site mutation c.1539+1G>A found to account for the enrichment of MEB within the Finnish population was detected in two patients (patients A21 and A22 respectively) (Diesen et al., 2004). Three further novel mutations were detected more than once, specifically the p.Tyr666Cys mutation in *POMT2* which was found both in the homozygous and heterozygous state in four patients. Segregation of this novel missense mutation was studied in a large pedigree and was found to segregate with the disease (patient A15). Parental samples where studied for 11 probands to ensure that compound heterozygous mutations were in *trans* and that apparent homozygous mutations in the proband were not masking undetected deletions. Where parental DNA was tested (22 families in total) a single paternal mutation was found to occur *de novo* (*POMT2*; c.2150T>C; p.Phe117Ser). A relatively similar frequency of patients with mutations detected in *POMT1*, *POMT2*, *POMGNT1* and *FKTN* was detected (Table 8). In contrast, only a single patient was found to have a pathogenic mutation in *LARGE* although we were unable to identify a second mutation (patient A25).

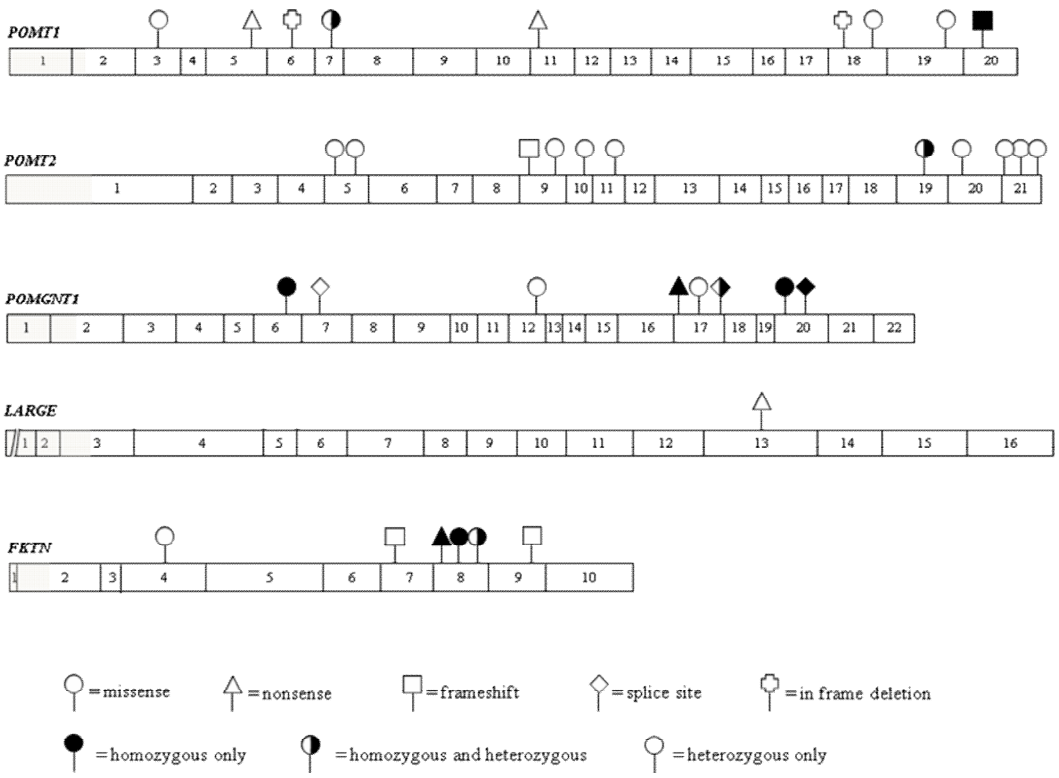

Figure 14. Distribution of mutations in *POMT1*, *POMT2*, *POMGNT1*, *FKTN* and *LARGE*.

White boxes represent individual coding exons, dark grey boxes indicate non-coding exons. All exons are numbered accordingly. The size of the box corresponds to the number of base pairs within each exon. Mutation types and locations are represented by symbols above the appropriate exon; circles represent missense mutations; triangles represent nonsense mutations; squares represent frameshift mutations; diamonds represent splice site mutations; crosses represent in frame deletions. Dark symbols indicate mutations found only in the homozygous state, white symbols indicate mutations found only in the heterozygous state and mixed symbols indicate mutations found in both states.

Patient A16 *POMT2*; c.2243G>C; p.Trp748Ser (exon21)

Patient A16 *POMT2*; c.551C>T; p.Thr184Met (exon5)

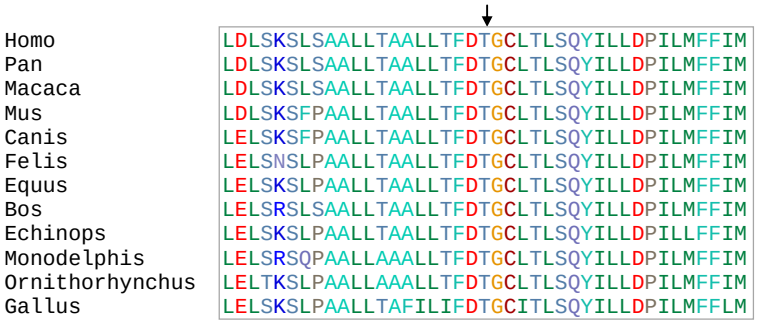

Patient A18 *POMGNT1*; c.526A>C; p.Thr176Pro (exon 6)

Patient A27 *FKTN*; c.915G>A; p.Trp305Cys (exon 8)

Figure 15. Protein alignment (homology) plots of *POMT2*, *POMGNT1* and *FKTN*.

A total of 12 vertebrate species are shown. The complete conservation of sequence variants detected in patients A16, A18 and A27 is indicated by arrows and are flanked by 40 amino acids.

Genotype-phenotype correlations

The spectrum of phenotypes associated with mutations in *POMT1* included WWS (1 case), MEB-FCMD (1 case), CMD-MR (3 cases) and LGMD-MR (3 cases). *POMT2* mutations were observed in patients with MEB-FCMD (6 cases), CMD-CRB (2 cases) and LGMD-MR (1 case). Six patients with *POMGNT1* mutations had WWS and a single case had LGMD-no MR. Phenotypes associated with mutations in *FKTN* were detected in patients with WWS (1 case), MEB-FCMD (1 case), CMD-no MR (1 case) and LGMD-no MR (3 cases). A mutation in *LARGE* was detected in a single patient with WWS (Table 5).

No clear difference in phenotype was observed between patients with and without mutations in any of these genes. The phenotypic spectrum of patients without identifiable mutations was similar to that of patients with mutations.

3.2.3 Functional Characterisation of the *POMGNT1* Variant p.Asp556Asn

The detection of a homozygous *POMGNT1* non-synonymous variant in a patient with LGMD-no MR warranted further investigation (patient A20, c.1666G>A; p.Asp556Asn). Thus far mutations in this gene have not been described in patients without associated brain involvement.

The sequence change was found to segregate with disease in all family members tested. This substitution causes a non-conservative amino acid change that affects an evolutionary conserved amino acid residue within the catalytic domain (Figure 16).

A

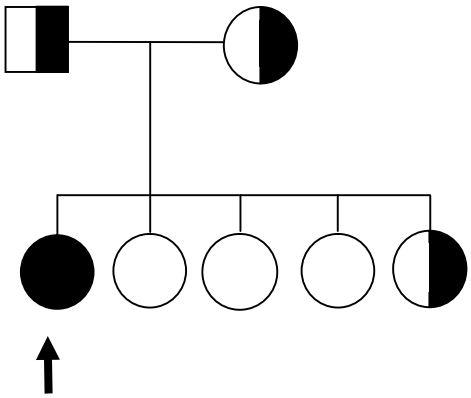

B

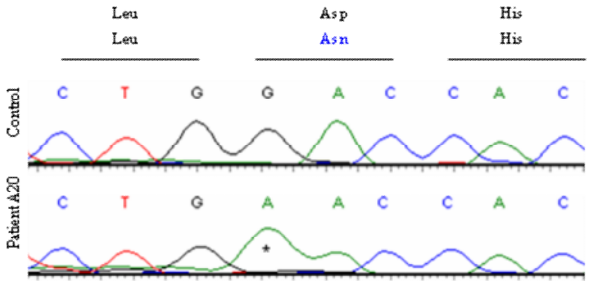

Figure 16. Sequence analysis: *POMGNT1* variant c.1666G>A; p.Asp556Asn.

A) The arrow indicates patient A20. Circles denote females and the square denotes a male. Fully shaded shapes indicate homozygosity for the *POMGNT1* variant, semi shaded shapes indicate carriers of this variant. B) Electropherograms showing the sequence variation in *POMGNT1*. An asterisk denotes the homozygous mutation (c.1666G>A) that leads to a predicted amino acid change (p.Asp556Asn).

Subcellular localisation of mutant *POMGNT1* constructs

To observe the effects of the variant found in patient A20 on *POMGNT1* expression and localization, I introduced the c.1666G>A; p.Asp556Asn variant into the wild-type *POMGNT1* tagged construct. The mutant construct appeared to be expressed at levels similar to the wild-type construct and retained co-localization with the Golgi apparatus marker GM130 in transfected myotubes (Figure 17).

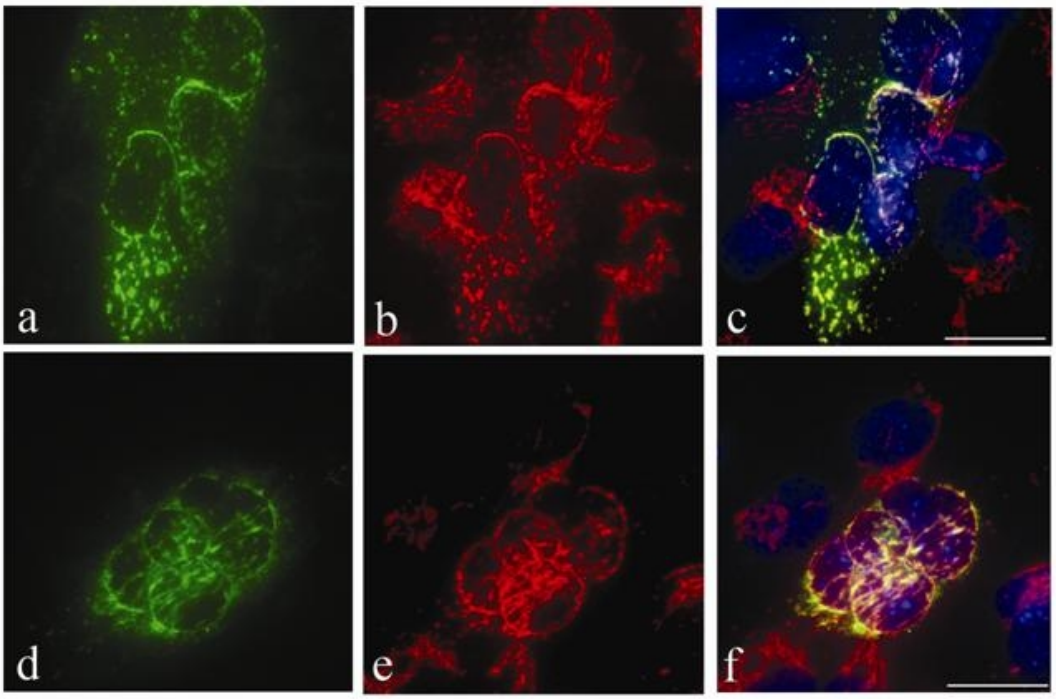

Figure 17. Double labelling of *POMGNT1*-V5 constructs and GM130 on transfected C2C12 myotubes.

The merged images (c and f) indicate that both wild-type (a-c) and mutant *POMGNT1* (c.1666G>A; p.Asp556Asn) constructs (d-f) colocalize with the Golgi apparatus marker GM130. Green channel; anti-V5 antibody; red channel; anti-GM130 antibody; blue channel; Hoechst 33342 nuclear stain. Scale bar; 10μm.

Investigating the creation of a novel *N*-glycosylation site

The c.1666G>A alteration results in a substitution of aspartic acid with an asparagine residue at position 556. This alteration creates a potential *N*-glycosylation site (Asn-X-Ser/Thr-X-, where X is any amino acid except proline) in the protein which is predicted to have no other such sites (Asp-His-Ser-Lys to Asn-His-Ser-Lys). To observe the effects of the variant detected in patient A20 on *POMGNT1* expression and localisation, I transfected C2C12 cells with human V5-tagged wild type and mutant (c.1666G>A; p.Asp556Asn) *POMGNT1*. Protein extracts from these cells were analysed by western blotting using a V5-specific antibody. No difference in molecular weight of mutant and wild type protein was observed in this system indicating that this mutation does not induce aberrant *N*-glycosylation at this site (Figure 18).

A

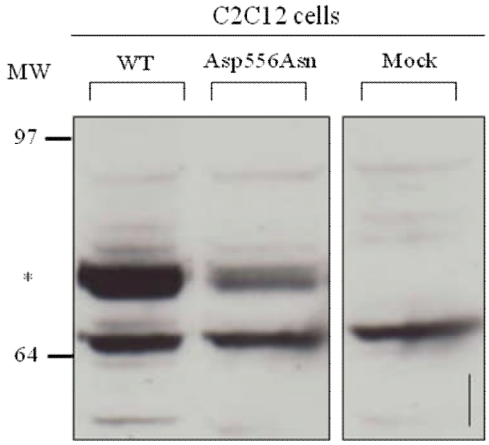

B

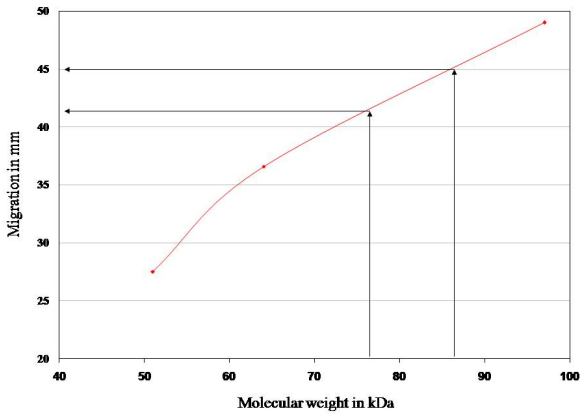

Figure 18. Investigating the creation of a novel *N*-glycosylation site in *POMGNT1*. C2C12 cells were transfected with wild-type (WT) and mutant *POMGNT1* (c.1666G>A; p.Asp556Asn) V5-tagged constructs. A) Proteins were resolved by SDS-PAGE and immunoblotted with an antibody to V5. MW, molecular weight in kDa. *POMGNT1* V5-tagged protein is indicated by an asterisk, whilst the band below this is a non specific band. * Indicates transfected V5-tagged *POMGNT1*. Vertical bar (approximately 3 mm) indicates the predicted change in migration of V5-tagged *POMGNT1* if aberrantly *N*-glycosylated. B) Graph showing calculations of predicted change in migration of *POMGNT1* if aberrantly *N*-glycosylated (Vogt et al., 2005).

Collaborative functional investigations; kinetic analysis

Quantifying the pathological consequence of *POMGNT1* mutations has been facilitated by the development of a functional assay measuring *POMGNT1* enzyme activity. This assay enables the detection of pathogenic *POMGNT1* alterations in both individuals with MEB as well as carriers of these mutations. Its implementation and has been used as a successful adjunct to diagnosis. In a collaborative study with Professor Harry Schachter's group in the department of Structural Biology and Biochemistry in Toronto, Canada, skin fibroblasts from patient A20 were analysed by methods previously described (Vajsar et al., 2006; Zhang et al., 2003). Conventional enzyme assays measuring apparent Vmax values detected no significant difference between controls and patient A20. During a more detailed analysis of patient 20's fibroblasts, *POMGNT1* activity was measured at four different substrate concentrations. An altered kinetic profile of the mutant enzyme was subsequently detected. The apparent K_m for UDP-GlcNAc is substantially higher and the V_{max} for Manα1-O-benzyl is substantially lower than in the control sample. Detailed descriptions of these results have been reported in Clement et al (Clement et al., 2008b).

Prevalence of the *POMGNT1* sequence change c.1666G>A

The *POMGNT1* sequence change c.1666G>A; p.Asp556Asn was excluded as a common polymorphism as it was not found in the dbSNP yet I detected the variant in 1 of 150 white European control chromosomes (please refer to section 2.1.1).

3.2.4 Further Collaborative Functional Investigations

Where available, fibroblasts from patients with detected sequence alterations were sent for analysis in Professor Kevin Campbell's laboratory (Howard Hughes Medical Institute, Department of Physiology and Biophysics, Department of Neurology, University of Iowa, USA). A complementation assay was performed by viral transfection of wild type constructs containing either human *POMT1*, *POMT2*, *POMGNT1*, *FKTN* or *FKRP*. Successful complementation was observed as a restoration of immunoreactivity to IIH6 on western blot. Fibroblasts from patients A8, A9, A12 and A30 were analysed.

As predicted, complementation was successful in cell lines from patient's A8, A12 and A30 using plasmids for *POMT1*, *POMT2* and *FKTN* respectively. All three patients harboured a mutation predicted to cause nonsense mediated decay. Patient A9, with two missense changes in *POMT2* was confirmed as having a *POMT2* defect.

3.3 DISCUSSION

Dystroglycanopathies are a recently defined, common group of muscular dystrophies encompassing an extremely wide spectrum of clinical severity and are caused by mutations in at least six genes encoding putative or demonstrated glycosyltransferases. The comparatively small coding region of *FKRP* has facilitated the rapid correlation between genotype and phenotype, allowing the discovery of pathogenic mutations in patients with LGMD2I, MDC1C, MEB-like and WWS-like disorders. However, there was no information regarding the frequency of involvement or the genotype-phenotype relationships for the remaining five glycosyltransferase genes in a large and unbiased population.

In this study we have systematically screened for mutations in *POMT1*, *POMT2*, *POMGNT1*, *FKTN* and *LARGE* in patients in whom we had previously ruled out *FKRP* gene involvement. Mutations were detected in 34% of these patients.

3.3.1 Genotype-Phenotype Correlations

Protein-*O*-mannosyltransferase 1 (*POMT1*)

Mutations in *POMT1* have previously been reported in patients with WWS, CMD-MR and LGMD-MR (LGMD2K). Within our cohort, all patients with mutations in *POMT1* had evidence of functional brain involvement either with no clear associated structural brain abnormalities (3 patients with LGMD2K (LGMD MR), and 3 patients with CMD-MR), or more severe conditions with structural brain defects (one patient with WWS, and one individual with a MEB-like phenotype). This suggests that the majority, if not all patients with *POMT1* mutations have either functional or structural central nervous system involvement, including those patients with relatively mild muscle weakness.

This is in contrast to patients in the present study with mutations in *FKTN* and to that previously reported for *FKRP* mutations.

Protein-*O*-mannosyltransferase 2 (*POMT2*)

Mutations in *POMT2* were confined to patients with evidence of brain involvement. Nine patients had pathogenic *POMT2* mutations; 6 with a MEB-FCMD phenotype, 2 with a CMD-CRB phenotype and a single patient with LGMD-MR. This latter patient has learning difficulties and remains ambulant at age 20 having presented, at 18 months of age, with developmental delay (patient A16). These findings indicate that like *POMT1*, the majority or all patients with mutations in *POMT2* have evidence of central nervous system involvement. In addition, we have identified the mildest phenotype associated with mutations in *POMT2* reported to date in an individual with LGMD-MR.

Protein *O*-linked mannose beta1,2-*N*-acetylglucosaminyltransferase (*POMGNT1*)

To date *POMGNT1* mutations have been described in patients with a phenotype consistent with MEB, although rare cases with more severe clinico-radiological features, resembling WWS, have also been reported (Taniguchi et al., 2003; Yoshida et al., 2001). The majority of patients in this study had an MEB- like disorder suggesting that *POMGNT1* mutations more frequently give rise to congenital disorders with associated structural brain involvement. A single patient possessing a LGMD phenotype and entirely normal intellectual function harboured a homozygous missense change. Applying the initial classification system, this variant was included in the mutation table yet further functional investigations uncovered a more complicated profile (please refer to section 3.3.2).

Like-glycosyltransferase (*LARGE*)

We were only able to identify a single potentially pathogenic *LARGE* mutation in a patient with typical WWS phenotype who died in the first few months of life (patient A25). Absent immunofluorescence staining was demonstrated on this patient's skeletal muscle biopsy using antibodies which recognise the glycosylated epitope of α-

dystroglycan. Unfortunately neither sufficient DNA nor frozen muscle from this patient was available to investigate the presence of a second, as yet undetected, mutation.

Fukutin (*FKTN*)

Mutations in *FKTN*, typically associated with FCMD in Japan were found in six patients, none of whom are of Japanese origin. Only two of these patients had structural brain involvement; one patient affected by WWS (patient A28) and one by a MEB-FCMD phenotype (patient A27). The remaining patients had no structural brain involvement; one case had CMD-no MR (patient A26) and never acquired the ability to walk but has normal IQ and 5 individuals from 3 families have entirely normal intellect and a mild LGMD phenotype (LGMD2L) (patients A29, A30, and A31). Interestingly in two of these families (A29 and A30), a dramatic response to steroid therapy was noted (Godfrey et al., 2006). In striking contrast to what has previously been reported in FCMD, none of these 5 patients have evidence of central nervous system involvement. Our findings together with the recent description by Murakami *et al.* of individuals with *FKTN* mutations presenting with a predominant cardiomyopathy, suggest that the majority of mutations outside Japan give rise to conditions milder than FCMD and are not usually associated with structural brain involvement (Murakami et al., 2006).

Further functional investigations were carried out on two mutations detected in patients A29 and A30 by members of the Dubowitz Neuromuscular Centre; p.Arg307Gln and Asp455fs were introduced into a wild type *FKTN* tagged construct. Both mutations appeared to be expressed at levels similar to the wild-type construct and retained co-localisation with the Golgi apparatus marker GM130 (data not shown). Detailed descriptions of these have been reported in Godfrey *et al*. (Godfrey et al., 2006).

Mutation frequencies

Mutations in *POMT2* were the most prevalent with 9 cases, followed by *POMT1* with 8 cases, *POMGNT1* with 7 cases, *FKTN* with 6 cases and finally *LARGE* with only a single case.

Members of the Dubowitz Neuromuscular Centre had previously identified *FKRP* mutations in 79 patients. Approximately 75% of these patients have a LGMD2I phenotype (Beltran-Valero de Bernabe et al., 2004; Brockington et al., 2001a; Mercuri et al., 2006; Topaloglu et al., 2003). The relative frequency of *FKRP* involvement needs to be considered with caution as it clearly reflects the genetic origin of patients studied within the Dubowitz Neuromuscular Centre. For example screening of 79 Australian LGMD dystroglycanopathy patients detected only two *FKRP* mutations. However, when amalgamating these results, it remains clear that *FKRP* mutations are the most frequent in this group of conditions. Both our department and others have previously published extensively on the spectrum of these mutations (Brockington et al., 2001a; Brockington et al., 2001b; Harel et al., 2004; Lin et al., 2007; Mercuri et al., 2003; Mercuri et al., 2006; Topaloglu et al., 2003; Vieira et al., 2006).

Genotype-phenotype correlations

Pathogenic mutations were detected in 3 of 5 patients with WWS syndrome (60%), 14 of 30 patients with a MEB/FCMD phenotype (47%), 2 of 4 patients with CMD-CRB (50%), 3 of 15 patients with CMD-MR (20%), 1 of 10 patients with CMD-no MR (10%), 4 of 5 patients with LGMD-MR (80%), and 4 of 20 patients with LGMD-no MR (20%) (Table 7).

Patients with associated structural brain defects belonging to the severe end of the clinical spectrum showed no apparent difference in their pattern of skeletal muscle weakness or central nervous system involvement in relation to the gene involved. However, the 4 LGMD patients with associated MR and microcephaly all had mutations in either *POMT1* or *POMT2*. No mutations were identified in the remaining patients. Conversely a number of patients with more severe muscle weakness and no brain involvement (CMD-no MR) were found to have mutations in *FKTN*, similar to that previously described in MDC1C (Brockington et al., 2001a). This suggests that there may be a hierarchical involvement of muscle and brain arising from individual gene mutations, with *POMT1* and *POMT2* being associated with significant central nervous system involvement even in patients with relatively mild weakness and who remain ambulant (LGMD2K). This does not appear to be a feature of *FKTN* or *FKRP*. These results suggest that in some individual subcategories certain genes are more likely to be

involved than others and this should be taken into account when undertaking mutation analysis in the dystroglycanopathies.

3.3.2 Functional Investigations

Without further RNA studies and functional biochemical analysis it is difficult to determine the pathogenicity of unclassified variants. This is exacerbated by the abundance of missense variants within these genes.

Further functional characterisation of the *POMGNT1* variant p.Asp556Asn was performed by me and others. This variant was detected in a patient with LGMD yet no associated brain involvement. Several lines of evidence initially suggested that the alteration identified in patient A20 was pathogenic. The variant was found to segregate with the disease in this large family. This substitution causes a non conservative amino acid change that affects an evolutionary conserved amino acid residue (Figure 19). The mutation causes a reversal of amino acid polarity in the substrate specific domain of *POMGNT1* which may be expected to have functional consequences. In addition, the detailed enzymatic studies offer support for this theory. *POMGNT1* activity was observed in the patient's fibroblasts yet differs in its kinetics from that of controls. This altered kinetic profile is less marked than in patients with MEB and in keeping with the relatively mild phenotype in our patient.

A

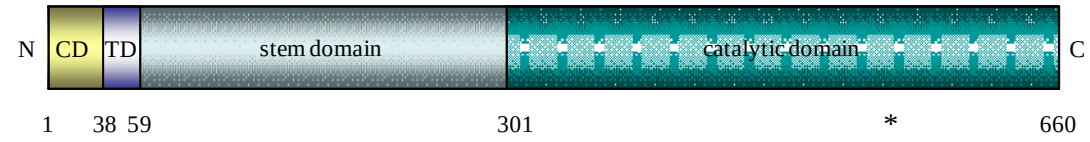

B

Figure 19. Sequence analysis *POMGNT1* variant p.Asp556Asn.

A) Location of an amino acid change in the catalytic substrate specificity domain of *POMGNT1*. Human *POMGNT1* is composed of a cytoplasmic domain (CD, amino acids 1-38), a transmembrane domain (TD, amino acids 39-59), a stem domain (amino acids 60-301) and a catalytic domain (amino acids 302-660). * Indicates the position of the patient mutation (p.Asp556Asn). B) Panel shows a protein alignment (homology) plot of the catalytic domain of *POMGNT1* in 16 vertebrate species, with complete conservation of Asp556Asn (arrow).

It is interesting to note that this mutation does not affect either the expression or subcellular localisation of a recombinant form of *POMGNT1*. The p.Asp556Asn mutation introduces a potential *N*-glycosylation site (Asn-X-Ser) into the protein which is predicted to have no other such sites. Vogt *et al.* reported that an unexpectedly high proportion of pathogenic mutations lead to the creation of *N*-glycosylation sites (Vogt et al., 2005). The authors demonstrated that the pathogenic effect of mutations in IFNγR2 was a direct consequence of the addition of *N*-linked carbohydrate. Although this study focussed on those proteins that undergo trafficking through the ER, some transmembrane proteins lacking a signal peptide or signal anchor can also be subjected to gains in glycosylation (Hammerle et al., 2000). It may be hypothesised that the presence of an *N*-glycan on *POMGNT1* within the substrate specific region of the catalytic domain may cause defective enzyme folding resulting in an active but inefficient enzyme. However no change in molecular weight on western blot was detected between wild-type and mutant *POMGNT1* constructs, therefore it is unlikely that this protein is aberrantly glycosylated. The *N*-glycosylation consensus sequence described is a prerequisite for modification; however not all of these sequons are glycosylated. *In silico* analysis to examine the sequence context of Asn-X-Ser sequon by NetNGlyc Server 1.0 (Technical University of Denmark) did not predict *N*-glycosylation at this site, adding to evidence that this variant does not cause the addition of aberrant carbohydrate moieties.

Subsequent to the publication of this study, we became aware that this sequence change had been detected within a French family. Both a patient with MEB disease and her apparently unaffected sibling were both homozygous for this change. In addition, this variant was detected in 8 out of 218 alleles from healthy French controls (Celin Bouchet, unpublished observation). This is surprising in view of our findings but, if confirmed will effectively exclude the p.Asp556Asn as being pathogenic. It therefore remains to be established whether the altered kinetic profile detected in *POMGNT1* is a polymorphism or contributes to the patient's phenotype. Indeed the alteration in *POMGNT1* kinetics may be due to a secondary effect of an as yet unidentified gene defect. We are currently awaiting a fibroblast cell line from the unaffected French sibling to ascertain *POMGNT1* function.

Functional characterisations were performed on a further four patient fibroblast cell lines by collaborators in America. Members of Professor K Campbell's department were able to confirm *POMT1*, *POMT2* and *FKTN* defects in four patients using a complementation assay. However, this approach was not useful to confirm/exclude the pathogenesis of a *POMGNT1* defect in patient A20's fibroblasts. To perform the assay, a dramatic reduction in immunoreactivity to the monoclonal antibody IIH6 is required. The mild reduction in α-dystroglycan epitope staining in patient A20's fibroblasts was not sufficient to detect a quantifiable improvement when transfected with a panel of virus.

The application of functional data to ascertain the pathological consequences of unclassified variants is an especially valuable tool in clinically and genetically heterogeneous disorders. Nevertheless, the investigation of the p.Asp556Asn variant in *POMGNT1* yielded a complex profile and highlights the difficulty in interpreting data in patients with atypical clinical presentations.

3.3.3 Conclusions

The results of this study demonstrate that the phenotypic spectrum of disorders associated with mutations in six of the known glycosyltransferase genes is significantly wider than initially suspected. In part this is due to the high prevalence of founder mutations within specific populations (Diesen et al., 2004; Kobayashi et al., 1998). We have expanded the clinical phenotypes associated with mutations in *POMT1*, *POMT2*, *FKTN* and *LARGE*. Despite this we have not observed a full spectrum of phenotypes associated with each gene, in particular *POMT1*, *POMT2* and *LARGE*. Numerous patients with clinicopathological features indistinguishable from the ones detailed in this study were not found to have mutations in any of the genes analysed.

This large and unbiased study redefines the clinical spectrum associated with each of the glycosyltransferases genes included. It identifies the frequency of individual gene defects and suggests that, after the exclusion of *FKRP*, the majority of patients with a dystroglycanopathy do not harbour mutations in any of the known genes. This work therefore suggests that further, as yet unknown genes will be involved in the

pathogenesis of the dystroglycanopathies. The identification of these genes will provide important information defining the pathway of glycosylation of α-dystroglycan.

CHAPTER 4. CANDIDATE GENE ANALYSIS

4 CANDIDATE GENE ANALYSIS

4.1 INTRODUCTION

At the time the study in chapter 3 was performed, pathogenic mutations had been identified in a total of six genes responsible for dystroglycanopathies. After the exclusion of *FKRP*, mutation screening of *POMT1*, *POMT2*, *POMGNT1*, *FKTN* and *LARGE* in a large cohort identified mutations in approximately a third of all cases. These findings reported for the first time the proportion of patients in whom a molecular diagnosis remains undefined. In addition it was noted that those patients without an identifiable mutation were clinically and pathologically indistinct from those with identified mutations. A clear limitation of this analysis is that only coding exons and bordering intronic splice sites were sequenced. It is therefore possible that some patients in cohort A (those screened in chapter 3) may instead harbour pathogenic structural or regulatory region defects in the genes studied. It is however, unlikely that these pathogenic variants account for a considerable proportion of patients in whom a gene defect remains undefined. It would be expected that if these mutations were highly prevalent within our population, an abundance of patients would have been identified as heterozygous for one clearly pathogenic mutation, but with no detectable second mutation. Only a single such case was identified in cohort A (patient A25). Therefore the high proportion of cases with no identifiable mutation strongly suggests that novel genes are likely to be involved in the pathogenesis of dystroglycanopathies. The challenge has therefore shifted focus to investigate novel genes. The identification of genetic defects in these patients would not only yield novel insights into the pathway of α-dystroglycan glycosylation but would improve the diagnosis, classification and counselling of patients and their families.

In the past, the analysis of linkage data from patient cohorts with specific clinical presentations has yielded fruitful results, specifically led to the identification of mutations in *FKTN* and *POMGNT1* (Kobayashi et al., 1998; Yoshida et al., 2001). The success of these studies relied on the elevated prevalence of specific mutations within distinct populations. The relatively high incidence of specific clinical phenotypes in Caucasian, Japanese and Finnish populations demonstrates the importance of founder effects in the aetiology of these diseases (Brockington et al., 2001b; Kobayashi et al.,

1998; Yoshida et al., 2001). Despite the success of this approach, those patients with no detectable mutations (described in chapter 3) are both clinically and ethnically diverse. This indicates that their underlying genetic defects are unlikely to be caused by a single mutation residing in a novel gene derived from a common ancestral chromosome. In support of this, evidence from homozygosity mapping performed on eleven unrelated consanguineous families with WWS failed to pinpoint a single loci indicating the presence of extensive genetic heterogeneity (van Reeuwijk et al., 2005b). The prospect remains that a large number of defective genes underlie the pathogenesis in these unresolved dystroglycanopathy cases. The contribution of novel genes could reflect that of *LARGE*, where the number of patients reported in the literature with mutations in this gene remains extremely low, despite its identification more than seven years ago (Longman et al., 2003; van Reeuwijk et al., 2007). The anticipated level of heterogeneity therefore challenges the appropriateness of using standard mapping strategies to identify novel genes, especially those involving the pooling of linkage data from a number of small pedigrees.

With such clinical, ethnic and presumed genetic heterogeneity within a cohort of sporadic cases, whole genome candidate gene analysis presents as an appropriate alternative strategy. Within the dystroglycanopathies alone, this methodology has proved successful in leading to the identification of mutations in *FKRP*, *POMT1*, *POMT2* and more recently, *DPM3*. This chapter describes the application of this approach to our cohort of molecularly unresolved dystroglycanopathy cases. I systematically screened a cohort of patients for mutations in a panel of candidate genes selected using a variety of rationales. In addition I functionally assessed the involvement of a subset of these genes in the pathway of α-dystroglycan glycosylation.

4.2 RESULTS

4.2.1 Clinical Findings

Patient cohort B comprised of 37 probands (patients B1-B37) from a range of ethnicities, the inclusion criteria of which is detailed in section 2.1.1. As previously stated, clinical data was analysed by Professor F Muntoni and Dr E Clement. Patients were classified into 1 of 7 broad clinical categories as described in section 3.2.1. The

cohort consisted of total of 22 patients with CMD and 15 patients with LGMD. A total of 21 patients had brain involvement. The division of phenotypes within the cohort is shown in Table 9.

Phenotypic category	Hypoglycosylation of α-dystroglycan	Muscle unavailable for α-dystroglycan studies	Total
Walker-Warburg syndrome	1	1	**2**
Muscle eye brain disease/Fukuyama CMD	8	2	**10**
CMD cerebellar involvement	1	1	**2**
CMD mental retardation	3	2	**5**
CMD no mental retardation	3	0	**3**
LGMD mental retardation	1	1	**2**
LGMD no mental retardation	9	4	**13**
Total	**26**	**11**	**37**

Table 9. Clinical classifications of 37 patients within cohort B.

CMD; Congenital Muscular Dystrophy, LGMD; Limb Girdle Muscular Dystrophy.

4.2.2 Identification of Novel Candidate Genes

I selected a total of seven genes as potential candidates for dystroglycanopathy (Table 12). The existence of naturally occurring and engineered animal dystroglycanopathy models provided a solid source of candidate genes. The analysis of functional candidates as well as the use of a bioinformatics approach identified a further four genes.

Animal models

Hypoglycosylation of α-dystroglycan has been demonstrated in a naturally occurring muscular dystrophy chicken (Saito et al., 2005). This was observed using the same monoclonal antibody routinely used in the diagnosis of dystroglycanopathy patients (Ervasti and Campbell, 1991; Saito et al., 2005). Linkage studies identified a homozygous region spanning approximately 1 Mb on chicken chromosome 2q containing only seven genes (Matsumoto H, 2007). A single homozygous missense alteration (c.1321G>A; p.Arg441Gln) was identified in the gene encoding ubiquitin ligase WW domain-containing protein 1 (*Wwp1*), although the pathogenic effect of this novel sequence variant has yet to be demonstrated (Matsumoto et al., 2008). E3 ubiquitin ligases are thought to function in the ubiquitin proteasome system; the major pathway responsible for protein degradation in eukaryotic cells through its ability to selectively target proteins for destruction. Ubiquitination is catalysed by three enzymes acting in a cascade; a ubiquitin activating enzyme (E1), a ubiquitin conjugating enzyme (E2) and a ubiquitin protein ligase (E3). The E3 ubiquitin ligase provides substrate specificity and catalyses isopeptide bond formation between ubiquitin and the substrate (Hirsch et al., 2009). The human *WWP1* ortholog resides on chromosome 8q21 and shares 83% amino acid identity with the chicken *Wwp1* protein (Matsumoto et al., 2008). Human *WWP1* is ubiquitously expressed with the highest expression in skeletal muscle and brain (Wood et al., 1998). This gene therefore warrants investigation as a candidate for human dystroglycanopathy.

The analysis of zebrafish is a powerful novel tool in the characterisation of gene function and in the dissection of disease pathogenesis. Very recently a novel zebrafish

morphant generated in the laboratory of our collaborator, Dr D Stemple at the Wellcome Trust Sanger Institute, Cambridge University, was found to suffer clinico-pathological features that were highly suggestive of a dystroglycanopathy (unpublished data). The knockdown of glycogenin (*Gyg*) expression caused a reduction in immunoreactivity to the monoclonal antibody IIH6, as well as causing a phenotype strikingly similar to that resulting from *Fkrp* knockdown in zebrafish (Kawahara et al., 2010; Thornhill et al., 2008). Glycogenin is a self-glucosylating protein primer that initiates the synthesis of glycogen. Humans possess two glycogenin genes: glycogenin 1 (*GYG1*) resides on chromosome 3q24-q25.1 and glycogenin 2 (*GYG2*) located at Xp22.3. Human *GYG2* is notably larger, and shares an overall amino acid identity with *GYG1* of 40-45% (Mu et al., 1997). Both human glycogenin proteins can self-glucosylate using UDP-glucose as a donor, the products of which are subsequently extended with glucose monomers by the action of glycogen synthase (encoded by *GYS*) [OMIM; 138570] (Lomako et al., 2004; Mu et al., 1997). The presence of *GYG2* paralogs are limited to mammals yet absent in rodent species (Figure 20). Many other organisms have been shown to harbour multiple glycogenin or glycogenin-like genes such as *Saccharomyces cerevisiae* which harbours two genes encoding self glucosylating proteins. Interestingly *GYG1*, *GYG2* and the proximal domain of *LARGE* demonstrate close homology to a bacterial GT8 glycosyltransferase protein family involved in lipooligosaccharide synthesis (Coutinho et al., 2003). This evidence indicates that both human glycogenin genes are promising candidates for dystroglycanopathy.

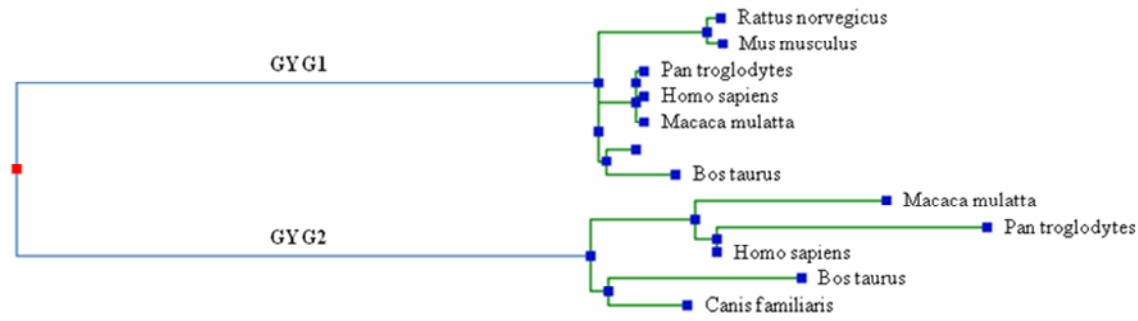

Figure 20. Phylogenetic tree depicting the mammalian glycogenin family.

Phylogenetic analysis of mammalian glycogenin reveals the *GYG1* paralog *GYG2*, is restricted to mammals and absent from rodent species. Figure generated using TreeFam (www.TreeFam.org).

Bioinformatic tools

In order to identify further candidate genes, I applied a bioinformatics approach to the whole genome. Endeavour software is based on the hypothesis that novel genes share either a similar role or biological processes with those genes known to be associated with disease (www.esat.kuleuven.be/endeavour/) (Aerts et al., 2006). In this study the ranking of candidates was derived from similarity to a 'training set' of genes which consisted of *POMT1*, *POMT2*, *POMGNT1*, *FKTN*, *FKRP* and *LARGE*. Data are subsequently mined from a range of bioinformatics resources (including information regarding annotation, sequence, expression, regulation and the available literature). Individual gene rankings are then merged into a global ranking of candidate genes (for more details please refer to section 2.2.10). Results are shown in Table 10. Two genes obtaining the highest rankings by the Endeavour search were Golgi apparatus resident proteins *GYLTL1B* and *β3GNT1*, both of which demonstrate significant homology to *LARGE* (Figure 21). Due to the only very recent discovery of α-dystroglycan hypoglycosylation in a patient with mutations in *DPM3*, this gene was absent from the 'training set' described above. Subsequent reanalysis generated with the inclusion of this gene retained *GYLTL1B* and *β3GNT* within the top six candidate genes (data not shown).

Rank *	Protein (*encoding gene*) **	Gene ID †	Location ††	Molecular function ‡	Subcellular localisation ‡‡
1	glycosyltransferase-like 1B (*GYLTL1B*)	120071	11p11.12	Glycosyltransferase	Golgi apparatus
2	UDP-GlcNAc:betaGal beta-1,3-*N*-acetylglucosaminyltransferase 1 (*β3GNT1*)	11041	11q13.2	Glycosyltransferase	Golgi apparatus
3	mannosyl (alpha-1,3-)-glycoprotein beta-1,2-*N*-acetylglucosaminyltransferase (*MGAT1*)	4245	5q35	Glycosyltransferase	Golgi apparatus
4	stromal cell-derived factor 2-like 1 (*SDF2L1*)	23753	22q11.21	Glycosyltransferase	Endoplasmic reticulum
5	beta-1,4-*N*-acetyl-galactosaminyl transferase 1 (*B4GALNT1*)	2583	12q13.3	Molecular function unclassified	Golgi apparatus

Table 10. Endeavour prioritised whole genome candidate genes.

* The top 5 ranked genes using the Endeavour gene prioritisation software (www.esat.kuleuven.be/endeavour/). The training set consisted of: *POMT1*, *POMT2*, *POMGNT1*, *LARGE*, *FCMD* and *FKRP*. ** Gene symbols and names as per HUGO nomenclature (www.genenames.org/). † Entrez Gene Identifier from the NCBI database (http://www.ncbi.nlm.nih.gov/). †† Denotes chromosomal location. ‡ Molecular function as classified by the PANTHER (Protein ANalysis THrough Evolutionary Relationships) Classification System (http://www.pantherdb.org/). ‡‡ Subcellular localisation as annotated via the Universal Protein Resource Knowledge Base (UniProtKB) (www.uniprot.org). Yellow shaded boxes indicate those genes investigated as candidate genes.

Glycosyltransferase-like 1B, encoded by *GYLTL1B*, is highly homologous to *LARGE* and present in a number of vertebrate species. Human *LARGE* and *GYLTL1B* share 68% amino acid identity indicating that the two genes are likely to have arisen via a gene duplication event (Grewal et al., 2005). *GYLTL1B* resides on chromosome 11p11.2 and encodes a 721 amino acid protein. Both *LARGE* and *GYLTL1B* have similar domain structure containing two catalytic domains, N-terminal cytoplasmic tails and variable stem region although *GYLTL1B* lacks the coil coil domain of *LARGE* (Figure 21). Epitope tagged *GYLTL1B* localises to the Golgi apparatus when over expressed in mouse myogenic C2C12 cells (Brockington et al., 2005; Grewal et al., 2005). Although the physiological functions of both *LARGE* and *GYLTL1B* remain elusive, intriguing properties of both proteins have recently been identified. The transient over expression of these genes in a variety of cells lines induced a dramatic increase in α-dystroglycan glycosylation which corresponds to an increase in high affinity binding to several extracellular matrix ligands (Barresi et al., 2004).

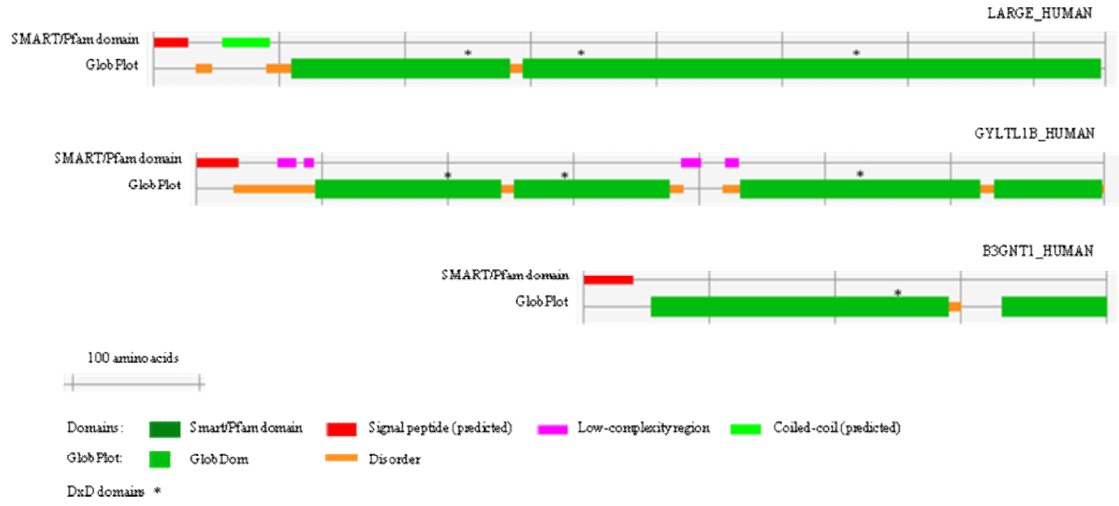

Figure 21. Schematic representation of the domain structures in human *LARGE*, *GYLTL1B* and *β3GNT1*.

Domains were predicted by the ELM server at http://elm.en.org. Conserved DxD motifs are indicated by *.

UDP-GlcNAc:betaGal beta-1,3-*N*-acetylglucosaminyltransferase 1, encoded by *β3GNT1*, is highly homologous to the N-terminal catalytic structural domain of *LARGE* (Figure 21) (Peyrard et al., 1999). The gene was originally identified by expression cloning as an enzyme that synthesises poly-*N*-acetyllactosamine, the production of which is essential for the formation of the i-antigen on human fetal blood cells (Sasaki et al., 1997). *β3GNT1* encodes a Golgi resident 397 amino acid protein and resides on chromosome 11q13.2. Bao *et al.* recently reported an association between the reduction in laminin-binding glycans and the decreased expression of *β3GNT1* in aggressive carcinoma cell lines. *β3GNT1* was subsequently found to be required for laminin-binding glycan synthesis through the formation of a complex with *LARGE* (Bao et al., 2009).

Therefore the application of a bioinformatics approach has identified two promising candidate dystroglycanopathy genes; *GYLTL1B* and *B3GNT1*.

Functional candidates

β1-6 *N*-acetylglucosaminyltransferase is a recently discovered glycosyltransferase functioning in the synthesis of *O*-mannosyl glycans (Inamori et al., 2003; Kaneko et al., 2003). The 792 amino acid protein is encoded by *MGAT5B* and resides on chromosome 17q25.3. *MGAT5B* has a type II membrane structure, typical of glycosyltransferases and is distinct from its homolog *GNTV* with regards to substrate specificity as it is capable of transferring to both *N*-linked and *O*-mannosyl linked acceptors (Inamori et al., 2004; Inamori et al., 2003; Inamori et al., 2006). In vitro studies reveal that *MGAT5B* prefers *O*-mannosyl acceptors catalysing the transfer of GlcNAc in β(1,6) linkage to the peptide-*O*-linked mannose, but only if the β(1,2) linked GlcNAc formed by *POMGNT1* is present (Figure 22) (Abbott et al., 2006). The NeuAcα2,3Galβ1,4GlcNAcβ1,2[NeuAcα2,3Galβ1,4GlcNAcβ1,6]Manα-*O* depicted in Figure 22 has been detected in abundance in the brain (Chai et al., 1999) (as depicted in Figure 4, section 1.2.1). Although *MGAT5B* can transfer to the Man(β1,2) GlcNAc found on non-galactosylated *N*-linked glycans, I selected *MGAT5B* as a candidate gene due to its putative functional involvement in the branching of *O*-mannosyl-linked glycans.

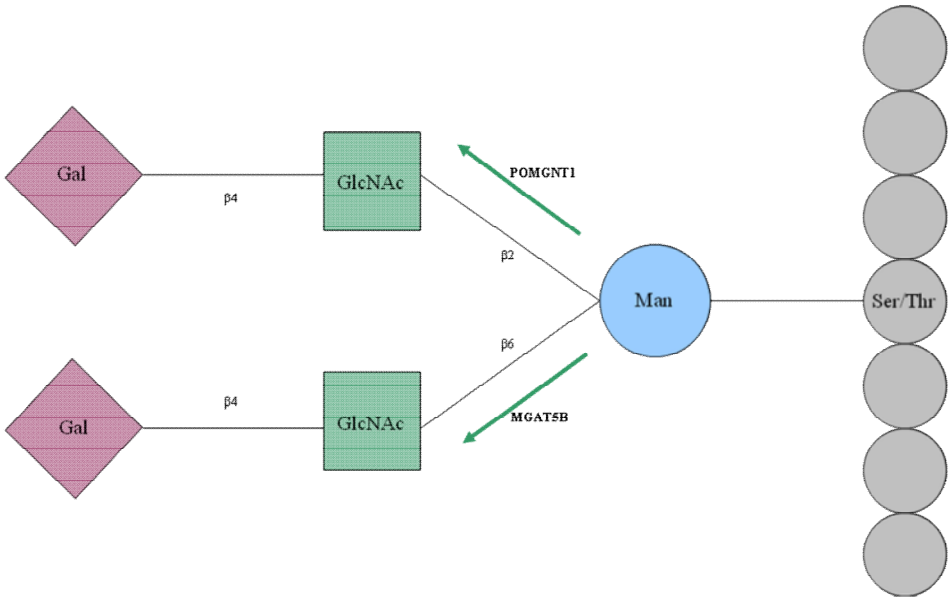

Figure 22. Diagrammatic representation of the branching action of *MGAT5B*.

This 2,6-branched structure is abundant amongst mammalian brain *O*-mannosyl glycans. *MGAT5B* has been shown to catalyse GlcNAc in β(1-6) linkage to the peptide-*O*-linked mannose only if the β(1-2) linked GlcNAc formed by *POMGNT1* is present. Ser; serine, Thr; threonine, Man; mannose, GlcNAc; *N*-acetylglucosamine, Gal; galactose,

Dystroglycan itself has long since been considered a poor candidate gene for dystroglycanopathy cases due to the deleterious effects of its abolition in mammalian animal models (Williamson et al., 1997). It is likely that a severe mutation giving rise to a dramatic reduction in protein production would not be viable. However the possibility remains that the presence of milder mutations may give rise to a dystroglycanopathy phenotype. It could be postulated, for example, that dystroglycan mutations affecting the binding affinity of *LARGE* to the N-terminal domain rather than its structural integrity, could perhaps induce a dystroglycanopathy-like phenotype. I therefore elected to include *DAG1* within the list of dystroglycanopathy candidate genes.

4.2.3 Mutation Analysis

To investigate whether these candidate genes are a cause of human dystroglycanopathy, I performed mutation screening of *GYLTL1B, β3GNT1, WWP1, GYG1, GYG2, MGAT5B* and *DAG1*. Cohort B comprised of patients in whom a mutation had not been detected after the screening of all known genes. For details of the inclusion criteria for cohort B please see section 2.1.1. I initially screened a subset of patients from cohort B for mutations in *GYLTL1B* and *MGAT5B.* The cohort subsequently expanded as additional cases were recruited. Therefore during the course of my studies, a total of thirty seven patients were screened for mutations in *β3GNT1, WWP1, GYG1, GYG2* and *DAG1*. Mutation screening of the candidate genes was performed by uni-directional sequencing on whole genome amplified DNA. DNA from the majority of patients was successfully amplified by multiple displacement amplification. In addition to the 37 patients detailed in Table 9, a further three patients met the inclusion criteria for cohort B yet DNA samples from these patients failed to amplify. There was insufficient DNA remaining to assess the quantity or quality of the starting material and these patients were excluded from further analysis. Sequencing results generated from multiple displacement amplification samples were indistinguishable from non amplified genomic DNA control samples.

Human *GYLTL1B, β3GNT1, WWP1, GYG1, GYG2, MGAT5B* and *DAG1* genes are organised into 13, 2, 23, 8, 12, 17 and 3 exons encoding 2.5 kb, 2.8 kb, 3.4 kb, 2 kb, 3.4 kb, 4.2 kb and 5.5 kb transcripts respectively. All sequence variations detected within +50 or -50 base pairs of the intron/exon boundary are recorded in Table 11. Good

quality sequencing reads from -20 to +10 base pairs of the intron/exon boundary was established as a minimum requirement for each amplicon in accordance with guidelines from the Clinical Molecular Genetics Society (www.cmgs.org). Both exonic and intronic alterations were categorised as polymorphisms if they were present on the dbSNP (http://www.ncbi.nlm.nih.gov). Variants were described in accordance with HGVS recommendations and verified using the Alamaut software package (Interactive software).

Gene	Intron/exon	Nucleotide change	Predicted amino acid change	Combined references
GYLTL1B	1	c.163C>T	p.Arg55Cys	- / 1 chromosome
GYLTL1B	1	c.83G>C	p.Gly28Ala	- / 1 chromosome
GYLTL1B	2	c.286-22dupC	intronic	-
GYLTL1B	2	c.286-33G>A	Intronic	- / 1 chromosome
GYLTL1B	3	c.492+9C>T	Intronic	- / 1 chromosome
GYLTL1B	11	c.1668C>T	synonymous	rs939105 / 30 chromosomes
GYLTL1B	11	c.1704C>T	synonymous	- / 10 chromosomes
GYLTL1B	12	c.1773A>C	synonymous	rs11038714 / 1 chromosome
β3GNT1	1	c.117G>A	synonymous	rs11537930 / 1 chromosome
WWP1	8	c.1157+16T>G	intronic	- / 1 chromosome
WWP1	9	c.1212C>T	synonymous	rs60177164 / 3 chromosomes
WWP1	10	c.1387+25A>G	intronic	- / 1 chromosome ‡
WWP1	10	c.1387+47delinsTCTCT	intronic	- / 9 chromosomes ‡
WWP1	10	c.1387+47delinsTCTCTCT	intronic	- / 18 chromosomes
WWP1	10	c.1387+60AT(6_25)	intronic	rs36186318 / 52 chromosomes ‡
WWP1	17	c.1999-16T>A	intronic	rs7012745 / 3 chromosomes
WWP1	19	c.2274-29C>T	intronic	rs10110096 / 20 chromosomes ‡

Gene	Intron/exon	Nucleotide change	Predicted amino acid change	Combined references
WWP1	20	c.2395-4C>T	intronic	- / 1 chromosome
WWP1	20	c.2395-6del	intronic	- / 12 chromosomes ‡
WWP1	22	c.2669+10A>G	intronic	rs7460650 / 20 chromosomes ‡
GYG1	5	c.552G>A	synonymous	rs4938 / 24 chromosomes ‡
GYG1	6	c.683C>T	p.Thr228Ile	- / 1 chromosome ‡
GYG2	7	c.707+35T>G	Intronic	rs5939133 / 4 chromosomes
GYG2	8	c.809C>T	p.Ala270Glu	- / 13 chromosomes
GYG2	9	c.938A>G	p.His313Arg	rs2306735 / 13 chromosomes
MGAT5B	1	c.68+21G>C	intronic	-
MGAT5B	3	c.208G>A	p.Val70Ile	rs571264 / 8 chromosomes ‡
MGAT5B	4	c.330-39G>A	intronic	rs571264 / 3 chromosomes
MGAT5B	4	c.330-47G>A	intronic	rs16969525 / 3 chromosomes
MGAT5B	4	c.346G>A	p.Gly116Ser	- / 1 chromosome
MGAT5B	4	c.376C>G	p.Gln126Glu	- / 1 chromosome
MGAT5B	5	c.446-12C>T	intronic	rs567207 / 6 chromosomes
MGAT5B	6	c.520-34C>T	intronic	rs537905 / 6 chromosomes
MGAT5B	7	c.691-45G>A	intronic	- / 2 chromosomes

Gene	Intron/exon	Nucleotide change	Predicted amino acid change	Combined references
MGAT5B	8	c.856-12T>C	intronic	- / 1 chromosome
MGAT5B	8	c.856-34C>T	intronic	- / 1 chromosome
MGAT5B	9	c.1050G>C	synonymous	rs3889145 / 5 chromosomes ‡
MGAT5B	9	c.1107C>T	synonymous	rs34056052 / 4 chromosomes ‡
MGAT5B	10	c.1158-27C>T	intronic	rs11653088 / 37 chromosomes ‡
MGAT5B	10	c.1158-43G>A	intronic	rs12450749 / 37 chromosomes ‡
MGAT5B	10	c.1185C>T	synonymous	rs33966966 / 3 chromosomes
MGAT5B	11	c.1323C>T	synonymous	- / 2 chromosomes
MGAT5B	13	c.1579-55T>C	intronic	rs920851 / 13 chromosomes ‡
MGAT5B	13	c.1671G>A	synonymous	rs8081793 / 8 chromosomes ‡
MGAT5B	13	c.1714A>G	p.Thr572Ala	-/ 1 chromosome ‡
MGAT5B	14	c.1746C>T	synonymous	- / 1 chromosome
MGAT5B	15	c.1863C>T	synonymous	rs8067984 / 17 chromosomes ‡
MGAT5B	16	c.2157C>T	Synonymous	- / 7 chromosomes
MGAT5B	17	c.2175-13T>C	intronic	rs9894270 / 46 chromosomes ‡
MGAT5B	17	c.2175-8C>G	intronic	rs57502449 / 12 chromosomes ‡
MGAT5B	17	c.2373+14G>A	3' UTR	- / 12 chromosomes ‡

Gene	Intron/exon	Nucleotide change	Predicted amino acid change	Combined references
DAG1	2	c.259A>G	p.Ile87Val het	- / 1 chromosome
DAG1	2	c.285+42T>C	intronic	rs2329024 / 74 chromosomes
DAG1	2	c.41C>G	p.Ser14Trp	rs2131107 / 74 chromosomes
DAG1	3	c.286-49G>A	intronic	- / 1 chromosome
DAG1	3	c.599C>G	p.Thr200Ser	rs41290704 / 1 chromosome
DAG1	3	c.2256C>T	synonymous	rs1801143 / 22 chromosomes ‡

Table 11. Summary of sequence alterations detected in candidate genes.

References to the dbSNP are provided where applicable. ‡ indicates those changes detected in the heterozygous state in patients with consanguineous parents.

All dystroglycanopathy cases reported to date have been compatible with a recessive pattern of inheritance. Animal models of *DAG1* and *WWP1* defects also demonstrate recessive inheritance. I therefore hypothesized that two mutations would need to be present in the candidate genes in order to give rise to disease.

A total of eight novel sequence variants were identified in *GYLTL1B*. Of these, two non-synonymous variations were detected, each occurring only once within the cohort studied (c.163C>T; p.Arg55Cys and c.83G>C; p.Gly28Ala). A single sequence variant was detected in *β3GNT1*. This synonymous change was recorded on the dbSNP. A total of six novel intronic sequence variants were identified in *WWP1*. A two base pair intronic deletion (c.2395-6delT) was detected in the heterozygous state in twelve individuals, two of whom had consanguineous parents. Three intronic heterozygous single base pair substitution variants were detected (c.1157+16T>G, c.2395-4C>T and c.1387+25A>G) each occurring only once within the cohort. Although the exact nomenclature of the c.1387+47delinsTCTCT and c.1387+47delinsTCTCTCT variants was not present on the SNP database, there are a number of additional variations recorded within this highly polymorphic stretch of intronic sequence (rs36226595, rs62510796 and rs9657012). A single novel variant was identified in *GYG1* (c.683C>T; p.Thr228Ile). This non synonymous heterozygous change was detected in a single patient born to consanguineous parents. A single novel variant was identified in *GYG2*. The non synonymous Ala270Glu change was detected in a total of 13 chromosomes. The highest number of variations was detected in *MGAT5B*. A total of 26 sequence changes were identified, eleven of which were novel. Three novel non synonymous variants were present, each occurring only once within the cohort. The Thr572Ala alteration was detected in the heterozygous state in a patient with consanguineous parents. A total of two novel variants were detected in *DAG1*. The Ile87Val change was detected in a single patient in whom no other variations were detected (patient B-1).

No splicing defects were predicted using the Alamut Splicing Prediction Module for any of the unclassified variants described in Table 11. In summary, although a large number of variants with unknown clinical significance were detected, no clearly pathogenic sequence alterations were identified in the candidate genes studied.

4.2.4 A Functional Assay to Investigate Ile87Val in *DAG1*

A missense change in *DAG1* (p.Ile87Val) was detected in a single patient with LGMD and no mental retardation. The variant is located within the region of *LARGE* binding (amino acids 30-316) and protein sequence alignment demonstrated that the Ile87 amino acid is conserved in all but three of the vertebrate species analysed (Figure 23). We therefore hypothesised that this variant could potentially lead to a reduction in *LARGE*-dependent modification. This change warranted further investigation using a functional assay previously optimised to examine the pathogenic implications of similar variations within this region. In a collaborative setting, experiments were performed by members of Professor K Campbell's laboratory in the Howard Hughes Medical Institute, University of Iowa, USA. Immunoreactivity to IIH6 was compared using Ile87Val mutant and wild type *DAG1* constructs transfected into *DAG1* null myoblast cell lines. No reduction in the production of the IIH6 epitope was observed when comparing wild type and mutant constructs, therefore indicating that the Ile87Val change does not impair *LARGE*-dependent dystroglycan modification in this system.

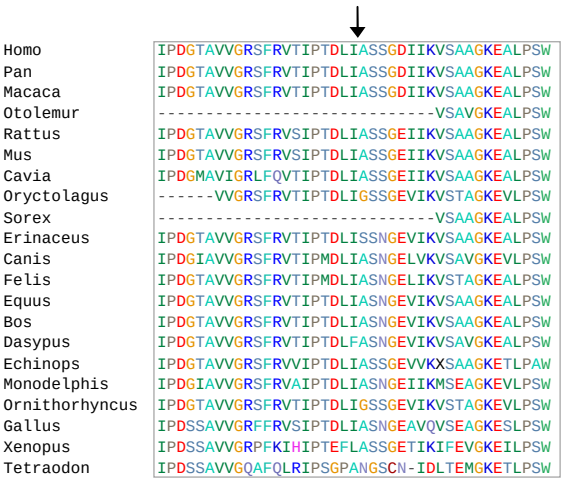

Figure 23. Protein alignment (homology) plot of the N-terminal amino region of *DAG1*. A total of 21 vertebrate species are shown. The arrow indicates complete conservation of the p.Ile87Val variant in 18 of the 21 vertebrate species analysed.

4.2.5 Modulation of Gene Expression During Myogenic Differentiation

To evaluate the functional involvement of candidate genes in the pathway of α-dystroglycan glycosylation, I modulated the expression of individual candidate genes in a mouse myogenic cell line using a ribonucleotide interference (RNAi) based strategy. Murine myoblast C2C12 cells are a well established model of myogenic differentiation. The differentiation of these cells is associated with a dramatic increase in the expression and glycosylation of α-dystroglycan. This characteristic suggests that the production of glycosylated α-dystroglycan could be modulated during myogenic cell differentiation by reducing the expression of individual genes. The transient regulation of gene expression was induced by the transfection of C2C12 cells with siRNA oligonucleotides targeted to specific candidate genes.

Initial experiments using Real Time PCR demonstrated only residual expression of *Gyltl1b*, *Mgat5b* and *Wwp1* in C2C12 cells as revealed by their high cycle threshold (>37 cycles) (data not shown). Transcripts were undetectable by Real Time PCR performed on samples from mouse skeletal muscle tissue (data not shown). Successful amplification of *Gyltl1b*, *Mgat5b* and *Wwp1* transcripts using gene specific Real Time probes was confirmed by the detection of expression in samples from whole mouse brain (data not shown). Insufficient expression of these candidate genes in C2C12 cells excluded their evaluation in this tissue culture model. As depicted in Figure 20, the glycogenin paralog *GYG2* is absent from rodent species therefore the evaluation of gene function in this system can only be performed on murine *Gyg*.

Therefore, of the seven candidate genes selected for study, the expression of only *Ggy* and *β3gnt1* could be modulated in this system to investigate their functional effect on dystroglycan glycosylation. Protocols were optimised using siRNA oligonucleotides targeted to *Pomt1*. Relative gene expression was assayed by Real Time PCR. The level of α-dystroglycan glycosylation was inferred on western blot. Immunoreactivity of whole cell protein lysates to IIH6 was evaluated relative to that of β-dystroglycan.

During assay optimisation a variety of cell densities, transfection agents, siRNA titrations and time frames were evaluated. No alteration in immunoreactivity to IIH6

was observed, with only a single transfection event at all cell densities and time points assayed (data not shown). Using siRNA oligonucleotides targeted to *Pomt1*, the most dramatic reduction of α-dystroglycan glycosylation was achieved using two successive transfection events at specific time points 48 hours apart.

The silencing of each transcript was maintained throughout the time course by transfecting C2C12 cells with siRNA oligonucleotides at 24 and 72 hours post cell plating. Real Time PCR assayed the effect on target gene expression at 48, 72 and 96 hours. The glycosylation of dystroglycan was examined 96 hours after plating by western blot analysis. Both a mock transfection and the use of a scramble siRNA oligonucleotide were included as controls. To assess the specificity of the siRNA oligonucleotides, two probes targeted to each candidate gene were used. Due to a lack of available antibodies to *Pomt1*, *Gyg* and *β3gnt1* it was not possible to investigate any induced reduction in protein production.

Efficient knockdown of *Pomt1*, *β3gnt1* and *Gyg* messenger RNA (mRNA) was obtained as confirmed by Real Time PCR analysis (Figure 24). Each probe successfully reduced target transcript levels to below 50% at all time points analysed, with the exception of *β3gnt1* which rose slightly above this threshold using the s99323 oligonucleotide at the 96 hour time point (0.56; $P > 0.05$). No significant reduction in gene silencing was detected when comparing gene expression in mock transfected cells against those transfected with a scramble oligonucleotide, with the exception of *Gyg* expression which was reduced at the 96 hour time point (0.7; $P > 0.05$).

A

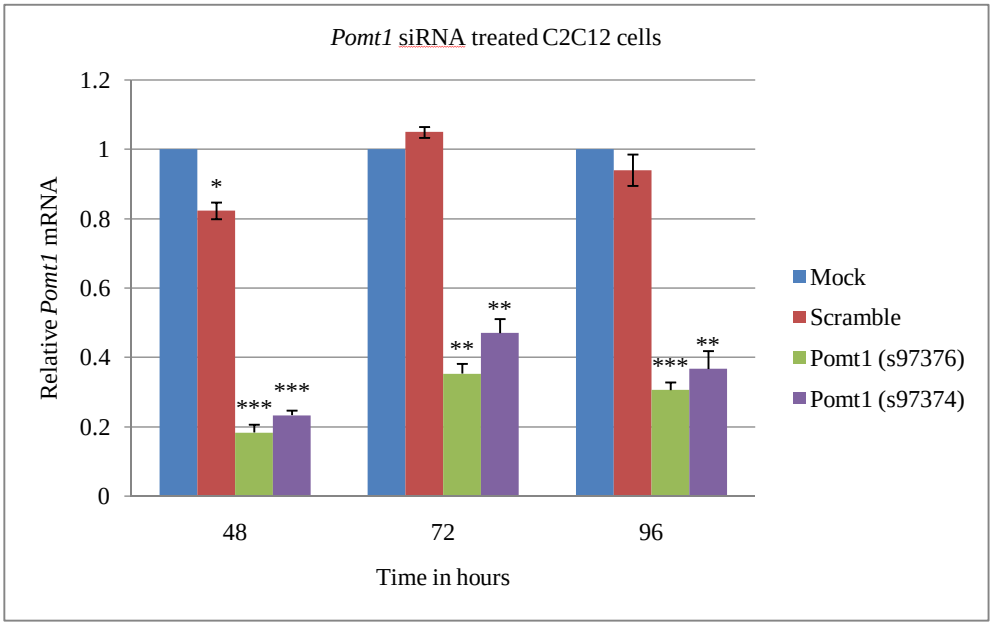
Pomt1 siRNA treated C2C12 cells
Relative Pomt1 mRNA
1.2
1
0.8
0.6
0.4
0.2
0
*
***
***
**
**
***
**
48
72
96
Time in hours
Mock
Scramble
Pomt1 (s97376)
Pomt1 (s97374)

B

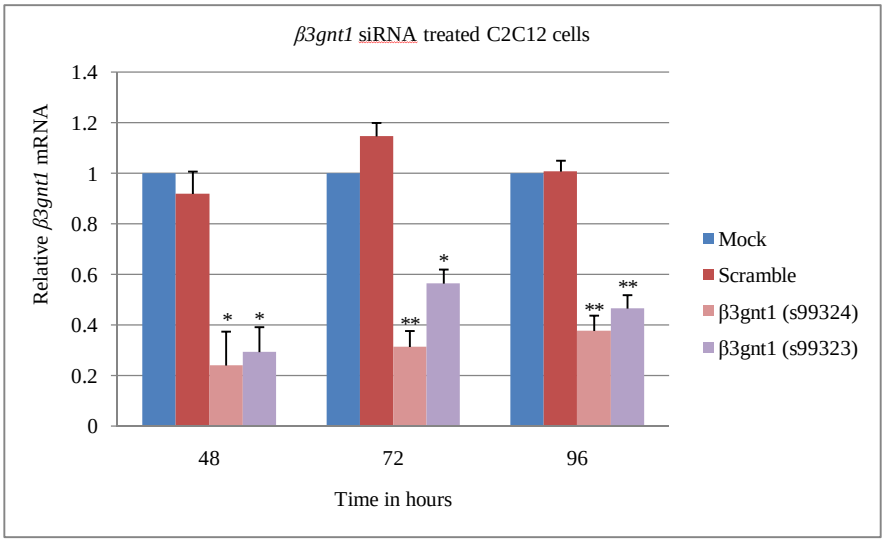
β3gnt1 siRNA treated C2C12 cells
Relative β3gnt1 mRNA
1.4
1.2
1
0.8
0.6
0.4
0.2
0
*
*
**
*
**
**
48
72
96
Time in hours
Mock
Scramble
β3gnt1 (s99324)
β3gnt1 (s99323)

C

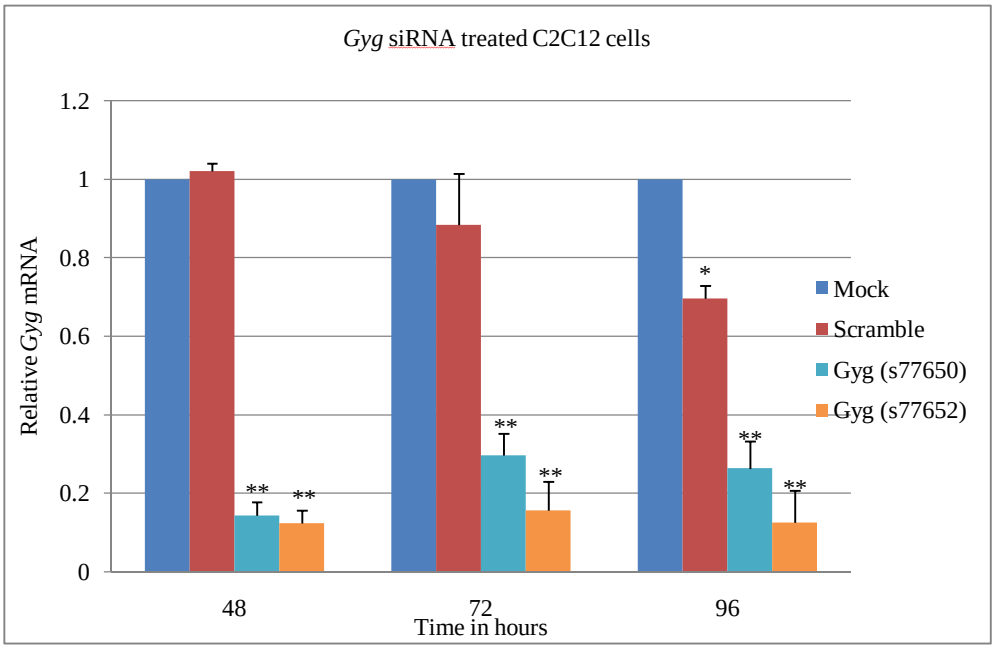

Figure 24. Modulation of gene expression during myogenic differentiation examined by Real Time PCR.

C2C12 cells were treated with siRNA oligonucleotides targeted to *Pomt1*, *β3gnt1* and *Gyg* at 24 hours and 72 hours post plating. Two different siRNA oligonucleotides per gene were tested; the reference to each is indicated in brackets. Bar graphs show relative expression levels of *Pomt1* (A), *β3gnt1* (B) and *Gyg* (C) at 48 hours, 72 hours and 96 hours post plating. Results are standardised against *β-actin* mRNA and expressed as a ratio versus mock transfected cells. Values are expressed as the mean ± SEM of three independent experiments (for each experiment, values are the average of three technical replicates). Differences between groups were examined using the unpaired *t*-test. **P* <0.05, ***P* <0.01 and ****P* <0.001 versus mock transfected cells.

A

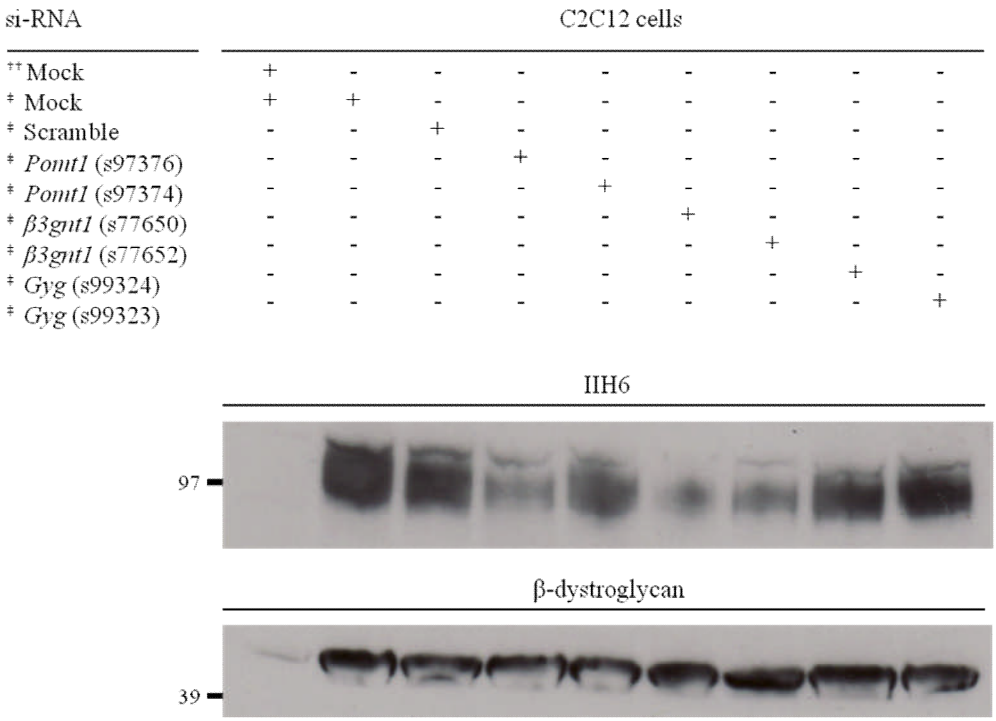

Figure 25. Modulation of α-dystroglycan glycosylation during myogenic differentiation examined by western blot.

Representative western blot showing IIH6 immunoreactivity relative to β-dystroglycan. C2C12 cells were treated with siRNA oligonucleotides targeted to *Pomt1*, *Gyg* and *β3gnt1*. Two different siRNA oligonucleotides per gene were tested, the reference to which is indicated in brackets. †† Protein assayed 24 hours after cell plating. ‡ Protein assayed 96 hours after cell plating.

A dramatic increase in the expression and glycosylation of dystroglycan during this cell culture system is demonstrated by comparing whole cell protein homogenates assayed at 24 hours and 96 hours after cell plating. The effect on α-dystroglycan glycosylation was examined on western blot by comparing immunoreactivity to IIH6 relative to that of β-dystroglycan. Western blot analysis was performed on triplicate samples; a representative western blot is shown in Figure 25. The inhibition of *Pomt1* gene expression was associated with a clear reduction in levels of glycosylated α-dystroglycan. When comparing the efficiency of both siRNA oligonucleotides targeted to *Pomt1*, the s97376 probe induced both a greater reduction in *Pomt1* expression levels and IIH6 immunoreactivity at all time points examined. When evaluating the effect of the two candidate genes studied, only the modulation of *β3gnt1* expression induced a detectable reduction in α-dystroglycan glycosylation. When comparing the efficiency of both siRNA oligonucleotides targeted to *β3gnt1*, the s99324 probe induced both a greater reduction in *β3gnt1* mRNA expression levels and IIH6 immunoreactivity at all time points examined. Both siRNA oligonucleotides targeted to *Gyg* reduced gene expression yet did not induce a marked reduction in IIH6 immunoreactivity.

4.2.6 The Exclusion of *DPM3* Mutations

Subsequent to the study performed in chapter 3, a further causative dystroglycanopathy gene has been identified; *DPM3* (please refer to section 1.3.1) (Lefeber et al., 2009). A single case study was reported and therefore no indication was provided as to the prevalence of mutations within this gene or indeed the clinical spectrum associated with this protein when defective. To ascertain whether patients comprising cohort B harboured alterations in *DPM3*, mutation screening was performed in collaboration with Professor Wevers' laboratory at the Institute of Genetic and Metabolic Disease, Nijmegen, The Netherlands. In this instance, a subset of 20 patients from cohort B was screened by members of Professor Wevers' laboratory yet no pathogenic sequence alterations were identified.

4.3 DISCUSSION

Specific gene defects have been detected in only the minority of dystroglycanopathy cases (Bouchet et al., 2007; Godfrey et al., 2007; Mercuri et al., 2009). To date, genes implicated in these disorders have either been putative and demonstrated glycosyltransferases or accessory proteins of glycosyltransferases. The discovery of mutations in the remaining molecularly undiagnosed patients presents as a challenge and work is currently underway to identify novel loci. Due to the genetic and clinically heterogeneous nature of these conditions as well as the lack of informative families, the whole genome candidate gene approach presents as a viable option. Within this study, evidence from the examination of animal models was initially used as a basis for candidate gene identification. It has recently been demonstrated that the genes responsible for human dystroglycanopathies are expressed in zebrafish (Moore et al., 2008). The targeted inactivation of zebrafish *Gyg* in Dr D Stemple's laboratory recapitulated various aspects of the pattern of muscle involvement seen in patients as well as recreating their specific immunohistochemical hallmark (unpublished data). Aberrant glycosylation of α-dystroglycan has also been demonstrated in a naturally occurring chicken with muscular dystrophy (Saito et al., 2005). A homozygous missense substitution in the E3 ubiquitin ligase gene *Wwp1* has been reported to underlie disease although its precise role in pathogenesis remains unknown (Matsumoto et al., 2008). I selected the mammalian homologs of both *Gyg* and *Wwp1* for candidate gene analysis. A bioinformatics approach was subsequently used and identified two Golgi resident genes (*GYLTL1B* and *β3GNT1*) both of which showed homology to *LARGE*. Two additional genes were selected on the basis of functional evidence; *DAG1* and *MGAT5B* which is thought to be responsible for the β1,6GlcNAc-branched structures of *O*-mannosyl glycans reported in brain glycoproteins (Inamori et al., 2003; Kaneko et al., 2003). A summary of the candidate genes analysed and their putative or demonstrated function is shown in Table 12.

*	**Protein (*encoding gene*) ****	**Gene ID †**	**location ††**	**Molecular function ‡**	**Subcellular localisation ‡‡**
Endeavour	glycosyltransferase-like 1B (*GYLTL1B*)	120071	11p11.12	Glycosyltransferase	Golgi apparatus
	UDP-GlcNAc:betaGal beta-1,3-*N*-acetylglucosaminyltransferase 1 (*β3GNT1*)	11041	11q13.2	Glycosyltransferase	Golgi apparatus
Animal models	WW domain containing E3 ubiquitin protein ligase 1 (*WWP1*)	602307	8q21	Ubiquitin-protein ligase	No entry
	Glycogenin 1 (*GYG1*)	603942	3q24-q25.1	Glycosyltransferase, other transferase	Cytosol
	Glycogenin 2 (*GYG2*)	300198	Xp22.3	Glycosyltransferase, other transferase	Cytosol
Function	Mannosyl (alpha-1,6-)-glycoprotein beta-1,6-*N*-acetyl-glucosaminyltransferase, isozyme B (*MGAT5B*)	612441	17q25.3	Glycosyltransferase	Golgi apparatus
	Dystroglycan 1 (*DAG1*)	1605	3p21	Other receptor	α-subunit; extracellular β-subunit; membrane

Table 12. Summary of candidate genes studied.

* Rationale for candidate gene selection; Endeavour; Endeavour gene prioritisation software. ** Gene symbols and names as per HUGO nomenclature (www.genenames.org/). † Entrez Gene Identifier from the NCBI database (http://www.ncbi.nlm.nih.gov/). †† Denotes chromosomal location. ‡ Molecular function as classified by the PANTHER (Protein ANalysis THrough Evolutionary Relationships) Classification System (http://www.pantherdb.org/). ‡‡ Subcellular localisation as annotated via the Universal Protein Resource Knowledge Base (UniProtKB) (www.uniprot.org).

To investigate whether mutations in any of these seven genes were present in a cohort of patients, I performed mutation screening. Although a number of sequence variants of unknown clinical significance were detected, no clearly pathogenic alterations were identified. A functional assay performed by collaborators to assess the effect of a *DAG1* variant was unable to demonstrate any pathogenic influence induced by this missense change (c.259A>G; p.Ile87Val). The identification of heterozygous polymorphisms indicates the exclusion of these loci in a number consanguineous families studied (Table 11). The possibility remains that rare mutations are present in these candidate genes within the population tested, yet remain unidentified by the mutation detection method chosen. Another possibility is that these genes are only very rarely involved in dystroglycanopathies, for example mutations in *LARGE* have been reported in only five cases worldwide since its original description in 2003 (Godfrey et al., 2007; Longman et al., 2003; Mercuri et al., 2009; van Reeuwijk et al., 2007). Therefore the screening of a larger patient cohort for mutations in *GYLTL1B*, *β3GNT1*, *WWP1*, *GYG1*, *GYG2*, *MGAT5B* and *DAG1* may be informative.

Although the inspection of expression profiling databases (GEO Profiles; www.ncbi.nlm.nih.gov) suggests that human *GYLTL1B* and *MGAT5B* are widely expressed, the level of tissue specific transcripts remains unclear. Northern blot analysis of human *GYLTL1B* and *MGAT5B* demonstrate their abundant expression in the brain yet these transcripts were undetectable in both human fetal and adult skeletal muscle samples by Real Time PCR (data not shown). Although *MGAT5B* is thought to be responsible for the branching of the 2,6-substituted mannose (NeuAcα2,3Galβ1,4GlcNAcβ1,2[NeuAcα2,3Galβ1,4GlcNAcβ1,6]Manα-O) detected in brain, there is currently no direct evidence to demonstrate that this glycan resides on dystroglycan itself or indeed outside the brain (Chai et al., 1999). Moore *et al.* recently reported the targeting of *GYLTL1B* in the zebrafish with morpholino oligonucleotides (Moore et al., 2008). Although IIH6 immunostaining was abolished, no significant morphological changes were observed. Both *GYLTL1B* and *MGAT5B* remain candidates for patients presenting with isolated central nervous system involvement such as cobblestone lissencephaly without any associated skeletal muscle involvement. Due to the rarity of this clinical manifestation it was not possible to collate a cohort of patients to investigate this further.

The expression and post-translational modification of dystroglycan is heavily developmentally regulated (Brown et al., 2004; Leschziner et al., 2000). Initial experiments demonstrated that the differentiation of mouse myogenic cells resulted in a dramatic increase in glycosylated α-dystroglycan. This suggested that the production of the IIH6 epitope could be modulated during cell differentiation by reducing the abundance of individual genes involved in the pathway of α-dystroglycan glycosylation. I therefore developed an RNA interference based strategy to decrease the expression of individual genes. The lack of *Gyltl1b*, *Mgat5b* and *Wwp1* expression in C2C12 cells precluded their functional investigation in this system. The targeting of siRNA oligonucleotides to murine *Pomt1*, *β3gnt1* and *Gyg* resulted in efficient gene silencing. The modulation of both *Pomt1* and *β3gnt1* induced a marked reduction in the production of the IIH6 epitope present on α-dystroglycan as observed on western blot. It is unlikely that any reduction in immunoreactivity to IIH6 was caused by the degradation of the core peptide as the molecular weight of β-dystroglycan remained unchanged. This finding confirms *β3gnt1* as a key enzyme functioning in the pathway of α-dystroglycan glycosylation.

Despite a significant reduction in *Gyg* expression, no detectable inhibition of the IIH6 epitope was induced. It is important to note that this finding does not exclude this gene in functioning to glycosylate α-dystroglycan and could be explained by the existence of remaining mRNA or by the recycling of pre-existing *Gyg* protein. Due to the lack of available antibodies against *Pomt1*, *β3gnt1* or *Gyg*, the modulation of protein production in this system could not be investigated.

Although the uncharacterised carbohydrate epitope present on α-dystroglycan and recognised by the monoclonal antibody IIH6 is conserved across species from invertebrates to mammals, the full extent of glycan heterogeneity between species is not known (Ervasti and Campbell, 1991; Moore et al., 2008). Therefore the possibility remains that although *Wwp1* and *Gyg* mutations cause hypoglycosylation in animal models, mutations in these genes are not responsible for a dystroglycanopathy in the human. Limb girdle muscular dystrophy type 2H (OMIM; 254110) is caused by mutations in the E3 ubiquitin ligase Trim32 and although its molecular pathogenesis is quite distinct from that of the dystroglycanopathies, this finding does implicate the ubiquitin pathway in muscular dystrophy.

As far as is currently understood the initiating *O*-mannosyltransferases and *N*-acetylglucosaminyl-transferases, known to be causative in human dystroglycanopathy, are pathway specific. Due to the common nature of post-translational modifications, enzymatic defects that affect more than one glycosylation pathway have been found to induce multi-systemic consequences (i.e. congenital disorders of glycosylation). Therefore genes such as glycogenin have long since been considered poor candidates for inducing a specific dystroglycanopathy phenotype as they are known to function in pathways other than those exclusively involved in dystroglycan glycosylation. This view is challenged by the detection of *DPM3* mutations in a patient with a spectrum of disease spanning dystroglycanopathy and the congenital disorders of glycosylation. It remains unknown as to whether the galactose and sialic acid monosaccharides present on the NeuAcα2,3Galβ1,4GlcNAcβ1,2Manα-*O*-Ser/Thr glycan structure are added by glycosyltransferases unique to this pathway or by those with more general specificity (chapter 1, Figure 4). Various galactosyltransferases and sialyltransferase were investigated as candidate genes for dystroglycanopathy by previous members of the Dubowitz Neuromuscular Centre, yet no pathogenic defects were detected.

In conclusion, mutation screening data indicate that defects in *GYLTL1B, β3GNT1, WWP1, GYG1, GYG2, MGAT5B* and *DAG1* are not frequent causes of human dystroglycanopathy. The optimisation of a cell culture model of dystroglycanopathy has allowed the functional evaluation of a subset of candidate genes. This revealed that the inhibition of *β3gnt1* is associated with the induction of a dystroglycanopathy hallmark as detected using the antibody IIH6. Although decreased *β3gnt1* expression has recently been associated with a reduction in laminin-binding glycans in invasive carcinoma cells, these data demonstrate for the first time its involvement in a mammalian skeletal muscle system (Bao et al., 2009). Further work is needed to understand the exact function of *β3gnt1* within the pathway of α-dystroglycan glycosylation. The future identification of novel genes in this pathway will provide insight into the pathological mechanisms underlying disease as well as offer potential clues as to new approaches to therapy.

CHAPTER 5. REANALYSIS OF A CONSANGUINEOUS PEDIGREE

5 REANALYSIS OF A CONSANGUINEOUS PEDIGREE

5.1 INTRODUCTION

Whole genome linkage mapping has long been an essential methodology used in the identification of novel loci responsible for genetic disease. The analysis of multiple pedigrees in neuromuscular disorders has led to the detection of a number of causative genes (Kobayashi et al., 1998; Yoshida et al., 2001). Due to the recent progress in delineating pathogenic processes underlying neuromuscular conditions, mutations have been identified in many of the large pedigrees previously recruited to the Dubowitz Neuromuscular Centre. The remaining molecularly uncharacterised pedigrees often include small informative families in whom affected patients have been lost to clinical follow-up, or where biological samples are either exhausted or in short supply. This chapter deals specifically with my analysis of one particular pedigree (referred to here as pedigree 1) which I re-evaluated in light of newly available pathology data and the potential application of emerging novel methodologies. This family from the United Arab Emirates includes four affected children born to consanguineous parents and has previously been extensively studied within the department (Figure 26). The clinical presentation of these children was first reported in the literature over a decade ago as a form of CMD characterised by proximal muscle weakness, muscle hypertrophy and early respiratory failure (Muntoni et al., 1998). Both the brain imaging and intellect of these affected children was found to be normal. For a more detailed summary of clinical information please refer to section 2.1.1.

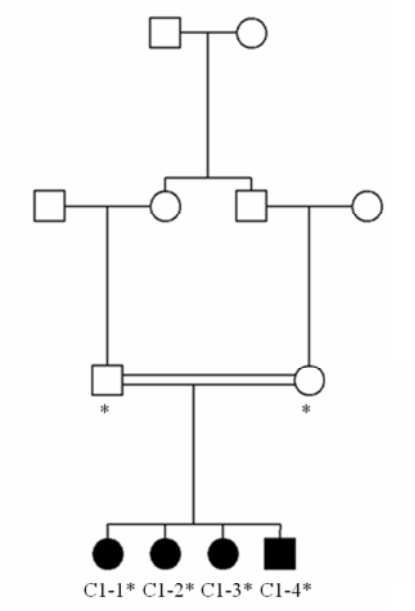

Figure 26. Pedigree 1.

The family depicted in pedigree 1 includes four affected members born to consanguineous parents. Squares indicate male family members and circles female family members; filled squares and circles indicate those patients affected. Double lines between parents indicate that the parents are related. Affected family members are referred to as C1-1, C1-2, C1-3 and C1-4. Asterisks indicate those individuals from whom DNA is available for study. Pedigree 1 has previously been described in Brockington *et al.* and Muntoni *et al.* (Brockington et al., 2000; Muntoni et al., 1998).

Initial immunostaining of skeletal muscle biopsies identified a reduction in laminin α-2, yet linkage to the *LAMA2* locus on chromosome 6q was excluded. In order to identify the disease loci in this family genome wide linkage analysis was subsequently performed (Brockington et al., 2000). DNA from each member of pedigree 1 was genotyped using 358 fluorescent high informative $(CA)_n$ repeat microsatellite markers located at an average of 10 cM intervals (the ABI linkage mapping set I). Homozygosity mapping identified a locus on chromosome 1q42 between flanking markers D1S2860 and D1S2800. A second small family with similar clinical and histopathological features was subsequently found to be compatible with this locus, generating a cumulative LOD score of 3.57 (Brockington et al., 2000). Extensive candidate gene analysis has been performed on this linkage interval, resulting in a number of genes being screened for mutations by sequencing (Table 13). Despite this, the causative mutation remains elusive.

Protein (*encoding gene*) *	**Gene ID ****	**Molecular function †**	**Subcellular localisation ‡**
ADP-ribosylation factor 1 (*ARF1*)	375	Small GTPase	Golgi apparatus and cytoplasm
beta-1,3-N-acetylgalactosaminyltransferase 2 (*β3GALNT2*)	148789	Glycosyltransferase	Golgi apparatus
UDP-N-acetyl-alpha-D-galactosamine: polypeptide N-acetylgalactosaminyltransferase 2 (*GALNT2*)	2590	Glycosyltransferase	Golgi apparatus and secreted
lectin, galactoside-binding, soluble, 8 (*LGALS8*)	3964	Other signaling molecule, Other cell adhesion molecule	Cytoplasm
nidogen 1 (*NID1*)	4811	Extracellular matrix glycoprotein	Secreted
Obscurin (*OBSCN*)	84033	Actin binding cytoskeletal protein, Guanyl-nucleotide exchange factor	Cytoplasm
Poly(ADP-ribose) polymerase family (*PARP1*)	142	Glycosyltransferase	Nucleus

Table 13. Candidate genes previously screened within the linkage interval detected on chromosome 1q42 using microsatellite data.

Genes that were previously screened by sequencing prior to my PhD. * Gene symbols and names as per HUGO nomenclature (www.genenames.org/). * Entrez Gene Identifier from the NCBI database (http://www.ncbi.nlm.nih.gov/). † Molecular function as classified by the PANTHER (Protein ANalysis THrough Evolutionary Relationships) Classification System (http://www.pantherdb.org/). ‡ Subcellular localisation as annotated via the Universal Protein Resource Knowledge Base (UniProtKB) (www.uniprot.org).

Recent reanalysis of the patients' muscle pathology revealed a reduction in IIH6 immunostaining. None of the known dystroglycanopathy loci reside within the region identified on chromosome 1q42. In addition to this, I included proband C1-1 in cohort A and therefore mutations in *FKRP*, *FKTN*, *POMT1*, *POMT2*, *POMGNT1* and *LARGE* were excluded by uni-directional sequencing (please refer to chapter 3).

The application of microsatellite markers for linkage mapping has now been superseded by the use of closely spaced single-nucleotide polymorphisms (SNPs). Despite the less informative nature of biallelic markers when compared to the use of highly polymorphic microsatellite markers, the sheer abundance of SNPs offers superior power to detect linkage. Studies comparing these two approaches have indicated that previous linkage analyses employing the use of sparse microsatellite markers could benefit from reanalysis with high density SNP maps (Evans and Cardon, 2004; Middleton et al., 2004).

Despite numerous investigations performed in the Dubowitz Neuromuscular Centre, the mutation underlying this family's condition has remained elusive. This chapter initially describes further candidate gene analysis performed by me using the microsatellite linkage data. In addition, with the greater coverage offered by the use of SNP arrays, whole genome linkage analysis was repeated, the expression profile of linked genes investigated and candidate gene analysis performed.

5.2 RESULTS

5.2.1 Genomic Mapping: Reanalysis of Microsatellite Data

Initially I confirmed that the order of fine mapping markers used in the original multipoint linkage analysis is consistent with the current physical maps (www.ncbi.nlm.nih.gov/unists). Therefore the calculated region of homozygosity remains flanked by the markers D1S2860 and D1S2800 (Figure 27). This large region is just under 17 Mb and contains in excess of 200 genes.

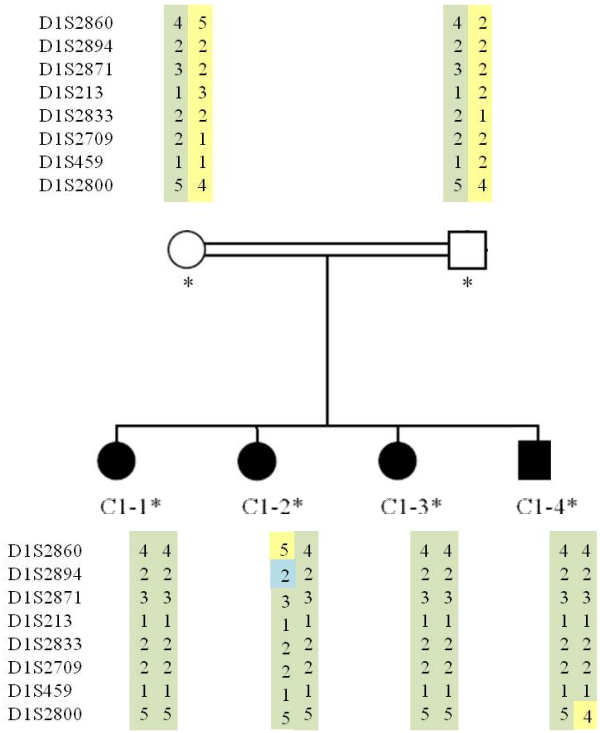

Figure 27. Haplotypes derived from chromosome 1q42 microsatellite markers.

Haplotypes from pedigree 1 from the original whole genome linkage report. The disease haplotype is denoted by green shaded bars. The blue section of the bar denotes an allele that could not be unequivocally assigned during the original analysis. The critical region identified during the study of pedigree 1 was defined by recombination events in patients C1-2 and C1-4. Asterisks indicate those individuals from whom DNA was available for analyses. Figure based on that from Brockington *et al.* (Brockington et al., 2000).

Candidate gene analysis

I further scrutinised those genes within the original loci identified on chromosome 1q for biological candidates. Those genes considered as more obvious targets for involvement had previously been excluded by members of the Dubowitz Neuromuscular Centre (Table 13). Therefore I employed a bioinformatics approach in order to identify novel candidates. Results generated by the gene ranking software Endeavour are shown in Table 14 (as previously described in chapter 4).

The genes ranked in second, third and fifth position by this method had already been excluded prior to this project being undertaken (UDP-N-acetyl-alpha-D-galactosamine: polypeptide N-acetylgalactosaminyltransferase 2; *GALNT2*, obscurin; *OBSCN* and poly(ADP-ribose) polymerase family; *PARP1*). Along with presenilin 2 (*PSEN2*) (identified as the highest scoring gene), the potassium channel subfamily K member 1 (*KCNK1*) was indicated as a novel candidate.

Due to the very recent discovery of α-dystroglycan hypoglycosylation in a patient with mutations in *DPM3*, this gene was absent from the 'training set' described above. Subsequent reanalysis generated with the inclusion of this gene retained *PSEN2* as the top scoring candidate as well as retaining *GALNT2*, *OBSCN*, *KCNK1* and *PARP1* within the top 20 genes (data not shown).

In addition to the above genes, I selected a further two for mutation screening; tetratricopeptide repeat domain 13 (*TTC13*) and lamin B receptor (*LBR*). *LBR* was included due to the involvement of nuclear envelope proteins in skeletal muscle pathology (Bonne et al., 1999; Capell and Collins, 2006). *TTC13* presented as a candidate due to its function as a glycosyltransferase.

	Rank *	Protein (*encoding gene*) **	Gene ID †	Molecular function ‡	Subcellular localisation ‡‡
Endeavour prioritised candidates	1	Presenilin 2 (*PSEN2*)	5664	Aspartic protease, other select calcium binding proteins	Endoplasmic reticulum and Golgi
	2	UDP-N-acetyl-alpha-D-galactosamine: polypeptide N-acetylgalactosaminyltransferase 2 (*GALNT2*)	2590	Glycosyltransferase	Golgi and secreted
	3	Obscurin (*OBSCN*)	84033	Actin binding cytoskeletal protein, Guanyl-nucleotide exchange factor	Cytoplasm
	4	Potassium channel, subfamily K, member 1 (*KCNK1*)	3775	Voltage-gated potassium channel	Membrane
	5	Poly(ADP-ribose) polymerase family (*PARP1*)	142	Glycosyltransferase	Nucleus
Others	N/A	Tetratricopeptide repeat domain 13 (*TTC13*)	79573	Glycosyltransferase	Unspecified
	N/A	Lamin B receptor (*LBR*)	3930	Receptor	Nuclear membrane

Table 14. Candidate genes identified within the linkage interval detected on chromosome 1q42 using microsatellite data.

* The top 5 ranked genes within the interval on 1q42 using the Endeavour gene prioritisation software (www.esat.kuleuven.be/endeavour/). The training set consisted of; *POMT1*, *POMT2*, *POMGNT1*, *LARGE*, *FCMD* and *FKRP*. ** Gene symbols and names as per HUGO nomenclature (www.genenames.org/). † Entrez Gene Identifier from the NCBI database (http://www.ncbi.nlm.nih.gov/). ‡ Molecular function as classified by the PANTHER (Protein ANalysis THrough Evolutionary Relationships) Classification System (http://www.pantherdb.org/). ‡‡ Subcellular localisation as annotated via the Universal Protein Resource Knowledge Base (UniProtKB) (www.uniprot.org). Blue shaded boxes indicate those genes previously screened by sequencing prior to my PhD. Yellow shaded boxes indicate those genes investigated by me as candidate genes.

Mutation screening

To investigate whether mutations resided within these candidate genes, I performed screening of *PSEN2, KCNK1, TTC13* and *LBR*. The human *PSEN2, KCNK1, TTC13* and *LBR* genes are organised into 13, 3, 23 and 14 exons and encode 2.3 kb, 2.2 kb, 3.3 kb and 3.7 kb transcripts respectively. To ensure the preservation of precious genetic material, uni-directional sequencing was performed on whole genome amplified DNA from patient C1-1. Sequencing results from the MDA sample were indistinguishable from non amplified genomic DNA control samples. No heterozygous or homozygous sequence variations were detected within the candidate genes studied. Good quality sequencing reads from -20 to +10 base pairs of the intron/exon boundary were established as a minimum requirement for each amplicon in accordance with guidelines from the Clinical Molecular Genetics Society (www.cmgs.org).

5.2.2 Genomic Mapping: SNP Genotyping Platforms

In order to identify the underlying disease locus a whole genome scan was performed on DNA samples from members of pedigree 1 using SNP genotyping platforms (GeneChip Human Mapping 500K Nsp array, Affymetrix). Prior to the submission of samples for analysis, I established the quantity and quality of DNA. Quantification was performed using the NanoDrop ND-1000 Spectrophotometer whereas agarose gel electrophoresis was used to establish the presence of high molecular weight DNA in stock samples. The DNA from patient C1-3 was found to be highly degraded. Due to the potential impact of degradation on genotype accuracy, other sources of DNA for this patient were investigated. A single section of skeletal muscle remained from this patient's OCT mounted biopsy measuring approximately 12 µm x 9 mm x 9 mm. In order to maximise the DNA yield extracted from this sample, I compared protocols involving QIAamp DNA Micro Kit (Qiagen) and MDA performed directly on tissue using control skeletal muscle samples. MDA performed directly on muscle sections using a modified protocol produced a consistently high yield. Both the quality and quantity of yield was determined using both the NanoDrop ND-1000 Spectrophotometer and agarose gel electrophoresis.

I submitted DNA samples from the mother, father and four affected children for analysis. DNA for patient C1-3 was submitted in duplicate; both the degraded sample and MDA products derived directly from tissue. Data were generated by the UCL Genomics facility (www.genomics.ucl.ac.uk) and genotypes examined by Professor R Kleta and Dr H Stanescu at the department of Internal Medicine, UCL (please refer to the methods section 2.2.1 for more detail). Comparable genotyping call rates were generated for each sample.

Parametric LOD scores were generated. Analyses performed using the multipoint linkage analysis programs Allegro and Simwalk revealed compatible regions of linkage on multiple chromosomes with a maximum LOD score of over 2.5 (Figure 28). Peaks on chromosomes 1, 2 and 17 were identified using both programs whereas an additional two peaks on chromosomes 3 and 8 were identified using the Simwalk program only. This most probably reflects false positive peaks deemed to appear towards the ends of the fragments that have been generated in order to perform the Simwalk run. Therefore those regions generated by the use of Allegro were initially interrogated.

Linkage detected on chromosome 1q contained regions consistent with both homozygosity and heterozygosity (Figure 29). A total of six regions of homozygosity were identified and localised between SNPs rs527213-rs1568804, rs2494195-rs1857623, rs3766934-rs17140182, rs4846992-rs701152, rs12068313-rs41406346, and rs6695181-rs10797534. Three regions of heterozygosity were detected between these regions of homozygosity and were located between SNPs rs1857623-rs3766934, rs17140182-rs4846992 and rs701152-rs12068313. These regions of interest located on chromosome 1 spanned just over 16 Mb and also contained two small regions of non compatibility. Two regions of homozygosity of approximately 0.7 Mb were detected on chromosome 2 between SNPs rs6708337-rs7589821 and rs17039367-rs10495987 (Figure 30). A single region of interest was identified on chromosome 17 (Figure 31). This region of approximately 4.7 Mb localised between SNPs rs854653 and rs16966014. In total these 12 regions contained 226 genes; 143 on chromosome 1, 82 on chromosome 17 and 1 located on chromosome 2 (Tables 15, 16, 17 and 18).

A

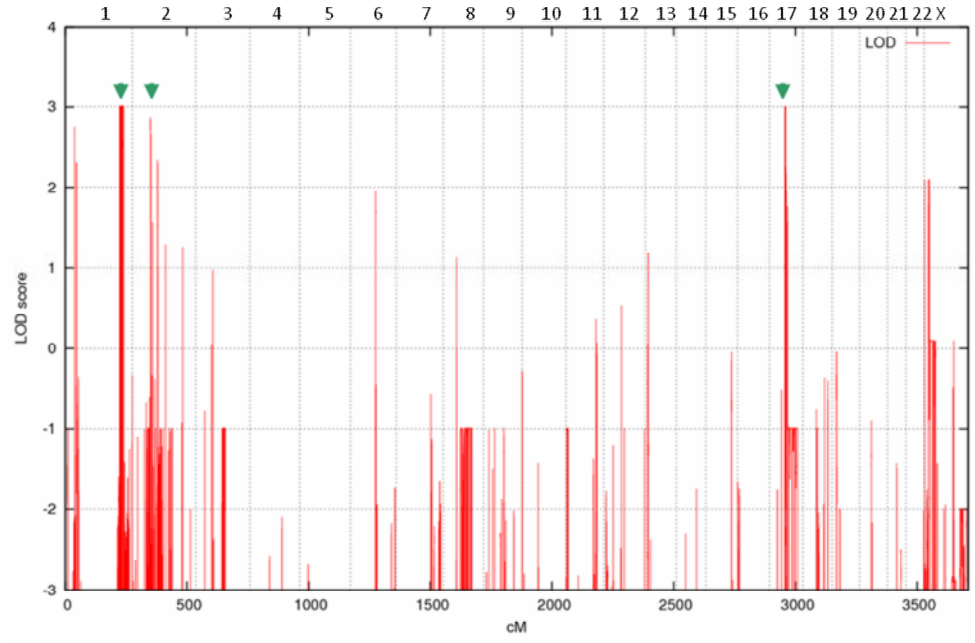

B

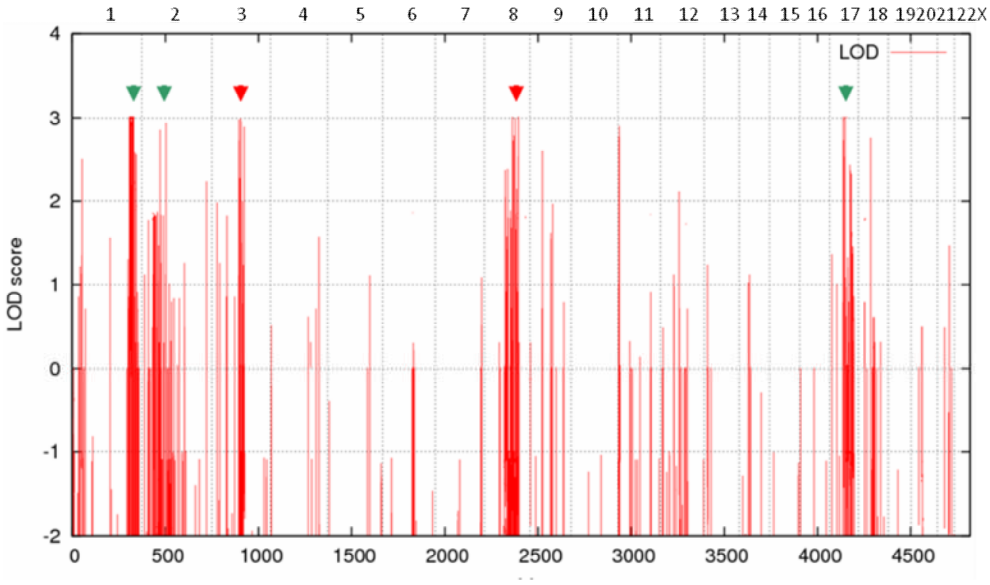

Figure 28. Whole genome linkage analysis using SNP data.

Peaks with a LOD score of approximately 3 are detected on multiple chromosomes. Analysis performed using the multipoint linkage analysis programs Allegro (A) and Simwalk (B). Arrow heads shown in green indicate peaks identified by both Allegro and Simwalk whereas those in blue denote those identified using Simwalk only. Genetic distance (in centimorgans) and individual chromosomes (1-22) are indicated on the lower and upper x axis, respectively.

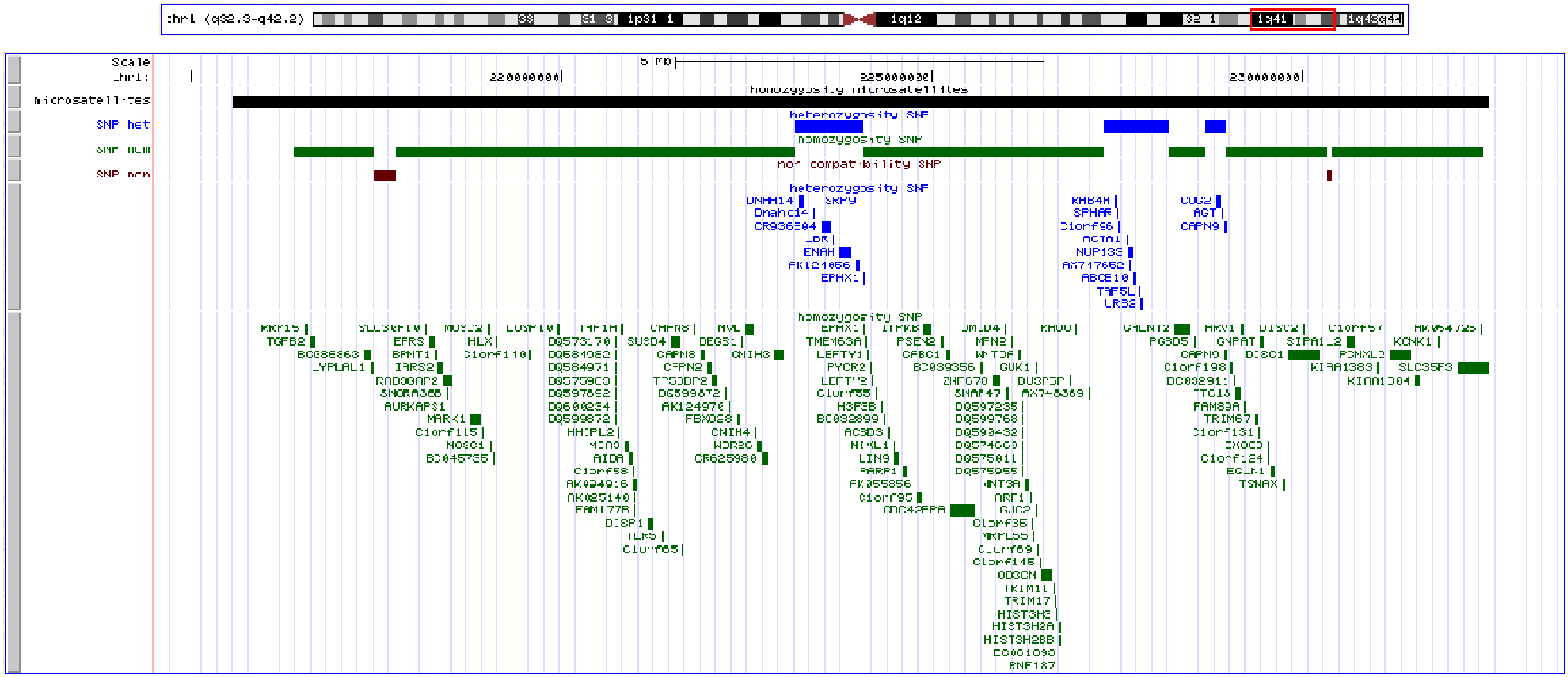

Figure 29. Depiction of the linkage intervals detected on chromosome 1q.

The black bar represents a region of homozygosity detected through the analysis of whole genome microsatellite arrays. Blue and green bars represent regions detected through the analysis of whole genome SNP arrays. Green and blue bars represent regions of homozygosity and heterozygosity respectively. Those genes lying within regions are shown below. Maroon bars represent regions of non compatibility detected within regions of heterozygosity. This figure was constructed using output from the UCSC Genome Browser (genome.ucsc.edu/).

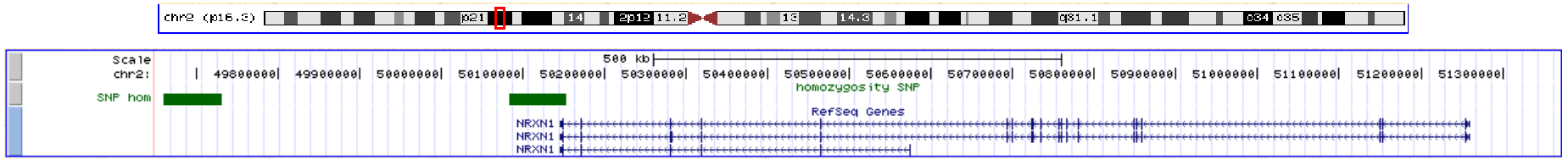

Figure 30. Depiction of the linkage intervals detected on chromosome 2p using SNP data.

Green bars indicated regions of homozygosity. No genes are located within the first region yet a single exon of *NRXN1* lies within the second region of homozygosity. This figure was constructed using output from the UCSC Genome Browser (genome.ucsc.edu/).

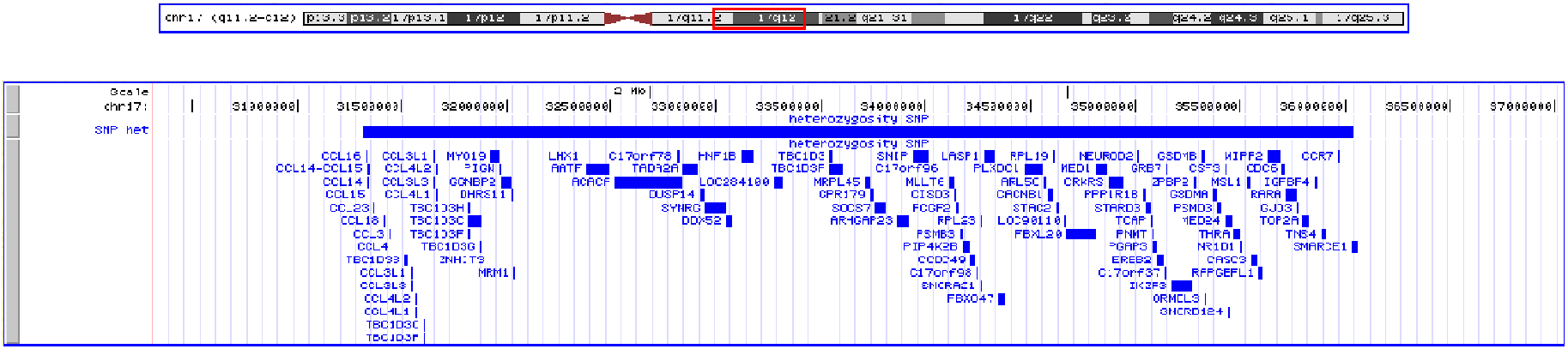

Figure 31. Depiction of the linkage interval detected on chromosome 17q using SNP data.

The blue bar indicates a region of heterozygosity detected through the analysis of whole genome SNP arrays. Those genes lying within this region are shown below the bar. This figure was constructed using output from the UCSC Genome Browser (genome.ucsc.edu/).

Symbol *	Protein	Molecular function **
ABCB10	ATP-binding cassette, sub-family B (MDR/TAP), member 10	ATP-binding cassette (ABC) transporter
ACTA1	actin, alpha 1, skeletal muscle	Actin and actin related protein
AGT	angiotensinogen (serpin peptidase inhibitor, clade A, member 8)	Serine protease inhibitor
AK124056	AK124056	N/A
AX747652	AX747652	N/A
C1orf96	chromosome 1 open reading frame 96	Molecular function unclassified
CAPN9	calpain 9	Cysteine protease
COG2	component of oligomeric golgi complex 2	Molecular function unclassified
CR936804	N/A	N/A
DNAH14	dynein, axonemal, heavy chain 14	N/A
Dnahc14	dynein, axonemal, heavy chain 14	N/A
ENAH	enabled homolog (*D. melanogaster*)	Non-motor actin binding protein
EPHX1	epoxide hydrolase 1, microsomal (xenobiotic)	Other hydrolase
LBR	lamin B receptor	Receptor
NUP133	nucleoporin 133kDa	Molecular function unclassified
RAB4A	RAB4A, member RAS oncogene family	Small GTPase
SPHAR	S-phase response (cyclin related)	N/A
SRP9	signal recognition particle 9kDa	Molecular function unclassified
TAF5L	TAF5-like RNA polymerase II, p300/CBP-associated factor (PCAF)-associated factor, 65kDa	Basal transcription factor
URB2	URB2 ribosome biogenesis 2 homolog (*S. cerevisiae*)	N/A

Table 15. Genes located within heterozygous linkage regions detected on chromosome 1 using SNP data.

* Gene symbols as per HUGO nomenclature. ** Molecular function as classified by the PANTHER (Protein ANalysis THrough Evolutionary Relationships) Classification System (http://www.pantherdb.org/). Chromosome 1 intervals; 223131228-224081640, 227318180-228204141 and 228695214-228979241.

Symbol *	Protein	Molecular function **
ACBD3	acyl-Coenzyme A binding domain containing 3	Molecular function unclassified
AIDA	axin interactor, dorsalization associated	Transmembrane receptor regulatory/adaptor protein
AK025140	AK025140	N/A
AK054726	AK054726	N/A
AK055856	AK055856	N/A
AK094916	AK094916	N/A
AK124970	AK124970	N/A
ARF1	ADP-ribosylation factor 1	Small GTPase
ARV1	ARV1 homolog (*S. cerevisiae*)	Molecular function unclassified
AURKAPS1	aurora kinase A pseudogene 1	N/A
AX748369	AX748369	N/A
BC032899	BC032899	N/A
BC032911	BC032911	N/A
BC039356	BC039356	N/A
BC045735	BC045735	N/A
BC061893	BC061893	N/A
BC086863	BC086863	N/A
BPNT1	3'(2'), 5'-bisphosphate nucleotidase 1	Nuclease, Other phosphatase
C1orf115	chromosome 1 open reading frame 115	Molecular function unclassified
C1orf124	chromosome 1 open reading frame 124	Molecular function unclassified
C1orf131	chromosome 1 open reading frame 131	Molecular function unclassified
C1orf140	N/A	Molecular function unclassified
C1orf145	chromosome 1 open reading frame 145	N/A
C1orf198	chromosome 1 open reading frame 198	Molecular function unclassified
C1orf35	chromosome 1 open reading frame 35	Molecular function unclassified
C1orf55	chromosome 1 open reading frame 55	Molecular function unclassified
C1orf57	chromosome 1 open reading frame 57	Biological process unclassified

Symbol *	Protein	Molecular function **
C1orf58	chromosome 1 open reading frame 58	Molecular function unclassified
C1orf65	chromosome 1 open reading frame 65	Molecular function unclassified
C1orf69	chromosome 1 open reading frame 69	Molecular function unclassified
C1orf95	chromosome 1 open reading frame 95	Molecular function unclassified
CABC1	chaperone, ABC1 activity of bc1 complex homolog (*S. pombe*)	Chaperone
CAPN2	calpain 2, (m/II) large subunit	Cysteine protease
CAPN8	calpain 8	Cysteine protease
CAPN9	calpain 9	Cysteine protease
CDC42BPA	CDC42 binding protein kinase alpha (DMPK-like)	Non-receptor serine/threonine protein kinase
CNIH3	cornichon homolog 3 (*D. melanogaster*)	Membrane-bound signaling molecule
CNIH4	cornichon homolog 4 (*D. melanogaster*)	Membrane traffic protein
CR625980	N/A	N/A
DEGS1	degenerative spermatocyte homolog 1, lipid desaturase (*D. melanogaster*)	Oxidoreductase
DISC1	disrupted in schizophrenia 1	Molecular function unclassified
DISC2	disrupted in schizophrenia 2 (non-protein coding)	N/A
DISP1	dispatched homolog 1 (*D. melanogaster*)	Molecular function unclassified
DQ573170	N/A	N/A
DQ574660	N/A	N/A
DQ575011	N/A	N/A
DQ575955	N/A	N/A
DQ575983	N/A	N/A
DQ584971	N/A	N/A
DQ584982	N/A	N/A
DQ590432	N/A	N/A
DQ597235	N/A	N/A
DQ597892	N/A	N/A
DQ599768	N/A	N/A

Symbol *	Protein	Molecular function **
DQ599872	N/A	N/A
DQ600234	N/A	N/A
DUSP10	dual specificity phosphatase 10	Kinase inhibitor, Protein phosphatase
DUSP5P	dual specificity phosphatase 5 pseudogene	N/A
EGLN1	egl nine homolog 1 (*C. elegans*)	Oxidoreductase
EPHX1	epoxide hydrolase 1, microsomal (xenobiotic)	Other hydrolase
EPRS	glutamyl-prolyl-tRNA synthetase	Aminoacyl-tRNA synthetase
EXOC8	exocyst complex component 8	Molecular function unclassified
FAM177B	family with sequence similarity 177, member B	N/A
FAM89A	family with sequence similarity 89, member A	Biological process unclassified
FBXO28	F-box protein 28	Molecular function unclassified
GALNT2	UDP-N-acetyl-alpha-D-galactosamine:polypeptide N-acetylgalactosaminyltransferase 2 (GalNAc-T2)	Glycosyltransferase
GJC2	gap junction protein, gamma 2, 47kDa	N/A
GNPAT	glyceronephosphate O-acyltransferase	Acyltransferase
GUK1	guanylate kinase 1	Nucleotide kinase
H3F3B	H3 histone, family 3B (H3.3B)	Chromatin packaging and remodeling
HHIPL2	HHIP-like 2	N/A
HIST3H2A	histone cluster 3, H2a	Histone
HIST3H2BB	histone cluster 3, H2bb	Molecular function unclassified
HIST3H3	histone cluster 3, H3	Histone
HLX	H2.0-like homeobox	N/A
IARS2	isoleucyl-tRNA synthetase 2, mitochondrial	Aminoacyl-tRNA synthetase, Ligase
ITPKB	inositol 1,4,5-trisphosphate 3-kinase B	Kinase Transferase
JMJD4	jumonji domain containing 4	Other receptor
KCNK1	potassium channel, subfamily K, member 1	Voltage-gated potassium channel
KIAA1383	KIAA1383	Molecular function unclassified
KIAA1804	N/A	N/A

Symbol *	Protein	Molecular function **
LEFTY1	left-right determination factor 1	Growth factor
LEFTY2	left-right determination factor 2	Growth factor
LIN9	lin-9 homolog (*C. elegans*)	Transcription cofactor
LYPLAL1	lysophospholipase-like 1	Phospholipase
MARK1	MAP/microtubule affinity-regulating kinase 1	Non-motor microtubule binding protein, Non-receptor serine/threonine protein kinase
MIA3	melanoma inhibitory activity family, member 3	Growth factor
MIXL1	Mix1 homeobox-like 1 (*X. laevis*)	Homeobox transcription factor, Other DNA-binding protein
MOSC1	MOCO sulphurase C-terminal domain containing 1	Molecular function unclassified
MOSC2	MOCO sulphurase C-terminal domain containing 2	Molecular function unclassified
MPN2	protease, serine, 38 (hugo gene name PRSS38)	Serine protease
MRPL55	mitochondrial ribosomal protein L55	Molecular function unclassified
NVL	nuclear VCP-like	Molecular function unclassified
OBSCN	obscurin, cytoskeletal calmodulin and titin-interacting RhoGEF	Actin binding cytoskeletal protein, Guanyl-nucleotide exchange factor
PARP1	poly (ADP-ribose) polymerase 1	Glycosyltransferase
PCNXL2	pecanex-like 2 (*D. melanogaster*)	Molecular function unclassified
PGBD5	piggyBac transposable element derived 5	Molecular function unclassified
PSEN2	presenilin 2 (Alzheimer disease 4)	Aspartic protease, Other select calcium binding proteins
PYCR2	pyrroline-5-carboxylate reductase family, member 2	Reductase
RAB3GAP2	RAB3 GTPase activating protein subunit 2 (non-catalytic)	G-protein modulator
RHOU	ras homolog gene family, member U	Small GTPase
RNF187	ring finger protein 187	Ubiquitin-protein ligase
RRP15	ribosomal RNA processing 15 homolog (*S. cerevisiae*)	N/A
SIPA1L2	signal-induced proliferation-associated 1 like 2	Other G-protein modulator

Symbol *	Protein	Molecular function **
SLC30A10	solute carrier family 30, member 10	Other transporter
SLC35F3	solute carrier family 35, member F3	Molecular function unclassified
SNAP47	synaptosomal-associated protein, 47kDa	N/A
SNORA36B	small nucleolar RNA, H/ACA box 36B	N/A
SUSD4	sushi domain containing 4	Molecular function unclassified
TAF1A	TATA box binding protein (TBP)-associated factor, RNA polymerase I, A, 48kDa	Molecular function unclassified
TGFB2	transforming growth factor, beta 2	Growth factor
TLR5	toll-like receptor 5	Receptor, Extracellular matrix
TMEM63A	transmembrane protein 63A	Molecular function unclassified
TP53BP2	tumor protein p53 binding protein, 2	Select regulatory molecule
TRIM11	tripartite motif-containing 11	Ubiquitin-protein ligase
TRIM17	tripartite motif-containing 17	Ubiquitin-protein ligase
TRIM67	tripartite motif-containing 67	Ubiquitin-protein ligase
TSNAX	translin-associated factor X	Single-stranded DNA-binding protein
TTC13	tetratricopeptide repeat domain 13	Glycosyltransferase
WDR26	WD repeat domain 26	Molecular function unclassified
WNT3A	wingless-type MMTV integration site family, member 3A	Other signaling molecule
WNT9A	wingless-type MMTV integration site family, member 9A	Other signaling molecule, Extracellular matrix structural protein
ZNF678	zinc finger protein 678	KRAB box transcription factor

Table 16. Genes located within homozygous linkage regions detected on chromosome 1 using SNP data.

* Gene symbols as per HUGO nomenclature. ** Molecular function as classified by the PANTHER (Protein ANalysis THrough Evolutionary Relationships) Classification System (http://www.pantherdb.org/). Chromosome 1 intervals; 216377616-217457828, 217755257-223131228, 224081640-227318180, 228204141- 228695214. 228979241-230328893 and 230395313-232447140.

Symbol *	Protein	Molecular function **
NRXN1	Neurexin 1	Other receptor

Table 17. Genes located within homozygous linkage regions detected on chromosome 2 using SNP data.

* Gene symbols as per HUGO nomenclature. ** Molecular function as classified by the PANTHER (Protein ANalysis THrough Evolutionary Relationships) Classification System (http://www.pantherdb.org/). Chromosome 2 intervals; 49660621-49731956 and 50083603-50153280.

Symbol *	Protein	Molecular function **
AATF	apoptosis antagonizing transcription factor	Other transcription factor
ACACA	acetyl-Coenzyme A carboxylase alpha	Other ligase
ARHGAP23	Rho GTPase activating protein 23	Molecular function unclassified
ARL5C	ADP-ribosylation factor-like 5C	N/A
C17orf37	chromosome 17 open reading frame 37	Oxidoreductase
C17orf78	chromosome 17 open reading frame 78	Molecular function unclassified
C17orf96	chromosome 17 open reading frame 96	N/A
C17orf98	chromosome 17 open reading frame 98	N/A
CACNB1	calcium channel, voltage-dependent, beta 1 subunit	Voltage-gated calcium channel
CASC3	cancer susceptibility candidate 3	Molecular function unclassified
CCDC49	coiled-coil domain containing 49	Molecular function unclassified
CCL14	chemokine (C-C motif) ligand 14	Chemokine
CCL14-CCL15	N/A	N/A
CCL15	chemokine (C-C motif) ligand 15	Chemokine
CCL16	chemokine (C-C motif) ligand 16	Chemokine
CCL18	chemokine (C-C motif) ligand 18 (pulmonary and activation-regulated)	Chemokine
CCL23	chemokine (C-C motif) ligand 23	Chemokine
CCL3	chemokine (C-C motif) ligand 3	Chemokine
CCL3L1	chemokine (C-C motif) ligand 3-like 1	Chemokine
CCL3L1	chemokine (C-C motif) ligand 3-like 1	Chemokine
CCL3L3	chemokine (C-C motif) ligand 3-like 3	Chemokine
CCL3L3	chemokine (C-C motif) ligand 3-like 3	Chemokine
CCL4	chemokine (C-C motif) ligand 4	Chemokine
CCL4L1	chemokine (C-C motif) ligand 4-like 1	Chemokine
CCL4L1	chemokine (C-C motif) ligand 4-like 1	Chemokine
CCL4L2	chemokine (C-C motif) ligand 4-like 2	Chemokine
CCL4L2	chemokine (C-C motif) ligand 4-like 2	Chemokine

Symbol *	Protein	Molecular function **
CCR7	chemokine (C-C motif) receptor 7	G-protein coupled receptor
CDC6	cell division cycle 6 homolog (S. cerevisiae)	Replication origin binding protein
CISD3	CDGSH iron sulfur domain 3	N/A
CRKRS	Cdc2-related kinase, arginine/serine-rich	Non-receptor serine/threonine protein kinase
CSF3	colony stimulating factor 3 (granulocyte)	Other cytokine
DDX52	DEAD (Asp-Glu-Ala-Asp) box polypeptide 52	RNA helicase
DHRS11	dehydrogenase/reductase (SDR family) member 11	N/A
DUSP14	dual specificity phosphatase 14	Kinase inhibitor, Protein phosphatase
ERBB2	v-erb-b2 erythroblastic leukemia viral oncogene homolog 2, neuro/glioblastoma derived oncogene homolog (avian)	Other miscellaneous function protein
FBXL20	F-box and leucine-rich repeat protein 20	Molecular function unclassified
FBXO47	F-box protein 47	N/A
GGNBP2	gametogenetin binding protein 2	Molecular function unclassified
GJD3	gap junction protein, delta 3, 31.9kDa	N/A
GPR179	G protein-coupled receptor 179	Molecular function unclassified
GRB7	growth factor receptor-bound protein 7	Transmembrane receptor regulatory/adaptor protein
GSDMA	gasdermin A	N/A
GSDMB	gasdermin B	N/A
HNF1B	HNF1 homeobox B	Other transcription factor, Nucleic acid binding
IGFBP4	insulin-like growth factor binding protein 4	Other miscellaneous function protein
IKZF3	IKAROS family zinc finger 3 (Aiolos)	KRAB box transcription factor, Other zinc finger transcription factor
LASP1	LIM and SH3 protein 1	Non-motor actin binding protein
LHX1	LIM homeobox 1	Homeobox transcription factor, Other zinc finger transcription factor, Nucleic acid binding
LOC284100	N/A	Other chaperones

Symbol *	Protein	Molecular function **
LOC90110	N/A	N/A
MED1	mediator complex subunit 1	Other DNA-binding protein, Other miscellaneous function protein
MED24	mediator complex subunit 24	Receptor
MLLT6	myeloid/lymphoid or mixed-lineage leukemia (trithorax homolog, *D. melanogaster*); translocated to, 6	Other zinc finger transcription factor, Nucleic acid binding
MRM1	mitochondrial rRNA methyltransferase 1 homolog (S. cerevisiae)	Molecular function unclassified
MRPL45	mitochondrial ribosomal protein L45	Molecular function unclassified
MSL1	male-specific lethal 1 homolog (*D. melanogaster*)	N/A
MYO19	myosin XIX	N/A
NEUROD2	neurogenic differentiation 2	Basic helix-loop-helix transcription factor, Nucleic acid binding
NR1D1	nuclear receptor subfamily 1, group D, member 1	Nuclear hormone receptor, Transcription factor, Nucleic acid binding
ORMDL3	ORM1-like 3 (S. cerevisiae)	Other miscellaneous function protein
PCGF2	polycomb group ring finger 2	Zinc finger transcription factor
PGAP3	post-GPI attachment to proteins 3	N/A
PIGW	phosphatidylinositol glycan anchor biosynthesis, class W	Acetyltransferase, AcyltransferasE
PIP4K2B	phosphatidylinositol-5-phosphate 4-kinase, type II, beta	Other kinase
PLXDC1	plexin domain containing 1	Molecular function unclassified
PNMT	phenylethanolamine N-methyltransferase	Methyltransferase
PPP1R1B	protein phosphatase 1, regulatory (inhibitor) subunit 1B	Other signaling molecule, Phosphatase inhibitor
PSMB3	proteasome (prosome, macropain) subunit, beta type, 3	Other proteases
PSMD3	proteasome (prosome, macropain) 26S subunit, non-ATPase, 3	Other enzyme activator
RAPGEFL1	Rap guanine nucleotide exchange factor (GEF)-like 1	Molecular function unclassified

Symbol *	Protein	Molecular function **
RARA	retinoic acid receptor, alpha	Nuclear hormone receptor, Transcription factor, Nucleic acid binding
RPL19	mitochondrial ribosomal protein L19	Ribosomal protein
RPL23	mitochondrial ribosomal protein L23	Ribosomal protein
SMARCE1	SWI/SNF related, matrix associated, actin dependent regulator of chromatin, subfamily e, member 1	Chromatin/chromatin-binding protein, Other DNA-binding protein
SNIP	Smad nuclear interacting protein 1	Molecular function unclassified
SNORA21	small nucleolar RNA, H/ACA box 21	N/A
SNORD124	small nucleolar RNA, C/D box 124	N/A
SOCS7	suppressor of cytokine signaling 7	Cytokine, Other miscellaneous function protein
STAC2	SH3 and cysteine rich domain 2	Molecular function unclassified
STARD3	StAR-related lipid transfer (START) domain containing 3	Other transfer/carrier protein, Other membrane traffic protein
SYNRG	synergin, gamma	N/A
TADA2A	transcriptional adaptor 2A	N/A
TBC1D3	TBC1 domain family, member 3	Other G-protein modulator
TBC1D3B	TBC1 domain family, member 3B	Other G-protein modulator
TBC1D3C	TBC1 domain family, member 3C	Other G-protein modulator
TBC1D3C	TBC1 domain family, member 3C	Other G-protein modulator
TBC1D3F	TBC1 domain family, member 3F	N/A
TBC1D3F	TBC1 domain family, member 3F	N/A
TBC1D3F	TBC1 domain family, member 3F	N/A
TBC1D3G	TBC1 domain family, member 3G	Other G-protein modulator
TBC1D3H	TBC1 domain family, member 3H	N/A
TCAP	titin-cap (telethonin)	Other cytoskeletal proteins
THRA	thyroid hormone receptor, alpha (erythroblastic leukemia viral (v-erb-a) oncogene homolog, avian)	Nuclear hormone receptor, Transcription factor
TNS4	tensin 4	Ribosomal protein

Symbol *	Protein	Molecular function **
TOP2A	topoisomerase (DNA) II alpha 170kDa	DNA topoisomerase, Select regulatory molecule, Isomerase
WIPF2	WAS/WASL interacting protein family, member 2	Molecular function unclassified
ZNHIT3	zinc finger, HIT type 3	Transcription cofactor
ZPBP2	zona pellucida binding protein 2	Molecular function unclassified

Table 18. Genes located within heterozygous linkage regions detected on chromosome 17 using SNP data.

* Gene symbols as per HUGO nomenclature. ** Molecular function as classified by the PANTHER (Protein ANalysis THrough Evolutionary Relationships) Classification System (http://www.pantherdb.org/). Chromosome 17 interval; 31317362-36039271.

Expression array analysis

A recent study combining linkage data with expression array analysis successfully pinpointed the causative gene in a rare form of epilepsy (Berkovic et al., 2008). Those transcripts significantly downregulated in affected compared to unaffected individuals were prioritised as candidate genes within the linkage interval. Analysis is based on the hypothesis that the causative mutation may affect mRNA stability. As lymphoblastoid cell lines were available from two affected members of pedigree 1, I used the approach described in order to identify down regulated transcripts lying within the linkage intervals previously detected. RNA from patient C1-1 and C1-4 was analysed against three unrelated control cell lines. I obtained two sex matched non disease controls from the European Collection of Cell Cultures' (ECACC) Human Random Collection and an unaffected age matched control was obtained from the ECACC's Human Genetic Collection (please refer to section 2.2.6, Table 3 for more detail). Samples were submitted to the UCL Genomics facility for analysis using the GeneChip(R) Human Gene 1.0 ST Arrays (Affymetrix). These expression arrays offer whole transcript analysis of well annotated coverage with each gene represented on the array by multiple probes spread across the full length of the gene. In order to identify significant differences between affected and unaffected individuals, data was analysed by the UCL Genomics facility with a two-way empirical Bayes ANOVA approach.

Analysis of the entire dataset showed large variation in the expression of genes within the Human Leukocyte Antigen (HLA) locus on chromosome 4. For example *HLA-DRB5, HLA-DRB1* and *HLA-DRB3* were found to be significantly dysregulated in patients C1-1 and C1-4 compared to the controls. I filtered the data generated from each probe set by genomic position using the NetAffx and Cytoband facilities (www.affymetrix.com). Analysis was confined to those probe sets mapping to the linkage intervals detailed above. In order to fully interrogate the data, all probes sets with a P value of less than or equal to 0.05 ranked by fold change (probe subset A) and all probes sets with a P value of less than or equal to 0.001 ranked by fold change (probe subset B) (Table 19). The gene *PSEN2*, detected by the probe set 7910156 and 7910147 was identified as the most down regulated transcript in probe subsets A and B respectively. The gene *KCNK1*, detected by the probe set 7910614 was identified as the most down regulated transcript in probe subset B. I had previously identified both these

genes as candidates during the reanalysis of microsatellite data and excluded mutations by uni-directional sequencing. The gene *NRXN1*, detected by the probe set 8052101 was identified as the second most down regulated gene in probe subset A. This candidate was down regulated over 2 fold in the affected members of pedigree 1 compared with that of control ($p<0.003$). The gene *NRXN1* encoding neurexin 1 was an appealing candidate due its function as an extracellular matrix ligand for α-dystroglycan. It is interesting to note that the most highly up-regulated transcript within the linkage intervals was CDC42 binding protein kinase alpha (DMPK-like) (*CDC42BPA*), lying within a region of homozygosity on chromosome 1 (Table 19).

	Symbol *	Probe ID set	Fold Change (Affected vs Control)	Fold Change (Description)	P-value **
Probe subset A (p≤0.01)	*PSEN2*	7910156	-2.34779	Affected down vs Control	0.000514556
	NRXN1	8052101	-2.30027	Affected down vs Control	0.00333748
	PCNXL2	7925122	-1.62803	Affected down vs Control	0.000574992
	RAB3GAP2	7924425	-1.56066	Affected down vs Control	0.00158968
	RAB3GAP2	7924420	-1.54135	Affected down vs Control	0.00962787

	Symbol *	Probe ID set	Fold Change (Affected vs Control)	Fold Change (Description)	P-value **
Probe subset B (p≤0.05)	*KCNK1*	7910614	-8.2585	Affected down vs Control	0.0476433
	PSEN2	7910147	-3.41015	Affected down vs Control	0.0161064
	ITPKB	7924762	-2.96634	Affected down vs Control	0.0378884
	TBC1D3B	8014383	-2.80814	Affected down vs Control	0.0156976
	TBC1D3B	8014405	-2.80814	Affected down vs Control	0.0156976

Table 19. The top 5 most down regulated transcripts detected by those probe sets lying within the 12 linkage intervals interrogated.
Two subsets of probe sets were ranked by fold reduction. Subset A; probe sets reaching a P value of 0.01 or less, subset B; probe sets reaching a P value of 0.05 or less. * Gene symbols as per HUGO nomenclature. ** P values calculated using ANOVA. Yellow shaded boxes indicate those genes investigated by me as candidate genes as part of the re-analysis of microsatellite linkage data. The blue shaded box indicates a novel candidate for further investigation.

Candidate gene analysis

I interrogated the intervals on chromosomes 1, 2 and 17 for the presence of candidate genes. The most promising novel candidate initially presented as *TCAP*. *TCAP* encodes telethonin and mutations in this gene have previously been associated with limb girdle forms of muscular dystrophy LGMD2G; NM_601954. The 12 genomic intervals were further scrutinised by the Endeavour software package (as previously described in chapter 4). As with the search performed on the genes lying within the original microsatellite linkage interval, both *PSEN2* and *OBSCN* were again identified as top ranking candidate genes (Table 20). Subsequent reanalysis generated with the inclusion of *DPM3* within the 'training set' recorded *PSEN2* as the top scoring candidate, *OBSCN* remained as the third highest scoring candidate (data not shown).

Mutation screening

Therefore to investigate novel candidate genes within the regions newly identified by whole genome SNP analysis, I performed mutation screening of *TCAP* and *NRXN1*. The human *TCAP* and *NRXN1* genes are organised into 2 and 22 exons encoding transcripts of 2.1 kb and 7.5 kb transcripts respectively. Uni-directional sequencing was carried out as described in section 2.2.3. No sequence variants were identified within these genes.

	Rank *	Protein (*encoding gene*) **	Gene ID †	Molecular function ‡	Subcellular localisation ‡‡
Endeavour prioritised candidates	1	Presenilin 2 (*PSEN2*)	5664	Aspartic protease, other select calcium binding proteins	Endoplasmic reticulum and Golgi
	2	Obscurin (*OBSCN*)	84033	Actin binding cytoskeletal protein, Guanyl-nucleotide exchange factor	Cytoplasm
	3	nuclear factor (erythroid-derived 2)-like 1 (*NFE2L1*)	4779	Other transcription factor	Nucleus
	4	inositol 1,4,5-trisphosphate 3-kinase B (*ITPKB*)	3707	Kinase, Transferase	No information
	5	guanylate kinase 1 (*GUK1*)	2987	Nucleotide kinase	Cytosol
Others	N/A	titin-cap (telethonin) (*TCAP*)	8557	Other cytoskeletal proteins	Cytoplasm
	N/A	Neurexin 1 (*NRXN1*)	9378	Other receptor	Integral to membrane

Table 20. Candidate genes identified from within the 12 linkage regions detected using high density SNP data.

* The top 5 ranked genes within the interval on 1q42 using the Endeavour gene prioritisation software (www.esat.kuleuven.be/endeavour/). The training set consisted of; *POMT1*, *POMT2*, *POMGNT1*, *LARGE*, *FCMD* and *FKRP*. ** Gene symbols and names as per HUGO nomenclature (www.genenames.org/). † Entrez Gene Identifier from the NCBI database (http://www.ncbi.nlm.nih.gov/). ‡ Molecular function as classified by the PANTHER (Protein ANalysis THrough Evolutionary Relationships) Classification System (http://www.pantherdb.org/). ‡‡ Subcellular localisation as annotated via the Universal Protein Resource Knowledge Base (UniProtKB) (www.uniprot.org). Blue shaded boxes indicate those genes previously screened by sequencing prior to the commencement of my PhD. Yellow shaded boxes indicate those genes investigated by me

as candidate genes. *PSEN2* was previously identified as a candidate gene within the linkage interval detected on chromosome 1q42 using the microsatellite data (Table 14).

5.3 DISCUSSION

This chapter comprises of work performed on a single family of Arabic descent originally recruited to the Dubowitz Neuromuscular Centre over twenty years ago (referred to here as pedigree 1). Four children from this consanguineous family are affected by a congenital form of muscular dystrophy characterised by proximal muscle weakness, muscle hypertrophy and early respiratory failure (Muntoni et al., 1998). Prior to the commencement of my PhD a genome wide linkage scan identified a region of homozygosity on chromosome 1q42 using a panel of microsatellite markers (Brockington et al., 2000). Candidate gene analysis had previously excluded a total of seven genes from this region by sequencing.

Recent years have seen a rapid expansion in the understanding of fundamental processes underlying CMD. Re-assessment of the pathology in pedigree 1 uncovered hypoglycosylation of α-dystroglycan in the remaining muscle biopsy samples. This provided further insight into the mechanism of disease in this family and part of my studies consisted of the re-evaluation of available data. After thorough inspection of the original region of homozygosity I generated a list of novel candidate genes. However, after screening four genes for mutations, the pathogenic alteration in this family remained elusive. The homozygous region on chromosome 1 contained a large number of genes and without further clues as to the causative gene's identity, I considered alternative approaches.

The use of microsatellite markers has more recently been superseded by the application of high density SNP genotyping platforms offering greater power to detect regions of linkage. Reports have demonstrated that the reanalysis of existing microsatellite scans with high density SNP arrays, have often detected regions of linkage missed by the initial scan (Middleton et al., 2004). Therefore in a collaborative project with the newly established UCL Genomics facility, Professor R Kleta and Dr H Stanescu at the Department of Internal Medicine UCL, DNA samples from members of pedigree 1 were examined by high density SNP genotyping platforms (GeneChip Human Mapping 500

Nsp array (Affymetrix)). This technology is capable of simultaneously genotyping 250,000 SNPs per sample with an average inter-marker distance of 5.8 kb.

Regions compatible with both homozygosity and compound heterozygosity were interrogated. Linkage to chromosome 1q was detected spanning approximately 16 Mb and lying within the original region reported in 2000. This peak reached a maximum LOD score of 3 and reduced the original region by around 1 Mb. Yet fine mapping of this interval revealed a much more complex pattern of inheritance than originally detected by the analysis of microsatellites. This interval consisted of six regions of homozygosity, three regions of heterozygosity and two smaller regions of non compatibility. In addition to those detected on chromosome 1, three further regions of suggestive linkage have also been identified consisting of two smaller regions of homozygosity on chromosome 2 (~666,000 bps and ~697,000 bps) and one region of heterozygosity on chromosome 17 (~4.7 Mb). Genomic regions on chromosomes 1, 2 and 17 total 22.1 Mb and contain 226 annotated reference genes.

Previous candidate gene analysis performed using the original microsatellite data by me and others, led to the exclusion of eleven genes. Using the intervals generated from the analysis of SNP data, three of these genes no longer locate to regions of compatibility (*B3GALNT2*, *LGALS8* and *NID1*). The remaining eight genes all reside within regions of homozygosity with the exception of *LBR*, which is now found to locate within a region of heterozygosity.

Within the twelve regions of linkage reaching a LOD score of over 2.5, a total of 226 reference genes are annotated. Initially *TCAP* presented as promising novel candidate gene. Telethonin (or titin-cap) encoded by *TCAP*, is a sarcomeric substrate of titin; a gigantic filamentous muscle protein essential for assembly of the sarcomere. Mutations have previously been found in cases of limb girdle muscular dystrophy (LGMD2G; NM_601954) and dilated cardiomyopathy (CMD1N; NM_607487) (Knoll et al., 2002; Moreira et al., 2000). Mutation screening of *TCAP* failed to detect any sequence variants in members of pedigree 1.

A recent study investigating the genes involved in a rare form of epilepsy combined both mapping data and expression analysis (Berkovic et al., 2008). The authors hypothesised that a reduction in mRNA levels of the defective protein may be a cause of disease. Expression microarrays were used to identify down regulated transcripts in lymphoblastoid cell lines of affected individuals compared to unaffected siblings from two families. Expression analysis was then used to prioritise candidate genes within regions of homozygosity. Truncating mutations in *SCARB2* were identified in all three families used for mapping (Action myoclonus–renal failure syndrome; OMIM 254900) (Berkovic et al., 2008). To explore whether the application of this approach could prove beneficial to the study of pedigree 1, expression analysis was performed. RNA profiles from lymphoblastoid cells from patients C1-1 and C1-4 were compared to that of control lymphoblastoid cells. This data was used to prioritise the 226 candidate genes identified by linkage. Linked transcripts found to be significantly down regulated in patients compared to controls were interrogated further. *PSEN2* and *KCNK1* were amongst those genes with the highest fold changes. Both these genes were also identified as candidates using the Endeavour prioritisation software although no mutations were identified upon mutation screening. Interestingly *NRXN1* was also identified as a significantly down regulated transcript in patients. Human neurexins are encoded by three genes (*NRXN1*; NM_600565, *NRXN2*; NM_600566 and *NRXN3*; NM_600567) which function as cell adhesion molecules and receptors. Thousands of neurexin isoforms are transcribed from these genes with the use of alternative promoters and alternative splicing (Tabuchi and Sudhof, 2002). Neurexins constitute neuronal dystroglycan ligands and recent evidence from collaborators has indicated that neurexin transcripts could also be expressed in skeletal muscle (unpublished observation from Professor D Górecki). Interestingly, respiratory impairment was found to be the cause of morbidity in α-*NRXN* deficient mice (Dudanova et al., 2006). The authors recorded spontaneous respiratory activity from brainstem slices showing dysfunctional rhythm output. Despite this, mutation screening of *NRXN1* failed to detect any sequence variants in members of pedigree 1.

The utility of the approach described by Berkovic *et al.* is heavily reliant on the mutation affecting mRNA stability. An adequate expression profile of the causative gene in control cell lines is also a prerequisite for study. A further limitation is that

without RNA from unaffected family members it is not possible to control for interfamilial or ethnic transcript level variation. If additional cell lines or sufficient skeletal muscle was available from members of pedigree 1, it would be interesting to confirm these transcript regulation alterations further and investigate their possible effect on protein production.

Regardless of the method used to prioritise candidate genes, a continuation of the systematic gene by gene mutation screening approach is problematic. In a data set comprising of such a large number of genes even robotically semi-automated Sanger sequencing becomes both time consuming and expensive. The advent of novel genomics based technologies now offers efficient alternatives to more traditional mutation detection techniques. Combining targeted sequence capture and massively parallel DNA sequencing offers a cost effective alternative to whole genome resequencing (Ng et al., 2010). Using high density sequence capture arrays either the entire exome (coding subsequences constituting approximately 5% of the whole genome), or specific genomic regions are captured on a microarray and subsequently sequenced. Therefore, work is currently underway within the department to design a custom hybridisation array for the enrichment and deep sequencing of those genomic regions identified on chromosomes 1, 2 and 17 which total 22.1 Mb.

In summary, I employed a combination of high density SNP genotyping platforms, expression microarrays and sequencing data to investigate the causes of congenital dystroglycanopathy in a single family. My analysis of this family has highlighted how linkage peaks can remain undetected due to the insufficient coverage or information content of sparse microsatellite makers used to generate whole genome linkage maps. Analysis of SNP mapping data revealed additional peaks on chromosomes 2 and 17 as well as uncovering an unexpectedly complex pattern of recombination within the original locus identified on chromosome 1. Regions identified on these peaks span over 22 Mb of genomic sequence and contain over 226 genes. After the exclusion of 13 genes by genomic sequencing, novel genomic based mutation detection approaches are now been applied in order to identify the causal mutation in this family.

CHAPTER 6. FINAL DISCUSSION

6 FINAL DISCUSSION

A reduction in α-dystroglycan's ligand-binding capacity is now associated with a growing subset of muscular dystrophies often associated with central nervous system pathogenesis (Michele et al., 2002). The term 'dystroglycanopathies' has been ascribed to these disorders which encompass a striking range of clinical severity (Brockington and Muntoni, 2005; Mercuri et al., 2006; Toda et al., 2003). Diagnosis is established upon the detection of hypoglycosylation of α-dystroglycan at the sarcolemma by immunolabeling of skeletal muscle sections (Brown et al., 2004; Dubowitz and Sewry, 2006). Hypoglycosylation of α-dystroglycan can also be observed as a reduction in molecular weight of α-dystroglycan on western blot (Michele et al., 2002).

Thus far, defects in seven genes have been identified in these autosomal recessive, genetically heterogeneous disorders (Beltran-Valero de Bernabe et al., 2002; Brockington et al., 2001a; Kobayashi et al., 1998; Lefeber et al., 2009; Longman et al., 2003; van Reeuwijk et al., 2005b; Yoshida et al., 2001). Six of these genes are thought to be involved in the addition of carbohydrate residues onto the α-dystroglycan peptide either via the process of *O*-mannosylation (*POMT1*, *POMT2*, *POMGNT1*) (Akasaka-Manya et al., 2004; Manya et al., 2003; Yoshida et al., 2001) or via other not fully characterised mechanisms (*FKTN*, *FKRP* and *LARGE*) (Brockington et al., 2005; Brown et al., 2004; Saito et al., 2006; Xiong et al., 2006). Mutations in a single patient have also been detected in *DPM3*, which functions in the synthesis of Dol-P-Man acting as the glycoyl donor for all mannosylation reactions resulting in hypoglycosylation of α-dystroglycan (Lefeber et al., 2009).

Prior to the molecular and biochemical defects being identified, it was not appreciated that these conditions belonged to the same broad category, nor the fact that individual gene defects were associated with such a broad spectrum of clinical severity. The prevalence of founder mutations in geographical subpopulations originally facilitated the identification of a number of causative genes (Diesen et al., 2004; Kobayashi et al., 1998). This led to the initial assumption that the severity of clinical features was dictated, not by the nature of mutation, but by the identity of the causative gene. However, since then a widening of the clinical spectrum associated with individual

genes has been observed. This is best exemplified by the finding of *FKRP* mutations in both congenital and limb girdle forms of MD (MDC1C and LGMD2I) (Brockington et al., 2001a; Brockington et al., 2001b). To assess the individual involvement of *POMT1*, *POMT2*, *POMGNT1*, *LARGE* and *FKTN* in chapter 3, I focussed on the study of a large cohort of dystroglycanopathy patients in whom *FKRP* involvement had been excluded. Not only did we expand the spectrum of clinical phenotype associated with each gene, but we also established for the first time, the frequency of involvement of these genes in a large population of dystroglycanopathy patients.

Interpreting the pathogenic significance of sequence alterations in chapter 3 was complicated by the abundance of previously unreported missense mutations. Investigations performed to ascertain the pathological significance of a *POMGNT1* sequence variant (section 3.2.3) highlight the importance of cautious interpretation of functional data, particularly when studying atypical clinical presentations. Further studies are needed to investigate the significance of the altered *POMGNT1* kinetic profile identified in patient A20. The implementation of enzymatic assays in the context of a diagnostic setting requires careful determination of kinetic parameters. Two of the novel mutations detected in chapter 3 have subsequently been reported as common founder mutations (Manzini et al., 2008; Yanagisawa et al., 2007). In particular the *FKTN* c.1167_1168insA alteration detected in patients A20 and A30 has a carrier frequency of 0.75% in the Ashkenazi Jewish population, therefore the pre-screening of this mutation in certain patients may be appropriate (Manzini et al., 2008).

A clear limitation of the mutation screening methods employed in this thesis is that structural and non coding variants remain undetected. The proportion of mutations that remain undetected has yet to be established. One of the few reports describing mutations in *LARGE* details a homozygous intragenic deletion spanning 63 kb in a WWS patient with consanguineous parents (van Reeuwijk et al., 2007). The deletion encompasses exons 9 and 10 and the intronic breakpoints were confirmed using a combination of Multiplex Ligation-dependent Probe Amplification and Multiplex Amplifiable Probe Hybridisation. The *Large*^{myd} mouse has a spontaneous deletion of approximately 100 kb encompassing exons 4, 5 and 6 (Browning et al., 2005). These findings highlight the importance of examining genomic deletions in this gene in particular. The gene *LARGE* spans over 660 kb of genomic DNA despite having a

coding sequence of only 4.4 kb (Peyrard et al., 1999). The overall exon content of *LARGE* is similar to that of *DMD* in which deletion mutations predominate (Ashton et al., 2008).

The refinement of a large cohort of patients in chapter 3 permitted further collaborative genotype-phenotype analyses focusing on additional parameters. A subset of patients in whom I had identified mutations in *POMT1*, *POMT2*, *POMGNT1*, *LARGE*, *FKRP* and *FKTN* were subsequently investigated further by members of the Dubowitz Neuromuscular Centre. A thorough analysis of muscle pathology for a subset of twenty four patients was performed (Jimenez-Mallebrera et al., 2008). A strong correlation between reduced α-dystroglycan epitope staining and clinical course was observed in patients with mutations in *POMT1*, *POMT2* and *POMGNT1*. However, this was not consistently found in patients with defects in *FKTN* or *FKRP*. Some of these patients with milder forms of LGMD and no brain involvement were found to have a profound depletion in α-dystroglycan epitope staining. Therefore this study indicates that it is not always possible to correlate clinical course with α-dystroglycan epitope labelling. In a further study focusing on brain involvement, magnetic resonance image brain scans from twenty seven patients were analysed (Clement et al., 2008a). This analysis expanded the spectrum of structural abnormalities associated with mutations in *POMT1*, *POMT2*, *POMGNT1* and *LARGE*. In particular this study demonstrated that infratentorial structures were often affected in isolation therefore highlighting their particular susceptibility in these conditions.

After the exclusion of *FKRP*, we detected mutations in approximately a third of all patients screened. Since the work in chapter 3 was performed, results from three other populations have been reported in which mutations in *POMT1*, *POMT2*, *POMGNT1*, *LARGE*, *FKTN* and *FKRP* were systematically screened. Each study focused on a defined clinical presentation and mutations were detected in a total of 53%, 40% and 51% of CMD, WWS and type II lissencephaly patient cohorts respectively (Bouchet et al., 2007; Manzini et al., 2008; Mercuri et al., 2009). In combination, these studies confirm our finding that a high proportion of patients remain without a definitive molecular diagnosis. Following the work of chapter 3 my research shifted focus towards to the identification of further causative loci.

The identification of causative dystroglycanopathy genes has been hindered by the extensive genetic and clinical heterogeneity present in these disorders. To compound these issues, as studies of common founder mutations and large informative pedigrees are exhausted, the detection of rarely mutated genes becomes more challenging. In order to tackle these issues I used a combination of strategies. Chapter 4 focused on the study of a large cohort of sporadic patients and the establishment of a cell culture model of dystroglycanopathy to assess various candidate genes. Chapter 5 focused on the analysis of a single consanguineous family using high density SNP genotyping and expression analysis. Despite these attempts no clearly pathogenic sequence alterations were identified in any of the novel genes screened. It is important to note that the exclusion of these candidate genes from the cohorts studied does not preclude their involvement in disease pathogenesis. However, it may be inferred that mutations in *GYLTL1B, β3GNT1, WWP1, GYG1, GYG2, MGAT5B* and *DAG1* are not a common cause of human dystroglycanopathy.

Chapter 4 described the establishment of a cell culture model of dystroglycanopathy by modulating individual gene expression in a mouse myogenic cell line. This enabled the functional assessment of individual genes in the pathway of α-dystroglycan glycosylation. A reduction in the IIH6 epitope, as observed on western blot, could not be induced by the modulation of *Gyg1* using the conditions optimised with *Pomt1* siRNA oligonucleotides. The lack of available antibodies to *Gyg1* prevented the confirmation of an induced reduction in protein production. A reduction in *β3gnt1* mRNA did, however, induce a reduction of the IIH6 epitope present on α-dystroglycan. Previous reports have demonstrated that *β3GNT1* is required for the production of laminin-binding glycans in aggressive human carcinoma cell lines (Bao et al., 2009). Due to the tissue specific nature of α-dystroglycan glycosylation it was important to confirm the involvement of *β3GNT1* in a skeletal muscle system. As an extension, the future development of this mouse skeletal muscle cell experimental approach using fluorescence activated cell sorting would facilitate the accurate quantification of α-dystroglycan epitopes. A number of candidate genes could not be studied with the cell culture assay due to the differing expression patterns and gene complements between the species studied. Despite the expression of *WWP1* in human and chicken skeletal muscle, this gene was not detectable at a sufficient level in C2C12 cells. The predominant expression of both *GYLTL1B* and *MGAT5B* in brain also precluded their

analysis in this mouse skeletal muscle cell system. As these genes remain candidates for patients with isolated lissencephaly, it would be interesting to modulate their expression in a neuronal cell system to investigate tissue specific glycosylation patterns. Evidently the generation of mouse models for these genes would facilitate the analysis of their function in a whole mammalian system and the assessment of potential clinic-pathological similarities to human dystroglycanopathy patients.

Despite the relatively low abundance of α-dystroglycan, 30% of all *O*-linked glycans detected in rabbit brain have been reported to be linked via mannose, indicating the presence of other proteins with *O*-linked mannose in the brain (Chai et al., 1999). Although only partial structural information is available, *O*-mannosyl glycans have been identified on both cell adhesion molecule, neural 1 and tenascin R [OMIM 11690 and 601995 respectively] (Endo, 1999; Wing et al., 1992). Further studies are needed to clarify the distribution of these structures throughout tissues, developmental stages and under pathological conditions. Although further insights have come about from the genetic and biochemical analysis of dystroglycanopathy patients, the exact glycans present, the function of these glycans in ligand binding and the glycosylation pathways involved remain uncharacterised (Yoshida-Moriguchi et al., 2010). It is likely that defects in proteins other than glycosyltransferases (such as nucleotide sugar transporters, convertases, glycosidases and conserved oligomeric Golgi proteins), which all participate in the process of glycosylation, may be identified in dystroglycanopathy patients (Muntoni et al., 2009).

The application of array based mutation detection techniques will be crucial to the identification of novel dystroglycanopathy loci. The Dubowitz Neuromuscular Centre is currently involved in a large European consortium based project aimed at designing, producing and validating novel DNA-chips for neuromuscular disease diagnostics. Arrays will be developed with oligonucleotide probes designed to all known neuromuscular disease genes as well as a large panel of novel genes. Each candidate gene discussed in chapter 4 has been included in the panel of candidate genes. In addition, DNA from a subset of patients from cohort B (screened in chapter 4) will be submitted for exome sequencing as part of the UK10K Project at the Wellcome Trust Sanger Institute, Cambridge. The interrogation of these data will provide a wealth of information as to the sequence variants present within patients.

The relative frequency of common mutations in dystroglycanopathies, such as the *FKRP* p.Leu276Ile in the Caucasian population, has been explained by the founder effect (Frosk et al., 2005). There has been speculation that selective advantage may also be contributing to the maintenance of these alleles (Frosk et al., 2005). A recent high profile study analysed over three million SNPs to detect areas of positive natural selection across the human genome (Sabeti et al., 2006). Four hundred and twenty chromosomes from three continents were genotyped. Evidence of positive selection was detected for loci within *LARGE* and *DMD* in the West African sample (Yoruba in Ibadan, Nigeria) where the Lassa virus is endemic. The Lassa virus causes severe hemorrhagic fever and is associated with a high mortality rate in humans. Alpha-dystroglycan functions as the receptor for a range of arenaviruses including the Lassa virus (Cao et al., 1998). Protein *O*-mannosylation and the specific post-translational modification induced by *LARGE* are crucial for infection (Kunz et al., 2005). The authors suggest that the presence of selected *LARGE* and *DMD* alleles in chromosomes from the Yoruba population may correlate with disease resistance (Sabeti et al., 2006). Detailed infection studies on genotyped cell lines as well as correlating haplotypes with clinical outcomes are needed to further investigate these observations.

In 2004, Campbell and colleagues reported that the function of *LARGE* could be exploited as a viable therapeutic strategy for dystroglycanopathy patients (Barresi et al., 2004). The overexpression of human *LARGE* in the *Large*^{myd} mouse model not only ameliorated symptoms but was well tolerated in skeletal muscle. Surprisingly the overexpression of *LARGE* in patient cell lines with *FKTN*, *POMGNT1* and *POMT1* mutations resulted in the production of the IIH6 antigen and a restoration of α-dystroglycan ligand binding. It is not yet clear how an increase in *LARGE* expression restores ligand binding and thus compensating for the defects in other causative dystroglycanopathy loci (Yoshida-Moriguchi et al., 2010). Transgenic mouse models with ubiquitous expression of human *LARGE* are currently being developed in the Dubowitz Neuromuscular Centre in order to assess any induced pathological changes, as well as to facilitate crossing with dystroglycanopathy mouse models (Brockington *et al.* submitted for publication). Although the correction of neuronal migration disorders occurring early in fetal development presents as a significant challenge, this treatment

could be valuable to patients at the milder end of the clinical spectrum in whom only skeletal muscle is involved.

Pharmacological regulation of *LARGE* expression is a possible avenue for therapy (Muntoni et al., 2009). Further studies are needed to identify pharmacological agents that may affect the transcription or recycling of *LARGE*. This approach would not be amenable in those patients with mutations in *LARGE*, although with only three cases reported worldwide, this excludes only a minority of dystroglycanopathy patients. Interestingly the production of the IIH6 antigen in cell lines can also be induced by the expression of *GYLTL1B* (Brockington et al., 2005). As demonstrated in this thesis, mutations in this gene are not a common cause of dystroglycanopathy in our cohort, therefore the modulation of this gene offers further therapeutic potential. The increase in ligand-binding glycans induced by *LARGE* overexpression requires the function of endogenous *β3GNT1* (Bao et al., 2009). Indeed Bao *et al*. reported that increasing *β3GNT1* expression substantially augmented the *LARGE*-mediated formation of α-dystroglycan ligand-binding glycans. The presence of mutations in *β3GNT1* in patients would therefore preclude the use of *LARGE* modulation as a therapeutic strategy. Therefore the exclusion of mutations in *β3GNT1* and *GYLTL1B* (chapter 4; cohort B) has been of significant benefit when evaluating the appropriateness of these therapeutic strategies amongst the dystroglycanopathy population.

To date, candidate gene analysis has mainly focussed on further putative and demonstrated glycosyltransferases (Muntoni et al., 2009). Through the application of next generation sequencing technologies it is likely that defects in a range of cellular pathways will be found to underlie dystroglycanopathy pathogenesis. Clues may also be offered by the further characterisation of α-dystroglycan processing. The recent identification of a phosphorylated *O*-mannosyl glycan on the mucin-like domain of α-dystroglycan may implicate those proteins participating in phosphoryl modifications (Yoshida-Moriguchi et al., 2010).

This thesis describes a variety of approaches used to further refine the genetics of muscular dystrophies with defective glycosylation of α-dystroglycan. Additional information regarding the pathogenic processes underlying these disorders will further

aid in the diagnosis, treatment and development of novel therapeutic approaches for these incapacitating diseases.

APPENDICES

Gene	Intron/exon	Nucleotide variant	Amino acid change	Combined references
FKTN	3	c.165-6A>G	intronic	rs41277795 / additional change
FKTN	4	c.165C>T	p.Arg56Cys	rs41277797 / additional change
FKTN	5	c.608A>G	p.Arg203Gln	rs34787999 / additional change / dmd.nl
FKTN	7	c.910+14G>A	intronic	- / additional change
FKTN	8	c.1026C>A	synonymous	rs17309806 / additional change / dmd.nl
FKTN	8	c.1044+44A>G	intronic	- / additional change
FKTN	8	c.1044+58C>T	intronic	- / additional change
FKTN	10	c.1336A>G	p.Asn446Asp	- / additional change / dmd.nl
LARGE	2	c.1-63C>T	intronic	- / additional change
LARGE	4	c.211G>A	p.Glu71Lys	- / additional change *
LARGE	5	c.435C>T	synonymous	- / additional change
LARGE	6	c.552G>A	synonymous	- / additional change
LARGE	10	c.1092C>T	synonymous	- / additional change *
LARGE	11	c.1287+105G>C	intronic	-
LARGE	11	c.1287+146T>C	intronic	- / additional change
LARGE	12	c.1451+38C>T	intronic	- *
LARGE	14	c.1878-24A>G	intronic	- *

Gene	Intron/exon	Nucleotide variant	Amino acid change	Combined references
LARGE	15	c.1994G>A	p.Arg665His	- / additional change
LARGE	15	c.2073+36C>T	intronic	- / additional change
LARGE	16	c.2100C>T	synonymous	- / additional change
POMGNT1	1	c.1-11G>A	intronic	- / additional change *
POMGNT1	3	c.235+33T>G	intronic	-
POMGNT1	4	c.355-27C>T	intronic	- *
POMGNT1	8	c.681A>G	synonymous	- / additional change
POMGNT1	13	c.111-23C>T	intronic	- / additional change
POMGNT1	20	c.1785+31C>A	intronic	- *
POMGNT1	21	c.1867A>G	p.Met623Val	rs6659553
POMGNT1	21	c.1895+30A>G	intronic	- *
POMT1	2	c.122-5dupT	intronic	- / additional change
POMT1	3	c.129C>T	synonymous	- / additional change *
POMT1	5	c.318G>A	synonymous	- *
POMT1	5	c.428-21C>T	intronic	rs11243404 / additional change
POMT1	7	c.751C>T	p.Gln251Trp	rs3887873
POMT1	7	c.752A>G	p.Gln251Trp	rs2296949

Gene	Intron/exon	Nucleotide variant	Amino acid change	Combined references
POMT1	8	c.766-43T>G	intronic	- / additional change
POMT1	8	c.766-48G>A	intronic	rs2018621 / additional change
POMT1	9	c.855G>C	p.Leu285Phe	- / dmd.nl
POMT1	10	c.922-65G>A	intronic	rs34159422 / additional change
POMT1	10	c.942C>T	synonymous	- / additional change / dmd.nl
POMT1	10	c.979G>A	p.Val327Ile	rs4740164 / additional change / dmd.nl
POMT1	11	c.1053-113C>G	intronic	rs10901068 / additional change
POMT1	11	c.1053-102G>A	intronic	- / additional change
POMT1	11	c.1053-39C>T	intronic	- *
POMT1	11	c.1113C>T	synonymous	rs3739494 / additional change / dmd.nl
POMT1	11	c.1148+16G>A	intronic	- / additional change / dmd.nl
POMT1	11	c.1148+45C>G	intronic	- / additional change
POMT1	12	c.1149-64C>T	intronic	-
POMT1	13	c.1299C>A	p.Asp433Glu	rs11243406 / additional change / dmd.nl
POMT1	13	c.1338+84C>T	intronic	- / additional change
POMT1	14	c.1432-61G>A	intronic	rs1547768 / additional change
POMT1	16	c.1565G>A	p.Arg522Lys	dmd.nl

Gene	Intron/exon	Nucleotide variant	Amino acid change	Combined references
POMT1	17	c.1764+48G>C	intronic	rs2277152 / additional change / dmd.nl
POMT1	17	c.1758G>A	synonymous	rs34954751 / additional change / dmd.nl
POMT1	19	c.1922C>T	p.Ala641Val	rs12115566
POMT1	19	c.2069+13C>T	intronic	rs4740165 / dmd.nl
POMT1	20	c.2244+41C>T	intronic	rs3739495 / additional change / dmd.nl
POMT2	3	c.439-45C>T	intronic	- / additional change
POMT2	3	c.439-98A>T	intronic	- *
POMT2	4	c.548-77C>G	intronic	- *
POMT2	6	c.817-26C>T	intronic	- *
POMT2	8	c.1007-32G>A	intronic	- / additional change
POMT2	8	c.1007-46C>T	intronic	- *
POMT2	9	c.1116+165C>T	intronic	- / additional change
POMT2	9	c.1116+35A>G	intronic	rs2302831 / additional change
POMT2	9	c.1116+91C>T	intronic	- / additional change *
POMT2	9	c.1117-20C>T	intronic	- / additional change
POMT2	13	c.1383A>G	synonymous	- / additional change / dmd.nl
POMT2	14	c.1654-6A>G	intronic	- / additional change

Gene	Intron/exon	Nucleotide variant	Amino acid change	Combined references
POMT2	15	c.1653+38G>A	intronic	- / additional change
POMT2	15	c.1654-41G>C	intronic	-
POMT2	16	c.1725+51G>C	intronic	- *
POMT2	17	c.1785T>C	synonymous	- / additional change
POMT2	18	c.1881G>A	synonymous	- / additional change
POMT2	18	c.1891A>G	synonymous	- / additional change
POMT2	19	c.1911T>G	synonymous	- / additional change / dmd.nl
POMT2	20	c.2148-18A>G	intronic	- / additional change
POMT2	21	c.2253+75C>T	intronic	- / additional change / dmd.nl

Appendix Table 1. List of non pathogenic variants detected in *POMT1*, *POMT2*, *POMGNT1*, *FKTN* and *LARGE*.
dbSNP references are provided where applicable. Additional changes in patients with a pathogenic mutation are annotated. * Variation detected in a single individual. Dmd.nl refers to the change recorded as a polymorphism on the Leiden database (www.dmd.nl).

PCR Protocol *	Exon	Primer name	Forward primer (5'–>3')	Primer name	Reverse primer (5'–>3')
PCR A	1	WWP1_1_F_T1_01	TTAGGGTTTTCTTTTAATGGGATG	WWP1_1_R_T1_01	TATTAATCATTTAAGGGCCAATGC
PCR A	2	WWP1_2_F_T1_02	AGTAGCCCTTTTGTATTGTTTCTT	WWP1_2_R_T1_02	TCACTCATTACTTTGAAGTCATTTT
PCR A	3	WWP1_3_F_T1_01	TAAGACTCCTGTGTTGGTGTTTTG	WWP1_3_R_T1_01	CCACAAAGTTAATCAATCACAAGC
PCR A	4	WWP1_4_F_T1_01	TATGCACAGAAGCAATTAAAGGTG	WWP1_4_R_T1_01	AAATATTCTACCTGGCAGTTGTCC
PCR A	5	WWP1_5_F_T1_01	TATAACAAACTGCAGCTCATCTCC	WWP1_5_R_T1_01	TGTGTGGCAAATTCTAAACTAAGG
PCR A	6	WWP1_6_F_T1_01	CATGTCATATCTTTGTTCATTACTC	WWP1_6_R_T1_01	ACAAAAAGGGAAGTGTAGGCATGG
PCR A	7	WWP1_7_F_T1_01	TCTGGATTAGGCTCTGAATAAGTG	WWP1_7_R_T1_01	CAATGAAAACATTTTATGCACAC
PCR A	8	WWP1_8_F_T1_01	TTAAAATGTGGGGTATTCTCTTCC	WWP1_8_R_T1_01	GCAGAATGAAAGAATCAAATTACG
PCR A	9	WWP1_9_F_T1_01	GGTAGAATGGGAAGGTAATTTAGG	WWP1_9_R_T1_01	ATGTGATTATGGTCAAGGGATAGC
PCR C	10-11	WWP1_10_F_T1_02	CTTGAACTCCTGGGCTTAAGTA	WWP1_11_R_T1_02	CACAAGATGAACCTTTTCTAGGTA
PCR A	12	WWP1_12_F_T1_01	AAGATCCAAGAACTCAAGGGTATG	WWP1_12_R_T1_01	ATTGTCAAATGAGAGCAAAGACAG
PCR A	13	WWP1_13_F_T1_01	CATAAATACAATGTCCTTCTTTGT	WWP1_13_R_T1_01	TTCTGCTAAAATCCTCCTTACCTG
PCR A	14	WWP1_14_F_T1_01	AATCTTCCTGTGGTATTTTGTTGG	WWP1_14_R_T1_01	AAAACAAAGGCACTCAACAAGTG
PCR A	15	WWP1_15_F_T1_01	TCATCTCTTGAGTTAAAAGCATTG	WWP1_15_R_T1_01	TCAGATCCTACATTTTGTACATTG
PCR A	16	WWP1_16_F_T1_01	AAATGGAGAGCCAGATCATAGAAG	WWP1_16_R_T1_01	TTGGTAACAAAACTTGTGAATAGC

PCR Protocol *	Exon	Primer name	Forward primer (5'–>3')	Primer name	Reverse primer (5'–>3')
PCR A	17	WWP1_17_F_T1_01	GATTGAGGCAGGGTATGGTAATAG	WWP1_17_R_T1_01	GCCACATTCTTCAATGTTGTTATC
PCR A	18	WWP1_18_F_T1_01	TCTGGATAAGGTTTGAAGATTTTG	WWP1_18_R_T1_01	TTTTCAAGAACATTGGTACTGGTG
PCR A	19	WWP1_19_F_T1_01	TGTTAGAACTGATTTCCTCAAATG	WWP1_19_R_T1_01	CAAATGAGAGGATTCAAGATTGTG
PCR A	20	WWP1_20_F_T1_01	TTGGTTTGAGTTCAATAAACATGG	WWP1_20_R_T1_01	TAAACTGTGTCCAAAAGCAGTCTC
PCR A	21	WWP1_21_F_T1_01	AACCTTTAGCACATCTTTTGAACC	WWP1_21_R_T1_01	TCTAAATGAAGCCCTACCTACAGC
PCR A	22	WWP1_22_F_T1_01	CTCTGCAACAATTTTCTTCTTCAG	WWP1_22_R_T1_01	AAAGTGTTCAGTTATAGAATGCTG
PCR A	23	WWP1_23_F_T1_01	AATTTAGATTACTCTAAATACTTC	WWP1_23_R_T1_01	CGGAAAACATACTTTGAGAGGTTC

Appendix Table 2. *WWP1* genomic PCR primers used for mutation analysis.

* PCR protocols are described in section 2.2.3.

PCR Protocol *	Exon	Primer name	Forward primer (5'–>3')	Primer name	Reverse primer (5'–>3')
PCR B	1	GNTIX_1_F_T1_01	CTCCCGGTCCCCAAAATGTGAAG	GNTIX_1_R_T1_01	ATCACCAGGGGTTGAAGTGTGAAC
PCR A	2	GNTIX_2_F_T1_01	CTCATTCGTAAAACATTTGTGCAG	GNTIX_2_R_T1_01	GACACCCAACTAAAGAAGCAACAC
PCR A	3	GNTIX_3_F_T1_01	CTTAGGAAATGATCCCAATGTCAC	GNTIX_3_R_T1_01	AATCTTCTCCAGATTCACAAAAGG
PCR A	4	GNTIX_4_F_T1_01	TTTCCCGTATGTCTGTAATGTGTG	GNTIX_4_R_T1_01	AGTTGTCCTGCTGAAAGCCTAAAC
PCR A	5	GNTIX_5_F_T1_01	CTGATGAGCTTTAAGGTGGGAAAG	GNTIX_5_R_T1_01	TTTAATCATTTGCTGTGAGAAAGC
PCR A	6	GNTIX_6_F_T1_01	GGTCCTGGTTCAATCTCTTCTCTG	GNTIX_6_R_T1_02	CTGGCAAGCAGCTCAGTCTCATTC
PCR A	7	GNTIX_7_F_T1_01	CCTTAGAAAGTGCAGGAGAAGCTG	GNTIX_7_R_T1_01	ACAGCTTGTTTGAAGACCTATTCC
PCR A	8	GNTIX_8_F_T1_01	GCAAGCACGTGACTATCTTGTTC	GNTIX_8_R_T1_01	GGATTAGGAGTGGTGATGTCCTG
PCR A	9	GNTIX_9_F_T1_01	TCCTTTCTGAGAGTCTGTGCTAAG	GNTIX_9_R_T1_01	CAGGACAGTATGTTCTCCCACCTG
PCR A	10	GNTIX_10_F_T1_01	CCTAGTCCAAGTGCTAACACACAC	GNTIX_10_R_T1_01	GTTCACACACTTATGGAGCAGGAG
PCR A	11	GNTIX_11_F_T1_01	GCTCTGATCTTTGTAGCAGTCTCC	GNTIX_11_R_T1_01	GGGTGTCTTTAAATAGCAGTTAGG
PCR A	12	GNTIX_12_F_T1_01	CATCTTCTGACTTCCAGACCAAAG	GNTIX_12_R_T1_01	CTATAGGACCTCTCCTGCCTGGTG
PCR A	13	GNTIX_13_F_T1_01	TTATAGCTCACATAACAGGCTGAG	GNTIX_13_R_T1_01	GACAAAGAAAGGTACCCCATACAC
PCR A	14	GNTIX_14_F_T1_01	GTGTATGGGGTACCTTTCTTTGTC	GNTIX_14_R_T1_01	CACCGTTTTCTAATCAGAGTGAAG
PCR A	15	GNTIX_15_F_T1_01	TGAGCTTTATCCTCATTGCAGTTG	GNTIX_15_R_T1_01	AACTCTGGGAAGAGACTGGACAGG

PCR Protocol *	Exon	Primer name	Forward primer (5'–>3')	Primer name	Reverse primer (5'–>3')
PCR B	16	GNTIX_16_F_T1_01	TGGTATTCAGTAAGCGCCCAGTAG	GNTIX_16_R_T1_01	TGACTCATTGGAAAGCATTACATC
PCR B	17	GNTIX_17_F_T1_01	CAGCAGGTGGGATAAAGGAGCCG	GNTIX_17_R_T1_02	CGGCATGCTGCCTCCTCCTATTC

Appendix Table 3. *MGAT5b* genomic PCR primers used for mutation analysis.

* PCR protocols are described in section 2.2.3.

PCR Protocol *	Exon	Primer name	Forward primer (5'–>3')	Primer name	Reverse primer (5'–>3')
PCR B	1	GYG_1_F_T1_01	CACGTGACGGCCGCTATAAGAGC	GYG_1_R_T1_01	GCTGAGGGCGGAGGAGAAGG
PCR A	2	GYG_2_F_T1_01	CTGGTTTTGCTGAATTACTGTTTG	GYG_2_R_T1_01	CTAGGAGGAGGTTTCAAATACAGC
PCR A	3	GYG_3_F_T1_01	AACTGGACATGCAAATAAACACAG	GYG_3_R_T1_01	ATTCCTCAAATGCCTACAGGTCTC
PCR A	4	GYG_4_F_T1_01	TTTTGTGTTGGATGACATAGGAAG	GYG_4_R_T1_01	CACACACAATATTTCCCAGAAGAG
PCR A	5	GYG_5_F_T1_01	GGTCCAGTTATGTGCTCCTATAAA	GYG_5_R_T1_01	CTATCTGTTATTTCCCTCGGAATG
PCR A	6	GYG_6_F_T1_01	AAGTGCTACTAAGTGCTGCTTATC	GYG_6_R_T1_01	ATGCTGCTAAATATTCCACATCTC
PCR A	7	GYG_7_F_T1_01	GCGGCTCTCTAGTTAGATTCTTTC	GYG_7_R_T1_01	GCAATAAATTGAAGACAGAAAAGC
PCR A	8	GYG_8_F_T1_01	TTTTTGCTACTTTGCATGATGATT	GYG_8_R_T1_01	CAGACTTTTCTCAACCCAGCTCTA

Appendix Table 4. *GYG* genomic PCR primers used for mutation analysis.

* PCR protocols are described in section 2.2.3.

PCR Protocol *	Exon	Primer name	Forward primer (5'–>3')	Primer name	Reverse primer (5'–>3')
PCR A	2	GYG2_2_F_T1_01	AGGTGACATGGAGTGGGTAGGAG	GYG2_2_R_T1_01	ACAAAAGGAAACTGGTGAAATCC
PCR A	3	GYG2_3_F_T1_01	AAGGTTCCTTCATACTCCTCCTG	GYG2_3_R_T1_01	AGAGTTACACTCCTGAGGGACAG
PCR A	4	GYG2_4_F_T1_01	GGAGAGGAGAGGAGGTGACTATG	GYG2_4_R_T1_01	TGGTTGGGAGAATGAACTGTAAC
PCR A	5	GYG2_5_F_T1_01	ATTCTCTTTGCATTCCACGTTTG	GYG2_5_R_T1_01	GTGGGAGAATCACTTGAACTCAG
PCR B	6	GYG2_6_F_T1_01	TGTAATCCCAGCTACTCAAGAGG	GYG2_6_R_T1_01	CTGAGCGAGGTGTGACTGTATG
PCR A	7	GYG2_7_F_T1_01	AGGCAAGTGTTTATGTTGAGAGC	GYG2_7_R_T1_01	TAAATATGCCGACAGCTGGTATG
PCR A	8	GYG2_8_F_T1_01	CATTGGGACAAGTCCTTCAGAG	GYG2_8_R_T1_01	CAGGTGCTTGCTTCTCAGTATTC
PCR A	9	GYG2_9_F_T1_01	TTATTTAATGATTGGCAGATGG	GYG2_9_R_T1_01	AAATAAATGCAGAGCCTTGAATG
PCR A	10	GYG2_10_F_T1_01	AACAAACACAGGTATTGGTGAGC	GYG2_10_R_T1_01	AACTTATTCCAGGTGGGAGAAAC
PCR B	11	GYG2_11_F_T1_01	CCTCCTAAAATGCTGGGATTAC	GYG2_11_R_T1_01	ATCAGACTTGAAGATGGCAAAAG
PCR A	12	GYG2_12_F_T1_01	ATCTCTTTTTGAGAACTGAGATGC	GYG2_12_R_T1_01	ATAGAGGCACAAGGTTCAACAG

Appendix Table 5. *GYG2* genomic PCR primers used for mutation analysis.

* PCR protocols are described in section 2.2.3.

PCR Protocol *	Exon	Primer name	Forward primer (5'–>3')	Primer name	Reverse primer (5'–>3')
PCR D	1	La2_1_F_T1_01	CCAGGGCTGAGTCTCCCATCTCGC	La2_1_R_T1_01	CAGGTACTGTGATTCCCGCAGATG
PCR B	2	La2_2_F_T1_01	GAATCACAGTACCTGGCGTCTGTC	La2_2_R_T1_01	AGGATGTTCTTACAACTGCCCTTC
PCR B	3	La2_3_F_T1_01	GGAAAAGCTCTTTGCAGATGG	La2_3_R_T1_01	GACTGATGATTCTCTTCTCCAACC
PCR A	4	La2_4_F_T1_01	CCTCTCCTCTGTGTCACTGCAAG	La2_4_R_T1_01	CTCTGGTTCTCCACAAGACCGATC
PCR A	5	La2_5_F_T1_01	CTTTGCTCACTTTTCTGGTGAGAG	La2_5_R_T1_01	GTTCTTTTCACAGCAATGTTCTTC
PCR B	6	La2_6_F_T1_01	AAAACAAAGGACACCTTCATGACC	La2_6_R_T1_01	TTGAGGTCAGACGCCTCAGAGTAG
PCR A	7	La2_7_F_T1_01	GCATGACAGCATCTCTTCATTGG	La2_7_R_T1_01	AAGAATTCCACATGCTTGTTCTTC
PCR B	8	La2_8_F_T1_01	GTCTCTGCTCAGGACATCTTCAAC	La2_8_R_T1_01	GGGATAGGGCAGAACAACACATC
PCR A	9	La2_9_F_T1_01	AATTTCTACCTGACCTTCCTGGAG	La2_9_R_T1_01	GTAGCTCACTACCACAGCATCAGG
PCR A	10	La2_10_F_T1_01	TAAAAGTATTTGAAGGGTGCTCAG	La2_10_R_T1_01	TAATACAAACCCCAATTGACAGAG
PCR A	11	La2_11_F_T1_01	GGTGGTCTAGTCCTGTGGCTAATG	La2_11_R_T1_01	ACCACCACGTAGGGTTCATAGTTG
PCR A	12	La2_12_F_T1_01	CCTTCAGGTAGGAGAGGCTACTTC	La2_12_R_T1_01	GGGCAGATTATTTTAATTCCACAG
PCR A	13	La2_13_F_T1_01	ACACCACTAGGCAACACTGTTAGA	La2_13_R_T1_01	CCCTTCCCAGAGACCTTAAATAAT

Appendix Table 6. *GYLTL1B* genomic PCR primers used for mutation analysis.

* PCR protocols are described in section 2.2.3.

PCR Protocol *	Exon	Primer name	Forward primer (5'–>3')	Primer name	Reverse primer (5'–>3')
PCR B	2	DAG_2_F_T1_01	GCTCAAGTCTAAACCTGCTTTTC	DAG_2_R_T1_01	CTCTTATGAACATCAGTGGCTGTC
PCR B	3	DAG_3a_F_T1_02	CTGTCACACAATTCAGGTTAACTG	DAG_3A_R_T1_02	GCTCTACTTCTGAGAAGCTCCGC
PCR B	3	DAG_3b_F_T1_01	GTATCATCTGCCTGTGCTGCGGAT	DAG_3B_R_T1_01	GAGGAGCAATGGCTGGAGATGTGG
PCR B	3	DAG_3c_F_T1_01	CAGATCCATGCTACACCCACACCT	DAG_3C_R_T1_01	GGTGATGGAAACTTTGGTGGTGAC
PCR B	3	DAG_3d_F_T1_01	CAACGCCTTCAACTGACTCCACC	DAG_3D_R_T1_01	GAACCTTGCAGGAGCCCTATCCCC
PCR B	3	DAG_3e_F_T1_01	CACGAGTATTTCATGCATGCCAC	DAG_3E_R_T1_01	CCTCTGAGGGCACTCTCCTGGGT
PCR B	3	DAG_3f_F_T1_01	CTGACTTTAAGGCCACAAGCATC	DAG_3F_R_T1_01	CGCATTGGGATCCTCATCCCGCAG
PCR B	3	DAG_3g_F_T1_01	CCTCCTGAGTACCCCAACCAGAG	DAG_3G_R_T1_01	CTAGGTCAGGTGTCGGCTCCCGG

Appendix Table 7. *DAG1* genomic PCR primers used for mutation analysis.

* PCR protocols are described in section 2.2.3.

PCR Protocol *	Exon	Primer name	Forward primer (5'–>3')	Primer name	Reverse primer (5'–>3')
PCR B	1	iGNT_1a_F_T1_01	CGGCAGGCTGCGGTAAATCCGGGC	iGNT_1a_R_T1_01	CCTCCCAGCGCTCCAGCAGACCCG
PCR B	1	iGNT_1b_F_T1_01	CCTGCTGAAGACCACCATGGACC	iGNT_1b_R_T1_01	CCACTGGTTGCTCTGATCCAGCAT
PCR B	1	iGNT_1c_F_T1_01	GGGCCAACTATGCCCTGGTGATCG	iGNT_1c_R_T1_01	CCAGGGCCACTCCTCATAACTCCC
PCR B	2	iGNT_2_F_T1_01	GAAGATCCAGGATACTTCCAGAGG	iGNT_2_R_T1_02	GTAAAGTGGAGCGACATTTCTTAC

Appendix Table 8. *β3GNT1* genomic PCR primers used for mutation analysis.

* PCR protocols are described in section 2.2.3.

PCR Protocol *	Exon	Primer name	Forward primer (5'–>3')	Primer name	Reverse primer (5'–>3')
PCR A	2	NRXN1_2A_F_T1_01	CCCCTTACCTTTCTGTCTCTC	NRXN1_2A_R_T1_01	GTCGATGAAGAGCGTGGTGTT
PCR A	2	NRXN1_2B_F_T1_01	AGCTCAGCTTCTCCATCTTCT	NRXN1_2B_R_T1_01	AGATTAGGAAGACCCCATGCAC
PCR A	3	NRXN1_3_F_T1_01	CCCCTTGAATGATAGTGATG	NRXN1_3_R_T1_01	AACAAGGGTTGGAGTTAAGC
PCR A	4	NRXN1_4_F_T1_01	GGGTTTGGTTGGATTTTAAG	NRXN1_4_R_T1_01	CTTTGCAGTGATGGTTTGAAAG
PCR A	5	NRXN1_5_F_T1_01	ACATGTCCTGATTGCATCTC	NRXN1_5_R_T1_01	ACACATATACCTACCTCCCAGTG
PCR A	6	NRXN1_6_F_T1_01	CTGTTTGACTGAGACAGAGTTCA	NRXN1_6_R_T1_01	GGAGCCCTGTATCATGTTG
PCR A	7	NRXN1_7_F_T1_01	GTGGGAGGCCTACTTGTTAG	NRXN1_7_R_T1_01	CAGAAGTTGACAGGAACAGG
PCR A	8	NRXN1_8_F_T1_01	GTTCCGTCATAGGTCTAAAAACA	NRXN1_8_R_T1_01	GAATTTAAAGTTGTGCCGTTT
PCR A	9	NRXN1_9_F_T1_01	CGTTGAAAGTTACATGAGCTG	NRXN1_9_R_T1_01	GGCTAAAGAAACAAATGCAG
PCR A	10	NRXN1_10_F_T1_01	CCTCCAAGGAGTTAACCATC	NRXN1_10_R_T1_01	TACGTTTCAATGGTCAGTGC
PCR A	11	NRXN1_11_F_T1_01	CTTTCCAGCTCACAGTTTTG	NRXN1_11_R_T1_01	CCATGGCAAACAGGCTAC
PCR A	12	NRXN1_12_F_T1_01	GAGAAAGTTGCAGCCAGTC	NRXN1_12_R_T1_01	TTTTACAACCCAGATGATGG
PCR A	13	NRXN1_13_F_T1_01	GTTGTCATTTTCCTTGCTTG	NRXN1_13_R_T1_01	GGATTGTGTGAATACATTTCAAG
PCR A	14	NRXN1_14_F_T1_01	GTACCAAGGAGGGATTTGG	NRXN1_14_R_T1_01	AGATGATTTAAACAAATGCCTTC
PCR A	15	NRXN1_15_F_T1_01	CACTGAATAATCCTCTTTGCTG	NRXN1_15_R_T1_01	GCAGAAGGTACAAACACACC

PCR Protocol *	Exon	Primer name	Forward primer (5'–>3')	Primer name	Reverse primer (5'–>3')
PCR A	16	NRXN1_16_F_T1_01	TTTAGCACTTTGGGGAAAAC	NRXN1_16_R_T1_01	GAATTTTGCTGGACAGTGAG
PCR A	17	NRXN1_17_F_T1_01	CAGCCTCTCAGTTCCTAATTC	NRXN1_17_R_T1_01	CATCATCACAGGATTTAGCC
PCR A	18	NRXN1_18_F_T1_01	AACTTGGTCCACTTTCTTGAG	NRXN1_18_R_T1_01	AAGGAAGCATCCAAGAAGC
PCR A	19	NRXN1_19_F_T1_01	TCAATTCCCTTGAAAGTGTG	NRXN1_19_R_T1_01	CCACAATTTGGTGAAACG
PCR A	20	NRXN1_20_F_T1_01	CTCATTATTCACCCCATAAAAG	NRXN1_20_R_T1_01	TTCATATTCAAACGGAATGC
PCR A	21	NRXN1_21_F_T1_01	TCTACAAGTTGGCTGTCACC	NRXN1_21_R_T1_01	AAGAGTCCTCATCTCACAATCAA
PCR A	22	NRXN1_22_F_T1_01	TCTCCCAGAGAACTTTAAATCAC	NRXN1_22_R_T1_02	TGTGCTTCATAAAAAGGAAAGT
PCR A	23	NRXN1_BETA1_F_T1_01	ACTGTCCGAAGGAGGGAGAG	NRXN1_BETA1_R_T1_01	GAGCCTTAGGAGCCCAGGAG

Appendix Table 9. *NRXN1* genomic PCR primers used for mutation analysis.

* PCR protocols are described in section 2.2.3.

PCR Protocol *	Exon	Primer name	Forward primer (5'–>3')	Primer name	Reverse primer (5'–>3')
PCR A	2	LBR_2_F_T1_01	CTAAATCATCCTCTCAAATGATTC	LBR_2_R_T1_01	GACTATGCCTCATTCATACATTC
PCR A	3	LBR_3_F_T1_01	TTTAGAGTTAATGGTAGCAGTTCC	LBR_3_R_T1_01	CAACTTAGATTTGATGTTTCAGTG
PCR A	4	LBR_4_F_T1_01	AATCTGTTTTATTGCTTGATTCC	LBR_4_R_T1_01	CAGCATCTCAATACAGCTATACAC
PCR A	5	LBR_5_F_T1_01	GTGTATAGCTGTATTGAGATGCTG	LBR_5_R_T1_01	CTACTCCATAATCCCTCAAAATG
PCR A	6	LBR_6_F_T1_01	AACGAGTTCTGATCTTAACAAATC	LBR_6_R_T1_01	TAAGTTCCTCCTAATAAGCAAGTG
PCR A	7	LBR_7_F_T1_01	ATTTAAGCACATTTAGTCTTGAGG	LBR_7_R_T1_01	ATAAACAGTTGCTCTTCCAACTAC
PCR A	8	LBR_8_F_T1_01	ATAGTGGCGTAAGTTTCATGTGAG	LBR_8_R_T1_01	GCAATCTATTCAAATCTGGAAATG
PCR A	9	LBR_9_F_T1_01	AGTGGAATTGTGAGCCTGGATAG	LBR_9_R_T1_01	TAACAGGGCATCTTAAACCTCTG
PCR A	10	LBR_10_F_T1_01	ATGGTGCTGAGATGTCTTATTC	LBR_10_R_T1_01	TAAACACAAGAACAGCTGATAAAC
PCR A	11	LBR_11_F_T1_01	TTAGAGATCTGTTATCTCCAGAGC	LBR_11_R_T1_01	AATGGCATGTTTCAAGTATGTAG
PCR A	12	LBR_12_F_T1_01	AATTTCCTCAGAGCATAGAAATC	LBR_12_R_T1_01	CAAACTAGCACTCTTCTGAAATG
PCR A	13	LBR_13_F_T1_01	CTTGCACGTAAGTATTGATTTATG	LBR_13_R_T1_02	AGCCAGAGGAGCTTCTACAGAG
PCR A	14	LBR_14_F_T1_01	GTGGTTCCATTTTTAGAGAATTTG	LBR_14_R_T1_01	CATAGTCCTGACTCAAAAAGAAAA

Appendix Table 10. *LBR* genomic PCR primers used for mutation analysis.

* PCR protocols are described in section 2.2.3.

PCR Protocol *	Exon	Primer name	Forward primer (5'–>3')	Primer name	Reverse primer (5'–>3')
PCR D	1	TTC13_1_F_T1_01	CACACAATGCTTCTCCCCTTGT	TTC13_1__R_T1_01	GGGCAGCCGGAGGCGTGAGG
PCR A	2	TTC13_2_F_T1_01	GTTGCCACTTTTAGTGTTATTCAC	TTC13_2__R_T1_01	GTTCTATGTCCAGAATAATCAACC
PCR A	3	TTC13_3_F_T1_01	ACTGAAAGCCATAAAGTGTAAAAC	TTC13_3__R_T1_01	AAAGCCAGTCTCTCTACTCCTTAC
PCR A	4	TTC13_4_F_T1_01	AGTGGTGAAAGTAGAAGAATTCAG	TTC13_4__R_T1_01	AGACTATGAGTAAATTGCTTGACC
PCR A	5	TTC13_5_F_T1_01	CACATTTCATACAAATGAGCTTTA	TTC13_5__R_T1_01	TGAAAGGAACTCAAACTCTAAGTC
PCR A	6	TTC13_6_F_T1_01	ATCTGTGGAATTTGTGATAGGTAG	TTC13_6__R_T1_01	TAAAGGCATTAAGTACCGACATAG
PCR A	7	TTC13_7_F_T1_01	GATACAACCCAGAATGTGAAATAG	TTC13_7__R_T1_01	TTAATTTCAGCTACAGAAAATGC
PCR A	8	TTC13_8_F_T1_01	AAAACTCCCAACTGTTTGAATG	TTC13_8__R_T1_01	ACTTATTAACCTTTGATCCTTTCC
PCR A	9	TTC13_9_F_T1_01	AGTCCTCCTAAAAGAAAATCTGTC	TTC13_9__R_T1_01	GATGAACGTTTTCTAGACCAATAC
PCR A	10	TTC13_10_F_T1_01	GAGCTGGTGAGATTTAGAAGTAAG	TTC13_10__R_T1_01	ACTAGTCTACAGGACAAGAGCAAT
PCR A	11	TTC13_11_F_T1_01	CTTAAGAACTTTAAGGTGAGCATC	TTC13_11__R_T1_01	CATACGAAACATAAAAGAGTCAAG
PCR A	12	TTC13_12_F_T1_01	CCCAGACTGACTGACTTATATTTG	TTC13_12__R_T1_01	GGATATTCACAGGCACAAGGATA
PCR A	13	TTC13_13_F_T1_01	GACTGAAGTAAGGATTATGTGGTC	TTC13_13__R_T1_01	AGTCTTCTTTCAGAATTCAGTTTG
PCR A	14	TTC13_14_F_T1_01	TACTATAGGAGTGAGGAAGAATGC	TTC13_14__R_T1_01	TAACAAACTTTAGAGAGGAAAACC
PCR A	15	TTC13_15_F_T1_01	GAGTAACCTTTGATATTCATTTGC	TTC13_15__R_T1_01	GTGCAGAGTCAATCAGTATGTTC

PCR Protocol *	Exon	Primer name	Forward primer (5'–>3')	Primer name	Reverse primer (5'–>3')
PCR A	16	TTC13_16_F_T1_01	ACTGAGTTTGATGCCAGAATAG	TTC13_16__R_T1_01	AATTTGATAGACCTTGTTTAGCC
PCR A	17	TTC13_17_F_T1_01	AGATGTTTCCTTAATTCTCATCTG	TTC13_17__R_T1_01	AATGTGTTCATACGAGTGATTTC
PCR A	18	TTC13_18_F_T1_01	CATCTCTTGTATCAGATGACCTC	TTC13_18__R_T1_01	TAACTGGTTATAACTGCTCACTGG
PCR A	19	TTC13_19_F_T1_01	AGGCAACTATCACATTTTATGAAG	TTC13_19__R_T1_01	TTATTATCCTCCCCATTACTGTAG
PCR A	20	TTC13_20_F_T1_01	TTTATCCAAGAGTTGCAGTTTAAG	TTC13_20__R_T1_01	GCACATGATACACAGTAAACTTTC
PCR A	21	TTC13_21_F_T1_01	TTATCTTTCATGATGGGAAGTC	TTC13_21__R_T1_01	GGAGATCTATGTAACTCGTGTACC
PCR D	22	TTC13_22_F_T1_01	AATGCTTGGTTATGTATTAAGTCC	TTC13_22__R_T1_01	GGATTACAGGTATGAGCTACTGTG
PCR A	23	TTC13_23_F_T1_01	AATGATAGGAATAAATATAAGCTCT	TTC13_23__R_T1_01	GGTTCAGAAAAGTAAAGAAAATGA

Appendix Table 11. *TTC13* genomic PCR primers used for mutation analysis.

* PCR protocols are described in section 2.2.3.

PCR Protocol *	Exon	Primer name	Forward primer (5'–>3')	Primer name	Reverse primer (5'–>3')
PCR D	1	KCNK1_1_F_T1_01	AGGAAAAGAAGGAAGAAAAACAT	KCNK1_1__R_T1_01	GGACGCCAGTAAGGGGAAGGTC
PCR A	2	KCNK1_2_F_T1_01	GCAGATGATAGGCATATATTGTTT	KCNK1_2__R_T1_01	CAAAATAGAGACAGAAGCCTGTAA
PCR A	3	KCNK1_3_F_T1_01	TAAAAATTAAGAAACTGGCAATGA	KCNK1_3__R_T1_01	TGCATTCTGATAAAAATGAACATA

Appendix Table 12. *KCNK1* genomic PCR primers used for mutation analysis.

* PCR protocols are described in section 2.2.3.

PCR Protocol *	Exon	Primer name	Forward primer (5'–>3')	Primer name	Reverse primer (5'–>3')
PCR A	4	PSEN2_4_F_T1_01	CTCTCAAGGCCTCTTGTTTTATG	PSEN2_4_R_T1_01	ATCCTCATCATTACTTCCCTTCTC
PCR A	5	PSEN2_5_F_T1_01	CAACATTCAAACTTCTCATTTCTG	PSEN2_5_R_T1_01	CAAGTAGGTCACAATCCAGGAG
PCR A	6	PSEN2_6_F_T1_01	CTGGAGGACAGGAACTGCTC	PSEN2_6_R_T1_01	TCTAAAGGCGGCTGTTTCAC
PCR A	7	PSEN2_7_F_T1_01	GAAGTAGCCTAATGAAGAGCATTC	PSEN2_7_R_T1_01	TTAAATCAGGAACGAGACAGAAAC
PCR A	8	PSEN2_8_F_T1_01	GGGAAGGAAATGTTAGTAAAGAGG	PSEN2_8_R_T1_01	CTGTTTTACAAAGGCGACTCTC
PCR A	9	PSEN2_9_F_T1_01	TGTGACTGGAGAATGAGAATTTG	PSEN2_9_R_T1_01	TGCTTCCTGTCCTAACTTTCTAAG
PCR A	10	PSEN2_10_F_T1_01	ACAACGGCCTCCTAACAATG	PSEN2_10_R_T1_01	TGGTTTTCAACGGACCTTTC
PCR A	11	PSEN2_11_F_T1_01	GAAGATTCAGCAAGTGTTGGAC	PSEN2_11_R_T1_01	CATCTTCTACTTTCACAGAGATGC
PCR A	12	PSEN2_12_F_T1_01	GTTTTACCTGAGTTTCAGAACTGC	PSEN2_12_R_T1_01	CTCAGAGGGAAGAGAAGAAATG
PCR A	13	PSEN2_13_F_T1_01	TAACAGGTGAGGTGATCTAATGG	PSEN2_13_R_T1_01	CCTCACCAAGTAAACACGTACT

Appendix Table 13. *PSEN2* PCR primers used for mutation analysis.

* PCR protocols are described in section 2.2.3.

PCR Protocol *	Exon	Primer name	Forward primer (5'–>3')	Primer name	Reverse primer (5'–>3')
PCR 1	1	TCAP_1_F_T1_01	TCTACTTATAGCATCTGACACCAG	TCAP_1_R_T1_01	CTGGTGGTAGGTCTCATGTCTC
PCR 1	2	TCAP_2_F_T1_01	AGCATGAAGCCCTGGAGAAAT	TCAP_2_R_T1_01	AACTCTGGGCAAACTACAAAGC

Appendix Table 14. *TCAP* genomic PCR primers used for mutation analysis.

* PCR protocols are described in section 2.2.3.

PUBLICATIONS PERTAINING TO THE WORK WITHIN THIS THESIS

Permission to reproduce these articles has been granted by Oxford University Press, John Wiley and Sons and Jama & Archives.

doi:10.1093/brain/awm212 *Brain* (2007), **130**, 2725–2735

Refining genotype–phenotype correlations in muscular dystrophies with defective glycosylation of dystroglycan

Caroline Godfrey,[1,2,*] Emma Clement,[1,*] Rachael Mein,[2] Martin Brockington,[1] Janine Smith,[3] Beril Talim,[4] Volker Straub,[5] Stephanie Robb,[1] Ros Quinlivan,[6] Lucy Feng,[1] Cecilia Jimenez-Mallebrera,[1] Eugenio Mercuri,[1] Adnan Y. Manzur,[1] Maria Kinali,[1] Silvia Torelli,[1] Susan C. Brown,[1] Caroline A. Sewry,[1,6] Kate Bushby,[5] Haluk Topaloglu,[7] Kathryn North,[3] Stephen Abbs[2] and Francesco Muntoni[1]

[1]Dubowitz Neuromuscular Unit, Hammersmith Hospital, Imperial College, London, [2]DNA Laboratory, Genetics Centre, Guy's Hospital, London, UK, [3]The Institute for Neuromuscular Research, The Children's Hospital at Westmead, University of Sydney, Australia, [4]Department of Paediatric Pathology, Hacettepe Children's Hospital, Ankara, Turkey, [5]Institute of Human Genetics, University of Newcastle upon Tyne, International Centre for Life, Newcastle upon Tyne, [6]Centre for Inherited Neuromuscular Disorders, Robert Jones and Agnes Hunt Orthopaedic Hospital, Oswestry, UK and [7]Department of Child Neurology, Hacettepe Children's Hospital, Ankara, Turkey

[*]These authors contributed equally to this work.

Correspondence to: Francesco Muntoni, Department of Paediatrics, Imperial College London, Hammersmith Hospital, Du Cane Road, London W12ONN, UK
E-mail: f.muntoni@ic.ac.uk

Muscular dystrophies with reduced glycosylation of α-dystroglycan (α-DG), commonly referred to as dystroglycanopathies, are a heterogeneous group of autosomal recessive conditions which include a wide spectrum of clinical severity. Reported phenotypes range from severe congenital onset Walker–Warburg syndrome (WWS) with severe structural brain and eye involvement, to relatively mild adult onset limb girdle muscular dystrophy (LGMD). Specific clinical syndromes were originally described in association with mutations in any one of six demonstrated or putative glycosyltransferases. Work performed on patients with mutations in the *FKRP* gene has identified that the spectrum of phenotypes due to mutations in this gene is much wider than originally assumed. To further define the mutation frequency and phenotypes associated with mutations in the other five genes, we studied a large cohort of patients with evidence of a dystroglycanopathy. Exclusion of mutations in *FKRP* was a prerequisite for participation in this study. Ninety-two probands were screened for mutations in *POMT1*, *POMT2*, *POMGnT1*, *fukutin* and *LARGE*. Homozygous and compound heterozygous mutations were detected in a total of 31 probands (34 individuals from 31 families); 37 different mutations were identified, of which 32 were novel. Mutations in *POMT2* were the most prevalent in our cohort with nine cases, followed by *POMT1* with eight cases, *POMGnT1* with seven cases, *fukutin* with six cases and *LARGE* with only a single case. All patients with *POMT1* and *POMT2* mutations had evidence of either structural or functional central nervous system involvement including four patients with mental retardation and a LGMD phenotype. In contrast mutations in *fukutin* and *POMGnT1* were detected in four patients with LGMD and no evidence of brain involvement. The majority of patients (six out of nine) with mutations in *POMT2* had a Muscle–Eye–Brain (MEB)-like condition. In addition we identified a mutation in the gene *LARGE* in a patient with WWS.
Our data expands the clinical phenotypes associated with *POMT1*, *POMT2*, *POMGnT1*, *fukutin* and *LARGE* mutations. Mutations in these five glycosyltransferase genes were detected in 34% of patients indicating that, after the exclusion of *FKRP*, the majority of patients with a dystroglycanopathy harbour mutations in novel genes.

Keywords: congenital muscular dystrophy; limb girdle muscular dystrophy; alpha dystroglycan; glycosylation; glycosyltransferase

Abbreviations: CMD = congenital muscular dystrophy, LGMD = limb girdle muscular dystrophy, α-DG = alpha-dystroglycan

Received May 11, 2007. Revised August 9, 2007. Accepted August 10, 2007. Advance Access publication August 18, 2007

Introduction

Muscular dystrophies with reduced glycosylation of α-dystroglycan (α-DG) are a clinically and genetically heterogeneous group of autosomal recessive muscular dystrophies with variable neurological and ophthalmic involvement. Pathologically these disorders share the common feature of a hypoglycosylated form of α-dystroglycan (α-DG) on skeletal muscle biopsy (Muntoni *et al.*, 2002) which led to the term dystroglycanopathy (Toda *et al.*, 2003; Brockington and Muntoni, 2005; Mercuri *et al.*, 2006). Alpha and beta dystroglycan are derived from the same precursor peptide and are major components of the dystrophin-associated glycoprotein complex (DGC) that forms a link between the actin associated cytoskeleton and the extracellular matrix. α-DG is a highly glycosylated peripheral membrane protein that binds many of its extracellular matrix partners through its carbohydrate modifications. In the dystroglycanopathies, these modifications are either absent or reduced resulting in the decreased binding of its ligands, such as laminin-2, agrin and perlecan in skeletal muscle and neurexin in the brain (Barresi and Campbell, 2006). Primary mutations in the gene encoding dystroglycan (*DAG1*) have never been reported and a dystroglycan knockout mouse is embryonically lethal (Williamson *et al.*, 1997).

To date, mutations in six known or putative glycosyltransferase genes have been identified in these disorders: *Protein-O-mannosyl transferase* 1 (*POMT1*; OMIM 607423), *Protein-O-mannosyl transferase 2* (*POMT2*; OMIM 607439), *Protein-O-mannose 1,2-N-acetylglucosaminyltransferase 1* (*POMGnT1*; OMIM 606822), *fukutin* (OMIM 607440), *Fukutin-related protein* (*FKRP*; OMIM 606596) and *LARGE* (OMIM 603590) (Kobayashi *et al.*, 1998; Brockington *et al.*, 2001*a*; Yoshida *et al.*, 2001; Beltran-Valero de Bernabe *et al.*, 2002; Longman *et al.*, 2003; van Reeuwijk *et al.*, 2005*b*). These genes are thought to be involved in the addition of carbohydrate residues onto the α-DG backbone either via the process of *O*-mannosylation (*POMT1, POMT2, POMGnT1*) (Yoshida *et al.*, 2001; Manya *et al.*, 2003; Akasaka-Manya *et al.*, 2004) or via other not fully characterized mechanisms (*fukutin, FKRP and LARGE*) (de Paula *et al.*, 2003; Brown *et al.*, 2004; Brockington *et al.*, 2005; Xiong *et al.*, 2006).

The phenotypic severity of dystroglycanopathy patients is extremely variable. At the most severe end of the clinical spectrum are Walker–Warburg Syndrome (WWS), Muscle–Eye–Brain (MEB) disease and Fukuyama congenital muscular dystrophy (FCMD). These conditions are characterized by congenital muscular dystrophy (CMD) with severe structural brain and eye abnormalities, which in WWS results in early infantile death (van Reeuwijk *et al.*, 2005*a*). Conversely, individuals at the mildest end of the clinical spectrum may present, in adult life, with limb-girdle muscular dystrophy (LGMD) with no associated brain or eye involvement (Brockington *et al.*, 2001*b*). A number of intermediate phenotypes between these extremes have also been described including congenital muscular dystrophy type 1C (MDC1C), a CMD variant in which the brain can be entirely normal and LGMD2K, a variant with microcephaly and mental retardation but a relatively mild LGMD-like phenotype (Brockington *et al.*, 2001*a*; Balci *et al.*, 2005).

These syndromes were originally described in association with mutations in specific genes: WWS [OMIM 236670] was associated with mutations in *POMT1* and *POMT2* (Beltran-Valero de Bernabe *et al.*, 2002; Currier *et al.*, 2005; van Reeuwijk *et al.*, 2005*b*); these enzymes form a heterodimer and have been shown to catalyse the first step in *O*-mannosylation (Akasaka-Manya *et al.*, 2006). MEB [OMIM 253280] was originally described within the Finnish population in association with mutations in *POMGnT1*, an enzyme involved in the second step of *O*-mannosylation of α-DG by transferring *N*-acetylglucosamine to a protein *O*-linked mannose (Yoshida *et al.*, 2001). Recent molecular genetic studies have demonstrated that the high prevalence of MEB in the Finnish population is due to a founder splice site mutation (Diesen *et al.*, 2004). FCMD [OMIM 253800] was described within the Japanese population where it is the second most common form of muscular dystrophy after Duchenne muscular dystrophy (Kobayashi *et al.*, 1998). The high incidence of FCMD in Japan is related to a founder retrotransposal mutation in the 3′UTR of *fukutin*, which is found in the homozygous state in ~90% of all Japanese FCMD patients. MDC1C [OMIM 606612] and MDC1D [OMIM 608840] are two rare CMD syndromes, secondary to mutations in *FKRP and LARGE* respectively (Brockington *et al.*, 2001*a*; Longman *et al.*, 2003). The increased availability of mutation analysis in patients with a dystroglycanopathy has subsequently led to the widening of the clinical spectrum observed for several of these genes. This is best exemplified by the range of phenotypes resulting from mutations in *FKRP*. Following the initial description of its involvement in MDC1C (Brockington *et al.*, 2001*a*), it has subsequently been shown to cause a very common and relatively mild variant, LGMD2I [OMIM 607155] (Brockington *et al.*, 2001*b*), and more recently CMD variants with associated mild structural brain [MDC1C and cerebellar cysts (Topaloglu *et al.*, 2003; Mercuri *et al.*, 2006)] or severe brain and eye involvement (WWS and MEB-like disorders) (Beltran-Valero de Bernabe *et al.*, 2004; Mercuri *et al.*, 2006). It has recently been documented that several of these genes are involved in both milder and more severe phenotypes than originally reported. This includes the finding of *fukutin* mutations in two families with WWS (de Bernabe *et al.*, 2003) and in two families with a LGMD variant (Godfrey *et al.*, 2006) as well as the involvement of *POMT1* in patients with LGMD2K, with associated microcephaly and mental retardation (Balci *et al.*, 2005).

All previous studies have been conducted on a small number of families or individuals. This causes inevitable difficulties in applying mutation frequencies to the general population. In addition such reports make it difficult to establish whether the described clinical spectrum is truly representative of the phenotypic variability as well as how common the originally described core phenotypes are for each of these genes. In order to address these points, we have systematically screened a large population of patients with a dystroglycanopathy phenotype for mutations in the associated genes. As the spectrum of phenotypes secondary to *FKRP* involvement has been previously reported by us and others, we studied 92 patients in whom involvement of this gene had been excluded before proceeding with analysis of the five remaining genes. Our large and unbiased study redefines the clinical spectrum associated with each of the glycosyltransferases genes studied, identifies the frequency of individual gene defects and suggests that, after the exclusion of *FKRP*, the majority of patients with a dystroglycanopathy do not harbour mutations in any of the known genes.

Patient and methods

Patients

The cohort consisted of 92 unrelated individuals. This included a large group of patients from Australia (27 patients) and Turkey (16 patients). The majority of the remaining patients were recruited via the Hammersmith Hospital National Commissioning Group (NCG) service and included DNA from individuals referred from across the UK and Europe with a few samples from further a field. Mutations in *FKRP* had previously been excluded in all cases (Brockington *et al.*, 2001*a*).

The inclusion criteria were specified as hypoglycosylation of α-DG at the sarcolemma by immunolabelling of skeletal muscle sections (Brown *et al.*, 2004; Dubowitz and Sewry, 2007). Eighty patients met this criteria whilst in the remaining 12 cases there was no muscle available to perform α-DG studies. This later group of patients were included due to their clinical phenotype being highly suggestive of a dystroglycanopathy and consisted of children with CMD, elevated serum CK and brain MRI evocative of a cobblestone lissencephaly. All the patients who had had a muscle biopsy, were studied by standard immunocytochemical and/or Western blotting analysis in order to rule out dystrophinopathy, LGMDs such as sarcoglycanopathies, calpainopathy and dysferlinopathy, merosin deficient CMD and collagen VI deficiency (Dubowitz and Sewry, 2007). Clinical data was collated and patients were divided into phenotypic categories. This study was approved by Hammersmith Hospital Ethics Committee REC 2000:/5802.

Molecular genetics

Genomic DNA was extracted in the referring centre's laboratory using standard protocols. All mutation scanning was performed in the DNA laboratory at Guy's Hospital. The complete coding regions, including intron/exon boundaries of *POMT1*, *POMT2*, *POMGnT1*, *fukutin* and *LARGE* were amplified by PCR (primers are available in supplementary information, Table 1). Single nucleotide polymorphisms (SNP) within the primer binding sites were avoided using the Diagnostic SNP Check software (www.ngrl.man.ac.uk/SNPCheck). Amplicons were screened for mutations using a combination of unidirectional sequencing (standard dideoxynucleotide methodology) and heteroduplex analysis as previously described (Godfrey *et al.*, 2006). Where available, parental DNA was studied once a sequence alteration was identified in the proband. In two families, further segregation analysis was carried out to investigate the potential pathogenicity of unclassified variants. In families where a *de novo* mutation was suspected, paternity was confirmed using 11 STR markers (data not shown). Mutation nomenclature based on the following GeneBank Accession numbers; *POMT1*; NM_007171.2, *POMT2*; NM_013382.3, *POMGnT1*; NM_017739.1, *fukutin*; NM_006731.1 and *LARGE*; NM_133642.2, with nucleotide number 1 corresponding to the first base of the translation initiation codon.

Results

Clinical findings

Patients were classified as having either a CMD or LGMD phenotype and further subdivided according to the degree of structural and functional brain involvement. CMD was defined as onset of weakness prenatally or within the first 6 months of life. LGMD was defined by later onset weakness, specifically after having acquired ambulation. The cohort consisted of a total of 64 patients with CMD and 25 patients with LGMD, a total of 59 patients had brain involvement. In three cases the clinical information available was insufficient to determine phenotypic classification. Patients were divided into 1 of 7 broad phenotypic categories described below;

(1) WWS (and WWS-like): Onset prenatally or at birth. Patients assigned to this category had severe structural brain abnormalities including complete agyria or severe lissencephaly with only rudimentary cortical folding, marked hydrocephalus, severe cerebellar involvement and complete or partial absence of the corpus callosum. Eye abnormalities including congenital cataracts, micropthalmia and buphthalmus were common. When MRI evidence was not available, death before 1 year of age was taken as suggestive of this category if other clinical findings were supportive (Cormand *et al.*, 2001). Motor development was typically absent in these patients. Five patients were assigned to this group.
(2) MEB/FCMD-like: These categories were merged due to the overlapping phenotypic features. Included in

Table 1 Clinical characteristics of 33 individuals from 31 families in whom mutations were detected

Patient	ADG	Phenotype	Age at onset[a]	CK	Motor ability[b]	Contractures[c]	Hypertrophy[d]	Spine[e]	Eyes[f]	Weakness[g]	IQ[h]	Microcephaly[i]	MRI[j]	Other[k]
								Sc, RS	Poor visual attention	LL>UL				
1	LOW	WWS	P	4000	NS	Y	Y	Sc, RS	CG	N/A	L	Y	H, CHy, WM, Lis	Gastrostomy
2	LOW	MEB-FCMD	P	3500	N/A	Y	N/A	N/A	CG	N/A	L	Y	H, BS,WM, CC,CHy	N/A
3	LOW	LGMD-MR	I	2000	W	N/A	Y	U	N/A	N/A	L	Y	Normal	N/A
4	LOW	CMD-MR	I	7800	NW 2yr	N/A	N/A	U	U	N/A	L	N/A	WM	N/A
5	LOW	LGMD-MR	I	4000	W	N	Y	U	U	N/A	L	Y	Normal	N/A
6	LOW	LGMD-MR	3 Yr	8000	W		Y	N/A	U	N/A	L	Y	WM- minimal	N/A
7	LOW	CMD-MR	I	3600	St	N	Y	U	U	N/A	L	Y	Normal	N/A
8	LOW	CMD-MR	4 m	18000	W	N/A	Y	RS	N/A	N/A	L	Y	WM- minimal	Choreic Movement disorder
9	LOW	MEB-FCMD	N	5500	S	Y	Y	RS, Sc	N/A	N/A	L	Y	WM, BS	N/A
10	LOW	MEB-FCMD	4 Yr	5200	NW	N	Y	U		N/A	L	Y	Encephalocele	N/A
11	LOW	MEB-FCMD	7 m	N/A	NS	Y	N	U	Hm	N/A		N/A	H, WM,CC,	N/A
12	LOW	MEB-FCMD	N	3100	NS	Y	N/A	RS		UL>LL	L	Y	WM	N/A
13	N/A	MEB-FCMD	8 m		W	N/A	Y	U	My	UL>LL	L	N	WM, CDys, CC,PMG	N/A
14	LOW	MEB-FCMD	N	6000	S	Y	Y	Sc	CC	N/A	L	Y	BS,H,WM	SE, RIP age 11yr
15a	N/A	CMD-cerebellar	I	4700	W	Y	Y	N/A	N/A	UL>LL	L	Y	N/A	N/A
15b	N/A	CMD-cerebellar	I	5200	S	N/A	N/A	N/A	N/A	N/A	L	N/A	CHy	Micropenis and cryptorchidism
16	LOW	LGMD-MR	18 m	1900	W	N	Y	U	N/A	N/A	L	N/A	NO MRI	RBBB on ECHO
17	LOW	MEB-FCMD	N	2000	NS	Y	Y	N/A	My	UL,LL	L	Y	CHy, H	Macroglossia
18	LOW	MEB-FCMD	I	780	NW	N	N	N/A	CG	N/A	L	N/A	BS,CC,WM,H	N/A
19	LOW	MEB-FCMD	P	1000	W	Y	Y	U	OA, My	N/A	L	N	WM,CC	SE, feeding difficulties
20	LOW	LGMD-NOMR	12 Yr	12000	R	N	Y	U	My	LL>UL	N	N		N/A
21	LOW	MEB-FCMD	N	1200	NONE	N	N	U	RD	N/A	L	N/A	H,WM,CC	SE, feeding difficulties.

22	LOW	MEB-FCMD	12 m	2800	R	N	N/A	U	Pt., RA	N/A	L	N/A	CHy, CC, WM,H	Dyspraxia, feeding difficulties, SE
23	LOW	MEB-FCMD	N/A	N/A	N/A	N/A	N/A	N/A	N/A	N/A	N/A	N/A	H,CC,WM	N/A
24	N/A	WWS	N	1300	NS	N/A	N/A	U	N/A	N/A	L	N/A	CC,CHy, WM, H,Lis	N/A
25	LOW	WWS	P	5700	NONE	Y			RDy		L		H,WM,CHy, Lis	Feeding difficulties. RIP 8 weeks
26	LOW	CMD-NOMR	3 Yr	3200	S	N	N	U	U	G	N	N/A	WM-MILD	hypothyroid
27	N/A	MEB-FCMD	I	4000	S	N	Y	U	U	N/A	L	N/A	CC,WM,H	
28	LOW	WWS	N	7000	N/A	Y	Y	U	RD,Mo	N/A		N/A	WM,CHy, BS, H	Dysmorphic
29a	LOW	LGMD-NOMR	4 m	10000	W	N	Y	N/A	N/A	UL>LL	N	N	N/A	Steroid responsive
29b	LOW	LGMD-NOMR	4 m	13000	W	N	Y	U	U	LL>UL	N	N	Normal	Steroid responsive
30	LOW	LGMD-NOMR	10 m	60000	W	N	Y	U	U	LL>UL	N	N	H-MILD	Steroid responsive
31a	LOW	LGMD-NOMR	4 yr	9000	R	Y	N/A	U	N/A	N/A	N	N/A	N/A	N/A
32b	LOW	LGMD-NOMR	9 m	5700	R	Y	Y	U	N/A	LL>UL	N	N/A	Normal	CDH. Increased weakness with fever.

WWS = Walker–Warburg Syndrome; MEB/FCMD = Muscle-Eye-Brain/Fukuyama Congenital Muscular Dystrophy Like; CMD-MR = Congenital Muscular Dystrophy with Mental Retardation; CMD-NOMR = Congenital Muscular Dystrophy with No Mental Retardation; CMD-Cerebellar = Congenital Muscular Dystrophy with cerebellar Involvement; LGMD-MR = Limb Girdle Muscular Dystrophy with Mental Retardation; LGMD-NOMR = Limb Girdle Muscular Dystrophy with No Mental Retardation.
[a]P = prenatal onset; N = neonatal onset; I = infant onset; Yr = years; m = months. [b]W = walk; S = sit; St = stand; R = run; Prefix N = never. [c]Y = yes; N = no. [d]Y = yes; N = no. [e]RS = rigid spine; Sc = scoliosis; U = unaffected [f]CG = congenital glaucoma; RD = retinal detachment; RA = Retinal Atrophy; CC = Congenital cataracts; OA = optic atrophy; My = myopia; Mo = micropthalmia; Pt = ptosis; U = unaffected; Hm = hypermetropia; RDy = retinal dysplasia [g]UL = Upper limbs; LL = lower limbs; G = generalised [h]N = Normal intelligence; L = low [i]Y = yes; N = no [j]H = Hydrocephalus; CC = cerebellar cysts; BS = brainstem involvement; WM = white matter abnormality; CHy = cerebellar hypoplasia; Lis = lissencephaly; CDys = cerebellar dysplasia [k]SE = seizures; CDH = congenital dislocation of hip; RBBB = Right bundle branch block.

this group were CMD with brain abnormality less severe than that seen with WWS. MRI findings include pachygyria with preferential fronto-parietal involvement, polymicrogyria, cerebellar hypoplasia, cerebellar dysplasia and frequent flattening of the pons and brainstem. Eye abnormalities are often seen and include congenital glaucoma, progressive myopia, retinal atrophy and juvenile cataracts. Individuals may, rarely, acquire the ability to walk although this is delayed. Rarely patients manage to learn a few spoken words. Thirty patients were assigned to this group, including one in whom the clinical information was limited.

(3) CMD-CRB (CMD with cerebellar involvement): This category included CMD with mental retardation and cerebellar involvement on MRI scan as the only structural abnormality. Cerebellar abnormalities may include cysts, as described relatively frequently in individuals with *FKRP* gene defects (Mercuri *et al.*, 2006), or cerebellar hypoplasia or dysplasia. Four patients were assigned to this group.

(4) CMD-MR (CMD with mental retardation): CMD with mental retardation and structurally normal brain. Patients with isolated microcephaly or minor white matter changes on MRI are included in this group. Fifteen patients were assigned to this group, including two with limited clinical information.

(5) CMD-no MR (CMD with no mental retardation): Several patients within this group have had no neuroimaging but had entirely normal intellectual function. Ten patients were assigned to this group, one with limited information.

(6) LGMD-MR (LGMD with mental retardation): LGMD with mental retardation and structurally normal brain. Patients with minor white matter abnormalities and microcephaly were included in this group. This category includes patients with a phenotype resembling LGMD-2K (Balci *et al.*, 2005). Five patients were assigned to this group.

(7) LGMD-no MR (LGMD with no mental retardation): LGMD with no mental retardation. This category includes the LGMD phenotypes resembling LGMD2I and 2L (Godfrey *et al.*, 2006). Twenty patients were assigned to this group, six with limited clinical information.

The division of phenotypes within the cohort is shown in Table 4. Detailed clinical information is contained in Table 1 for those patients in whom pathogenic mutations were detected.

Mutation analysis

Mutation screening of *POMT1*, *POMT2*, *POMGnT1*, *fukutin* and *LARGE* was performed on 92 probands in whom *FKRP* mutations had been previously excluded. Homozygous and compound heterozygous mutations were detected in a total of 31 probands (34 individuals from 31 families). Thirty-seven different mutations were identified, 32 of which had not been previously reported. Pathogenic mutations are summarized in Table 2 and the comparative mutation frequencies between genes are represented in Table 4.

Without further RNA studies and functional biochemical analysis it is difficult to determine the pathogenicity of unclassified variants within these genes, this is exacerbated by the abundance of missense variants. For the purposes of this study, nonsense mutations, insertions and deletions, splice-site mutations as well as previously reported mutations were classified as pathogenic. Both exonic and intronic sequence alterations were categorized as polymorphisms if they were present on The Single Nucleotide Polymorphism database (http://www.ncbi.nlm.nih.gov), the Leiden database (http://www.dmd.nl) or present as an additional change in a patient with two proven pathogenic mutations (polymorphisms are available in supplementary information, Table 2). Amino acid substitutions were classified as pathogenic if they were detected in conjunction with a clearly pathogenic mutation or if they have been shown to segregate with disease in a large pedigree. In addition, two patients with homozygous missense mutations and one patient with compound heterozygous missense mutations have been included in Table 2 as they are non-conservative amino acid changes that affected an evolutionary conserved amino acid residue (Patient 16, Patient 18 and Patient 27). Patients in whom only a single-sequence alteration was detected are summarized in Table 3. We have been unable to determine whether these are rare polymorphisms or pathogenic alterations in patients who harbor a second undetectable mutation. These six patients have not been included in the 34% of patients detected with mutations. Patient 25 has been included in Tables 1, 2 and 4 despite the absence of a second detectable mutation due to the presence of a nonsense mutation.

A variety of mutation types were identified; 37 missense mutations; 7 nonsense mutations; 9 frameshift mutations; 1 insertion/deletion mutation; 1 deletion and 6 splice-site mutations. No mutation hotspots were identified. From a total of 37 mutations, 8 were found to be recurrent within the cohort. The p.Ala200Pro mutation in *POMT1*, previously described as prevalent within the Turkish population (Balci *et al.*, 2005), was detected in three patients, two of Turkish origin and one of Greek decent (Patient 8). The *POMGnT1* donor splice-site mutation c.1539 + 1G>A found to account for the enrichment of MEB within the Finnish population was detected in two patients (Diesen *et al.*, 2004). Three further novel mutations were detected more than once, specifically the p.Tyr666Cys mutation which was found both in the homozygous and heterozygous state in four patients. Segregation of this novel missense mutation was studied in a large pedigree and was found to

Table 2 A summary of pathogenic mutations detected in this study

Patient	Gene	Exon/intron	Nucleotide change	Predicted amino acid change	Mutation type	Reference
1	*POMT1*	20	c.2179_2180delTC	p.Ser727fs	Frameshift	Novel
	POMT1	20	c.2179_2180delTC	p.Ser727fs	Frameshift	Novel
2	*POMT1*	20	c.2179_2180delTC	p.Ser727fs	Frameshift	Novel
	POMT1	20	c.2179_2180delTC	p.Ser727fs	Frameshift	Novel
3	*POMT1*	7	c.598G>C	p.Ala200Pro	Missense	Leiden database
	POMT1	7	c.598G>C	p.Ala200Pro	Missense	Leiden database
4	*POMT1*	18	c.1847_1849delGGT	p.Trp616del	Deletion	Novel
	POMT1	3	c.193G>A	p.Gly65Arg	Missene	Leiden database
5	*POMT1*	11	c.1081C>T	p.Gln361X	Nonsense	Novel
	POMT1	19	c.2005G>A	p.Ala669Thr	Missene	Novel
6	*POMT1*	6	c.517_523delTTCTTCAinsG	p.Phe173AsnI175delinsAsp	Insertion/deletion	Novel
	POMT1	18	c.1868G>C	p.Arg623Thr	Missene	Novel
7	*POMT1*	7	c.598G>C	p.Ala200Pro	Missense	Leiden database
	POMT1	7	c.598G>C	p.Ala200Pro	Missense	Leiden database
8	*POMT1*	5	c.427G>T	p.Glu143X	Nonsense	Novel
	POMT1	7	c.598G>C	p.Ala200Pro	Missene	Leiden database
9	*POMT2*	21	c.2150T>C	p.Phe717Ser	Missense	Novel [a]
	POMT2	21	c.2177G>A	p.Gly726Glu	Missene	Leiden database
10	*POMT2*	19	c.1997A>G	p.Tyr666Cys	Missense	Novel
	POMT2	19	c.1997A>G	p.Tyr666Cys	Missense	Novel
11	*POMT2*	19	c.1997A>G	p.Tyr666Cys	Missense	Novel
	POMT2	11	c.1238G>C	p.Arg413Pro	Missene	Novel
12	*POMT2*	20	c.2047A>C	p.Thr683Pro	Missense	Novel
	POMT2	9	c.105delG	p.Ala35Ifs	Framshift	Novel
13	*POMT2*	5	c.593T>A	p.Ile198Asn	Missense	Novel
	POMT2	19	c.1997A>G	p.Tyr666Cys	Missene	Novel
14	*POMT2*	10	c.1117G>T	p.Val373Phe	Missense	Novel
	POMT2	5	c.593T>A	p.Ile198Asn	Missene	Novel
15a, 15b [b]	*POMT2*	19	c.1997A>G	p.Tyr666Cys	Missense	Novel
	POMT2	19	c.1997A>G	p.Tyr666Cys	Missense	Novel
16	*POMT2*	5	c.551C>T	p.Thr184Met	Missense	Novel
	POMT2	21	c.2243G>C	p.Trp748Ser	Missene	Novel
17	*POMT2*	9	c.1057G>A	p.Gly353Ser	Missense	Novel[1]
	POMT2	21	c.2177G>A	p.Gly726Glu	Missene	Novel[1]
18	*POMGnT1*	6	c.526A>C	p.Thr176Pro	Missense	Novel
	POMGnT1	6	c.526A>C	p.Thr176Pro	Missense	Novel
19	*POMGnT1*	7	c.652+1G>A	Donor splice site	Splice site	Novel
	POMGnT1	17	c.1469G>A	p.Cys490Tyr	Missene	Leiden database
20 [b]	*POMGnT1*	20	c.1666G>A	p.Asp556Asn	Missense	Novel[2]
	POMGnT1	20	c.1666G>A	p.Asp556Asn	Missense	Novel[2]
21	*POMGnT1*	17	c.1539+1G>A	Donor splice site	Splice site	Leiden database
	POMGnT1	17	c.1539+1G>A	Donor splice site	splice site	Leiden database
22	*POMGnT1*	12	c.1100G>A	p.Arg367His	Missense	Novel
	POMGnT1	17	c.1539+1G>A	Donor splice site	Splice site	Leiden database
23	*POMGnT1*	20	c.1785+2T>G	Donor splice site	Splice site	Novel
	POMGnT1	20	c.1785+2T>G	Donor splice site	Splice site	Novel
24	*POMGnT1*	17	C1425G>A	p.Trp475X	Nonsense	Novel
	POMGnT1	17	C1425G>A	p.Trp475X	Nonsense	Novel
25	*LARGE*	13	c.1548C>G	p.Trp516X	Nonsense	Novel
26	*fukutin*	8	c.920G>A	p.Arg307Gln	Missense	Leiden database
	fukutin	8	c.920G>A	p.Arg307Gln	Missense	Leiden database
27	*fukutin*	8	c.915G>A	p.Trp305Cys	Missense	Novel
	fukutin	8	c.915G>A	p.Trp305Cys	Missense	Novel
28	*fukutin*	8	c.919C>T	p.Arg307X	Nonsense	Novel
	fukutin	8	c.919C>T	p.Arg307X	Nonsense	Novel
29a, 29b	*fukutin*	8	c.920G>A	p.Arg307Gln	Missense	Novel[3]

(continued)

Table 2 Continued

Patient	Gene	Exon/intron	Nucleotide change	Predicted amino acid change	Mutation type	Reference
	fukutin	9	c.1167dupA	p.Phe390fs	Frameshift	Leiden database[3]
30	fukutin	9	c.1167dupA	p.Phe390fs	Frameshift	Leiden database[3]
	fukutin	10	c.1363delG	p.Asp455fs	Frameshit	Novel[3]
31a, 31b	fukutin	4	c.340G>A	p.Ala114Thr	Missense	Novel
	fukutin	7	c.859delA	p.Thr286fs	Frameshift	Novel

Probands are numbered, affected siblings are indicated with letters.
[a]*de novo* mutation. [b]Family studies carried out to investigate segregation of the variant through the pedigree.
The following patients were included in this cohort and have recently been reported individually; [1]Patients previously described in Mercuri *et al*., 2006. [2]Patient described individually in Clement *et al*., 2007, *Archives of Neurology* in press. [3]Patients previously described in Godfrey *et al*., 2006.

Table 3 Summary of unclassified variants

Patient	Gene	Exon/intron	Nucleotide change	Predicted amino acid change	Mutation type	Reference
32	*POMT1*	9	c.905T>G	p.Phe302Cys	missense	Novel
33	*POMT1*	19	c.1922C>T	p.Ala641Val	missense	Novel
34	*POMT1*	20	c.2203C>T	p.Arg735Cys	missense	Novel
35	*POMT1*	20	c.2244+5A>G	intronic	intronic	Novel
	POMT1	20	c.2244+5A>G	intronic	intronic	Novel
36	*POMT1*	20	c.2246G>A	synonymous	synonymous	Novel
37,38,39	*POMGnT1*	21	c.1867A>G	p.Met623Val	missense	Novel
39	*LARGE*	4	c.309C>A	synonymous	synonymous	Novel
40	*LARGE*	12	c.1431C>T	synonymous	synonymous	Novel
41	*LARGE*	13	c.1640G>A	p.Arg547His	missense	Novel
42,43	*LARGE*	14	c.1827A>T	synonymous	synonymous	Novel

Table 4 The phenotypic distribution of patients within the cohort, the frequency of mutations in each of the five glycosyltransferase genes analysed and the comparative mutation frequencies for individual clinical categories

	Number of patients							
	WWS	MEB FCMD	CMD CRB	CMD MR	CMD no MR	LGMD MR	LGMD no MR	Total
POMT1	1	1	–	3	–	3	–	8
POMT2	–	6	2	–	–	1	–	9
POMGnT1	–	6	–	–	–	–	1	7
fukutin	1	1	–	–	1	–	3	6
LARGE	1	–	–	–	–	–	–	1
Mutation detected	3 (60%)	14 (47%)	2 (50%)	3 (20%)	1 (10%)	4 (80%)	4 (20%)	31 (34%)
Total	5	30	4	15	10	5	20	92[a]

WWS = Walker–Warburg syndrome; MEB/FCMD = muscle eye brain syndrome/Fukuyama congenital muscular dystrophy; CMD CRB = congenital muscular dystrophy with cerebellar involvement; CMD-MR = congenital muscular dystrophy with mental retardation; CMD-no MR = congenital muscular dystrophy with no mental retardation; LGMD-MR = limb girdle muscular dystrophy with mental retardation; LGMD-no MR = limb girdle muscular dystrophy with no mental retardation.
[a]Includes three patients not assigned a clinical classification due to insufficient clinical information.

segregate with the disease (Patient 15). Parental samples were studied for 11 probands to ensure that compound heterozygous mutations were in *trans* and that apparent homozygous mutations in the proband were not masking undetected deletions. Where parental DNA was tested (22 families in total) a single paternal mutation was found to occur *de novo* (p.Phe117Ser, *POMT2*). A relatively similar frequency of patients with mutations were detected

in *POMT1*, *POMT2*, *POMGnT1* and *fukutin* (Table 4). In contrast, only a single patient was found to have a pathogenic mutation in *LARGE* although we were unable to identify a second mutation (Patient 25).

Genotype–phenotype correlations

The spectrum of phenotypes associated with mutations in *POMT1* included WWS (one case), MEB-FCMD (one case), CMD-MR (three cases) and LGMD-MR (three cases). *POMT2* mutations were observed in patients with MEB-FCMD (six cases), CMD-CRB (two cases) and LGMD-MR. Six patients with *POMGnT1* mutations had WWS and a single case had LGMD-no MR. Phenotypes associated with mutations in *fukutin* were detected in patients with WWS (one case), MEB-FCMD (one case), CMD-no MR (one case) and LGMD-no MR (three cases). A mutation in *LARGE* was detected in a single patient with WWS.

Although α-DG immunostaining was not systematically quantified as part of this study, we noticed a broad correlation between the amount of depleted glycosylated epitope and phenotypic severity. For example the WWS patient found to have a mutation in *LARGE* had complete absence in immunostaining, while the previously reported milder case of MDC1D had only a reduction in the amount of immunofluorescence (Longman *et al.*, 2003). Similarly the *POMGnT1* patient with LGMD-no MR (Patient 20) had only a subtle deficiency in immunofluorescence (Clement *et al.*, 2007, *Archives of Neurology*, in press), in contrast to the virtually absent expression in patients with MEB-FCMD.

There was no clear difference in phenotype or pattern of dystroglycan expression between patients with and without mutations in any of these genes. The phenotypic spectrum of patients without identifiable mutations was similar to that of patients with mutations.

Discussion

Dystroglycanopathies are a recently defined, common group of muscular dystrophies encompassing an extremely wide spectrum of clinical severity and are caused by mutations in at least sex genes encoding putative or demonstrated glycosyltransferases. The comparatively small coding region of *FKRP* has facilitated the rapid correlation between genotype and phenotype, allowing the discovery of pathogenic mutations in patients with LGMD2I, MDC1C, MEB-like and WWS-like disorders. However, there is no information regarding the frequency of involvement or the genotype–phenotype relationships for the remaining five glycosyltransferase genes in a large and unbiased population.

In this study we have systematically screened for mutations in *POMT1*, *POMT2*, *POMGnT1*, *fukutin* and *LARGE* in patients in whom we had previously ruled out *FKRP* gene involvement. Mutations were detected in 34% of these patients.

Fukutin mutations

Mutations in *fukutin*, typically associated with FCMD in Japan were found in six patients, none of whom are of Japanese origin. Only two of these patients had structural brain involvement; one patient affected by WWS (Patient 28) and one by a MEB-FCMD phenotype (Patient 27). The remaining patients had no structural brain involvement; one case had CMD-no MR (Patient 26) and never acquired the ability to walk but has normal IQ and five individuals from three families have entirely normal intellect and a mild LGMD phenotype (LGMD2L) (Patients 29, 30 and 31). Interestingly in the latter two of these families, a dramatic response to steroid therapy was noted (Godfrey *et al.*, 2006). In striking contrast to what has previously been reported in FCMD, none of these five patients have evidence of central nervous system involvement. Our findings together with the recent description of individuals with *fukutin* mutations presenting with a predominant cardiomyopathy (Murakami *et al.*, 2006), suggest that the majority of mutations outside Japan give rise to conditions milder than FCMD and are not usually associated with structural brain involvement.

POMGnT1 mutations

Mutations in *POMGnT1* were also associated with a wider than reported spectrum of clinical severity, which include a relatively mild form of LGMD. The majority of patients (6) had an MEB like disorder with only a single patient possessing a LGMD phenotype, suggesting that *POMGnT1* mutations more frequently give rise to congenital disorders with associated structural brain involvement. The LGMD patient (Patient 20) has entirely normal intellectual function and disease onset in the second decade of life, dramatically expanding the phenotypes associated with mutations in *POMGnT1* (Clement *et al.*, 2007, *Archives of Neurology*, in press).

POMT1 mutations

Mutations in *POMT1* have previously been reported in patients with WWS, CMD-MR and LGMD-MR (LGMD-2K). Within our cohort, all patients with mutations in *POMT1* had evidence of functional brain involvement either with no clear associated structural brain abnormalities (three patients with LGMD2K, and three patients with CMD-MR), or more severe conditions with structural brain defects (one patient with WWS, and one individual with a MEB-like phenotype). This suggests that the majority, if not all patients with *POMT1* mutations have either functional or structural central nervous system involvement, including those patients with relatively mild muscle weakness. This is in contrast to patients in the present study with mutations in *fukutin* and *POMGnT1* and to that previously reported for *FKRP* mutations.

POMT2 mutations

Mutations in *POMT2* were confined to patients with evidence of brain involvement. Nine patients had pathogenic *POMT2* mutations; six with a MEB-FCMD phenotype, two with a CMD-cerebellar phenotype and a single patient with LGMD-MR. This latter patient has learning difficulties and remains ambulant at age 20 having presented, at 18 months of age, with developmental delay (Patient 16). These findings indicate that like *POMT1*, the majority or all patients with mutations in *POMT2* have evidence of central nervous system involvement. In addition, we have identified the mildest phenotype associated with mutations in *POMT2* reported to date in an individual with LGMD-MR.

LARGE mutations

We were only able to identify a single pathogenic *LARGE* mutation in a patient with typical WWS phenotype who died in the first few months of life (Patient 25). Absent immunofluorescence staining was demonstrated on this patient's skeletal muscle biopsy using antibodies which recognise the glycosylated epitope of α-DG. Unfortunately neither sufficient DNA nor frozen muscle from this patient was available to investigate the presence of a second, as yet undetected, mutation. However, it remains possible that this mutation contributed to the patient's phenotype.

Mutation frequencies

Mutations in *POMT2* were the most prevalent with nine cases, followed by *POMT1* with eight cases, *POMGnT1* with seven cases, *fukutin* with six cases and finally *LARGE* with only a single case.

We have previously identified *FKRP* mutations in 79 patients. Approximately 75% of these patients have a LGMD2I phenotype (Brockington *et al.*, 2001*a*; Topaloglu *et al.*, 2003; Beltran-Valero de Bernabe *et al.*, 2004; Mercuri *et al.*, 2006). The relative frequency of *FKRP* involvement needs to be considered with caution as it clearly reflects the genetic origin of patients studied in our unit. For example screening of 79 Australian LGMD patients detected only two *FKRP* mutations. However, when amalgamating these results, it remains clear that *FKRP* mutations are the most frequently found mutations in this group of conditions. Both ourselves and others have previously published extensively on the spectrum of these mutations (Brockington *et al.*, 2001*a*, *b*; Mercuri *et al.*, 2003; Topaloglu *et al.*, 2003; Harel *et al.*, 2004; Mercuri *et al.*, 2006; Vieira *et al.*, 2006; Lin *et al.*, 2007).

Genotype–phenotype correlations

Pathogenic mutations were detected in 3 of 5 patients with WWS syndrome (60%), 14 of 30 patients with a MEB/FCMD phenotype (47%), 2 of 4 patients with CMD CRB (50%), 3 of 15 patients with CMD-MR (20%), 1 of 10 patients with CMD-no MR (10%), 4 of 5 patients with LGMD-MR (80%) and 4 of 20 patients with LGMD-no MR (20%) (Table 4).

Patients with associated structural brain defects belonging to the severe end of the clinical spectrum showed no apparent difference in their pattern of skeletal muscle weakness or central nervous system involvement in relation to the gene involved. However, the four LGMD patients with associated MR and microcephaly all had mutations in either *POMT1* or *POMT2*. No mutations were identified in the remaining patients. Conversely a number of patients with more severe muscle weakness and no brain involvement (CMD-no MR) were found to have mutations in *fukutin*, similar to that previously described in MDC1C (Brockington *et al.*, 2001*a*). This suggests that there may be a hierarchical involvement of muscle and brain arising from individual gene mutations, with *POMT1* and *POMT2* being associated with significant central nervous system involvement even in patients with relatively mild weakness and who remain ambulant (LGMD2K). This does not appear to be a feature of *fukutin* or *FKRP*. These results suggest that in some individual subcategories, certain genes are more likely to be involved than others and this should be taken into account when undertaking mutation analysis in the dystroglycanopathies.

The results of this study demonstrate that the phenotypic spectrum of disorders associated with mutations in the six known glycosyltransferase genes is significantly wider than initially suspected, in part due to the high prevalence of founder mutations within specific populations (Kobayashi *et al.*, 1998; Diesen *et al.*, 2004). We have expanded the clinical phenotypes associated with mutations in *POMT1*, *POMT2*, *POMGnT1*, *fukutin* and *LARGE*, although we have not observed a full spectrum of phenotypes associated with each gene, in particular *POMT1*, *POMT2* and *LARGE*. A large number of patients with clinico-pathological features indistinguishable from the ones detailed in this manuscript were not found to have mutations in any of the genes studied. Finally, this work suggests that more, as yet undefined, genes are likely to be involved in the pathogenesis of the dystroglycanopathies. The identification of these genes may provide additional information on the pathway of glycosylation of α-dystroglycan.

Supplementary material

Supplementary material is available at *Brain* online.

Acknowledgements

The authors wish to thank the Muscular Dystrophy Campaign for the centre grants and research grants (No's PC3143 and PC0916) supporting the Dubowitz Neuromuscular Centre. The authors also wish to thank the support from National Commissioning Group (NCG) for the diagnostic work in the CMD population, the

patients who participated in this study and the colleagues who have referred patients to the service. K.N.N. was supported by an NH&MRC project grant (No. 284533); J.S. was supported an NH&MRC Medical Postgraduate Research Scholarship; and B.T. by a Hacettepe University grant (No. 02G129).

References

Akasaka-Manya K, Manya H, Kobayashi K, Toda T, Endo T. Structure-function analysis of human protein O-linked mannose beta1,2-N-acetylglucosaminyltransferase 1, POMGnT1. Biochem Biophys Res Commun 2004; 320: 39–44.

Akasaka-Manya K, Manya H, Nakajima A, Kawakita M, Endo T. Physical and functional association of human protein O-mannosyltransferases 1 and 2. J Biol Chem 2006; 281: 19339–45.

Balci B, Uyanik G, Dincer P, Gross C, Willer T, Talim B, et al. An autosomal recessive limb girdle muscular dystrophy (LGMD2) with mild mental retardation is allelic to Walker-Warburg syndrome (WWS) caused by a mutation in the POMT1 gene. Neuromuscul Disord 2005; 15: 271–5.

Barresi R, Campbell KP. Dystroglycan: from biosynthesis to pathogenesis of human disease. J Cell Sci 2006; 119: 199–207.

Beltran-Valero de Bernabe D, Currier S, Steinbrecher A, Celli J, van Beusekom E, van der Zwaag B, et al. Mutations in the O-mannosyltransferase gene POMT1 give rise to the severe neuronal migration disorder Walker-Warburg syndrome. Am J Hum Genet 2002; 71: 1033–43.

Beltran-Valero de Bernabe D, Voit T, Longman C, Steinbrecher A, Straub V, Yuva Y, et al. Mutations in the FKRP gene can cause muscle-eye-brain disease and Walker-Warburg syndrome. J Med Genet 2004; 41: e61.

Brockington M, Blake DJ, Prandini P, Brown SC, Torelli S, Benson MA, et al. Mutations in the fukutin-related protein gene (FKRP) cause a form of congenital muscular dystrophy with secondary laminin alpha2 deficiency and abnormal glycosylation of alpha-dystroglycan. Am J Hum Genet 2001*a*; 69: 1198–209.

Brockington M, Muntoni F. The modulation of skeletal muscle glycosylation as a potential therapeutic intervention in muscular dystrophies. Acta Myol 2005; 24: 217–21.

Brockington M, Torelli S, Prandini P, Boito C, Dolatshad NF, Longman C, et al. Localization and functional analysis of the LARGE family of glycosyltransferases: significance for muscular dystrophy. Hum Mol Genet 2005; 14: 657–65.

Brockington M, Yuva Y, Prandini P, Brown SC, Torelli S, Benson MA, et al. Mutations in the fukutin-related protein gene (FKRP) identify limb girdle muscular dystrophy 2I as a milder allelic variant of congenital muscular dystrophy MDC1C. Hum Mol Genet 2001*b*; 10: 2851–9.

Brown SC, Torelli S, Brockington M, Yuva Y, Jimenez C, Feng L, et al. Abnormalities in alpha-dystroglycan expression in MDC1C and LGMD2I muscular dystrophies. Am J Pathol 2004; 164: 727–37.

Cormand B, Pihko H, Bayes M, Valanne L, Santavuori P, Talim B, et al. Clinical and genetic distinction between Walker-Warburg syndrome and muscle-eye-brain disease. Neurology 2001; 56: 1059–69.

Currier SC, Lee CK, Chang BS, Bodell AL, Pai GS, Job L, et al. Mutations in POMT1 are found in a minority of patients with Walker-Warburg syndrome. Am J Med Genet A 2005; 133: 53–7.

de Bernabe DB, van Bokhoven H, van Beusekom E, Van den Akker W, Kant S, Dobyns WB, et al. A homozygous nonsense mutation in the fukutin gene causes a Walker-Warburg syndrome phenotype. J Med Genet 2003; 40: 845–8.

de Paula F, Vieira N, Starling A, Yamamoto LU, Lima B, de Cassia Pavanello R, et al. Asymptomatic carriers for homozygous novel mutations in the FKRP gene: the other end of the spectrum. Eur J Hum Genet 2003; 11: 923–30.

Diesen C, Saarinen A, Pihko H, Rosenlew C, Cormand B, Dobyns WB, et al. POMGnT1 mutation and phenotypic spectrum in muscle-eye-brain disease. J Med Genet 2004; 41: e115.

Dubowitz V, Sewry CA. Muscle biopsy - a practical approach: [Saunders]; 2007.

Godfrey C, Escolar D, Brockington M, Clement EM, Mein R, Jimenez-Mallebrera C, et al. Fukutin gene mutations in steroid-responsive limb girdle muscular dystrophy. Ann Neurol 2006; 60: 603–10.

Harel T, Goldberg Y, Shalev SA, Chervinski I, Ofir R, Birk OS. Limb-girdle muscular dystrophy 2I: phenotypic variability within a large consanguineous Bedouin family associated with a novel FKRP mutation. Eur J Hum Genet 2004; 12: 38–43.

Kobayashi K, Nakahori Y, Miyake M, Matsumura K, Kondo-Iida E, Nomura Y, et al. An ancient retrotransposal insertion causes Fukuyama-type congenital muscular dystrophy. Nature 1998; 394: 388–92.

Lin YC, Murakami T, Hayashi YK, Nishino I, Nonaka I, Yuo CY, et al. A novel FKRP gene mutation in a Taiwanese patient with limb-girdle muscular dystrophy 2I. Brain Dev 2007; 29: 234–8.

Longman C, Brockington M, Torelli S, Jimenez-Mallebrera C, Kennedy C, Khalil N, et al. Mutations in the human LARGE gene cause MDC1D, a novel form of congenital muscular dystrophy with severe mental retardation and abnormal glycosylation of alpha-dystroglycan. Hum Mol Genet 2003; 12: 2853–61.

Manya H, Sakai K, Kobayashi K, Taniguchi K, Kawakita M, Toda T, et al. Loss-of-function of an N-acetylglucosaminyltransferase, POMGnT1, in muscle-eye-brain disease. Biochem Biophys Res Commun 2003; 306: 93–7.

Mercuri E, Brockington M, Straub V, Quijano-Roy S, Yuva Y, Herrmann R, et al. Phenotypic spectrum associated with mutations in the fukutin-related protein gene. Ann Neurol 2003; 53: 537–42.

Mercuri E, Topaloglu H, Brockington M, Berardinelli A, Pichiecchio A, Santorelli F, et al. Spectrum of brain changes in patients with congenital muscular dystrophy and FKRP gene mutations. Arch Neurol 2006; 63: 251–7.

Muntoni F, Brockington M, Blake DJ, Torelli S, Brown SC. Defective glycosylation in muscular dystrophy. Lancet 2002; 360: 1419–21.

Murakami T, Hayashi YK, Noguchi S, Ogawa M, Nonaka I, Tanabe Y, et al. Fukutin gene mutations cause dilated cardiomyopathy with minimal muscle weakness. Ann Neurol 2006; 60: 597–602.

Toda T, Kobayashi K, Takeda S, Sasaki J, Kurahashi H, Kano H, et al. Fukuyama-type congenital muscular dystrophy (FCMD) and alpha-dystroglycanopathy. Congenit Anom (Kyoto) 2003; 43: 97–104.

Topaloglu H, Brockington M, Yuva Y, Talim B, Haliloglu G, Blake D, et al. FKRP gene mutations cause congenital muscular dystrophy, mental retardation, and cerebellar cysts. Neurology 2003; 60: 988–92.

van Reeuwijk J, Brunner HG, van Bokhoven H. Glyc-O-genetics of Walker-Warburg syndrome. Clin Genet 2005a; 67: 281–9.

van Reeuwijk J, Janssen M, van den Elzen C, Beltran-Valero de Bernabe D, Sabatelli P, Merlini L, et al. POMT2 mutations cause alpha-dystroglycan hypoglycosylation and Walker-Warburg syndrome. J Med Genet 2005b; 42: 907–12.

Vieira NM, Schlesinger D, de Paula F, Vainzof M. Mutation analysis in the FKRP gene provides an explanation for a rare cause of intrafamilial clinical variability in LGMD2I. Neuromuscul Disord 2006; 16: 870–3.

Williamson RA, Henry MD, Daniels KJ, Hrstka RF, Lee JC, Sunada Y, et al. Dystroglycan is essential for early embryonic development: disruption of Reichert's membrane in Dag 1-null mice. Hum Mol Genet 1997; 6: 831–41.

Xiong H, Kobayashi K, Tachikawa M, Manya H, Takeda S, Chiyonobu T, et al. Molecular interaction between fukutin and POMGnT1 in the glycosylation pathway of alpha-dystroglycan. Biochem Biophys Res Commun 2006; 350: 935–41.

Yoshida A, Kobayashi K, Manya H, Taniguchi K, Kano H, Mizuno M, et al. Muscular dystrophy and neuronal migration disorder caused by mutations in a glycosyltransferase, POMGnT1. Dev Cell 2001; 1: 717–24.

Fukutin Gene Mutations in Steroid-Responsive Limb Girdle Muscular Dystrophy

Caroline Godfrey, BSc,[1] Diana Escolar, MD,[2] Martin Brockington, BSc,[3] Emma M. Clement, MD,[3] Rachael Mein, BSc,[1] Cecilia Jimenez-Mallebrera, PhD,[3] Silvia Torelli, PhD,[3] Lucy Feng, PhD,[3] Susan C. Brown, PhD,[3] Caroline A. Sewry, PhD,[3,4] Mary Rutherford, MD, PhD,[5] Yehuda Shapira, MD,[6] Stephen Abbs, PhD,[1] and Francesco Muntoni, MD[3]

Objective: Defects in glycosylation of α-dystroglycan are associated with several forms of muscular dystrophy, often characterized by congenital onset and severe structural brain involvement, collectively known as dystroglycanopathies. Six causative genes have been identified in these disorders including *fukutin.* Mutations in *fukutin* cause Fukuyama congenital muscular dystrophy. This is the second most common form of muscular dystrophy in Japan and is invariably associated with mental retardation and structural brain defects. The aim of this study was to determine the genetic defect in two white families with a dystroglycanopathy.

Methods: The six genes responsible for dystroglycanopathies were studied in three children with a severe reduction of α-dystroglycan in skeletal muscle.

Results: We identified pathogenic *fukutin* mutations in these two families. Affected children had normal intelligence and brain structure and shared a limb girdle muscular dystrophy (LGMD) phenotype, had marked elevation of serum creatine kinase, and were all ambulant with remarkable steroid responsiveness.

Interpretation: Our data suggest that *fukutin* mutations occur outside Japan and can be associated with much milder phenotypes than Fukuyama congenital muscular dystrophy. These findings significantly expand the spectrum of phenotypes associated with *fukutin* mutations to include this novel form of limb girdle muscular dystrophy that we propose to name LGMD2L.

Ann Neurol 2006;60:603–610

The dystroglycanopathies form a group of muscular dystrophies that share the common pathological feature of aberrant α-dystroglycan glycosylation (hypoglycosylation).[1–3] α-Dystroglycan is a peripheral membrane component of the dystrophin-glycoprotein complex that associates with β-dystroglycan at the sarcolemma, forming a link between the extracellular matrix and the actin-associated cytoskeleton.[4] α-Dystroglycan is heavily glycosylated and interacts with several extracellular matrix proteins including laminin-1 and -2, agrin, neurexin, and perlecan.[5] In the dystroglycanopathies, these carbohydrate moieties are either absent or reduced, resulting in decreased binding of extracellular matrix ligands.[2,6] Mutations in genes encoding six known or putative glycosyltransferases have been identified in this group of disorders: *Protein O-mannosyl transferase 1* (*POMT1;* OMIM 607423), *Protein O-mannosyl transferase 2* (*POMT2;* OMIM 607439), *Protein O-mannose β-1, 2*-N-*acetylglucosaminyltransferase* (*POMGnT1;* OMIM 606822), *Fukutin* (OMIM 607440), *Fukutin-related protein* (*FKRP;* OMIM 606596), and *LARGE* (OMIM 603590). The phenotypic spectrum arising from mutations in these genes ranges from forms with a congenital onset and severe structural brain abnormalities (Walker–Warburg syndrome [WWS; OMIM 236670], muscle-eye-brain disease [OMIM 253280] and Fukuyama congenital muscular dystrophy [FCMD; OMIM 253800]), to forms with a congenital onset and absent or mild-to-moderate brain involvement (MDCIC [OMIM 606612] and MDCID [OMIM 608840]), through to forms with later onset limb girdle presentations that may also be associated with mental retardation but no structural brain defects (LGMD2I [OMIM 607155] and LGMD2K) (reviewed in Muntoni and Voit[7]). The phe-

From the [1]DNA Laboratory, Genetics Centre, Guy's Hospital, London, United Kingdom; [2]Research Center for Genetic Medicine, Children's National Medical Center, George Washington University, Washington, DC; [3]Dubowitz Neuromuscular Centre, Department of Paediatrics, Hammersmith Campus, Imperial College London, London; [4]Centre for Inherited Neuromuscular Disorders, Robert Jones & Agnes Hunt Orthopaedic Hospital, Oswestry; [5]Robert Steiner Magnetic Resonance Unit, Clinical Sciences Centre, Hammersmith Hospital, Imperial College London, London, United Kingdom; and [6]Division of Child Neurology, Hadassah University Hospital, Jerusalem, Israel.

Received Jun 19, 2006, and in revised form Sep 8. Accepted for publication Sep 12, 2006.

C.G. and D.E. contributed equally to this article.

Published online Oct 16, 2006, in Wiley InterScience (www.interscience.wiley.com). DOI: 10.1002/ana.21006

Address correspondence to Prof Muntoni, Dubowitz Neuromuscular Centre, Department of Paediatrics, Division of Medicine, Hammersmith Campus, Imperial College, Du Cane Road, London W12 ONN, United Kingdom. E mail: f.muntoni@imperial.ac.uk

Published by Wiley-Liss, Inc., through Wiley Subscription Services

notypes arising from mutations in several of these glycosyltransferases are more diverse than originally thought. The best example of this is the identification of mutations in the *FKRP* gene in patients spanning the entire spectrum, from WWS and muscle-eye-brain disease–like disorders through to adult-onset limb girdle muscular dystrophy (LGMD2I).[8–12] The phenotypic severity of some of the dystroglycanopathies therefore appears dependent on the severity of individual gene mutations rather than the gene primarily involved.

The FCMD gene encodes a 461-amino acid protein, termed *fukutin,*[13] that has features typical of many glycosyltransferases.[14] α-Dystroglycan glycosylation was subsequently shown to be affected in FCMD.[15] This is the second most frequent form of muscular dystrophy in Japan after Duchenne muscular dystrophy, due to the presence of a founder mutation within this population.[16] About 87% of FCMD chromosomes harbor a 3Kb retrotransposal element in the 3′ untranslated region of the fukutin gene. Reports of mutations in *fukutin* outside the Japanese population are limited to two Turkish patients with a severe WWS-like phenotype. These individuals harbor homozygous null mutations,[18,19] indicating that unlike the situation in mice, complete loss of *fukutin* function is not embryonic lethal,[20] but results in a phenotype considerably more severe than FCMD. There are no reports of patients with mutations in *fukutin* and absent brain involvement either inside or outside of the Japanese population.

Here, we report *fukutin* mutations in three affected children from two unrelated families who presented with a novel form of LGMD. In contrast with previous cases, these patients had no brain involvement and a remarkable clinical response to corticosteroids.

Patients and Methods

Patients

Three siblings from two nonconsanguineous white families affected by an early-onset form of muscular dystrophy were studied. The finding of abnormal glycosylation of α-dystroglycan on muscle biopsy was the criterion for inclusion into this study, which was approved by the Hammersmith Hospital Trust Ethics committee.

Histology and Immunohistochemistry

Frozen 10μm sections were stained with hematoxylin and eosin using a standard technique.[21] Frozen 7μm sections were incubated with monoclonal antibodies to laminin-α2 (1/4,000 MAB1922 [Chemicon, Temecula, CA] and 1/200 4H8 [Alexis Corporation, San Diego, CA] to the 80kDa C-terminal and 300kDa N-terminal fragments, respectively); to laminin-β1 and laminin-γ1 chains (MAB1928 and MAB1914; 1/4,000; Chemicon); to α-Dystroglycan (IIH6; kind gift of Kevin Campbell, University of Iowa, Iowa City, IA); a sheep polyclonal antibody to the core protein of chick α-dystroglycan (kind gift of Stephan Kroger, University of Mainz, Mainz, Germany); monoclonal antibodies to major histocompatibility complex (MHC) class I (M0736; 1/400; Dako, Carpinteria, CA); CD4 (M0716; 1/50; Dako); CD8 (M0707; 1/100; Dako); and CD20 (M0755, 1/600; Dako).

Primary antibodies were applied for 1 hour and shown with an appropriate biotinylated secondary antibody (1:200; Amersham, Braunschweig, Germany) for 30 minutes, followed by either streptavidin conjugated to Alexa 594 (Molecular Probes, Eugene, OR) or to horseradish peroxidase, according to standard procedures.[21] All dilutions and washings were made in phosphate-buffered saline. Sections labeled for fluorescence were mounted in aqueous mountant and viewed with a Leica DMR microscope linked to Metamorph (Universal Imaging, Downington, PA). Control sections were labeled without primary antibodies, and all sections were compared with age-matched control samples from other neuromuscular disorders and with normal muscle.

Mutation Analysis

The complete coding regions of *FKRP, POMT1, POMT2, POMGnT1, LARGE,* and *fukutin* were screened for mutations by heteroduplex analysis and characterized by sequencing. Heteroduplex analysis was performed by temperature-gradient capillary electrophoresis on a Reveal Discovery System (model RVL 9612 96 capillary SpectruMedix LLC, State College, PA). Polymerase chain reaction fragments were amplified from genomic DNA. Raw data were collected by SpectruMedix Checkmate software and processed by Revelation 2.4 mutation analysis software (SpectruMedix LLC). Heteroduplex peaks were characterized by sequence analysis to identify pathogenic mutations. Nonfluorescent primers were used with a 24bp tag sequence attached to the 5′ end. Polymerase chain reactions were amplified using Qiagen Multiplex Buffer (Qiagen, Chatsworth, CA). Exons were sequenced using BigDye Cycle sequencing kit v3.1 (Applied Biosystems, Foster City, CA). Products were detected using an ABI3730 automated genetic analyser (Applied Biosystems). Analysis of bidirectional sequence traces was performed using Mutation Surveyor software version 2.61 (SoftGenetics, State College, PA).

Construction of Expression Plasmids and Site-Directed Mutagenesis

Total human brain RNA (ClonTech, Palo Alto, CA) was reverse transcribed using Superscript III (Invitrogen, La Jolla, CA). The coding sequence of *fukutin* (National Center for Biotechnology Information accession number NM_006731) was amplified using Advantage HF Polymerase (ClonTech). The amplified product was cloned into the pcDNA3.1/V5-His TOPO expression vector (Invitrogen) following the manufacturer's instructions. This vector directs the synthesis of a fusion protein tagged at its C-terminal end with the V5 epitope. Polymerase chain reaction–directed mutagenesis was performed on plasmid DNA using overlapping mismatch primers and Advantage HF Polymerase (ClonTech). Amplified products were digested with *Dpn*I (10U) to remove contaminating parental plasmid DNA and subsequently transformed into One Shot TOP10 Chemically Competent *Escherichia coli* cells (Invitrogen). Mutations were confirmed

by DNA sequencing. The sequences of the primers used are available on request.

Cell Culture, Transfection, and Immunocytochemistry

Chinese hamster ovary cells (ECACC) were cultured on glass coverslips in Nutrient Mixture F-12 HAM (high glucose; Sigma, St. Louis, MO) supplemented with 2mM L-glutamine plus 10% fetal bovine serum. Cell transfection was performed using Gene Juice (Novagen, Madison, WI) in serum-free media. After 24 hours, cells were fixed in 2% paraformaldehyde.

Cells were permeabilized in phosphate-buffered saline with 0.05% Triton X-100 (Sigma). For double labeling, cells were first incubated for 1 hour with monoclonal anti-GM130 (BD Biosciences, San Jose, CA), followed by an anti–mouse conjugated to Alexa 594 (Molecular Probes) for 30 minutes. After washing, fluorescein isothiocyanate–conjugated goat anti–V5-His (Bethyl Lab, Montgomery, TX) was applied for 1 hour. Cell nuclei were counterstained with Hoechst 33342 (Molecular Probes). All dilutions and washings were made in phosphate-buffered saline, and incubations were performed at room temperature. Coverslips were mounted in aqueous mountant and viewed with epifluorescence using a Leica Diaphot microscope and digitally captured using Metamorph (Universal Imaging).

Results

Clinical Findings

FAMILY 1. Patient 1 is a girl born to nonconsanguineous Israeli parents. Concerns were raised in the first few months about hypotonia, but by 10 months she could sit and stand with support. At this age she developed a febrile illness with skin vesicles. An acute and dramatic deterioration in functional ability followed, and she became paralyzed, retaining only eye movement. A muscle biopsy showed changes consistent with muscular dystrophy. She made a gradual recovery, and by 18 months of age, she was standing independently. At this time, another febrile illness led to functional deterioration, leaving her unable to stand. Creatine kinase (CK) level was 60,000IU/L, and repeat muscle biopsy showed an inflammatory picture, leading to a diagnosis of polymyositis. She was commenced on prednisolone 2mg/kg for 5 days, which was weaned over some weeks to a maintenance dose of 0.75mg/kg alternate days. This led to a rapid improvement, and 3 days into treatment, she had regained standing ability with a reduction in her fever. Her CK level quickly declined to 800IU/L, and she acquired the ability to walk shortly after. Her intellectual development progressed entirely normally. At 6 years of age, steroids were discontinued; at 8 years of age, she was referred to the Hammersmith Hospital because of progressive muscle weakness. On examination, she had proximal weakness with lower limbs affected more than upper limbs; flexors were stronger than extensors. She could walk 20m with difficulty but not rise from the floor. She had hypertrophy of brachioradialis and triceps, thighs, and calves. Normal motor nerve conduction studies were recorded (peroneal and ulnar nerves). MRI showed a structurally normal brain (Fig 1A). Muscle biopsy taken from the quadriceps showed a dystrophic picture with severely reduced α-dystroglycan immunolabeling, suggestive of a dystroglycanopathy (Fig 2). In addition, there was minimal focal inflammation. Labeling of MHC class I antigen was normal. The inflammatory cells consisted of macrophages and a few $CD8^+$ lymphocytes scattered in the endomysium. No B lymphocytes were detected (CD20), and no eosinophils were present (not shown). Laminin-α2, -β1, and -γ1 were all mildly reduced on the sarcolemma, as reported previously in FCMD.[21]

She was restarted on intermittent prednisolone, using a similar regimen to the one used in Duchenne muscular dystrophy.[22] She partially responded to this with increased endurance and less frequent falls. She is now 11 years old; an attempt to stop steroids at the age of 10 resulted in rapid deterioration of muscle strength, frequent falls, and a leg fracture. Steroids were started again with partial response and regain of ambulation, although for only short distances.

FAMILY 2. Two siblings (a boy and a girl) were affected in the second family; parents were unrelated, of Jewish and Indian origin (Fig 3). Both children were the product of normal pregnancies and deliveries. The boy (Patient 3) had started to develop normally, when at 4 months of age he suffered a Coxsackie virus infection with oral blisters. He became hypotonic and lost the ability to lift his head and turn. The illness resolved, and 2 weeks later, he had regained the ability to control his head, but not to roll. From that point he showed gross motor developmental delay and hypotonia. At 18 months, he was referred to one of the au-

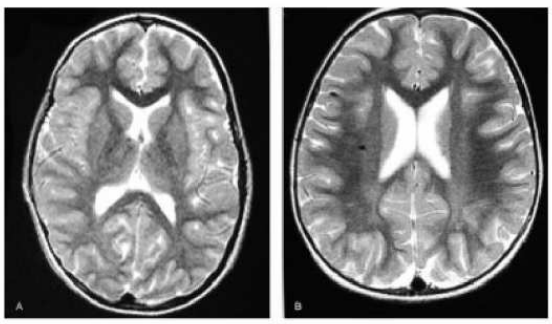

Fig 1. (A) T2-weighted brain magnetic resonance images (MRIs) acquired in the transverse plane of Patient 1 aged 8 years showing mild ventriculomegaly with normal white matter and cortical folding. (B) Brain MRI of Patient 2 aged 3 years. Both white matter and cortical folding are normal.

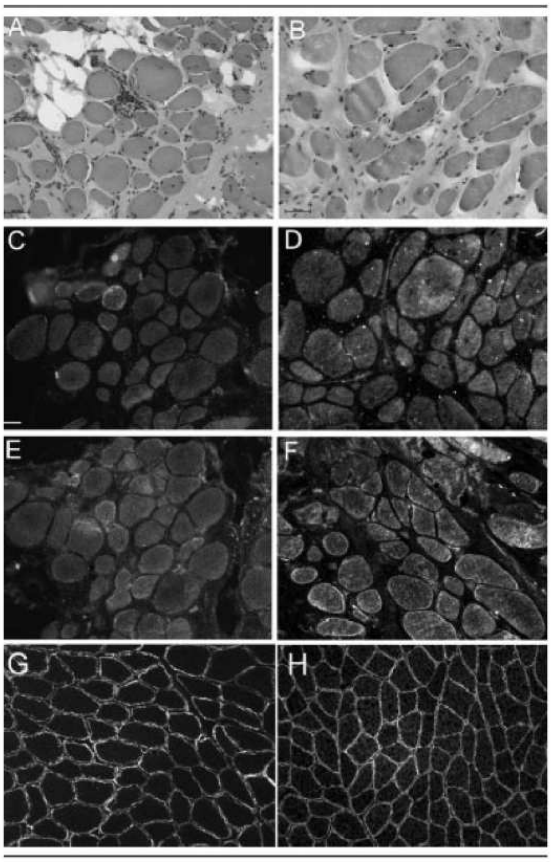

Fig 2. Muscle biopsies of Patient 1 (A, C, E), Patient 2 (B, D, F), and a control subject (G, H). Dystrophic appearance on hematoxylin and eosin staining (A, B) showing a focus of inflammatory cells in Patient 1 (A). Reduced labeling of the glycosylated epitope of α-dystroglycan with IIH6 antibody (C, D) and with an antibody to the core of the dystroglycan protein (E, F). Control muscle with normal labeling of α-dystroglycan with the IIH6 antibody (G) and with antibody to the core protein (H).

thors (D.E.) and found to have a CK level of 9,951IU/L with proximal upper extremity weakness and periscapular atrophy. Lower extremities were also affected; he was able to support weight on legs, but not to stand independently. Brain MRI was normal. A muscle biopsy showed a dystrophic pattern with infiltrating cells mainly comprising macrophages with a few T lymphocytes. There was moderate expression of MHC class I on the sarcolemma. He began prednisone therapy at a dose of 2mg/kg daily for 2 weeks, weaned to 1mg/kg/day on reevaluation at 1 month. He also had a 5-day course of intravenous immunoglobulins at a dose of 0.4gm/kg/day. One month after onset of therapy, his CK level was 857 IU/L, he could raise his arms above his head, and was cruising on furniture. Three months into treatment, he was walking independently. This boy has been followed for 9 years. Attempts to lower or stop steroids have resulted in increased weakness. He is now maintained on a prednisone dose of 0.75mg/kg/day. His upper extremities remain more affected than lower extremities, and he has weakness of wrist and finger extensors, as well as wrist flexors. He also developed hypertrophy affecting mostly the lateral gastrocnemius. Intelligence is unaffected.

His younger sister (Patient 2) was evaluated at birth and subsequently every month (D.E.). She developed normally until 4 months of age. At this point, she developed increased truncal weakness and hypotonia. At 3 months of age, CK level was 13,000IU/L. The weakness progressed; she sat at 7 months, but by the age of 1 year, she could not roll, sit, or support her weight and had no antigravity movements of her arms. She had distal and proximal weakness, with the legs more affected than the arms. At 13 months, she began prednisone therapy at a dosage of 0.75mg/kg/day with rapid improvement and the acquisition of independent ambulation by 24 months. By the age of 3 years, she had hypertrophy of the lateral gastrocnemius and peroneal muscle weakness. At 7 years of age, she is able to

Fig 3. Clinical photographs of the affected siblings in Family 2. (right) Patient 2. (left) Patient 3.

get up from the floor and remains stable on steroids. As in the previous case, at 3 years of age, a febrile illness in the midst of having reduced and stopped the steroids resulted in acute muscle weakness and hypotonia. She was placed back on prednisone therapy and strength returned to her baseline before the illness occurred. Intelligence is normal, and a brain MRI was also normal except for a frontal small subarachnoid cyst (see Fig 1B). Muscle biopsy at age 4.5 years showed virtually absent glycosylated α-dystroglycan (see Fig 2). Laminin-α2, -β1, and -γ1 were all mildly reduced, as observed previously in patients with *fukutin* mutations (data not shown). Macrophages around necrotic fibers and in the endomysium were seen, but no eosinophils. Lymphocyte markers showed only a few T cells and no B cells (Data not shown).

Sequencing Mutation Analysis

Two heterozygous mutations in the *fukutin* gene were found in Patient 1. One, 1167dupA, which has been reported previously, occurred in exon 9. This is predicted to result in a frameshift at Phe390 and premature termination of translation after the addition of a further 13 residues (amino acid 403). The second was a novel mutation found in exon 10,1363delG. This is predicted to cause a frameshift at Asp455 and termination of translation after the addition of a further 11 amino acids, including 5 encoded by the 3′ untranslated region (Fig 4A). Parental studies showed that the exon 9 mutation was inherited from the mother and the exon 10 mutation from the father. Analysis of her two healthy siblings showed that one had inherited no mutations, whereas the other carried the exon 9 mutation.

Patients 2 and 3 also harbored two heterozygous *fukutin* mutations. The first was the same single A insertion after nucleotide 1167 (exon 9) found in Patient 1. The second was a novel missense mutation in exon 8, c.920G>A, predicted to result in a p.Arg307Gln change (see Fig 4A). The exon 8 mutation was inherited from the mother and the exon 9 mutation from the father. A schematic representation of the *fukutin* protein with the sites of these mutations is represented in Figure 4B.

Expression and Subcellular Localization of Mutant Fukutin *Constructs*

A tagged human *fukutin* complementary DNA vector was transfected into Chinese hamster ovary cells. Strong colocalization of wild-type constructs with GM130 (a marker for the Golgi apparatus) was seen in transfected cultures. To observe the effects of the mu-

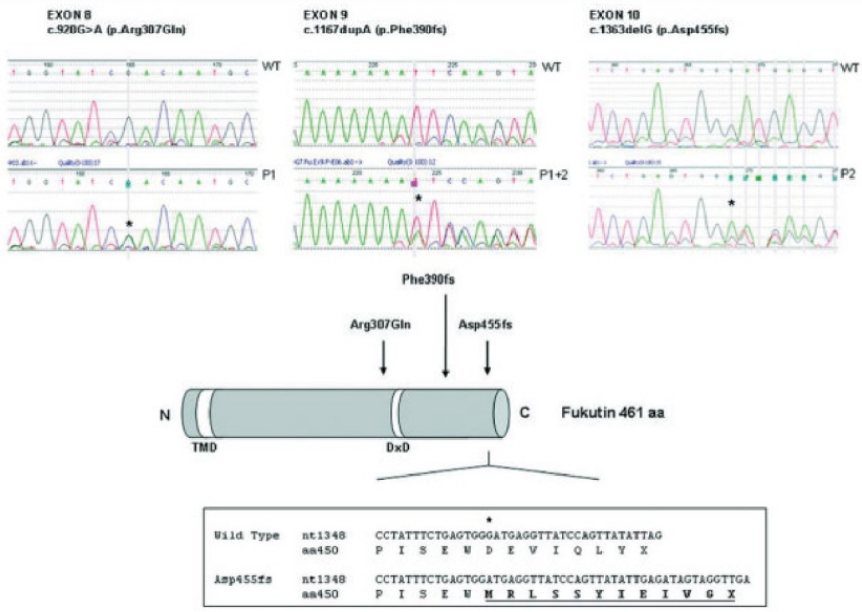

Fig 4. (A) Sequencing chromatograms obtained from Patients 1 and 2 showing the presence of heterozygous fukutin mutations. The mutations are indicated by an asterisk. *WT = wild type; P1 = Patient 1 (Family 1) carries the exon 8 and 9 mutations; P2 = Patient 2 (Family 2) carries the exon 9 and 10 mutations. (B) A schematic representation of fukutin showing the localization of mutations found in Families 1 and 2. The box shows the expanded C-terminal sequence predicted from the presence of the Asp455 frameshift mutation showing extension into the 3′ untranslated region. The locations of the transmembrane domain (TMD) and conserved DxD motif are also indicated.*

tations found in Patients 1 and 2 on *fukutin* expression and localization, we introduced the Arg307Gln and Asp455fs mutations into the wild-type *fukutin* tagged construct. Both mutant constructs appeared to be expressed at levels similar to the wild-type construct and retained colocalization with the Golgi marker GM130 (Fig 5). We did not introduce the Phe390fs mutation because this mutation is located in exon 9 (therefore not in the last exon), and the stop signal in this exon is predicted to create unstable messenger RNA as a result of the nonsense-mediated decay.[23]

Discussion

FCMD was first described by Yukio Fukuyama in 1960.[24] Affected children have generalized muscle weakness, severe brain involvement with mental retardation, seizures, and abnormal eye structure and/or function.[25] First symptoms occur at birth; there is marked delay of motor milestones, and most patients progress only to sitting unsupported or standing with support. Structural brain malformations are an integral feature of FCMD and include the "cobblestone" polymicrogyria-pachygyria complex. Seizures are common.[25,26] Complete agyria has been described in two Turkish patients with nonsense *fukutin* mutations and a WWS-like phenotype.[18,19] Pseudohypertrophy of the tongue, calves, and quadriceps muscles is common. Progressive weakness then develops, and respiratory failure in the mid-to-late teens is an invariable complication. CK levels are elevated between 10 and 50 times normal. A FCMD patient who was able to stand with support and had only mild mental retardation has been reported; however, analysis of the *fukutin* gene identified the founder mutation on one allele only, with no other mutations.[27] For this reason, the primary role of *fukutin* in this patient has yet to be established.

Our three patients have a phenotype that overlaps between congenital muscular dystrophy and LGMD. On balance, their condition is best described as a LGMD variant. They all acquired independent ambulation and share a complete absence of central nervous system involvement. In addition, the main reason for bringing them to medical attention in the first year of life was the acute and severe weakness after intercurrent illness. Interestingly, they each showed some cellular infiltrates in the muscle biopsy and demonstrated a remarkable response to steroids to the point that a polymyositis was considered as an alternative diagnosis. Muscle inflammation is usually a nonspecific phenomenon that accompanies several forms of muscular dystrophy. An association between calpain-3 deficiency and eosinophilic myositis has been reported.[28] More commonly, the infiltrate in other forms of dystrophies comprises macrophages and $CD8^+$ cytotoxic T cells. In some instances, the severity of the infiltrate can lead to the erroneous diagnosis of polymyositis, particularly in dysferlinopathies (see Brown and Amato for a recent review[29]). Severe inflammatory infiltrates resembling polymyositis have been reported previously not only in laminin-α2 deficiency congenital muscular dystrophy (MDC1A),[30] but also in an infant eventually diagnosed as affected by FCMD.[31] The inflammatory response in our patients was mainly macrophages and a few lymphocytes. No eosinophils were observed. There was moderate expression of MHC-I in one of the patients. Such sarcolemmal MHC-I expression can occur in several conditions, including Duchenne muscular dystrophy, Becker muscular dystrophy, and LGMD2B, and also occurs on regenerating fibers. The severe depletion of glycosylated α-dystroglycan suggested a dystroglycanopathy, and the analysis of *fukutin* allowed identification of heterozygous pathogenic mutations. The mutation common to both families in exon 9 is expected to be severe because it is predicted to lead to premature termination of translation at amino acid 403 and subsequent nonsense-mediated messenger RNA decay.[23] The severe nature of this mutation is supported by its occurrence in a Japanese patient in association with the retrotransposal element where the resultant phenotype was more severe than in homozygotes for the insertion.[17] The mutation had apparently occurred de novo in this Japanese patient[17] but was inherited in our two families, who share an Israeli origin, suggesting that it might be common in this population. In contrast, the two novel *fukutin* mu-

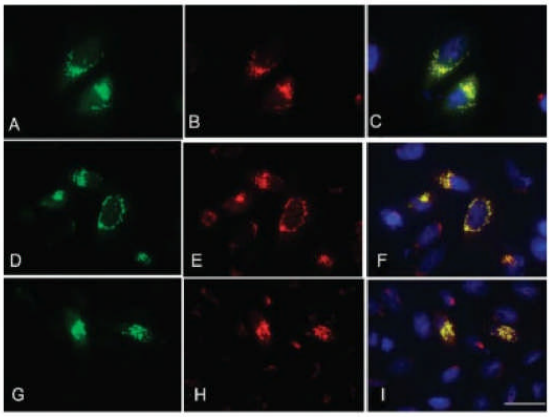

Fig 5. Double labeling of Fukutin-V5 constructs and GM130 on Chinese hamster ovary (CHO) cell cultures. The merged images (C, F, I) indicate that both wild-type (A–C) and mutant fukutin constructs (D–F: Asp455fs; G–I: Arg307Gln) perfectly colocalize with the Golgi marker GM130. Moreover, the fukutin mutant constructs did not appear to be less stable than wild type. Green channel = anti-V5 antibody; red channel = anti-GM130 antibody; blue channel = Hoechst 33342 nuclear stain. Scale bar = 20μm.

tations reported here possibly represent the mildest so far described. These mutations result in proteins that are expressed and localized correctly; we assume that they exert their effect by disrupting *fukutin* function or its interaction with other Golgi proteins. These data also suggest that the retrotransposal insertion is probably a rather severe mutation.

The demonstration of vastly differing phenotypes associated with *fukutin* mutations is reminiscent of the spectrum of disorders attributed to *FKRP* mutations. A significant variability of clinical severity recently has been reported for mutations in *POMT1,* with phenotypes ranging from severe WWS[32] to a form of LGMD with associated mental retardation and microcephaly, now known as LGMD2K.[33]

Although enhancing our understanding of the role of glycosyltransferases in dystroglycanopathies, the finding of mutations in *fukutin* in mildly affected individuals again reinforces the wide phenotypic spectrum within this group of disorders. The inflammatory infiltrates found in our cases and the remarkable response to corticosteroid therapy raise two important issues: first, a dystroglycanopathy should now be considered in the differential diagnosis of polymyositis; and second, further studies aimed at assessing the role of steroids in dystroglycanopathies should be considered. In view of the significant clinical differences between our patients and those previously described with FCMD, we propose to name this milder subgroup LGMD2L.

This work was supported by the Muscular Dystrophy Campaign (MDC; PC3143, F.M.) and an MDC clinical research fellowship (PC0916, E.M.C.).

We acknowledge the National Specialist Commissioning Advisory Group (UK) support to the Hammersmith Hospital Congenital Muscular Dystrophy Centre. We also thank Dr F. Roncaroli for his help in characterizing the inflammatory cells.

References

1. Muntoni F, Brockington M, Blake DJ, et al. Defective glycosylation in muscular dystrophy. Lancet 2002;360:1419–1421.
2. Muntoni F, Brockington M, Torelli S, Brown SC. Defective glycosylation in congenital muscular dystrophies. Curr Opin Neurol 2004;17:205–209.
3. Toda T, Kobayashi K, Takeda S, et al. Fukuyama-type congenital muscular dystrophy (FCMD) and alpha-dystroglycanopathy. Congenit Anom Kyoto 2003;43:97–104.
4. Henry MD, Campbell KP. Dystroglycan inside and out. Curr Opin Cell Biol 1999;11:602–607.
5. Michele DE, Barresi R, Kanagawa M, et al. Post-translational disruption of dystroglycan-ligand interactions in congenital muscular dystrophies. Nature 2002;418:417–422.
6. Michele DE, Campbell KP. Dystrophin-glycoprotein complex: post-translational processing and dystroglycan function. J Biol Chem 2003;278:15457–15460.
7. Muntoni F, Voit T. The congenital muscular dystrophies in 2004: a century of exciting progress. Neuromuscul Disord 2004;14:635–649.
8. Brockington M, Blake DJ, Prandini P, et al. Mutations in the fukutin-related protein gene (FKRP) cause a form of congenital muscular dystrophy with secondary laminin alpha2 deficiency and abnormal glycosylation of alpha-dystroglycan. Am J Hum Genet 2001;69:1198–1209.
9. Brockington M, Yuva Y, Prandini P, et al. Mutations in the fukutin-related protein gene (FKRP) identify limb girdle muscular dystrophy 2I as a milder allelic variant of congenital muscular dystrophy MDC1C. Hum Mol Genet 2001;10:2851–2859.
10. Topaloglu H, Brockington M, Yuva Y, et al. FKRP gene mutations cause congenital muscular dystrophy, mental retardation, and cerebellar cysts. Neurology 2003;60:988–992.
11. van Reeuwijk J, Janssen M, van den Elzen C, et al. POMT2 mutations cause alpha-dystroglycan hypoglycosylation and Walker-Warburg syndrome. J Med Genet 2005;42:907–912.
12. Mercuri E, Topaloglu H, Brockington M, et al. Spectrum of brain changes in patients with congenital muscular dystrophy and FKRP gene mutations. Arch Neurol 2006;63:251–257.
13. Kobayashi K, Nakahori Y, Miyake M, et al. An ancient retrotransposal insertion causes Fukuyama-type congenital muscular dystrophy. Nature 1998;394:388–392.
14. Aravind LK, Koonin EV. The fukutin protein family—predicted enzymes modifying cell-surface molecules. Curr Biol 1999;9:R836–R837.
15. Hayashi YK, Ogawa M, Tagawa K, et al. Selective deficiency of alpha-dystroglycan in Fukuyama-type congenital muscular dystrophy. Neurology 2001;57:115–121.
16. Toda T, Kobayashi K, Kondo-Iida E, et al. The Fukuyama congenital muscular dystrophy story. Neuromuscul Disord 2000;10:153–159.
17. Kondo-Iida E, Kobayashi K, Watanabe M, et al. Novel mutations and genotype-phenotype relationships in 107 families with Fukuyama-type congenital muscular dystrophy (FCMD). Hum Mol Genet 1999;8:2303–2309.
18. Silan F, Yoshioka M, Kobayashi K, et al. A new mutation of the fukutin gene in a non-Japanese patient. Ann Neurol 2003;53:392–396.
19. de Bernabe DB, van Bokhoven H, van Beusekom E, et al. A homozygous nonsense mutation in the fukutin gene causes a Walker-Warburg syndrome phenotype. J Med Genet 2003;40:845–848.
20. Takeda S, Kondo M, Sasaki J, et al. Fukutin is required for maintenance of muscle integrity, cortical histiogenesis and normal eye development. Hum Mol Genet 2003;12:1449–1459.
21. Dubowitz V, Sewry CA. Muscle biopsy: a practical approach. 3rd ed. London: WB Saunders, 2006.
22. Kinali M, Mercuri E, Main M, et al. An effective, low-dosage, intermittent schedule of prednisolone in the long-term treatment of early cases of Duchenne dystrophy. Neuromuscul Disord 2002;12(suppl 1):S169–S174.
23. Baker KE, Parker R. Nonsense-mediated mRNA decay: terminating erroneous gene expression. Curr Opin Cell Biol 2004;16:293–299.
24. Fukuyama Y, Kwazura M, Haruna H. A peculiar form of congenital muscular dystrophy. Paediatr Univ Tokyo 1960;4:5–8.
25. Fukuyama Y, Osawa M, Suzuki H. Congenital progressive muscular dystrophy of the Fukuyama type: clinical, genetic and pathological considerations. Brain Dev 1981;3:1–29.
26. Takada K, Nakamura H, Tanaka J. Cortical dysplasia in congenital muscular dystrophy with central nervous system involvement (Fukuyama type). J Neuropathol Exp Neurol 1984;43:395–407.

27. Akiyama T, Ohtsuka Y, Takata T, et al. The mildest known case of Fukuyama-type congenital muscular dystrophy. Brain Dev 2006;28:537–540.
28. Krahn M, Lopez de Munain A, Streichenberger N, et al. CAPN3 mutations in patients with idiopathic eosinophilic myositis. Ann Neurol 2006;59:905–911.
29. Brown RH Jr, Amato A. Calpainopathy and eosinophilic myositis. Ann Neurol 2006;59:875–877.
30. Pegoraro E, Mancias P, Swerdlow SH, et al. Congenital muscular dystrophy with primary laminin alpha2 (merosin) deficiency presenting as inflammatory myopathy. Ann Neurol 1996;40:782–791.
31. Kinoshita M, Iwasaki Y, Wada F, Segawa M. [A case of congenital polymyositis—a possible pathogenesis of "Fukuyama type congenital muscular dystrophy" (author's transl)]. Rinsho Shinkeigaku 1980;20:911—916.
32. Beltran-Valero de Bernabe D, Currier S, Steinbrecher A, et al. Mutations in the O-mannosyltransferase gene POMT1 give rise to the severe neuronal migration disorder Walker-Warburg syndrome. Am J Hum Genet 2002;71:1033–1043.
33. Balci B, Uyanik G, Dincer P, et al. An autosomal recessive limb girdle muscular dystrophy (LGMD2) with mild mental retardation is allelic to Walker-Warburg syndrome (WWS) caused by a mutation in the POMT1 gene. Neuromuscul Disord 2005;15:271–275.

OBSERVATION

Mild *POMGnT1* Mutations Underlie a Novel Limb-Girdle Muscular Dystrophy Variant

Emma M. Clement, MB, ChB; Caroline Godfrey, BSc; Jenny Tan, PhD; Martin Brockington, BSc; Silvia Torelli, PhD; Lucy Feng, PhD; Susan C. Brown, PhD; Cecilia Jimenez-Mallebrera, PhD; Caroline A. Sewry, PhD; Cheryl Longman, MD; Rachael Mein, BSc; Steve Abbs, PhD; Jiri Vajsar, MD; Harry Schachter, MD, PhD; Francesco Muntoni, MD

Background: Mutations in protein-O-mannose-β1,2-N-acetylglucosaminyltransferase 1 (*POMGnT1*) have been found in muscle-eye-brain disease, a congenital muscular dystrophy with structural eye and brain defects and severe mental retardation.

Objective: To investigate whether mutations in *POMGnT1* could be responsible for milder allelic variants of muscular dystrophy.

Design: Screening for mutations in *POMGnT1*.

Setting: Tertiary neuromuscular unit.

Patient: A patient with limb-girdle muscular dystrophy phenotype, with onset at 12 years of age, severe myopia, normal intellect, and decreased α-dystroglycan immunolabeling in skeletal muscle.

Results: A homozygous *POMGnT1* missense mutation (c.1666G>A, p.Asp556Asn) was identified. Enzyme studies of the patient's fibroblasts showed an altered kinetic profile, less marked than in patients with muscle-eye-brain disease and in keeping with the relatively mild phenotype in our patient.

Conclusions: Our findings widen the spectrum of disorders known to result from mutations in *POMGnT1* to include limb-girdle muscular dystrophy with no mental retardation. We propose that this condition be known as *LGMD2M*. The enzyme assay used to diagnose muscle-eye-brain disease may not detect subtle abnormalities of *POMGnT1* function, and additional kinetic studies must be carried out in such cases.

Arch Neurol. 2008;65(1):137-141

Author Affiliations: Dubowitz Neuromuscular Unit, Department of Paediatrics, Hammersmith Hospital, Imperial College London (Drs Clement, Torelli, Feng, Brown, Jimenez-Mallebrera, Sewry, Longman, and Muntoni), Ms Godfrey, Mr Brockington, and DNA Laboratory, Genetics Centre, Guy's Hospital (Mss Godfrey and Mein and Dr Abbs), London, and Centre for Inherited Neuromuscular Disorders, Robert Jones and Agnes Hunt Orthopaedic Hospital, Oswestry (Dr Sewry), England; and Department of Structural Biology and Biochemistry (Drs Tan and Schachter) and Division of Neurology (Dr Vajsar), Hospital for Sick Children, and Faculty of Medicine, University of Toronto (Drs Vajsar and Schachter), Toronto, Ontario, Canada.

THE DYSTROGLYCANOPATHIES are a group of heterogeneous autosomal recessive disorders characterized by reduced glycosylation of α-dystroglycan (α-DG) on the sarcolemma of skeletal muscle fibers[1]. These disorders share the common clinical feature of muscular dystrophy with a variable neurologic and ophthalmic phenotype.

Protein-O-mannose-β1,2-N-acetylglucosaminyltransferase 1 (*POMGnT1*; Online Mendelian Inheritance in Man database 606822) mutations were first detected in 2001 in patients with a typical muscle-eye-brain (MEB) disease phenotype.[2] Muscle-eye-brain disease is a severe form of congenital muscular dystrophy typically presenting with weakness at birth or in the first few months of life and ocular abnormalities including myopia, retinal defects, and congenital glaucoma. Patients invariably have mental retardation and typically have absent expressive language. Magnetic resonance imaging brain scans show abnormalities including frontoparietal cortical pachygyria, cerebellar hypoplasia, flattened brain stem, and ventricular dilatation.[3-5] More recently *POMGnT1* mutations have been found in patients with phenotypes resembling Walker-Warburg syndrome,[5] a more serious disorder that develops prenatally and is associated with absent motor development and severe structural brain and eye defects. Walker-Warburg syndrome is usually fatal within the first year of life.[4,6]

POMGnT1 is a glycosyltransferase gene involved in the glycosylation of α-DG and is responsible for the transfer of *N*-acetylglucosamine (GlcNAc) to mannose.[2,7] Quantifying the pathologic consequence associated with *POMGnT1* mutations has been facilitated by the development of a functional assay of POMGnT1 enzyme activity. This assay enables the detection of pathogenic *POMGnT1* alterations in individuals with MEB and the identification of carriers of these mutations, and has been used as a successful adjunct to diagnosis.[8,9]

Herein we report a homozygous *POMGnT1* mutation in a patient with a novel form of limb-girdle muscular dystrophy without mental retardation, ex-

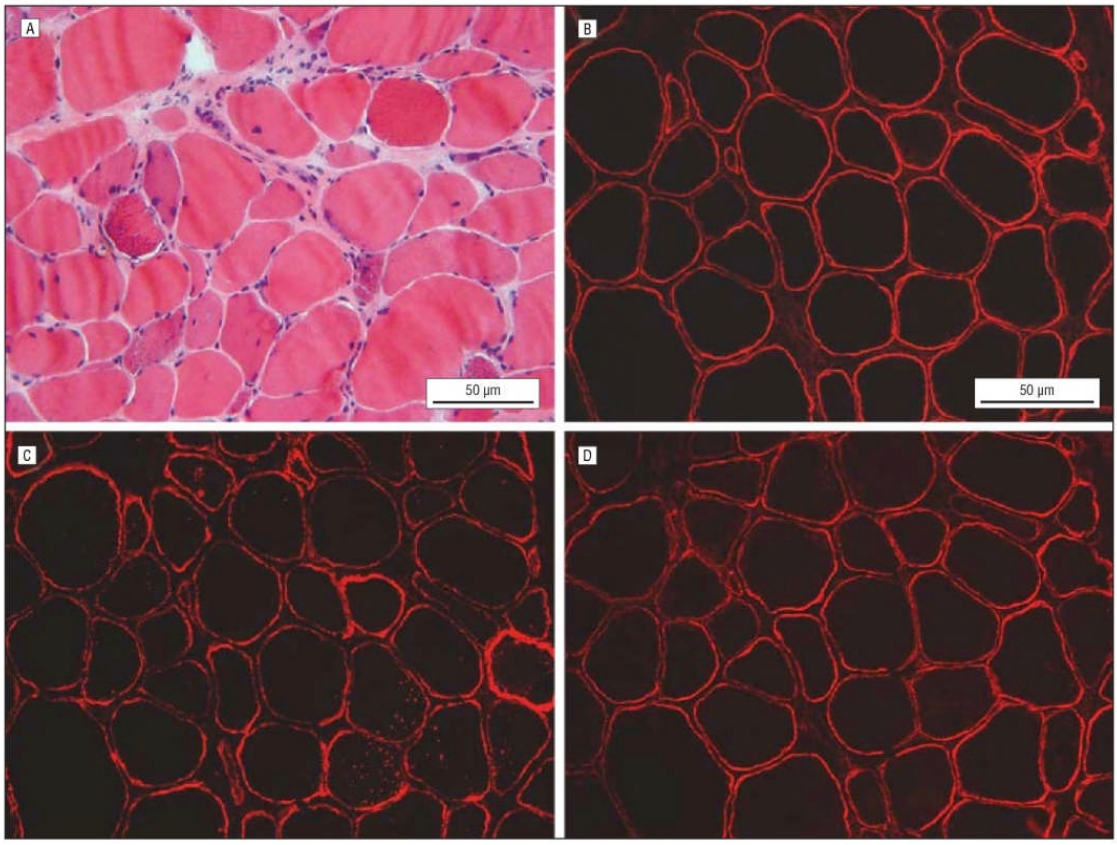

Figure 1. Muscle biopsy specimen. A, Note dystrophic changes and granular fibers with vacuoles (hematoxylin-eosin). B, Immunolabeling for β-dystroglycan. C and D, Labeling for α-dystroglycan using an antibody to the glycosylated epitope IIH6 (C) and the core protein (D).

panding the spectrum of diseases derived from mutations of this gene. This mutation led to a subtle abnormality in POMGnT1 enzyme activity not typical of that seen in MEB.

METHODS

PATIENT

A patient with limb-girdle muscular dystrophy was studied. The finding of abnormal glycosylation of α-DG in a muscle biopsy specimen was the criterion for inclusion in this study, which was approved by the Hammersmith Hospital Trust Ethics Committee (Research Ethical Committee 2000/5802).

HISTOLOGIC ANALYSIS AND IMMUNOHISTOCHEMISTRY

Frozen 10-µm muscle sections were stained with hematoxylin-eosin using a standard technique.[10] Frozen 7-µm sections were incubated with mouse monoclonal antibodies to spectrin and dystrophin (spectrin DYS1, DYS2, and DYS3; Novocastra Laboratories Ltd, Newcastle upon Tyne, England); laminin-α2 (MAB1922; Chemicon International Inc, Temecula, California); the 80-kDa C-terminal fragment; β-dystroglycan (43DAG; Novocastra Laboratories Ltd); and an α-dystroglycan, IIH6; and with a sheep polyclonal antibody to the core protein of chick α-dystroglycan. Immunostaining was performed as previously described by Godfrey et al.[11]

SINGLE-SECTION WESTERN BLOT AND OVERLAY ASSAYS

Proteins from control and patient muscle biopsy specimens were extracted from sections using the method published by Cooper et al.[12] In brief, sections were collected in sample buffer consisting of 4% sodium dodecylsulfate, 125mM Tris (pH 8.8), 40% glycerol, protease inhibitor cocktail, 100mM dithiothreitol, and bromophenol blue, and were boiled for 3 minutes. After centrifugation to sediment particulate material, the supernatant was used for Western blot analysis and for the laminin overlay. Samples were loaded into a NuPAGE Pre-Cast Gel System (4%-12% Bis–Tris gel; Invitrogen Corp, Carlsbad, California), then transferred electrophoretically to nitrocellulose membrane. Nitrocellulose strips were blotted with α-dystroglycan IIH6 antibody (Upstate Biotechnology, Waltham, Massachusetts) and β-dystroglycan antibody (Novocastra Laboratories Ltd) as described by Longman et al.[13] The laminin overlay assay was performed as described by Longman et al.[13]

MUTATION ANALYSIS

Genomic DNA was isolated from total blood samples using standard extraction protocols. The complete coding regions of

FKRP, *POMT1*, *POMT2*, *POMGnT1*, *LARGE*, and *fukutin* were screened as described by Godfrey et al[11] (GenBank Accession numbers: *FKRP*, NM_024301; *POMT1*, NM_007171.2; *POMT2*, NM_013382.3; *POMGnT1*, NM_017739.1; *fukutin*, NM_006731.1; and *LARGE*, NM_133642.2).

KINETIC ANALYSIS OF POMGnT1 ENZYME ACTIVITY

Kinetic analysis of POMGnT1 was carried out by a modification of a previously reported method.[8,14] Fibroblasts from a control subject without congenital muscular dystrophy and from the patient were scraped off dishes without trypsin. Cells containing about 1 mg of protein were homogenized at 4°C in 0.2 mL of homogenizing buffer (2.0% Triton X-100, 0.2M sodium chloride in phosphate-buffered saline solution) containing one-fourth of a tablet of protease inhibitor cocktail (Roche Boehringer Mannheim Diagnostics, Basel, Switzerland). The assay incubations contained, in a total volume of 0.020 mL, 0.015 mL of fibroblast extract (approximately 0.05-0.07 mg of protein per assay), 75mM 2-(*N*-morpholino) ethanesulfonic acid buffer (pH 6.0), 10mM manganese chloride, 5mM adenosine monophosphate, 0.2M GlcNAc, and 8 combinations of donor and acceptor concentrations: (1) 0.25, 0.5, 0.75, and 1.0mM uridine diphosphate (UDP)–(^{3}H)GlcNAc (New England Nuclear Corp, Boston, Massachusetts; 125 000 dpm/nmol) and 62.5mM Manα1-O-benzyl (Toronto Research Chemicals Inc, North York, Ontario, Canada), and (2) 5, 10, 15, and 20mM Manα1-O-benzyl and 0.5mM UDP–(^{3}H)GlcNAc. Incubations were carried out at 37°C for 2 hours. SepPak C18 cartridges (Waters Corp, Milford, Massachusetts) were used to determine the amount of radioactive product as previously described.[15,16] Control assays were routinely carried out in the absence of an acceptor, and the value obtained was subtracted from all assays. All assays were carried out in duplicate.

RESULTS

CLINICAL DESCRIPTION

Our patient is one of 5 children born to healthy nonconsanguineous Irish parents. She first developed proximal limb muscle weakness at the age of 12 years, with difficulty rising from a sitting position and climbing stairs. Her early motor milestones were normal. The weakness progressed rapidly, and by age 14 years was more proximal than distal, with the neck, hip girdle, and shoulder abductor muscles particularly affected. Her Gower sign was positive. There was hypertrophy of the calves and quadriceps and wasting of the hamstring and deltoid muscles. She had a lordotic stance and poor heel strike because of Achilles tendon tightening. Facial expression was normal. Progressive weakness resulted in loss of ambulation at age 19 years after a leg fracture. Her general health remains excellent. She has myopia (+6); at the age of 6 years, she underwent surgery to correct a convergent squint. Her intellect is normal, and she is attending a university and is 21 years old. Results of initial investigation included serum creatine kinase concentration consistently elevated between 5000 and 12 000 U/L and electromyographic findings suggestive of a myopathic process.

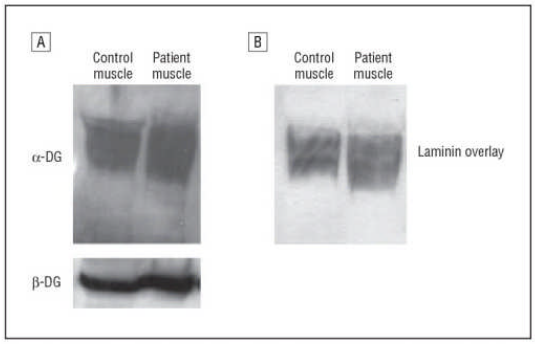

Figure 2. Single-section skeletal muscle analysis. A, Western blot analysis using the IIH6 antibody (α-DG) shows that expression and molecular weight of patient muscle were similar to those of control muscle. β-Dystroglycan expression (β-DG) was similar to control and demonstrates equal loading between samples. B, Laminin overlay assay. The patient's α-DG shows the same ability to bind laminin compared with the control muscle. α-DG and β-DG indicate α- and β-dystroglycan, respectively.

HISTOLOGIC ANALYSIS AND IMMUNOHISTOCHEMISTRY

The muscle biopsy specimen exhibited dystrophia with abnormal variation in fiber size, necrosis, increased endomysial connective tissue and fat, and basophilic fibers, some of which were granular and had vacuoles (**Figure 1**A). Immunolabeling of β-spectrin, dystrophin, and laminin-α2 yielded normal findings (data not shown). A percentage of these fibers were also weaker with the anti-β-dystroglycan antibody and may correspond to basophilic fibers (Figure 1B). Labeling with IIH6 antibody to the glycosylated epitope of α-DG was variable between fibers (Figure 1C). Some fibers showed a mild reduction; others were brightly labeled. Similarly, labeling with the core antibody was weaker on some small fibers (Figure 1D). Further examination of the biopsy specimen demonstrated normal findings at Western blot analysis of dystrophin, sarcoglycans, laminin-α2, caveolin, emerin, calpain 3, dysferlin, and telethonin.

SINGLE-SECTION WESTERN BLOT AND OVERLAY ASSAYS

Western blot analysis of skeletal muscle showed an expression of α-DG similar to that in the control sample using an antibody that recognizes a glycosylated epitope (IIH6; **Figure 2**A). β-Dystroglycan expression was normal and demonstrates equal protein loading. The laminin overlay assay showed that α-DG ability to bind laminin was similar to that in the control sample (Figure 2B).

MUTATION ANALYSIS

A novel homozygous point mutation, c.1666G>A, was detected in exon 20 of *POMGnT1*. This change is predicted to result in the substitution of a conserved aspartic acid at amino acid 556 to asparagine (p.Asp556Asn) in the POMGnT1 protein. No other sequence variations were detected in the other known dystroglycanopathy genes (*FKRP*, *POMT1*, *POMT2*, *fukutin*, or *LARGE*), and

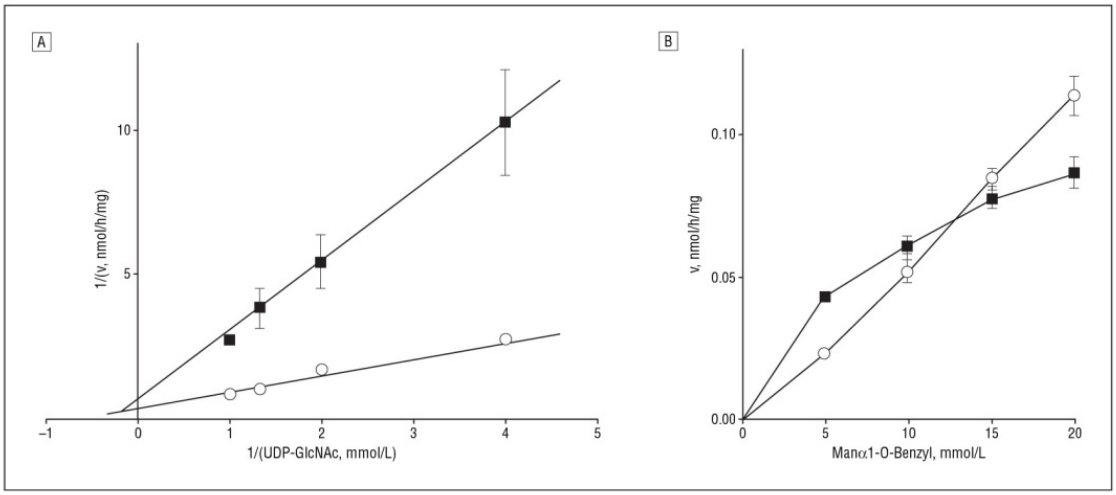

Figure 3. Kinetic analysis of protein-O-mannose-β1,2-N-acetylglucosaminyltransferase 1 (POMGnT1) enzyme activity. A, Reciprocal plot of enzyme rate vs uridine diphosphate–*N*-acetylglucosamine (UDP-GlcNAc) concentration (0.25, 0.5, 0.75, and 1.0 mmol/L) at 62.5 mmol/L of Manα1-O-benzyl for control (circles) and patient (squares) fibroblasts. The plots are linear, showing classic Michaelis-Menten behavior. The apparent Michaelis-Menten constant (K_m) and maximum velocity (V_{max}) values are, respectively, 2.2 and 6.1 mmol/L (highly significant difference) and 3.4 and 2.5 nmol/h/mg (difference not statistically significant) for control and patient fibroblasts. Standard deviation bars are shown. B, Plot of enzyme rate vs Manα1-O-benzyl concentration (5, 10, 15, and 20 mmol/L) at 0.5 mmol/L of UDP-GlcNAc for control and patient fibroblasts. The plot for the control fibroblasts is linear, as previously described,[14] indicating relatively large K_m and V_{max} values. The plot for patient fibroblasts is hyperbolic. The reciprocal plot (not shown) is linear, yielding apparent K_m and V_{max} values of 9 mmol/L and 0.1 nmol/h/mg, respectively. The slopes of the 2 reciprocal plots are significantly different at the 95% confidence interval. v indicates velocity.

linkage to the *MDC1B* locus on 1q42 was excluded.[17] Both parents were found to be carriers of the mutation, and none of the 4 unaffected siblings tested were homozygous for this change. This alteration was not detected in more than 100 disease control samples (data not shown).

KINETIC ANALYSIS OF POMGnT1 ENZYME ACTIVITY

Kinetic analysis of POMGnT1 activity at 4 different concentrations of UDP-GlcNAc (**Figure 3**A) showed apparent Michaelis-Menten constant (K_m) values of 2.2 and 6.1 mmol/L for control and patient fibroblasts, respectively. The respective apparent maximum velocity (V_{max}) values were 3.4 and 2.5 nmol/h/mg of protein (difference not statistically significant). It is impossible to obtain accurate K_m and V_{max} values for Manα1-O-benzyl with normal POMGnT1 because these parameters are both so large that a plot of enzyme rate vs acceptor concentration shows a straight line through the origin, up to the maximum soluble concentration of 60 mmol/L of Manα1-O-benzyl.[14] However, a similar analysis of patient fibroblasts (Figure 3B) showed a qualitative change from a straight line to a classic hyperbolic Michaelis-Menten plot (apparent K_m and V_{max} values of 9 mmol/L and 0.1 nmol/h/mg of protein, respectively).

COMMENT

To date, the identification of *POMGnT1* mutations has been restricted to patients with congenital muscular dystrophy and brain abnormalities. Most of these patients have a phenotype consistent with MEB, although some cases resembling Walker-Warburg syndrome have also been reported.[2,5] One of the unanswered questions about the genotype-phenotype correlation for *POMGnT1* mutations is whether it can cause mild as well as severe phenotypes, as noted in other dystroglycanopathy genes, most notably *FKRP*[18,19] but more recently also *fukutin*.[11]

The p.Asp556Asn mutation reported herein is predicted to be located in the substrate-specific region of the catalytic domain. Several lines of evidence indicate that this alteration is pathogenic. First, the patient's skeletal muscle biopsy specimen demonstrated findings consistent with a muscular dystrophy and suggestive of dystroglycanopathy. No mutations were detected in the 5 other dystroglycanopathy genes screened. The reduction of α-DG labeling was subtle at immunocytochemistry, and no substantial reduction in molecular weight was observed at Western blot analysis. This highlights the difficulty in detecting mild α-DG abnormalities and has been previously observed with mild *FKRP* mutations in limb-girdle muscular dystrophy type 2I.[20] Second, the mutation segregated with the disease in this large family. Third, the mutation causes a reversal of amino acid polarity in the substrate-specific domain of POMGnT1, which may be expected to have functional consequences. In addition, the detailed enzyme studies offer support for this theory. The POMGnT1 activity is observed but differs in its kinetics from that of control samples. The apparent K_m for UDP-GlcNAc is substantially higher and the apparent V_{max} for Manα1-O-benzyl is substantially lower than in the control sample. Application of the POMGnT1 assay conditions that were previously used for analysis in patients with MEB (1 mmol/L of UDP-GlcNAc and 62.5 mmol/L of Manα1-O-benzyl)[8] to our patient with limb-girdle muscular dystrophy yields a POMGnT1 rate that is significantly higher than the val-

ues found in patients with MEB. Reliable diagnosis in patients such as ours, therefore, requires determination of kinetic parameters.

This mutation had no effect on the subcellular localization or expression of a recombinant form of *POMGnT1* when overexpressed in C2C12 myotubes (data not shown). However, the p.Asp556Asn mutation introduces a potential *N*-glycosylation site (Asn-X-Ser) into the protein, which is predicted to have no other such sites. The presence of an *N*-glycan at this position may cause defective enzyme folding that results in an active but inefficient enzyme.

CONCLUSION

This article substantially expands the spectrum of disorders associated with *POMGnT1* mutations, and our patient has the mildest POMGnT1 deficiency described. The finding of normal POMGnT1 activity at conventional enzyme assay but the identification of altered kinetic properties of the mutant enzyme highlight the importance of careful interpretation of functional data, especially when studying atypical clinical findings.

This finding reinforces the presence of glycosyltransferase mutations among the limb-girdle muscular dystrophies. We propose to name this new phenotype *LGMD2M*.

Accepted for Publication: May 2, 2007.
Correspondence: Francesco Muntoni, MD, Dubowitz Neuromuscular Unit, Department of Paediatrics, Hammersmith Hospital, Imperial College London, Du Cane Road, London W12 ONN, England (f.muntoni@imperial.ac.uk).
Author Contributions: Dr Clement and Ms Godfrey contributed equally to the manuscript. *Study concept and design:* Clement, Godfrey, Abbs, and Muntoni. *Acquisition of data:* Clement, Godfrey, Tan, Brockington, Torelli, Feng, Jimenez-Mallebrera, Sewry, Longman, Mein, Abbs, and Schachter. *Analysis and interpretation of data:* Clement, Godfrey, Tan, Torelli, Feng, Brown, Jimenez-Mallebrera, Sewry, Mein, Abbs, Vajsar, and Schachter. *Drafting of the manuscript:* Clement, Godfrey, Tan, Brockington, Torelli, Feng, Jimenez-Mallebrera, Sewry, Longman, Mein, Abbs, Schachter, and Muntoni. *Critical revision of the manuscript for important intellectual content:* Clement, Godfrey, Brown, Jimenez-Mallebrera, Mein, Abbs, Vajsar, and Muntoni. *Statistical analysis:* Tan and Schachter. *Obtained funding:* Abbs and Muntoni. *Administrative, technical, and material support:* Clement, Godfrey, Brockington, Feng, Brown, Jimenez-Mallebrera, Sewry, Longman, Mein, Abbs, Vajsar, and Schachter. *Study supervision:* Clement, Godfrey, Mein, Abbs, and Muntoni.
Financial Disclosure: None reported.
Funding/Support: This work was supported by grants PC3143 from the Muscular Dystrophy Campaign (MDC) (Dr Muntoni) and MT-3285 from the Canadian Institutes of Health Research (Dr Schachter). Dr Clement and Ms Godfrey received MDC research fellowships PO0916 and RA3/734, respectively.
Additional Contributions: The National Specialist Commissioning Advisory Group Diagnostic and Advisory Service (NSCAG) provided support to the Dubowitz Neuromuscular Centre, Hammersmith Hospital, Imperial College London. Kate Bushby, MD, FRCP, of the Limb Girdle Muscular Dystrophies NSCAG Centre in Newcastle upon Tyne, England, performed the Western blot analysis of proteins involved in our patient with limb-girdle muscular dystrophy. The α-dystroglycan IIH6 was a gift of Kevin Campbell, University of Iowa, Iowa City, and the sheep polyclonal antibody to the core protein of chick α-dystroglycan was a gift of Stephan Kroger, University of Mainz, Mainz, Germany.

REFERENCES

1. Muntoni F, Voit T. The congenital muscular dystrophies in 2004: a century of exciting progress. *Neuromuscul Disord.* 2004;14(10):635-649.
2. Yoshida A, Kobayashi K, Manya H, et al. Muscular dystrophy and neuronal migration disorder caused by mutations in a glycosyltransferase, POMGnT1. *Dev Cell.* 2001;1(5):717-724.
3. Santavuori P, Somer H, Sainio K, et al. Muscle-eye-brain disease (MEB). *Brain Dev.* 1989;11(3):147-153.
4. Cormand B, Pihko H, Bayés M, et al. Clinical and genetic distinction between Walker-Warburg syndrome and muscle-eye-brain disease. *Neurology.* 2001;56(8):1059-1069.
5. Taniguchi K, Kobayashi K, Saito K, et al. Worldwide distribution and broader clinical spectrum of muscle-eye-brain disease. *Hum Mol Genet.* 2003;12(5):527-534.
6. Dobyns WB, Pagon RA, Armstrong D, et al. Diagnostic criteria for Walker-Warburg syndrome. *Am J Med Genet.* 1989;32(2):195-210.
7. Manya H, Sakai K, Kobayashi K, et al. Loss-of-function of an *N*-acetylglucosaminyltransferase, POMGnT1, in muscle-eye-brain disease. *Biochem Biophys Res Commun.* 2003;306(1):93-97.
8. Zhang W, Vajsar J, Cao P, et al. Enzymatic diagnostic test for muscle-eye-brain type congenital muscular dystrophy using commercially available reagents. *Clin Biochem.* 2003;36(5):339-344.
9. Vajsar J, Zhang W, Dobyns WB, et al. Carriers and patients with muscle-eye-brain disease can be rapidly diagnosed by enzymatic analysis of fibroblasts and lymphoblasts. *Neuromuscul Disord.* 2006;16(2):132-136.
10. Dubowitz V, Sewry CA. *Muscle Biopsy: A Practical Approach.* 3rd ed. Philadelphia, PA: WB Saunders Co; 2007.
11. Godfrey C, Escolar D, Brockington M, et al. Fukutin gene mutations in steroid-responsive limb girdle muscular dystrophy. *Ann Neurol.* 2006;60(5):603-610.
12. Cooper ST, Lo HP, North KN. Single section Western blot: improving the molecular diagnosis of the muscular dystrophies. *Neurology.* 2003;61(1):93-97.
13. Longman C, Brockington M, Torelli S, et al. Mutations in the human LARGE gene cause MDC1D, a novel form of congenital muscular dystrophy with severe mental retardation and abnormal glycosylation of alpha-dystroglycan. *Hum Mol Genet.* 2003;12(21):2853-2861.
14. Zhang W, Betel D, Schachter H. Cloning and expression of a novel UDP-GlcNAc: alpha-D-mannoside beta1,2-*N*-acetylglucosaminyltransferase homologous to UDP-GlcNAc:alpha-3-D-mannoside beta1,2-*N*-acetylglucosaminyltransferase I. *Biochem J.* 2002;361(pt 1):153-162.
15. Palcic MM, Heerze LD, Pierce M, Hindsgaul O. The use of hydrophobic synthetic glycosides as acceptors in glycosyltransferase assays. *Glycoconj J.* 1988;5(1):49-63. doi:10.1007/BF01048331.
16. Sarkar M. Expression of recombinant rabbit UDP-GlcNAc: alpha 3-D-mannoside beta-1,2-*N*-acetylglucosaminyltransferase I catalytic domain in Sf9 insect cells. *Glycoconj J.* 1994;11(3):204-209.
17. Brockington M, Sewry CA, Herrmann R, et al. Assignment of a form of congenital muscular dystrophy with secondary merosin deficiency to chromosome 1q42. *Am J Hum Genet.* 2000;66(2):428-435.
18. Brockington M, Yuva Y, Prandini P, et al. Mutations in the fukutin-related protein gene (FKRP) identify limb girdle muscular dystrophy 2I as a milder allelic variant of congenital muscular dystrophy MDC1C. *Hum Mol Genet.* 2001;10(25):2851-2859.
19. Silan F, Yoshioka M, Kobayashi K, et al. A new mutation of the fukutin gene in a non-Japanese patient. *Ann Neurol.* 2003;53(3):392-396.
20. Brown SC, Torelli S, Brockington M, et al. Abnormalities in alpha-dystroglycan expression in MDC1C and LGMD2I muscular dystrophies. *Am J Pathol.* 2004;164(2):727-737.

Brain Involvement in Muscular Dystrophies with Defective Dystroglycan Glycosylation

Emma Clement, MBChB,[1,2] Eugenio Mercuri, MD,[1,3] Caroline Godfrey, BSc,[1] Janine Smith, MBChB,[4] Stephanie Robb, MD,[1] Maria Kinali, MRCPCH, MD,[1,2] Volker Straub, MD,[5] Kate Bushby, MD,[5] Adnan Manzur, FRCPCH,[1] Beril Talim, MD,[6] Frances Cowan, MD, PhD,[2,7] Ros Quinlivan, FRCPCH,[8] Andrea Klein, MD,[9] Cheryl Longman, MD,[10] Robert McWilliam, FRCPCH,[11] Haluk Topaloglu, MD,[6] Rachael Mein, BSc,[12] Stephen Abbs, PhD,[12] Kathryn North, MD,[4] A. James Barkovich, MD,[13] Mary Rutherford, MD, PhD,[14] and Francesco Muntoni, MD[1,2]

Objective: To assess the range and severity of brain involvement, as assessed by magnetic resonance imaging, in 27 patients with mutations in *POMT1* (4), *POMT2* (9), *POMGnT1* (7), *Fukutin* (4), or *LARGE* (3), responsible for muscular dystrophies with abnormal glycosylation of dystroglycan (dystroglycanopathies).

Methods: Blinded review of magnetic resonance imaging brain scans from 27 patients with mutations in 1 of these 5 genes.

Results: Brain magnetic resonance images were normal in 3 of 27 patients; in another 5, only nonspecific abnormalities (ventricular dilatation, periventricular white matter abnormalities, or both) were seen. The remaining 19 patients had a spectrum of structural defects, ranging from complete lissencephaly in patients with Walker–Warburg syndrome to isolated cerebellar involvement. Cerebellar cysts and/or dysplasia and hypoplasia were the predominant features in four patients. Polymicrogyria (11/27) was more severe in the frontoparietal regions in 6, and had an occipitofrontal gradient in 2. Pontine clefts, with an unusual appearance to the corticospinal tracts, were seen in five patients with a muscle-eye-brain–like phenotype, three patients with POMGnT1, one with LARGE, and one with POMT2 mutations. Prominent cerebellar cysts were always seen with *POMGnT1* mutations, but rarely seen in *POMT1* and *POMT2.* Brainstem and pontine abnormalities were common in patients with *POMT2, POMGnT1,* and *LARGE* mutations.

Interpretation: Our results expand the spectrum of brain involvement associated with mutations in *LARGE, POMGnT1, POMT1,* and *POMT2.* Pontine clefts were visible in some dystroglycanopathy patients. Infratentorial structures were often affected in isolation, highlighting their susceptibility to involvement in these conditions.

Ann Neurol 2008;64:573–582

The "dystroglycanopathies" are a group of muscular dystrophies resulting from mutations in genes encoding known or putative glycosyltransferase enzymes.[1,2] A reduction in glycosylated α-dystroglycan (ADG) expression in muscle is the hallmark of these conditions. They include congenital muscular dystrophy (CMD) variants with structural changes affecting the brain and eyes (Fukuyama CMD [FCMD], muscle-eye-brain disease [MEB], Walker–Warburg syndrome [WWS]), as well as more recently described milder forms, characterized by subtle or absent brain involvement and ranging in severity from CMD (MDC1C, MDC1D) to milder limb girdle muscular dystrophy (LGMD) forms (LGMD2I, LGMD2K, LGMD2L, LGMD2M).[2–5] So

From the [1]Dubowitz Neuromuscular Unit, Institute of Child Health and Great Ormond Street Hospital; [2]Department of Paediatrics, Hammersmith Hospital, Imperial College London, London, United Kingdom; [3]Department of Pediatric Neurology, Catholic University, Rome, Italy; [4]Institute for Neuromuscular Research, Children's Hospital at Westmead, Faculty of Medicine, University of Sydney, Sydney, Australia; [5]Institute of Human Genetics, University of Newcastle upon Tyne, International Centre for Life, Newcastle upon Tyne, United Kingdom; [6]Hacettepe Children's Hospital, Ankara, Turkey; [7]Department of Imaging Sciences, Imperial College, Hammersmith Hospital, London; [8]Centre for Inherited Neuromuscular Disorders, Robert Jones and Agnes Hunt Orthopaedic Hospital, Oswestry, United Kingdom; [9]Department of Neurology, University Children's Hospital Zurich, Zurich, Switzerland; [10]Ferguson Smith Centre for Clinical Genetics and [11]Fraser of Allander Neurosciences Unit, Royal Hospital for Sick Children,Yorkhill Hospitals, Glasgow; [12]DNA Laboratory, Genetics Centre, Guy's and St Thomas' National Health Service Foundation Trust, London, United Kingdom; [13]Department of Radiology, University of California at San Francisco, San Francisco, CA; and [14]Robert Steiner Magnetic Resonance Unit, Clinical Sciences Centre, Hammersmith Hospital, Imperial College London, United Kingdom.

Received Feb 5, 2008, and in revised form Jun 17. Accepted for publication Jul 11, 2008.

Additional Supporting Information may be found in the online version of this article.

Published online in Wiley InterScience (www.interscience.wiley.com). DOI: 10.1002/ana.21482

E.C. and E.M. contributed equally to this work.

Potential conflict of interest: Nothing to report.

Address correspondence to Prof. Muntoni, Professor of Paediatric Neurology, Dubowitz Neuromuscular Centre, Institute of Child Health and Great Ormond Street Hospital for Children, 30 Guilford Street, London WC1N 1EH, United Kingdom.
E-mail: f.muntoni@ich.ucl.ac.uk

Published by Wiley-Liss, Inc., through Wiley Subscription Services

far mutations in six different genes (Protein-O-mannosyl transferase 1 [*POMT1;* OMIM 607423], Protein-O-mannosyl transferase 2 [*POMT2;* OMIM 607439], Protein-O-mannose 1,2-*N*-acetylglucosaminyltransferase 1 [*POMGnT1;* OMIM 606822], *Fukutin* [OMIM 607440], *Fukutin*-related protein [*FKRP;* OMIM 606596] and *LARGE* [OMIM 603590])[6–11] have been identified in patients with a dystroglycanopathy. Although the genotype-phenotype correlations initially suggested a tight association with specific phenotypes for each individual gene mutation, it has subsequently become clear that the severity of the skeletal muscle involvement associated with mutations in each gene is variable.[12]

Brain involvement is a frequent but not constant feature in patients with dystroglycanopathies. We have previously reported that the spectrum of brain involvement in patients with mutations in *FKRP,* the gene most commonly mutated in patients with a dystroglycanopathy in the white population, is wide[13]; this ranges from normal cognitive development and normal brain magnetic resonance imaging (MRI), as seen in the patients described when the first *FKRP* mutations were identified,[10,14] to severe structural brain abnormality in patients with associated learning difficulties. These include a hierarchical pattern of changes from isolated cerebellar cysts[15,16] to more severe structural involvement affecting the brainstem and pons, and also polymicrogyria and cobblestone lissencephalic changes indistinguishable from those found in MEB and WWS, affecting frontoparietal regions more than the occipital and temporal regions.[13,17] Ventricular dilatation and white matter abnormalities were also variably present in these patients.[13,16,18]

More recently, it has become obvious that mutations in the other genes encoding known or putative glycosyltransferases can also be associated with variable brain involvement. Mutations in *POMT1* and *POMT2,* originally associated with WWS phenotype,[6,7] were recently associated with milder brain involvement such as in patients with cerebellar hypoplasia[19–22] or even associated with normal brain MRI in patients with microcephaly and mild mental retardation.[23] Similarly, mutations in *Fukutin,* originally identified in Japanese patients with FCMD, typically associated with severe structural brain changes including polymicrogyria-pachygyria, occasional hemispheric fusion, cerebellar cystic lesions, and transient dysmyelination,[24] have been reported in a few patients with clinical and brain imaging features almost identical to those previously identified in WWS.[25,26] More recently, we and others described several families with milder allelic mutations in *Fukutin* associated with normal intelligence and brain MRI.[12,27]

In contrast, mutations in *POMGnT1,* originally identified in Finnish and Turkish patients with MEB,[8] have so far been described in patients with clinical and imaging features evocative of a MEB phenotype.[28,29] Mutations in *LARGE* were initially reported in a patient with frontoparietal pachygyria and brainstem hypoplasia,[11] and have more recently been associated with WWS-like features.[12,30]

The aim of this study is to report brain MRI findings in 27 patients with muscular dystrophy and mutations in *POMT1, POMT2 , POMGnT1, Fukutin,* and *LARGE* to establish the spectrum of brain involvement associated with each individual gene, as well as any genotype-phenotype correlations.

Patients and Methods

Twenty-seven patients with mutations in *POMT1, POMT2, POMGnT1, Fukutin,* or *LARGE* were selected because they had MRI brain scans available for review. Godfrey and colleagues[12] reported on all but six of these patients, and as such they were recruited by hypoglycosylation of ADG on muscle biopsy or clinical features highly evocative of α-dystroglycanopathy. Four (Patients 13, 14, 23, and 26) of these six patients have reduction of ADG evident on skeletal muscle biopsy, and the remaining two (Patients 18 and 20) have a phenotype suggestive of a dystroglycanopathy (see supplementary information). Details of genetic and pathological methods are as Godfrey and colleagues[12] described. Patients with *FKRP* mutations were excluded from this study because we have previously reported their spectrum of brain involvement; however, their findings are summarized for completion in Table 2.[13]

Brain Magnetic Resonance Imaging

All patients had undergone a brain MRI scan by the time the mutations were detected. Imaging studies were reviewed by at least two investigators who were blinded to clinical information and results of molecular genetic testing. The scans were reviewed using a proforma in which the following abnormalities were recorded: infratentorial—cerebellar abnormalities (vermian and/or hemispheric involvement, including presence of cerebellar cysts or other signs of cerebellar dysplasia), shape and size of the brainstem and pons; and supratentorial—cortical malformation (severity and location), white matter changes, and ventriculomegaly. Any additional abnormalities were also recorded. Regarding the nomenclature used when interpreting the dysplastic changes, this is qualified at the beginning of the discussion section.

Results

Twenty-seven patients fulfilled the inclusion criteria; all but one had two allelic mutations in one of the genes studied. One patient had a single pathogenic *LARGE* mutation: He had a typical WWS phenotype and died in the first few months of life (Patient 27).[12] Four patients had *Fukutin* mutations, four patients had *POMT1* mutations, nine patients had *POMT2* mutations, seven patients had *POMGnT1* mutations, and three patients had *LARGE* mutations. All patients had CMD with the exception of five with LGMD. The age

at brain MRI scan ranged from 3 weeks to 16 years (mean age, 4.04 years; 11 scans were obtained before 2 years of age). Only four patients were reported to have normal cognitive development, but this was not always formally tested. Phenotypic details can be found in the supplementary information.

MRI findings are shown in Table 1. In summary, eight patients had normal brain scans (Patients 1–3) or minimal changes (Patients 4–8) such as periventricular white matter changes, mild ventricular dilatation, or both. Two patients (Patients 9 and 10) had evidence of cerebellar hypoplasia with no cortical abnormality. Two other patients (Patients 11 and 12) had cerebellar cysts or hypoplasia and pontine abnormalities but no obvious cortical changes. Two patients (Patients 13 and 14) had frontoparietotemporal polymicrogyria but no involvement of the cerebellum or brainstem (Fig 1). Three patients (Patients 15–17) had cortical abnormalities with cerebellar dysplasia and posterior concavity abnormality of the brainstem (two of three) but a normal appearance to the pons. Eight patients (Patients 18–25) showed changes consistent with MEB (Figs 2 and 3A). The remaining two patients (Patients 26 and 27) had features consistent with a WWS phenotype.

Brainstem abnormalities were seen in a total of 14 patients. A thin brainstem with flattening of the pons was common, occurring in 13 of 27 scans, including those without cortical involvement. In the more abnormal scans, the brainstem had an unusual concavity to the posterior aspect best seen when viewed in sagittal sections (see Fig 2). In five patients, there was an abnormally thin brainstem with ventral and dorsal clefts of the pons (see Figs 2 and 3B). This was associated with an abnormal appearance to the corticospinal tracts with excessive areas of rounded short T1 and short T2 (see Fig 3B). Three of these patients had *POMGnT1* mutations (Patients 20, 21, and 25), one patient had a *POMT2* mutation (Patient 19), and one patient had a *LARGE* mutation (Patient 18).

Correlation between Brain Magnetic Resonance Imaging Findings and Gene Mutations

The four patients with *Fukutin* mutations all had a normal MRI or minimal ventricular dilatation. Six of seven patients with *POMGnT1* mutations had changes consistent with MEB, and the remaining patient had cerebellar cysts and a flat pons but no obvious signs of cortical dysplasia on a scan performed at 9 months.

Three of the four patients with *POMT1* mutations had minimal periventricular white matter changes, and one had cerebellar cysts and cortical changes but a normal pons.

The nine patients with *POMT2* mutations had abnormalities that ranged from mild ventricular dilatation to isolated cerebellar hypoplasia to generalized cobblestone lissencephaly, resembling WWS.

The three patients with *LARGE* mutations had both diffuse cortical and white matter changes; one had cerebellar cysts and features entirely consistent with a MEB-like disorder; and in one, the severity of the lissencephaly was consistent with a WWS diagnosis. These results are summarized in Table 2.

Discussion

The findings reported in this study expand the spectrum of structural brain involvement associated with mutations in several of the genes involved in dystroglycanopathies and show that the range of central nervous system involvement caused by individual gene defects is much wider than originally described.

The cortical abnormalities of patients with dystroglycanopathies has been described in multiple pathology reports and chapters. Three types of gross pathology have been described in the cerebral cortex of affected brains[31–33]: (1) verrucose dysplasia in which nodules of cellular cortical tissue protrude through the pial basement membrane superficial to normally laminated cortex (chiefly in temporal lobes); (2) unlayered polymicrogyria with haphazardly oriented cortical neurons forming irregular clusters, separated by gliovascular strands extending from the pia (chiefly in frontal and parietal lobes); and (3) agyric regions with four distinctive layers (superficial layer containing myelinated fibers obscuring the molecular layer, thick cellular layer with disorganized and occasionally aggregated neurons, cell-sparse layer of white matter, and heterotopic nodules of neurons). The agyric regions are located chiefly in the occipital lobes. Takada and colleagues[33] note that small, superficial nodules are seen on the surface in all regions and suggested that the appearance seen on the surface of what are now called *dystroglycanopathies* is best called *cobblestone cortex*. It should be noted that both polymicrogyria and agyria are heterogeneous disorders. Forman and coworkers[34] have described at least four different histological types of agyria.[35] Of note, these authors do not consider the agyric regions of dystroglycanopathies in their classification, instead classifying them separately as "cobblestone lissencephaly." In this article, we have followed their nomenclature. Regarding polymicrogyria, although it is possible that many different histological subtypes of polymicrogyria can be identified, and some of these subtypes may also be separable by their imaging characteristics, such separation was not attempted in this study. We separated the cortical abnormalities identified in our patients into two broad categories, based on the MRI appearance: polymicrogyria and cobblestone lissencephaly (verrucose dysplasia cannot be detected by MRI). Polymicrogyria was diagnosed when either multiple microgyri were identified in the cerebral cortex on individual images or a slightly thickened (4–7mm) cortex was seen, with irregularity of the cortical-white

Table 1. **Brain Magnetic Resonance Imaging Findings**

Patient No.	Age at scan	Gene	Ventricular Dilatation	White Matter Changes	Cerebellar Cysts	Other Cerebellar Abnormality	Brainstem Abnormality	Pontine Abnormality	Cortical Abnormality
1	5 yr	fukutin	−	−	−	−	−	−	−
2	10 yr	fukutin	−	−	−	−	−	−	−
3	3 yr	fukutin	−	−	−	−	−	−	−
4	8 yr	fukutin	+	−	−	−	−	−	−
5	6 yr	POMT2	±	−	−	−	−	−	−
6	3 yr	POMT1	−	PV	−	−	−	−	−
7	2 yr	POMT1	−	PV	−	−	−	−	−
8	7 yr	POMT1	+	PV	−	−	−	−	−
9	3 yr	POMT2	−	PV	−	Hypoplastic	−	−	−
10	3 yr	POMT2	+	PV	+	Hypoplastic	−	Hypoplasia	−
11	16 yr	POMGnT1	+	Diffuse abnormality	+	−	−	Hypoplasia	−
12	9 mo	POMT2	−	PV and FP	−	Hypoplastic vermis	Posterior concavity	−	−
13	3 mo	POMT2	−	−	−	−	−	−	FPT polymicrogyria
14	14 yr	LARGE	−	PV, T	−	−	Posterior concavity	Hypoplasia	FP pachygyria
15	3 wk	POMT1	++	TO>FP	+	Dysplastic vermis	Posterior concavity	−	TO polymicrogyria
16	1 yr	POMT2	+	FP reduced WM	+	Dysplastic vermis	Posterior concavity	−	Focal polymicrogyria (A>P)
17	13 yr	POMT2	−	PV	+	Dysplastic vermis	−	−	Posterior polymicrogyria
18	1 yr	LARGE	+	Abnormal	+	Dysplastic vermis	Posterior concavity	Hypoplasia and cleft	FP polymicrogyria
19	3 yr	POMT2	++	Diffuse abnormality	+	Cerebellar cleft	Posterior concavity	Hypoplasia, cleft + abnormal corticospinal tract	FP polymicrogyria
20	5 mo	POMGnT1	++	Abnormal	++	Dysplastic vermis	Posterior concavity	Hypoplasia, cleft + abnormal corticospinal tract	Diffuse polymicrogyria, slight FP gradient
21	3 yr	POMGnT1	++	Abnormal foci	+	Dysplastic	Posterior concavity	Hypoplasia, cleft + abnormal corticospinal tract	FP pachygyria. polymicrogyria T lobes, cobblestone cortex
22	5 mo	POMGnT1	++	Reduced WM	+	Hypoplastic vermis	Posterior concavity	Hypoplasia	Frontal pachygyria; cyst in T pole
23	8 mo	POMGnT1	++	Diffuse abnormality	++	Dysplastic, hypoplastic	Posterior concavity	Hypoplasia	FPT polymicrogyria
24	N/A	POMGnT1	++	Diffuse abnormality	+	Dysplastic	Hypoplasia	Hypoplasia	Polymicrogyria (A>P) and pachygyria
25	18 mo	POMGnT1	+++	Diffuse abnormality	+	Dysplastic, hypoplastic	Anterior concavity	Hypoplasia, cleft + abnormal corticospinal tract	Diffuse polymicrogyria
26	5 wk	POMT2	+++			Hypoplastic	Hypoplasia	Hypoplasia	Thin lissencephalic cortical mantle
27	4 wk	LARGE	+++	Diffuse abnormality		Dysplastic, hypoplastic	Posterior concavity	Hypoplasia	Posterior lissencephaly, cobblestone variant

+ = presence, − = absence of abnormality; PV = periventricular; FP = frontoparietal; FPT = frontoparietotemporal; T = temporal; TO>FP = temporooccipital > frontoparietal; TO = temporooccipital; F = frontal; WM = white matter; A>P = anterior > posterior.

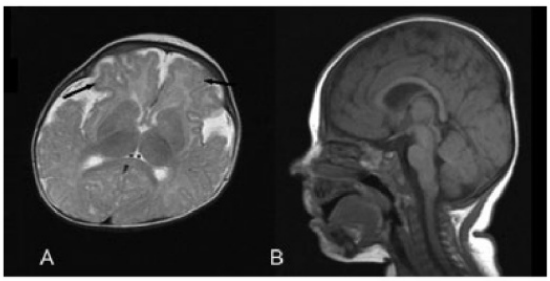

Fig 1. (A) T2-weighted image in the transverse plane of a 3-month-old infant with POMT2 mutations (Patient 13). Note the predominant frontal cortical polymicrogyria (arrows) *and (B) T1-weighted image showing the normal appearance of pons, brainstem, and cerebellar vermis in the sagittal plane.*

matter junction.[36] Polymicrogyria has different appearances on MRI depending on the state of myelination at the time of the scan.[37] The individual microgyri are easily seen in the unmyelinated brain, but as myelination ensues, the cortex begins to appear thick and can superficially resemble pachygyria. The two entities can be differentiated, however, by the lesser thickness (4–7mm) and irregularity of the junction between the cortex and white matter in polymicrogyria (the junction is smooth in pachygyria). Cobblestone lissencephaly was diagnosed when the cortex was thick (>7mm), the outer surface of the cortex was smooth, the inner surface of the cortex was irregular, and a layer of irregularly shaped nodules of gray matter formed a layer approximately 2mm deep to the cortex; in many cases, these nodules appeared to be radially oriented immediately below a bundle of radially oriented, spindle-shaped gray matter in the cortex.

Three of the 27 patients studied had normal scans, and another 5 had only mild changes such as minimal ventricular dilatation with periventricular white matter changes of long T2. These changes are nonspecific and can be observed in low-risk full-term infants with a normal outcome.[38] The remaining 18 patients all had structural brain changes that almost invariably affected infratentorial structures, with the exception of one patient in whom only the frontoparietotemporal regions were polymicrogyric. In 4 of these 18 patients, the infratentorial involvement was found in isolation, whereas in the remaining 14 patients, it was associated with supratentorial cortical and white matter involvement. In this latter group of patients, the supratentorial involvement ranged from diffuse periventricular white matter changes with focal areas of polymicrogyria to diffuse cortical structural abnormalities including cobblestone lissencephaly and an almost absent cortical mantle. In two patients, severe supratentorial findings were combined with abnormalities of the posterior fossa, consistent with the diagnosis of WWS.[39] Infratentorial involvement included hypoplastic or dysplastic vermis, cerebellar cysts, a concavity in the brainstem at the floor of the fourth ventricle, and pontine hypoplasia.

We correlated the results of the scans with the genotype of the patients and compared them with the previously documented changes in *FKRP*-related dystrophies.[13,15,17] Although some of the lesion patterns were more frequently associated with individual gene mutations, there was no unique defect that allowed unequivocal prediction of the primary gene defect. Florid cerebellar cysts were seen in all patients with *POMGnT1* mutations but were also found in 3 of 9 patients with *POMT2* mutations, in 1 of 4 patients with *POMT1* mutations, and in 1 of 3 with LARGE mutations. To the best of our knowledge, cerebellar cysts have not been previously associated with any of these genotypes. Interestingly, cerebellar cysts in patients with *POMGnT1* mutations were also found in the absence of supratentorial white matter or cortical involvement, as we have previously reported for patients with *FKRP* mutations,[13] suggesting that the cerebellum is particularly vulnerable to the underlying disease process in patients with mutations in these two genes. Targeted screening of *POMGnT1* and *FKRP* should, therefore, be considered where cerebellar cysts are the predominant abnormality. In contrast, none of our patients with *Fukutin* mutations had cerebellar cysts. All our patients with *Fukutin* mutations were cognitively normal, in contrast with reports of individuals with FCMD where cerebellar polymicrogyria with or without cysts was found in 90% of patients.[40] Increasingly, it is possible to recognize a subgroup of *Fukutin*-associated phenotypes that are distinct from the classic FCMD reported in Japan where learning difficulties and structural brain involvement are invariable. This is not surprising considering that virtually all Japanese patients carry the same founder mutation,[9] a relatively severe mutation that has not been reported in non-Japanese patients. In patients with *Fukutin* mutations, the spectrum of brain MRI findings, ranging from normal MRI[27] to the previously reported WWS-like changes,[25,26] resemble the spectrum we previously documented in patients with *FKRP* mutations.[13]

Mutations in *POMT1, POMT2, POMGnT1,* and *LARGE* were not associated with the same range of brain MRI findings reported for *FKRP* and *Fukutin.* Indeed, with the partial exception of *POMT2,* the other genes showed a relatively narrow range of findings; it is, however, of note that the patterns of lesions observed for an individual gene defect in this study are often different from those previously reported for the same gene. This was particularly evident for patients with *POMT2* mutations, originally associated with either a WWS or a cerebellar hypoplasia phenotype[7,21]; only two of the nine cases we studied had these previ-

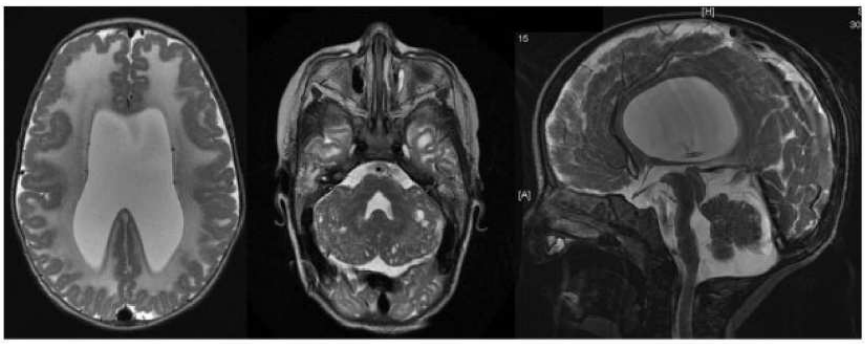

Fig 2. T2-weighted images in transverse, coronal, and sagittal planes of a 5-month-old (Patient 19) with POMGnT1 mutations. There is widespread polymicrogyria in frontal and parietal lobes, and abnormal high signal intensity throughout the white matter. There are multiple cysts in the hypoplastic cerebellar hemispheres in the transverse view. There are clefts in the dorsal and ventral pons. In the sagittal plane, the pons is thinned with a concave posterior border, and the midbrain tectum is abnormally large.

ously reported changes. In the other seven cases, the brain changes ranged from isolated mild ventricular dilatation or cerebellar dysplasia to various degree of cortical involvement, including isolated frontoparietotemporal polymicrogyria, which has not been reported previously. We also identified some patients with *POMGnT1* and *POMT1* mutations with previously unreported findings such as isolated cerebellar cysts in *POMGnT1* and relatively mild cortical involvement without pons and brainstem abnormalities in *POMT1*. We also identified a patient with novel mutations in the *LARGE* gene, leading to a MEB-like picture with

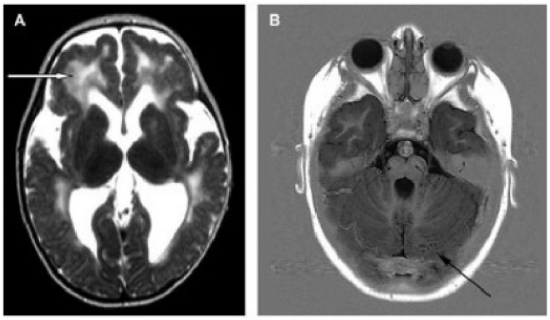

Fig 3. (A) T2-weighted image in the transverse plane of an 8-month-old (Patient 22) with heterozygous POMGnT1 mutations. There is widespread bilateral polymicrogyria affecting predominantly the frontal and parietal lobes. The white matter is reduced in volume with abnormally high signal intensity. Areas of lower signal intensity, mainly within the anterior white matter (arrow), *may represent heterotopic cells or variations in myelination. (B) T1-weighted image in the transverse plane of a 3-year-old (Patient 20) with heterozygous POMGnT1 mutations. There is a small ventral cleft in the pons. There is an exaggerated rounded appearance to the high signal myelinated corticospinal tracts* (thin black arrows). *There are several* (thick black arrow) *cerebellar cysts.*

associated cerebellar cysts. It may well be that as further work and patients with mutations in these genes are identified, the spectrum of changes found in these three genes also widens. Notably, we have previously reported a case of *POMGnT1* mutation with normal intelligence[41]; unfortunately, this patient had never had a brain MRI scan.

Other findings of this study were also of interest. In two patients, the cortical changes affected predominantly the temporal and occipital regions. In one, the posterior cortical changes were associated with normal appearances to the pons and brainstem, whereas in the other, the scan was performed at 3 weeks at an age when the extent and severity of cortical involvement cannot always be fully appreciated. The predominant posterior cortical involvement is at variance with the anteroposterior gradient described in *FKRP* mutations[13] and *POMGnT1*.[28,42] Predominantly posterior cortical malformation is a feature of merosin-negative CMD,[43] whereas the coexistence of frontoparietal polymicrogyria and occipital agyria has been reported in FCMD patients.[40]

We documented a ventral pontine cleft in five cases: four with a MEB-like condition (secondary to *POMGnT1* mutations in three and *LARGE* in another) and one with a more severe phenotype falling between the disease spectrum of MEB and WWS, carrying *POMT2* mutations. Such an abnormal appearance of the pons has not been reported in patients with a dystroglycanopathy before and is most likely caused by the absence of the ventral transverse pontine fibers, at the decussation of the middle cerebellar peduncles.[44] Indeed, these fibers migrate tangentially, and their migration is impaired in the Large^{myd} mouse.[45] Magnetic resonance diffusion tensor imaging studies may elucidate the exact position of pontine tracts and the structural basis for these abnormal imaging appearances.[44]

Table 2. **Distribution of Magnetic Resonance Imaging Brain Changes according to Gene Mutation**

Gene	Normal MRI (n = 3)		Normal Cortex and Cerebellum, Minimal vd+/− pv Changes (n = 5)		Cerebellar Hypoplasia, No Cortical Abnormalities (n = 2)		Cerebellar Cysts or Hypoplasia, No Cortical Changes (n = 2)		White Matter Cortical Changes, Cerebellum Normal (n = 2)		Cortex and Cerebellar Abnormality, Normal Pons (n = 3)		MEB-like Changes (n = 8)		WWS-like Changes (n = 2)	
	Our Cohort	Other Studies[a]	Our Cohort	Other Studies[a]	Our Cohort	Other Studies[a]	Our Cohort	Other Studies[a]	Our Cohort	Other Studies[a]	Our Cohort	Other Studies[a]	Our Cohort	Other Studies[a]	Our Cohort	Other Studies[a]
FUKUTIN (n = 4)	•	5	•	5										33		25
POMT1 (n = 4)		4, 19, 20, 57	•			20, 57					•			20		6, 20
POMT2 (n = 9)			•		•	21, 22	•		•		•		•		•	7
POMGnT1 (n = 7)							•						•	8, 28, 29		
LARGE (n = 3)									•	11			•		•	30
FKRP[b]		13		13				13		13				13		

Phenotypes described in this study are indicated with bullets. [a]Previously reported phenotypes, with the main references listed. [b]FKRP is not part of this study, results published previously. MRI = magnetic resonance imaging; MEB = muscle-eye-brain disease; WWS = Walker–Warburg syndrome; VD = ventricular dilatation; PV = periventricular.

The MRI changes reported here are highly evocative of a "dystroglycanopathy." There is, however, an overlap with other conditions. Patients with *GPR56* mutations have bilateral frontoparietal polymicrogyria seen in an anteroposterior distribution, bilateral patchy white matter changes, and brainstem and cerebellar hypoplasia.[46] Although the MRI findings are clearly similar to those seen in the midgroup of patients reported here (Patients 12–23), the polymicrogyria seen in patients with GPR56 mutations affects predominantly the frontoparietal regions and not the temporal and occipital areas also seen in patients with a dystroglycanopathy.[47] In addition, cerebellar cysts or scalloped appearance to the back of the brainstem has not been reported in patients with GPR56 mutations.

A question that remains to be answered relates to whether patients exist with brain changes within the spectrum described with mutations in one of the dystroglycanopathy genes but with minimal/absent muscle involvement. We are aware of one patient with *POMGnT1* mutations in whom serum creatine kinase concentrations were normal, but ADG expression was reduced on muscle biopsy (F. Muntoni, P. Guicheney, and T. Voit, presented at the 158th ENMC Workshop on Congenital Muscular Dystrophy), but there are no systematic studies where the analysis of the putative or demonstrated glycosyltransferases mutated in dystroglycanopathies has been performed in patients without skeletal muscle phenotype.

In addition to looking for a correlation between different genes and phenotypes, we also correlated the type of mutations with the brain MRI findings. Somewhat unsurprisingly, the three scans with the most abnormal appearance (Patients 25–27) resulted from nonsense mutations but in three different genes: *POMGnT1, POMT2,* and *LARGE.* Interestingly however, two patients with apparently severe mutations had less brain involvement than Patients 25 to 27. Patient 15 has a homozygous truncating mutation in *POMT1,* whereas Patient 4, who had no structural brain lesions, was homozygous for two frameshifting mutations in *Fukutin.* These findings may be explained by the location of these mutations in the most 3′ exon, meaning that the mutant products may not be subject to nonsense-mediated RNA decay.[5]

A limitation of this study relates to the fact that the scans had been performed in various centers, at different ages of the patients, and not always optimized with thin (ie, 1.5mm) slices to detect subtle dysplastic changes, because most scans were 5mm in thickness. Nevertheless, these are the diagnostic scans routinely available in clinical settings; hence, our findings are of relevance for this group of patients.

The reason for the varied abnormalities of brain involvement seen in patients carrying mutations in these different genes is not fully understood. All these gene products have so far been involved only in the glycosylation of ADG, a key cellular receptor expressed in neurons and oligodendrocytes, important in development of the fetal brain. ADG is modified by the process of O-mannosylation and other rare O-glycosylations that account for its differing molecular weights in various tissues. The appropriate glycosylation of ADG plays a crucial role for its function as it regulates its binding to extracellular matrix proteins such as laminin, neurexin, perlecan, and agrin.[48] Al-

though the role of ADG in brain development is not fully understood, it has been shown to be important for normal basement membrane formation and neuronal migration. ADG null mice have discontinuous pial basement membranes surrounding the cerebral cortex and loss of interhemispheric fissures.[48] Such discontinuities are also seen around the pial basement membrane of the cerebellum. Similar fusion of the cerebral cortices may be observed in patients with WWS.[49]

Normal basement membrane formation is essential for neuronal migration. During CNS development, cells proliferate in the ventricular zone of the neuroepithelium and migrate via radial glia to the cortical plate. These radial glia cells have end feet attached to the pial basement membrane. Targeted inactivation or spontaneous mutations of genes involved in the formation of the pial-glial membranes results in cobblestone lissencephaly,[50–52] and pathological studies in patients affected by FCMD, MEB, and WWS have identified disordered cortical layering and clusters of neurons and glia beyond the pial basement membrane, suggesting the involvement of a similar phenomenon. Because ADG is highly expressed in the pial membranes, it is likely that its abnormal glycosylation results in reduced integrity and the resulting breaches observed in these CMD variants.[53] Recent pathological studies in *POMGnT1* knock-out mice have indeed identified pial basement membrane breaches during rapid cerebral cortical expansion at E13.5 with radial end feet growing out of the neural boundary.[54] These abnormalities resemble closely those found in *FKRP*-deficient mice (S.C. Brown and F. Muntoni, unpublished data). The subsequent disruption caused disappearance of the basement membrane and glia limitans, and formation of a superficial diffuse cell zone above the original boundary of the basement membrane. Basement membranes breaches are also found in chimeric mice of *Fukutin* knock-out mice[55] and in the LARGE^{myd} mouse.[48,54,56,57]

In addition to the role of ADG in basement membrane stability, recent studies also suggest that this molecule is involved in the process of migration of cerebellar neurons.[58]

The difference observed in the pattern of brain involvement in patients carrying different gene mutations may suggest that some of these demonstrated or putative glycosyltransferases have targets other than ADG in brain, although this has never been demonstrated; another possibility is that it may reflect differences in the pattern of expression of individual glycosyltransferases in different brain regions; less likely, it may reflect a mutation-specific effect on the ability of these glycosyltransferases to differentially bind with interacting proteins. Further work on the relevant animal models will help to clarify these issues.

This work was supported by the Muscular Dystrophy Campaign (ICH centre grant 2HTC, research fellowship (EC) PC0916, research studentship (CA) RA3/734) and Telethon (EM) GUP 060004. MR acknowledges the support of the Medical Research Council.

Acknowledgment

The support of the Department of Health (NCG) is also gratefully acknowledged (FM).

References

1. Toda T, Chiyonobu T, Xiong H, et al. Fukutin and alpha-dystroglycanopathies. Acta Myol 2005;24:60–63.
2. Muntoni F, Brockington M, Torelli S, Brown SC. Defective glycosylation in congenital muscular dystrophies. Curr Opin Neurol 2004;17:205–209.
3. Muntoni F, Voit T. The congenital muscular dystrophies in 2004: a century of exciting progress. Neuromuscul Disord 2004;14:635–649.
4. Balci B, Uyanik G, Dincer P, et al. An autosomal recessive limb girdle muscular dystrophy (LGMD2) with mild mental retardation is allelic to Walker-Warburg syndrome (WWS) caused by a mutation in the POMT1 gene. Neuromuscul Disord 2005;15:271–275.
5. Godfrey C, Escolar D, Brockington M, et al. Fukutin gene mutations in steroid-responsive limb girdle muscular dystrophy. Ann Neurol 2006;60:603–610.
6. Beltran-Valero de Bernabe D, Currier S, Steinbrecher A, et al. Mutations in the O-mannosyltransferase gene POMT1 give rise to the severe neuronal migration disorder Walker-Warburg syndrome. Am J Hum Genet 2002;71:1033–1043.
7. van Reeuwijk J, Janssen M, van den Elzen C, et al. POMT2 mutations cause alpha-dystroglycan hypoglycosylation and Walker-Warburg syndrome. J Med Genet 2005;42:907–912.
8. Yoshida A, Kobayashi K, Manya H, et al. Muscular dystrophy and neuronal migration disorder caused by mutations in a glycosyltransferase, POMGnT1. Dev Cell 2001;1:717–724.
9. Kobayashi K, Nakahori Y, Miyake M, et al. An ancient retrotransposal insertion causes Fukuyama-type congenital muscular dystrophy. Nature 1998;394:388–392.
10. Brockington M, Blake DJ, Prandini P, et al. Mutations in the fukutin-related protein gene (FKRP) cause a form of congenital muscular dystrophy with secondary laminin alpha2 deficiency and abnormal glycosylation of alpha-dystroglycan. Am J Hum Genet 2001;69:1198–1209.
11. Longman C, Brockington M, Torelli S, et al. Mutations in the human LARGE gene cause MDC1D, a novel form of congenital muscular dystrophy with severe mental retardation and abnormal glycosylation of alpha-dystroglycan. Hum Mol Genet 2003;12:2853–2861.
12. Godfrey C, Clement E, Mein R, et al. Refining genotype phenotype correlations in muscular dystrophies with defective glycosylation of dystroglycan. Brain 2007;130:2725–2735.
13. Mercuri E, Topaloglu H, Brockington M, et al. Spectrum of brain changes in patients with congenital muscular dystrophy and FKRP gene mutations. Arch Neurol 2006;63:251–257.
14. Mercuri E, Brockington M, Straub V, et al. Phenotypic spectrum associated with mutations in the fukutin-related protein gene. Ann Neurol 2003;53:537–542.

15. Topaloglu H, Brockington M, Yuva Y, et al. FKRP gene mutations cause congenital muscular dystrophy, mental retardation, and cerebellar cysts. Neurology 2003;60:988–992.
16. Louhichi N, Triki C, Quijano-Roy S, et al. New FKRP mutations causing congenital muscular dystrophy associated with mental retardation and central nervous system abnormalities. Identification of a founder mutation in Tunisian families. Neurogenetics 2004;5:27–34.
17. Beltran-Valero de Bernabe D, Voit T, Longman C, et al. Mutations in the FKRP gene can cause muscle-eye-brain disease and Walker-Warburg syndrome. J Med Genet 2004;41:e61.
18. Quijano-Roy S, Marti-Carrera I, Makri S, et al. Brain MRI abnormalities in muscular dystrophy due to FKRP mutations. Brain Dev 2006;28:232–242.
19. D'Amico A, Tessa A, Bruno C, et al. Expanding the clinical spectrum of POMT1 phenotype. Neurology 2006;66: 1564–1567; 1461.
20. van Reeuwijk J, Maugenre S, van den Elzen C, et al. The expanding phenotype of POMT1 mutations: from Walker-Warburg syndrome to congenital muscular dystrophy, microcephaly, and mental retardation. Hum Mutat 2006;27: 453–459.
21. Mercuri E, D'Amico A, Tessa A, et al. POMT2 mutation in a patient with 'MEB-like' phenotype. Neuromuscul Disord 2006; 16:446–448.
22. Yanagisawa A, Bouchet C, Van den Bergh PY, et al. New POMT2 mutations causing congenital muscular dystrophy. Neurology 2007;69:1254–1260.
23. Biancheri R, Bertini E, Falace A, et al. POMGnT1 mutations in congenital muscular dystrophy: genotype-phenotype correlation and expanded clinical spectrum. Arch Neurol 2006;63: 1491–1495.
24. Kondo-Iida E, Kobayashi K, Watanabe M, et al. Novel mutations and genotype-phenotype relationships in 107 families with Fukuyama-type congenital muscular dystrophy (FCMD). Hum Mol Genet 1999;8:2303–2309.
25. de Bernabe DB, van Bokhoven H, van Beusekom E, et al. A homozygous nonsense mutation in the fukutin gene causes a Walker-Warburg syndrome phenotype. J Med Genet 2003;40: 845–848.
26. Silan F, Yoshioka M, Kobayashi K, et al. A new mutation of the fukutin gene in a non-Japanese patient. Ann Neurol 2003; 53:392–396.
27. Murakami T, Hayashi YK, Noguchi S, et al. Fukutin gene mutations cause dilated cardiomyopathy with minimal muscle weakness. Ann Neurol 2006;60:597–602.
28. Diesen C, Saarinen A, Pihko H, et al. POMGnT1 mutation and phenotypic spectrum in muscle-eye-brain disease. J Med Genet 2004;41:e115.
29. Taniguchi K, Kobayashi K, Saito K, et al. Worldwide distribution and broader clinical spectrum of muscle-eye-brain disease. Hum Mol Genet 2003;12:527–534.
30. van Reeuwijk J, Grewal PK, Salih MA, et al. Intragenic deletion in the LARGE gene causes Walker-Warburg syndrome. Hum Genet 2007;121:685–690.
31. Friede R. Developmental neuropathology. Berlin: Springer-Verlag, 1989:339–340.
32. Haltia M, Leivo I, Somer H, et al. Muscle-eye-brain disease: a neuropathological study. Ann Neurol 1997;41:173–180.
33. Takada K, Nakamura H, Tanaka J. Cortical dysplasia in congenital muscular dystrophy with central nervous system involvement (Fukuyama type). J Neuropathol Exp Neurol 1984;43: 395–407.
34. Forman MS, Squier W, Dobyns WB, Golden JA. Genotypically defined lissencephalies show distinct pathologies. J Neuropathol Exp Neurol 2005;64:847–857.
35. Takada K, Nakamura H, Takashima S. Cortical dysplasia in Fukuyama congenital muscular dystrophy (FCMD): a Golgi and angioarchitectonic analysis. Acta Neuropathol 1988;76: 170–178.
36. Barkovich AJ, Koch TK, Carrol CL. The spectrum of lissencephaly: report of ten patients analyzed by magnetic resonance imaging. Ann Neurol 1991;30:139–146.
37. Takanashi J, Barkovich AJ. The changing MR imaging appearance of polymicrogyria: a consequence of myelination. AJNR Am J Neuroradiol 2003;24:788–793.
38. Mercuri E, Dubowitz L, Brown SP, Cowan F. Incidence of cranial ultrasound abnormalities in apparently well neonates on a postnatal ward: correlation with antenatal and perinatal factors and neurological status. Arch Dis Child Fetal Neonatal Ed 1998;79:F185–F189.
39. Dobyns WB, Pagon RA, Armstrong D, et al. Diagnostic criteria for Walker-Warburg syndrome. Am J Med Genet 1989;32: 195–210.
40. Aida N, Tamagawa K, Takada K, et al. Brain MR in Fukuyama congenital muscular dystrophy. AJNR Am J Neuroradiol 1996; 17:605–613.
41. Clement EM, Godfrey C; Tan J, et al. Mild POMGnT1 mutations underlie a novel limb girdle muscular dystrophy variant. Arch Neurol 2008;65:137–141.
42. Vervoort VS, Holden KR, Ukadike KC, et al. POMGnT1 gene alterations in a family with neurological abnormalities. Ann Neurol 2004;56:143–148.
43. Sunada Y, Edgar TS, Lotz BP, et al. Merosin-negative congenital muscular dystrophy associated with extensive brain abnormalities. Neurology 1995;45:2084–2089.
44. Barkovich AJ, Millen KJ, Dobyns WB. A developmental classification of malformations of the brainstem. Ann Neurol 2007; 62:625–639.
45. Qu Q, Crandall JE, Luo T, et al. Defects in tangential neuronal migration of pontine nuclei neurons in the Largemyd mouse are associated with stalled migration in the ventrolateral hindbrain. Eur J Neurosci 2006;23:2877–2886.
46. Piao X, Hill RS, Bodell A, et al. G protein-coupled receptor-dependent development of human frontal cortex. Science 2004; 303:2033–2036.
47. Piao X, Chang BS, Bodell A, et al. Genotype-phenotype analysis of human frontoparietal polymicrogyria syndromes. Ann Neurol 2005;58:680–687.
48. Moore SA, Saito F, Chen J, et al. Deletion of brain dystroglycan recapitulates aspects of congenital muscular dystrophy. Nature 2002;418:422–425.
49. Cormand B, Pihko H, Bayes M, et al. Clinical and genetic distinction between Walker-Warburg syndrome and muscle-eye-brain disease. Neurology 2001;56:1059–1069.
50. Zarbalis K, Siegenthaler JA, Choe Y, et al. Cortical dysplasia and skull defects in mice with a Foxc1 allele reveal the role of meningeal differentiation in regulating cortical development. Proc Natl Acad Sci U S A 2007;104:14002–14007.
51. Niewmierzycka A, Mills J, St-Arnaud R, et al. Integrin-linked kinase deletion from mouse cortex results in cortical lamination defects resembling cobblestone lissencephaly. J Neurosci 2005; 25:7022–7031.
52. Beggs HE, Schahin-Reed D, Zang K, et al. FAK deficiency in cells contributing to the basal lamina results in cortical abnormalities resembling congenital muscular dystrophies. Neuron 2003;40:501–514.

Acta Myologica • 2007; XXVI; p. XX-XX

ORIGINAL ARTICLES

Muscular dystrophies due to defective glycosylation of dystroglycan

F. Muntoni[1], M. Brockington[1], C. Godfrey[1], M. Ackroyd[1], S. Robb[1], A. Manzur[1], M. Kinali[1], E. Mercuri[1], M. Kaluarachchi[1], L. Feng[1], C. Jimenez-Mallebrera[1], E. Clement[1], S. Torelli[1], C.A. Sewry[1,2], S.C. Brown[1]

[1] Dubowitz Neuromuscular Centre, Department of Paediatrics, Imperial College London, Hammersmith Hospital, Du Cane Road, London, UK; [2] Wolfson Centre for Inherited Neuromuscular Diseases, Robert Jones & Agnes Hunt Orthopaedic Hospital, Oswestry, UK

Muscular dystrophies are a clinically and genetically heterogeneous group of disorders. Until recently most of the proteins associated with muscular dystrophies were believed to be proteins of the sarcolemma associated with reinforcing the plasma membrane or in facilitating its re-sealing following injury. In the last few years a novel and frequent pathogenic mechanism has been identified that involves the abnormal glycosylation of alpha-dystroglycan (ADG). This peripheral membrane protein undergoes complex and crucial glycosylation steps that enable it to interact with LG domain containing extracellular matrix proteins such as laminins, agrin and perlecan.

Mutations in six genes (*POMT1*, *POMT2*, *POMGnT1*, *fukutin*, *FKRP* and *LARGE*) have been identified in patients with reduced glycosylation of ADG. While initially a clear correlation between gene defect and phenotype was observed for each of these 6 genes (for example, Walker Warburg syndrome was associated with mutations in *POMT1* and *POMT2*, Fukuyama congenital muscular dystrophy associated with *fukutin* mutations, and Muscle Eye Brain disease associated with *POMGnT1* mutations), we have recently demonstrated that allelic mutations in each of these 6 genes can result in a much wider spectrum of clinical conditions. Thus, the crucial aspect in determining the phenotypic severity is not which gene is primarily mutated, but how severely the mutation affects the glycosylation of ADG.

Systematic mutation analysis of these 6 glycosyltransferases in patients with a dystroglycan glycosylation disorder identifies mutations in approximately 65% suggesting that more genes have yet to be identified.

Key words: Muscular dystrophy, glycoslyation, alpha dystroglycan, neuronal migration, glycosyltransferases

Introduction

A significant number of muscular dystrophies (MD) are secondary to mutations in proteins located in the extracellular matrix, sarcolemma or nuclear envelope. Most of these proteins play a major structural role in muscle fibres although some have also been implicated in signaling or in chromatin binding and organization. However, recently it has become evident that a number of forms of congenital muscular dystrophy (CMD) and several variants of limb girdle muscular dystrophy (LGMD) are associated with mutations in a number of genes encoding for proteins that are either putative or demonstrated glycosyltransferases (1-5). These include four severe forms of CMD that are associated with severe structural brain involvement and variable associated eye abnormalities: Walker-Warburg syndrome (WWS), Muscle-Eye-Brain disease (MEB), Fukuyama congenital muscular dystrophy (FCMD) and congenital muscular dystrophy type 1D (MDC1D). The CMD variant MDC1C and a relatively mild form of limb girdle muscular dystrophy (LGMD2I) are not typically associated with brain involvement. A characteristic and diagnostic feature of these MD variants is their association with abnormalities in the glycosylation of α-dystroglycan (ADG), and this has led to the suggestion of the name "dystroglycanopathy" to identify them (6-10). The abnormal glycosylation of ADG was only described in 2001 but is now a recognized common pathogenetic mechanism responsible for several forms of muscular dystrophy. Mutations in 6 genes have been identified in patients with dystroglycanopathies, initially each associated with a specific clinical entity. However it is now clear that allelic mutations in each of these 6 genes are responsible for an extremely wide spectrum of clinical conditions; in addition thorough genetic analysis of these 6 genes in patients with a dystroglycanopathy only identifies mutations in ~ 65% of cases suggesting that further genetic heterogeneity exists.

Address for correspondence: Francesco Muntoni, FRCPCH, FMedSci, Dubowitz Neuromuscular Centre, Institute of Child Health & Great Ormond Street Hospital, 30 Guilford Street, London WC1N 1EH, UK

Glycosylation defects and muscular dystrophies

There are two main forms of protein glycosylation: N-linked glycosylation in which the oligosaccharide is attached to the amide group of an asparagine residue and *O*-linked glycosylation where the oligosaccharide is attached to a hydroxyl group of a serine or threonine residue. *O*-mannosylation is a very rare form of glycosylation and in humans only ADG has so far been shown to contain these modified glycans (1, 11-16). ADG is a very heavily glycosylated glycoprotein: while its primary sequence predicts a molecular mass of 72 kDa, its molecular mass in mammalian skeletal and cardiac muscle is 156 kDa and 140 kDa respectively and in brain and peripheral nerve 120 kDa. Although *O*-mannosylation does not represent the only form of *O*-glycosylation on ADG, it is required for binding to a number of LG domain containing extracellular matrix proteins such as laminin, perlecan and agrin in muscle, and neurexin in the brain (17).

To date, mutations in 6 known or putative glycosyltranferase genes have been identified in dystroglycanopathies. *Protein-O-mannosyl transferase* 1 (*POMT1*; OMIM 607423), *Protein-O-mannosyl transferase 2* (*POMT2*; OMIM 607439), *Protein-O-mannose 1,2-N-acetylglucosaminyltransferase 1* (*POMGnT1*; OMIM 606822), *fukutin* (OMIM 607440), *Fukutin-related protein* (*FKRP*; OMIM 606596) and *LARGE* (OMIM 603590) (18-23). Three of these genes are clearly involved in the process of *O*-mannosylation (*POMT1, POMT2, POMGnT1*) (20, 24, 25), while the function of the remaining 3 genes, *fukutin, FKRP and LARGE* is still not clear (26-29). Of these 6 genes, the most frequently mutated in the Caucasian population is *FKRP*. While this was the first gene to be associated with an extremely wide range of clinical severity, more recent data suggests that this is also a common theme for mutations in other genes.

The *FKRP* gene

Our group originally described mutations in the fukutin-related protein gene (*FKRP*) in patients with a form of CMD (MDC1C) characterized by onset at birth or in the first few months of life with profound weakness, markedly elevated serum CK and inability to achieve independent ambulation or standing (22). Intelligence was preserved and brain imaging normal. These patients had a significant reduction of the glycosylation of ADG both on immunocytochemistry and Western blot analysis (22). Shortly after our group also identified involvement of the *FKRP* gene in a much milder variant of limb girdle muscular dystrophy, LGMD2I, which had already been mapped to chromosome 19q13 where the *FKRP* gene lies (30). In contrast with MDC1C, the onset of the condition in LGMD2I varied from childhood to late adult life; typical patients with LGMD2I have a hypertrophic phenotype and a proximal distribution of weakness, limited or no contractures, markedly elevated serum CK and frequent cardiac complications (30-32). Both intelligence and brain imaging are entirely normal.

Surprisingly, this form of LGMD was subsequently found to be the most common LGMD variant in the UK population, due to the high frequency of a C826A mutation, with an estimated heterozygote frequency of ~1:400 (32). This particular mutation was also found at high frequency in other Caucasian populations, such as in Germany (33) and Scandinavian countries (34), while it was less common in Italians, and even less common in LGMD patients from Brazil (27, 35) and Japan. The expression of glycosylated ADG was only moderately reduced in LGMD2I, in keeping with the less severe muscle involvement compared to children with MDC1C (28).

Subsequent studies clarified that the originally described MDC1C phenotype did not represent the most severe end of the clinical spectrum, as we then identified *FKRP* mutations in patients with a CMD variant resembling MDC1C but with additional features such as mental retardation and cerebellar dysplasia and cysts on brain MRI (36), followed by the identification of mutations in patients with severe supratentorial cortical dysplasia and structural eye involvement, mimicking classical Muscle-Eye Brain disease (MEB) and Walker Warburg syndrome (WWS) (37). The severity of loss of ADG glycosylation in these patients was more severe than previously found in MDC1C, in keeping with their more severe clinical phenotype. None of the FKRP patients described was ever found to be homozygous for nonsense mutations and this led to the speculation that the homozygosity for *FKRP* null alleles might be incompatible with life. Despite the frequency of the involvement of this gene and the observation that ADG hypoglycosylation is associated with these forms of muscular dystrophy, there is no clear idea of the precise role of FKRP. Several studies have localized recombinant FKRP proteins to the Golgi apparatus of cultured cells (38-40), and more recent studies have noted an association of FKRP with the dystroglycan complex in skeletal muscle (41). While some authors have described mislocalisation of mutant proteins in transfected cells (39, 42), we have not confirmed these findings in our experiments (38, 43), suggesting that the pathogenesis of this condition is due to impaired function rather than altered localisation within the cell. In order to further evaluate this aspect our group has recently generated an animal model with reduced FKRP expression that recapitulates the severe brain and eye involvements observed in patients with MEB. These mice also have a very marked reduction of glycosylated ADG in their skeletal muscle. The detailed characterization of the phenotype of this animal model is currently being undertaken.

The *POMT1* and *POMT2* genes

Mutations in the *O*-mannosyltransferase 1 (*POMT1*) were originally described in a proportion (20%) of patients affected by the severe condition Walker Warburg syndrome (20). POMT1 catalyses in combination with POMT2 the first step in *O*-mannosyl glycan synthesis (44); as ADG is so far the only protein in which this type of glycosylation has been demonstrated, the finding of its abnormal processing in patients with *POMT1* mutations is not a surprise. A few years after the identification of *POMT1* mutations in WWS, mutations in *POMT2* were also identified in a subgroup of patients with WWS (19). Both conditions are characterized by a very severe depletion of ADG recognized by an antibody which recognises a glycosylated epitope, but also a marked reduction of the epitope recognized by an antibody raised to the core ADG originally produced by Kroger (45), though not by an anti-core ADG antibody produced in the laboratory of Campbell (46). These observations indicate that ADG may not be completely absent but rather abnormally glycosylated thus exposing different epitopes. Markedly reduced expression of glycosylated ADG in peripheral nerve has also been documented in WWS patients with a *POMT1* mutation (47).

More recent studies have indicated a wider spectrum of clinical and pathological features for mutations in both *POMT1* and *POMT2* genes than originally reported (48, 49). Allelic mutations in the *POMT1* gene have been recently been described in ambulant patients with a phenotype resembling LGMD, but with associated microcephaly and mental retardation, despite apparently normal brain scan (LGMD2K) (50). Milder allelic *POMT2* mutations have also been recently reported in patients with milder features compared to WWS, ranging from MEB-like phenotypes to ambulant patients with microcephaly and mental retardation, with features indistinguishable from LGMD2K (51, 52).

POMT1/2 enzymatic activity can be measured in both fibroblasts and lymphocytes, and this has been exploited as a diagnostic test in patients with mutations in these 2 genes. It has also been proposed that the finding of reduced POMT enzymatic activity could be used as a more rapid form of patient screening (53).

Targeted inactivation of *Pomt1* has been achieved in mice but is embryonic lethal in the homozygous mice due to defects in the formation of Reichert's membrane, the first basement membrane to form in the embryo which requires normally glycosylated dystroglycan (54).

The *POMGnT1* gene

The *POMGnT1* gene encodes protein *O*-linked mannose ß1,2-*N*-acetylglucosaminyltransferase 1, an enzyme involved in the transfer of an *N*-acetylglucosamine residue to an *O*-linked mannose (25). Mutations in *POMGnT1* were originally identified in patients affected by typical MEB, a condition characterized by CMD together with cortical dysplasia and ocular involvement (20). Following the original demonstration of *POMGnT1* mutations in the Finnish and Turkish MEB patient population, collaborative papers highlighted the spectrum of phenotypes in a world wide study, which ranged from typical MEB to more severe patients with structural brain involvement overlapping WWS. Mutations located at the 5' end of the gene were on the whole associated with a more severe phenotype than those located at the 3' end of the gene (55). *POMGnT1* enzymatic activity can also be measured from frozen muscle, lymphocytes and fibroblasts (56).

Regarding the spectrum of clinical severity in patients with *POMGnT1* mutations, our group very recently identified a patient with a form of LGMD with onset in the second decade of life, with entirely normal intelligence, who followed a relatively rapid progression of muscle weakness, becoming wheelchair dependent aged 19 following a fracture. Enzymatic studies on the patient's fibroblasts showed an altered kinetic profile, however this was less marked than in patients with MEB, and in keeping with the patient's relatively mild phenotype. This patient therefore is the mildest patient with *POMGnT1* mutations reported so far and her phenotype is that of a LGMD with proximal muscle weakness and markedly elevated serum CK (Godfrey et al manuscript in press).

An animal model of MEB due to mutations in *POMGnT1* exists, following the introduction of null alleles in this gene. These mutant mice were viable with multiple developmental defects in muscle, eye, and brain, similar to the phenotypes observed in human MEB disease (57, 58).

The *Fukutin* gene

Fukuyama-type congenital muscular dystrophy (FCMD) is a condition confined to Japan. Similar to MEB and WWS, it is characterized by the combination of CMD and central nervous system involvement. On the whole the severity of brain involvement is milder than WWS and MEB, and the eyes are only occasionally severely affected. A high proportion (87%) of FCMD patients carry a retrotransposon insertion into the 3' untranslated region of the *fukutin* gene which leads to a reduction in *fukutin* mRNA levels (21). This ancestral mutation explains the high prevalence of the disease in Japan where it represents the second most common form of muscular dystrophy after Duchenne. Patients homozygous for this mutation are relatively mild compared to those with compound heterozygosity between the ancestral mutation and a more severe loss-of-function mutation.

Inactivation of the *fukutin* gene in mice leads to lethality at embryonic day 6.5-7.5 (59), hence mice chimeric for normal and fukutin deficient cells have been generated (60). Those with a high proportion of fukutin

deficient cells show a typical muscular dystrophy with reduced survival and a marked disorganisation of the laminar structures of both the cerebral and cerebellar cortices with pathological features of a cobblestone lissencephaly, and eye abnormalities.

Several recent reports have significantly increased the spectrum of conditions due to *fukutin* mutations, mostly due to patients outside Japan, without the retrotransposonal insertion in the fukutin gene (61). Initially patients resembling WWS with homozygous null alleles of the *fukutin* gene were identified. These patients had a more profound depletion of ADG immunolabelling compared to typical FCMD patients. More recently the spectrum has been expanded towards milder patients: we recently described three children with CMD and no structural brain involvement, and in addition three families with a LGMD-like condition, with onset in the first few years of life, without any evidence of central nervous system involvement (62). In two of these families with LGMD the affected children where initially considered to have an inflammatory myopathy, and were administered corticosteroids which resulted in a significant clinical improvement. Even milder patients have recently been described carrying intragenic fukutin mutations: six patients were identified with dilated cardiomyopathy with the absence of, or minimal limb girdle muscle involvement and normal intelligence (63).

The *LARGE* gene

Mutations in the Large gene were originally identified in the myodystrophy mouse (*myd*; now renamed Large^{myd}), a spontaneous model of CMD (64). Several detailed studies of the skeletal and cardiac muscles, eyes and central nervous system involvement of these mice have been reported (65-68). These mice also show a profound deficiency of glycosylated ADG. We originally reported mutations in the *LARGE* gene in a single family, where the propositus was affected by congenital onset of weakness, profound mental retardation, white matter changes and subtle structural abnormalities on brain MRI; this novel condition was named MDC1D (23). A moderate reduction of glycosylated ADG was identified. More recently, allelic mutations in LARGE were identified in a patient with a severe form of CMD resembling WWS (69). This patient had an out of frame intragenic deletion, leading to a complete loss of LARGE function, and thereby explaining the milder phenotype of the previously described patient with missense mutations. We also recently identified a patient with a WWS-like phenotype, who carried a nonsense mutation at the heterozygous state. These results therefore identify LARGE as a gene rarely involved in CMD, with severity ranging from MDC1D to WWS.

Six genes: how many clinical phenotypes?

Mutations in the 6 genes described above all result in the reduced glycosylation of ADG; originally, mutations in individual genes were associated with specific phenotypes (i.e. fukutin mutations in FCMD, or POMGnT1 mutations in MEB). However, as illustrated by the wide spectrum of phenotypes secondary to FKRP mutations, and more recently also by allelic mutations in fukutin and other genes in rare cases with milder phenotypes, it is likely that full spectrum of clinical conditions secondary to mutations of each of these genes is also very wide. We have recently performed a large and unbiased study on the mutation frequency and phenotypes associated with mutations in the *POMT1*, *POMT2*, *POMGnT1*, *fukutin* and *LARGE* genes (70). The only inclusion criterion was the evidence of a dystroglycanopathy. Ninety two probands were screened for these 5 genes (FKRP had been previously excluded) irrespective of their age, ethnicity and clinical features, including the presence or absence of central nervous system involvement. We identified mutations in a total of 31 probands (34 individuals from 31 families); 37 different mutations were identified, of which 32 were novel. Con-

Table 1.

	Number of patients							
	WWS	MEB FCMD	CMD CRB	CMD MR	CMDno MR	LGMD MR	LGMD noMR	Total
POMT1	1	1	–	3	–	3	–	8
POMT2	–	6	2	–	–	1	–	9
POMGnT1	–	6	–	–	–	–	1	7
fukutin	1	1	–	–	1	–	3	6
LARGE	1	–	–	–	–	–	–	1
Mutation detected	3 (60%)	14 (47%)	2 (50%)	3 (20%)	1 (10%)	4 (80%)	4 (20%)	31 (34%)
Total	5	30	4	15	10	5	20	92

cerning the frequency of involvement of individual gene defects in this cohort, mutations in *POMT2* were the most prevalent with 9 cases, followed by *POMT1* with 8 cases, *POMGnT1* with 7 cases, *fukutin* with 6 cases and finally *LARGE* with only a single case (Table 1).

Regarding phenotype/genotype correlations for *POMT1*, *POMT2*, *POMGnT1*, *fukutin* and *LARGE*, we detected pathogenic mutations in 3 of 5 patients with WWS syndrome, 14 of 30 patients with a MEB/FCMD phenotype, in 2 of 4 patients with CMD and cerebellar involvement, 3 of 15 patients with CMD-mental retardation but otherwise structurally normal brain, 1 of 10 patients with CMD and absent mental retardation (resembling what previously described in MDC1C), 4 of 6 patients with LGMD and associated reduced IQ (resembling what has been previously described for LGMD2K), and 4 of 23 patients with LGMD-and no mental retardation or other evidence of central nervous system involvement. In most instances there was no apparent difference in the pattern of skeletal muscle weakness or central nervous system involvement in patients with associated structural brain defects belonging to the severe end of the clinical spectrum such as in WWS. However, regarding the LGMD subgroups with mental retardation and microcephaly (ie.LGMD2K and similar phenotypes), we found this specific phenotype only in patients with mutations either in *POMT1* or *POMT2* (70). On the other hand, we identified a number of patients with considerably more severe muscle weakness than LGMD2K, clinically resembling MDC1C (i.e. non ambulant children), with absent brain involvement, due to mutations in *fukutin*. This suggests that while involvement of any of these genes can give rise to a very wide spectrum of clinical syndromes with overlapping features, there might be at the same time subtle differences in the involvement of brain and muscle secondary to specific gene mutations, with *POMT1* and *POMT2* being apparently associated with more severe central nervous system involvement even in patients with relatively mild weakness who remain ambulant (LGMD2K): this phenotype has so far not been observed for *POMGnT1*, *LARGE*, *fukutin* or *FKRP*. These results may therefore allow the targeting of specific gene defects in individual subcategories of patients with dystroglycanopathies.

The results also suggest that the original descriptions of several "core phenotypes" associated with each of these genes is related to the high prevalence of founder mutations within specific populations, such as the "Finnish" *POMGnT1* mutation in MEB disease, and the "Japanese" *fukutin* mutation responsible for FCMD, and not to the fact that mutations in these genes are not capable of inducing different conditions.

These observations therefore expand the clinical phenotypes associated with mutations in *POMT1*, *POMT2*, *POMGnT1*, *fukutin* and *LARGE*, and provide an indication of the relative frequency of their involvement in Caucasian patients with a dystroglycanopathy. Adding together the patients recently studied for mutations in *POMT1*, *POMT2*, *POMGnT1*, *fukutin* and *LARGE,* and those in whom we have previously identified FKRP mutations (77 cases, Muntoni et al, personal observation) we have been able to identify causative mutations in approximately 65% of patients with a dystroglycanopathy. This means that a significant number of patients did not have mutations in any of the genes we know are associated with this phenotype, suggesting that more, as yet undefined, gene(s) are likely to be implicated in the pathogenesis of the dystroglycanopathies. The identification of these other genes may provide additional information on the pathway of glycosylation of α-dystroglycan.

Conclusions

All these forms of muscular dystrophies are characterized by the hypoglycosylation of ADG in both patients skeletal muscle biopsies and the skeletal muscle of equivalent animal models, suggesting the existence of a common pathogenetic pathway. Whilst *POMT1*, *POMT2* and *POMGnT1* encode enzymes involved in the biosynthesis of *O*-mannosylated glycans on dystroglycan, the function of *fukutin*, *FKRP* and *LARGE* have yet to be identified. In keeping with the hypothesis of a common pathogenetic pathway, allelic mutations of any of these genes results in conditions of variable severity broadly correlated with the degree of ADG hypoglycosylation. Molecular genetic analysis of patients with a dystroglycanopathy therefore should include all these 6 genes; however, approximately 35% of patients have no identifiable mutations, strongly pointing towards further genetic heterogeneity. Genetic analysis suggests that the possibility of a single major locus accounting for the remaining dystroglycanopathies is unlikely and we must be prepared to search for multiple genes associated with the glycosylation of ADG.

Acknowledgement

The authors wish to thank the ENMC CMD consortium for the ongoing collaboration. The financial support of the Muscular Dystrophy Campaign and of the Department of Health (NCG) is gratefully acknowledged. The group at Guy's Hospital Trust London involved in the NCG diagnostic work (Dr Stephen Abbs; Dr Rachael Mein; Dr Judith Pagan) is also gratefully acknowledged.

References

1. Endo T, Toda T. Glycosylation in congenital muscular dystrophies. Biol Pharm Bull 2003;26:1641-7.
2. Toda T, Kobayashi K, Takeda S, et al. Fukuyama-type congenital muscular dystrophy (FCMD) and alpha-dystroglycanopathy. Congenit Anom Kyoto 2003;43:97-104.
3. Martin-Rendon E, Blake DJ. Protein glycosylation in disease: new insights into the congenital muscular dystrophies. Trends Pharmacol Sci 2003;24:178-83.

4. Hewitt JE, Grewal PK. Glycosylation defects in inherited muscle disease. Cell Mol Life Sci 2003;60:251-8.
5. Muntoni F, Brockington M, Blake DJ, Torelli S, Brown SC. Defective glycosylation in muscular dystrophy. Lancet 2002;360:1419-21.
6. Martin PT. Mechanisms of Disease: congenital muscular dystrophies-glycosylation takes center stage. Nat Clin Pract Neurol 2006;2:222-30.
7. Martin PT. The dystroglycanopathies: the new disorders of O-linked glycosylation. Semin Pediatr Neurol 2005;12:152-8.
8. Toda T, Chiyonobu T, Xiong H, et al. Fukutin and alpha-dystroglycanopathies. Acta Myol 2005;24:60-3.
9. Muntoni F, Voit T. The congenital muscular dystrophies in 2004: a century of exciting progress. Neuromuscul Disord 2004;14:635-49.
10. Muntoni F, Brockington M, Torelli S, Brown SC. Defective glycosylation in congenital muscular dystrophies. Curr Opin Neurol 2004;17:205-9.
11. Chiba A, Matsumura K, Yamada H, et al. Structures of sialylated O-linked oligosaccharides of bovine peripheral nerve alpha-dystroglycan. The role of a novel O-mannosyl-type oligosaccharide in the binding of alpha-dystroglycan with laminin. J Biol Chem 1997;272:2156-62.
12. Endo T. O-mannosyl glycans in mammals. Biochim Biophys Acta 1999;1473:237-46.
13. Martin PT. Dystroglycan glycosylation and its role in matrix binding in skeletal muscle. Glycobiology 2003;13:55R-66R.
14. Seifert J, Ogawa T, Kurono S, Ito Y. Syntheses of alpha-dystroglycan derived glycosyl amino acids carrying a novel mannosyl serine/threonine linkage. Glycoconj J 2000;17:407-23.
15. Martin PT. Congenital muscular dystrophies involving the O-mannose pathway. Curr Mol Med 2007;7:417-25.
16. Endo T, Manya H. O-mannosylation in mammalian cells. Methods Mol Biol 2006;347:43-56.
17. Michele DE, Campbell KP. Dystrophin-glycoprotein complex: post-translational processing and dystroglycan function. J Biol Chem 2003;278:15457-60.
18. de Bernabe DBV, Currier S, Steinbrecher A, et al. Mutations in the O-mannosyltransferase gene POMT1 give rise to the severe neuronal migration disorder Walker-Warburg syndrome. Am J Hum Genet 2002;71:1033-43.
19. van Reeuwijk J, Janssen M, van den Elzen C, et al. POMT2 mutations cause alpha-dystroglycan hypoglycosylation and Walker-Warburg syndrome. J Med Genet 2005;42:907-12.
20. Yoshida A, Kobayashi K, Manya H, et al. Muscular dystrophy and neuronal migration disorder caused by mutations in a glycosyltransferase, POMGnT1. Dev Cell 2001;1:717-24.
21. Kobayashi K, Nakahori Y, Miyake M, et al. An ancient retrotransposal insertion causes Fukuyama-type congenital muscular dystrophy. Nature 1998;394:388-92.
22. Brockington M, Blake DJ, Prandini P, et al. Mutations in the fukutin-related protein gene (FKRP) cause a form of congenital muscular dystrophy with secondary laminin alpha2 deficiency and abnormal glycosylation of alpha-dystroglycan. Am J Hum Genet 2001;69:1198-209.
23. Longman C, Brockington M, Torelli S, et al. Mutations in the human LARGE gene cause MDC1D, a novel form of congenital muscular dystrophy with severe mental retardation and abnormal glycosylation of alpha-dystroglycan. Hum Mol Genet 2003;12:2853-61.
24. Akasaka-Manya K, Manya H, Kobayashi K, Toda T, Endo T. Structure-function analysis of human protein O-linked mannose beta1,2-N-acetylglucosaminyltransferase 1, POMGnT1. Biochem Biophys Res Commun 2004;320:39-44.
25. Manya H, Sakai K, Kobayashi K, et al. Loss-of-function of an N-acetylglucosaminyltransferase, POMGnT1, in muscle-eye-brain disease. Biochem Biophys Res Commun 2003;306:93-7.
26. Xiong H, Kobayashi K, Tachikawa M, et al. Molecular interaction between fukutin and POMGnT1 in the glycosylation pathway of alpha-dystroglycan. Biochem Biophys Res Commun 2006;350:935-41.
27. de Paula F, Vieira N, Starling A, et al. Asymptomatic carriers for homozygous novel mutations in the FKRP gene: the other end of the spectrum. Eur J Hum Genet 2003;11:923-30.
28. Brown SC, Torelli S, Brockington M, et al. Abnormalities in alpha-dystroglycan expression in MDC1C and LGMD2I muscular dystrophies. Am J Pathol 2004;164:727-37.
29. Brockington M, Torelli S, Prandini P, et al. Localization and functional analysis of the LARGE family of glycosyltransferases: significance for muscular dystrophy. Hum Mol Genet 2005;14:657-65.
30. Brockington M, Yuva Y, Prandini P, et al. Mutations in the fukutin-related protein gene (FKRP) identify limb girdle muscular dystrophy 2I as a milder allelic variant of congenital muscular dystrophy MDC1C. Hum Mol Genet 2001;10:2851-9.
31. Mercuri E, Brockington M, Straub V, et al. Phenotypic spectrum associated with mutations in the fukutin-related protein gene. Ann Neurol 2003;53:537-42.
32. Poppe M, Cree L, Bourke J, et al. The phenotype of limb-girdle muscular dystrophy type 2I. Neurology 2003;60:1246-51.
33. Walter MC, Petersen JA, Stucka R, et al. FKRP (826C > A) frequently causes limb-girdle muscular dystrophy in German patients. J Med Genet 2004;41:e50.
34. Sveen ML, Schwartz M, Vissing J. High prevalence and phenotype-genotype correlations of limb girdle muscular dystrophy type 2I in Denmark. Ann Neurol 2006;59:808-15.
35. Vieira NM, Schlesinger D, de Paula F, Vainzof M, Zatz M. Mutation analysis in the FKRP gene provides an explanation for a rare cause of intrafamilial clinical variability in LGMD2I. Neuromuscul Disord 2006;16:870-3.
36. Topaloglu H, Brockington M, Yuva Y, et al. FKRP gene mutations cause congenital muscular dystrophy, mental retardation, and cerebellar cysts. Neurology 2003;60:988-92.
37. de Bernabe DBV, Voit T, Longman C, et al. Mutations in the FKRP gene can cause Muscle-Eye-Brain disease and Walker-Warburg syndrome. J Med Genet 2004;41:e61.
38. Dolatshad NF, Brockington M, Torelli S, et al. Mutated fukutin-related protein (FKRP) localises as wild type in differentiated muscle cells. Exp Cell Res 2005;309:370-8.
39. Esapa CT, McIlhinney RA, Blake DJ. Fukutin-related protein mutations that cause congenital muscular dystrophy result in ER-retention of the mutant protein in cultured cells. Hum Mol Genet 2005;14:295-305.
40. Matsumoto H, Noguchi S, Sugie K, et al. Subcellular localization of fukutin and fukutin-related protein in muscle cells. J Biochem 2004;135:709-12.
41. Beedle AM, Nienaber PM, Campbell KP. Fukutin-related protein associates with the sarcolemmal dystrophin-glycoprotein complex. J Biol Chem 2007;282:16713-7.
42. Keramaris-Vrantsis E, Lu PJ, Doran T, et al. Fukutin-related protein localizes to the Golgi apparatus and mutations lead to mislocalization in muscle in vivo. Muscle Nerve 2007;36:455-65.
43. Torelli S, Brown SC, Brockington M, et al. Sub-cellular localisation of fukutin related protein in different cell lines and in the muscle of patients with MDC1C and LGMD2I. Neuromuscul Disord 2005;15:836-43.
44. Manya H, Chiba A, Yoshida A, et al. Demonstration of mammalian protein O-mannosyltransferase activity: coexpression of POMT1 and POMT2 required for enzymatic activity. Proc Natl Acad Sci USA 2004;101:500-5.

45. Herrmann R, Straub V, Blank M, et al. Dissociation of the dystroglycan complex in caveolin-3-deficient limb girdle muscular dystrophy. Hum Mol Genet 2000;9:2335-40.
46. Brown SC, Fassati A, Popplewell L, et al. Dystrophic phenotype induced in vitro by antibody blockade of muscle alpha-dystroglycan-laminin interaction. J Cell Sci 1999;112:209-16.
47. Sabatelli P, Columbaro M, Mura I, et al. Extracellular matrix and nuclear abnormalities in skeletal muscle of a patient with Walker-Warburg syndrome caused by POMT1 mutation. Biochim Biophys Acta 2003;1638:57-62.
48. van Reeuwijk J, Maugenre S, van den Elzen C, et al. The expanding phenotype of POMT1 mutations: from Walker-Warburg syndrome to congenital muscular dystrophy, microcephaly, and mental retardation. Hum Mutat 2006;27:453-9.
49. D'Amico A, Tessa A, Bruno C, et al. Expanding the clinical spectrum of POMT1 phenotype. Neurology 2006;66:1564-7.
50. Balci B, Uyanik G, Dincer P, et al. An autosomal recessive limb girdle muscular dystrophy (LGMD2) with mild mental retardation is allelic to Walker-Warburg syndrome (WWS) caused by a mutation in the POMT1 gene. Neuromuscul Disord 2005;15:271-5.
51. Yanagisawa A, Bouchet C, Van den Bergh PY, et al. New POMT2 mutations causing congenital muscular dystrophy. Neurology 2007.
52. Mercuri E, D'Amico A, Tessa A, et al. POMT2 mutation in a patient with 'MEB-like' phenotype. Neuromuscul Disord 2006;16:446-8.
53. Manya H, Bouchet C, Yanagisawa A, et al. Protein O-mannosyltransferase activities in lymphoblasts from patients with alpha-dystroglycanopathies. Neuromuscul Disord 2007 [Epub ahead of print].
54. Willer T, Prados B, Falcon-Perez JM, et al. Targeted disruption of the Walker-Warburg syndrome gene Pomt1 in mouse results in embryonic lethality. Proc Natl Acad Sci USA 2004;101:14126-31.
55. Taniguchi K, Kobayashi K, Saito K, et al. Worldwide distribution and broader clinical spectrum of muscle-eye-brain disease. Hum Mol Genet 2003;12:527-34.
56. Zhang W, Vajsar J, Cao P, et al. Enzymatic diagnostic test for Muscle-Eye-Brain type congenital muscular dystrophy using commercially available reagents. Clin Biochem 2003;36:339-44.
57. Hu H, Yang Y, Eade A, Xiong Y, Qi Y. Breaches of the pial basement membrane and disappearance of the glia limitans during development underlie the cortical lamination defect in the mouse model of muscle-eye-brain disease. J Comp Neurol 2007;501:168-83.
58. Liu J, Ball SL, Yang Y, et al. A genetic model for muscle-eye-brain disease in mice lacking protein O-mannose 1,2-N-acetylglucosaminyltransferase (POMGnT1). Mech Dev 2006;123:228-40.
59. Kurahashi H, Taniguchi M, Meno C, et al. Basement membrane fragility underlies embryonic lethality in fukutin-null mice. Neurobiol Dis 2005;19:208-17.
60. Takeda S, Kondo M, Sasaki J, et al. Fukutin is required for maintenance of muscle integrity, cortical histiogenesis and normal eye development. Hum Mol Genet 2003;12:1449-59.
61. de Bernabe DB, van Bokhoven H, van Beusekom E, et al. A homozygous nonsense mutation in the fukutin gene causes a Walker-Warburg syndrome phenotype. J Med Genet 2003;40:845-8.
62. Godfrey C, Escolar D, Brockington M, et al. Fukutin gene mutations in steroid-responsive limb girdle muscular dystrophy. Ann Neurol 2006;60:603-10.
63. Murakami T, Hayashi YK, Noguchi S, et al. Fukutin gene mutations cause dilated cardiomyopathy with minimal muscle weakness. Ann Neurol 2006;60:597-602.
64. Grewal PK, Holzfeind PJ, Bittner RE, Hewitt JE. Mutant glycosyltransferase and altered glycosylation of alpha-dystroglycan in the myodystrophy mouse. Nat Genet 2001;28:151-4.
65. Qu Q, Crandall JE, Luo T, McCaffery PJ, Smith FI. Defects in tangential neuronal migration of pontine nuclei neurons in the Large-myd mouse are associated with stalled migration in the ventrolateral hindbrain. Eur J Neurosci 2006;23:2877-86.
66. Litwack ED, Lee Y, Mallott JM. Absence of the basilar pons in mice lacking a functional Large glycosyltransferase gene suggests a defect in pontine neuron migration. Brain Res 2006;1117:12-7.
67. Levedakou EN, Chen XJ, Soliven B, Popko B. Disruption of the mouse Large gene in the enr and myd mutants results in nerve, muscle, and neuromuscular junction defects. Mol Cell Neurosci 2005;28:757-69.
68. Holzfeind PJ, Grewal PK, Reitsamer HA, et al. Skeletal, cardiac and tongue muscle pathology, defective retinal transmission, and neuronal migration defects in the Large(myd) mouse defines a natural model for glycosylation-deficient muscle - eye - brain disorders. Hum Mol Genet 2002;11:2673-87.
69. van Reeuwijk J, Grewal PK, Salih MA, et al. Intragenic deletion in the LARGE gene causes Walker-Warburg syndrome. Hum Genet 2007;121:685-90.
70. Godfrey C, Clement E, Mein R, et al. Refining genotype phenotype correlations in muscular dystrophies with defective glycosylation of dystroglycan. Brain 2007;130:2725-35.

Brain Pathology ISSN 1015-6305

RESEARCH ARTICLE

A Comparative Study of α-Dystroglycan Glycosylation in Dystroglycanopathies Suggests that the Hypoglycosylation of α-Dystroglycan Does Not Consistently Correlate with Clinical Severity

Cecilia Jimenez-Mallebrera[1]; Silvia Torelli[1]; Lucy Feng[1]; Jihee Kim[1]; Caroline Godfrey[1]; Emma Clement[1]; Rachael Mein[2]; Stephen Abbs[2]; Susan C. Brown[1,7]; Kevin P. Campbell[3]; Stephan Kröger[4]; Beril Talim[5]; Haluk Topaloglu[10]; Ros Quinlivan[6]; Helen Roper[8]; Anne M. Childs[9]; Maria Kinali[1]; Caroline A. Sewry[1,6]; Francesco Muntoni[1]

[1] Dubowitz Neuromuscular Centre, Institute of Child Health and Great Ormond Street Hospital for Children, UCL, London, UK.
[2] DNA Laboratory, Genetics Centre, Guy's Hospital, London, UK.
[3] Howard Hughes Medical Institute, Department of Molecular Physiology and Biophysics, Internal Medicine and Neurology, University of Iowa Carver College of Medicine, Iowa City, Ia.
[4] Physiological Institute, Ludwig-Maximilians-University, Munich, Germany.
[5] Department of Paediatric Pathology, Hacettepe Children's Hospital, Ankara, Turkey.
[6] Wolfson Centre for Inherited Neuromuscular Diseases, Robert Jones and Agnes Hunt Orthopaedic Hospital, Oswestry, UK.
[7] Division of Neurosciences, Imperial College London, London, UK.
[8] Department of Paediatrics, Birmingham Heartlands Hospital, Birmingham, UK.
[9] Department of Paediatric Neurosciences, Leeds General Infirmary, Leeds, UK.
[10] Child Neurology Unit, Department of Pediatrics, Hacettepe University, Ankara, Turkey.

Keywords
α-dystroglycan, congenital muscular dystrophy, glycosylation, immunohistochemistry, limb–girdle muscular dystrophy.

Corresponding author:
Cecilia Jimenez-Mallebrera, PhD, BSc, Dubowitz Neuromuscular Centre, Institute of Child Health and Great Ormond Street Hospital for Children, UCL, London, UK. (E-mail: *c.jimenez@imperial.ac.uk*)

Received 24 April 2008; accepted 13 June 2008.

doi:10.1111/j.1750-3639.2008.00198.x

Abstract

Hypoglycosylation of α-dystroglycan underpins a subgroup of muscular dystrophies ranging from congenital onset of weakness, severe brain malformations and death in the perinatal period to mild weakness in adulthood without brain involvement. Mutations in six genes have been identified in a proportion of patients. *POMT1*, *POMT2* and *POMGnT1* encode for glycosyltransferases involved in the mannosylation of α-dystroglycan but the function of *fukutin*, *FKRP* and *LARGE* is less clear. The pathological hallmark is reduced immunolabeling of skeletal muscle with antibodies recognizing glycosylated epitopes on α-dystroglycan. If the common pathway of these conditions is the hypoglycosyation of α-dystroglycan, one would expect a correlation between clinical severity and the extent of hypoglycosylation. By studying 24 patients with mutations in these genes, we found a good correlation between reduced α-dystroglycan staining and clinical course in patients with mutations in *POMT1*, *POMT2* and *POMGnT1*. However, this was not always the case in patients with defects in *fukutin* and *FKRP*, as we identified patients with mild limb–girdle phenotypes without brain involvement with profound depletion of α-dystroglycan. These data indicate that it is not always possible to correlate clinical course and α-dystroglycan labeling and suggest that there might be differences in α-dystroglycan processing in these disorders.

INTRODUCTION

α-Dystroglycan is a component of the dystrophin-associated protein (DAP) complex, which binds to various ligands in the extracellular matrix of muscle and other tissues, including laminin-α2, perlecan, neurexin and agrin (21, 35, 46). At the muscle cell surface, α-dystroglycan binds to β-dystroglycan, thus linking the extracellular matrix to dystrophin and the actin cytoskeleton (9, 16, 17, 46). Dystroglycan plays an important role in the organization of laminins during the development of basement membranes in muscle and nonmuscle tissues (13, 45, 47). In skeletal muscle, dystroglycan and integrin α7B1D function as the receptors for laminin-α2, and this interaction is necessary for the organization of laminin and the reorganization of the actin cytoskeleton. In turn, the presence of functional laminin-α2 is necessary to organize dystroglycan, integrin, dystrophin and spectrin at the sarcolemma and costameres (13, 47).

Laminin-α2 binding to α-dystroglycan is mediated by the C-terminal globular LG domains (LG 4-5) in the laminin molecule and the O-linked carbohydrate moieties in the mucin-like domain

of dystroglycan (13, 46). Differential glycosylation of the α-dystroglycan domain confers tissue-specific functional variability and results in different dystroglycan glycoforms (33). A number of different glycans have been demonstrated on α-dystroglycan, of which O-linked mannose represents one of the best characterized ones (10). Its formation involves the action of several enzymes (collectively referred to as glycosyltransferases) that add different monosaccharides in a stepwise manner. These carbohydrate groups also mediate binding with the LG domains of other ligands such as perlecan, agrin and neurexin (2).

Disruption of the interaction between α-dystroglycan and its ligands has severe consequences for muscle and brain function and structure and results in a group of muscular dystrophies with and without central nervous system involvement (11, 22, 35, 36). These disorders are now collectively referred to as "dystroglycanopathies" (2, 24, 30, 38) and are caused by gene defects in *fukutin* (OMIM 607440), fukutin-related protein (*FKRP*; OMIM 606596), protein-O-mannose 1,2-N-acetylglucosaminyltransferase 1 (*POMGnT1*; OMIM 606822), protein-O-mannosyl transferases (*POMT1* and *POMT2*; OMIM 607423 and 607439, respectively) and *LARGE* (OMIM 603590). However, mutations in these six genes account for only a proportion of patients with dystroglycan glycosylation defects (19), indicating that other unknown genes are involved.

Dystroglycanopathies constitute a heterogeneous and complex group of disorders as mutations in any of these genes can result in various phenotypes ranging from severe forms of congenital muscular dystrophy (CMD) to milder limb–girdle muscular dystrophy (LGMD) forms (4, 8, 18, 19, 30, 38, 42). Conversely, similar phenotypes can be caused by mutations in the different genes. This has led to the concept that it is the specific mutation that determines the severity of the phenotype rather than the individual gene. To reflect this complexity, a different classification/categorization has been suggested based on the age at onset of weakness (CMD if within the 6 months of life or LGMD if after acquiring ambulation), presence of mental retardation and/or structural brain abnormalities, and eye involvement, rather than on the specific gene defect and the original clinical entity (19).

At the pathological level, these conditions have in common a reduction in the glycosylated epitopes on α-dystroglycan. The degree of reduction is variable, and while in some patients with severe Walker–Warburg syndrome (WWS) there is virtual absence of these epitopes in muscle, other patients with a mild phenotype only show a minimal reduction (12, 24).

Genotype–phenotype correlations have been described in only a small number of patients with defects in the individual genes (1, 4, 6, 14, 26, 44). Early studies of patients with *FKRP* mutations showed a broad correlation between the levels of α-dystroglycan immunolabeling and the clinical severity, such that severely affected patients with the MDC1C phenotype had a more marked reduction than milder LGMD2I patients (6). More recently, the number of genes involved, the spectrum of clinical severity and our understanding of these conditions have significantly expanded. The aims of this study were to (i) determine if the previous correlation noted in patients with defects in *FKRP* could also be applied to the remaining dystroglycanopathies, and (ii) investigate whether the status α-dystroglycan glycosylation and/or other pathological features could be used to differentiate between the different primary gene defects.

For this purpose, we have correlated clinical and pathological data in a cohort of 24 patients with confirmed mutations in *POMT1*, *POMT2*, *POMGnT1*, *fukutin*, *LARGE* or *FKRP* from whom muscle biopsies were available.

MATERIALS AND METHODS

Patients

All biopsies were obtained with informed written consent and studied under ethical approval. Details of the 24 patients in this study, the clinical categories and mutations are listed in Table 1. Four cases had mutations in the gene encoding *POMT1*, five in *POMT2*, two in *POMGnT1*, two in *fukutin*, 10 in *FKRP* and one in *LARGE*. Some of these cases have been reported previously as indicated in Table 1. The phenotypic categorization in order of severity and as described in Godfrey *et al* (19) is as follows:

(i) WWS (and WWS-like): onset prenatally or at birth; severe structural brain abnormalities (complete agyria or severe lissencephaly), severe cerebellar involvement, and complete or partial absence of the corpus callosum; eye abnormalities are common; motor development is absent.

(ii) Muscle–eye–brain disease/Fukuyama congenital muscular dystrophy-like (MEB/FCMD-like): CMD with brain abnormality less severe than that seen with WWS (pachygyria with preferential frontoparietal involvement and polymicrogyria), cerebellar hypoplasia and dysplasia, and frequent flattening of the pons and brainstem; eye abnormalities are frequent; individuals may, rarely, acquire the ability to walk, although this is delayed; marked speech delay.

(iii) CMD with cerebellar involvement (CMD-CRB): CMD with mental retardation and cerebellar involvement on magnetic resonance imaging (MRI) scan as the only structural abnormality (including cysts, hypoplasia or dysplasia).

(iv) CMD with mental retardation (CMD-MR): CMD with mental retardation and structurally normal brain; patients with isolated microcephaly or minor white matter changes on MRI are included in this group.

(v) CMD with no mental retardation (CMD-No MR): patients with CMD and normal intellectual function.

(vi) LGMD with mental retardation (LGMD-MR): LGMD with mental retardation and structurally normal brain; patients with minor white matter abnormalities and microcephaly were included in this group; this category would include patients with LGMD2I (4, 6) and LGMD2K (1).

(vii) LGMD with no mental retardation (LGMD-No MR): LGMD with no mental retardation; this category would include the LGMD phenotypes such as LGMD2I and 2L (18).

Muscle biopsy

Needle or open muscle biopsies taken from the quadriceps, except patient P13, who had a biopsy taken from a foot muscle, were transversely orientated, mounted in OCT (Tissue-Tek, Sakura Finetek, Zoeterwoude, The Netherlands) and frozen in isopentane cooled in liquid nitrogen. Standard histological and histochemical techniques were applied to cryostat sections, including hematoxylin and eosin, Gomori trichrome, periodic acid Schiff, nicotinamide

Table 1. Summary of genetic and clinical features. Abbreviations: CK = creatine kinase; N/A = not available; WWS = Walter–Warburg syndrome; MEB = muscle–eye–brain disease; FCMD = Fukuyama congenital muscular dystrophy; CMD-CRB = congenital muscular dystrophy with cerebellar involvement; CMD-MR = congenital muscular dystrophy with mental retardation; LGMD-MR = limb–girdle muscular dystrophy with mental retardation; LGMD-No MR = limb–girdle muscular dystrophy without mental retardation; het = heterozygous.

Patient	Gene	Inheritance	Type of mutation	Reference	CK	Maximum motor ability	Phenotypic category
P1	*POMT1*	Homozygous	Frameshift	(19)	3 400	Never sat	MEB-FCMD
P2	*POMT1*	Homozygous	Frameshift	(19)	4 000	Never sat	WWS
P3	*POMT1*	Compound het	Insertion/deletion Missense	(19)	8 000	Walking	LGMD-MR
P4	*POMT1*	Compound het	Nonsense Missense	(19)	19 000	Walking	CMD-MR
P5	*POMT2*	Compound het	Missense Missense	(19)	5 500	Sitting with support	MEB-FCMD
P6	*POMT2*	Compound het	Missense Missense	(19, 34)	2 000	Sitting with support	MEB-FCMD
P7	*POMT2*	Compound het	Missense Missense	(19)	6 000	Never sat	MEB-FCMD
P8	*POMT2*	Compound het	Missense Frameshift	(19)	3 000	Sitting	CMD-CRB
P9	*POMT2*	Compound het	Missense		3 000	Walking	CMD-MR
P10	*POMGnT1*	Homozygous	Splice site		1 000	Sitting	MEB-FCMD
P11	*POMGnT1*	Homozygous	Missense	(12)	5 000–12 000	Walking	LGMD-No MR
P12	*LARGE*	Compound het	Missense Frameshift	(28)	500–4 500	Walking	MEB-FCMD
P13	*fukutin*	Compound het	Frameshift Frameshift	(18, 19)	13 000	Walking	LGMD-No MR
P14	*fukutin*	Compound het	Missense Frameshift	(18, 19)	60 000	Walking	LGMD-No MR
P15	*FKRP*	Homozygous	Missense		8 000	Walking	LGMD-No MR (2I-DMD-like)
P16	*FKRP*	Compound het	Missense		24 000	Sitting	CMD-No MR
P17	*FKRP*	Homozygous	Missense	(41, 43)	6 500	Sitting	CMD-CRB
P18	*FKRP*	Homozygous	Missense*		25 000	Walking	LGMD-MR (2I-BMD-like)
P19	*FKRP*	Compound het	Missense* Nonsense		4 900	Walking	LGMD-No MR (2I-BMD-like)
P20	*FKRP*	Compound het	Missense* Missense		N/A	Walking	LGMD-No MR (2I-BMD-like)
P21	*FKRP*	Compound het	Missense Frameshift		11 814	Walking	LGMD-No MR (2I-DMD-like)
P22	*FKRP*	Compound het	Missense* Missense		3 607	Walking	LGMD-No MR (2I-mild)
P23	*FKRP*	Compound het	Missense* Missense		5 500	Walking	LGMD-No MR (2I-mild)
P24	*FKRP*	Homozygous	Missense*		N/A	Walking	LGMD-No MR (2I-mild)

*Common mutation p.Leu276Ile.

adenine dinucleotide dehydrogenase-tetrazolium reductase (NADH-TR), succinic dehydrogenase and cytochrome oxidase (15).

Immunohistochemistry

Dystroglycan antibodies were β-dystroglycan (NCL-b-DAG, 1/50; Novocastra, Leica-microcystems, Wetzlar, Germany), α-dystroglycan mouse monoclonal IIH6, 1/200 (a gift from K. Campbell) and α-dystroglycan goat polyclonal GT20ADG, 1/50 (25, 27, 35). Antibody GT20ADG was raised against the entire dystroglycan glycoprotein complex and purified against a hypoglycosylated full-length α-dystroglycan human fusion protein expressed in HEK-293 cells. Anti-α-dystroglycan sheep polyclonal (a kind gift of S. Kröger) was raised against a synthetic peptide corresponding to the last 20 amino acids of chick α-dystroglycan 1/500 (20).

Other antibodies used were laminin-α2 (MAB1922 Chemicon (Millipore, Billerica, MA, USA) to the 80-kDa C-terminal fragment, 1/4000, and 4H8 Alexis Corporation (Lausen, Switzerland) to the 300-kDa N-terminal fragment, 1/100), spectrin (NCL-SPEC1, 1/20), dystrophin (NCL-DYS1, 1/3, NCL-DYS2, 1/20, and NCL-DYS3, 1/10), neonatal isoform of myosin heavy chain (NCL-MHCn, 1/15), developmental isoform of myosin (NCL-MHCd, 1/20) and utrophin (NCL-DRP2, 1/5), all from Novocastra. Caveolin-3 was from Becton Dickinson (Franklin Lakes, NJ, USA) (C38320, 1/400), and the HLA (Major Histocompatibility Complex I) was from Dako (Glostrup, Denmark) (1/400).

Cryostat sections (8 μm) were incubated with primary antibodies for 1 h at room temperature, followed by incubation with an appropriate biotinylated secondary antibody [anti-mouse IgM (Dako), 1/200 for IIH6; anti-mouse IgG (Amersham, plc, Little Chalfont, Buckinghamshire, UK), 1/200; anti-goat or anti-sheep IgG (Jackson Immunoresearch, West Grove, PA, USA), 1/500] for 30 minutes, and visualized by streptavidin conjugated to Alexa 594 (Molecular Probes, Invitrogen, Carlsbad, CA, USA, 1/1000) for 15 minutes. All dilutions and washings were made in phosphate buffered saline. Sections were mounted in aqueous mountant (Hydromount; National Diagnostics, Atlanta, GA, USA) and viewed with epifluorescence using a Leica DMR microscope (Leica Microsystems, Wetzlar, Germany) linked to Metamorph Molecular Devices (Sunnyvale, CA, USA). Control sections were labeled without primary antibodies, and all sections were compared with age-matched control samples from other neuromuscular disorders and with normal muscle.

The level of dystroglycan labeling was scored using a scale based on the proportion of positive fibers and intensity relative to the controls used in each sample set. In order to obtain an objective indication of intensity, we used control sections to set the exposure time and scale settings for the digital capturing system. Two independent observers scored the results blindly (C.J.M. and S.T.). The scale is as follows:

++++ = normal (based on the control sample in the same sample set)
+++/++++ = minimal reduction
+++ = mild reduction
++ = significant reduction
+ = very marked reduction
0/+ = weak traces
0 = negative

RESULTS

Pathology

All samples had features compatible with a muscular dystrophy, but these were variable in type and degree (Table 2). There were variable degrees of variation in fiber size, with atrophy and hypertrophy of fibers, fibrosis, adipose tissue, internal nuclei, necrosis and regeneration (basophilic fibers and expression of neonatal and/or developmental myosins). It was not possible to exclude the influence of factors such as sampling and size of biopsy on some of the features. Some of the biopsies (P1, P2, P5, P7 and P6) contained only a small number of fibers surrounded by connective tissue and fat. There was no correlation between the degree of pathology and age, nor with the defective gene. P1, aged 2 months, and P2, aged 5 years, both had marked connective tissue and fat proliferation (Figure 1A,B). On the other hand, patients with mutations in the same gene and of similar age at the time of biopsy showed different degrees of pathology (P5 and P9, both with *POMT2* mutations) (Figure 1C,H). As reported for other neuromuscular disorders (15), there was no correlation between the degree of pathology and clinical severity (compare P10 and P9; Figure 1E,H).

Proliferation of endomysial connective tissue was seen in all cases except P10 (Figure 1E) and was often extensive even in the clinically milder cases. Basophilic fibers were present in some cases, and all biopsies contained a proportion of fibers expressing

Table 2. Muscle pathology. Abbreviations: N/A = not available; NMY + ve = fibers positive for neonatal myosin.

Patient	Gene	Age at biopsy	Fibrosis	Adipose tissue	Internal nuclei	Regeneration	Necrosis
P1	*POMT1*	2 months	Marked	No	A few	No basophilia, many NMY + ve	No
P2	*POMT1*	5 years	Marked	Marked	A few	No basophilia, a few NMY + ve	No
P3	*POMT1*	3 years	Marked	Mild	Yes	Basophilia, many NMY + ve	Yes
P4	*POMT1*	2 years	Yes	Yes	Yes	Basophilia, several NMY + ve	Yes
P5	*POMT2*	2 years	Yes	Yes	Yes	No basophilia, some NMY + ve	No
P6	*POMT2*	1 year	Yes	Marked	Yes	Basophilia	No
P7	*POMT2*	10 years	Yes	Yes	Yes	Several NMY + ve	No
P8	*POMT2*	15 months	Yes	Some	Yes	Basophilia, many NMY + ve	Yes
P9	*POMT2*	2 years	Yes	Yes	Yes	Basophilia, some NMY + ve	No
P10	*POMGnT1*	2 years	No	No	A few	Basophilia, many NMY + ve	No
P11	*POMGnT1*	14 years	Some	Yes	Some	Basophilia, many NMY + ve	Yes
P12	*LARGE*	17 years	Traces	No	Yes	Basophilia, few NMY + ve	Yes
P13	*fukutin*	4 years	Yes	Yes	Yes	Basophilia, few NMY + ve	Yes
P14	*fukutin*	7 years	Yes	Yes	Yes	Basophilia, many NMY + ve	Yes
P15	*FKRP*	2 years	Yes	No	Yes	No basophilia, several NMY + ve	Yes
P16	*FKRP*	1 year	Yes	Yes	Yes	Basophilia, many NMY + ve	Yes
P17	*FKRP*	4 years	Marked	Mild	Few	Basophilia	Yes
P18	*FKRP*	14 years	Yes	Yes	Yes	Yes, NMY + ve	Yes
P19	*FKRP*	11 years	Yes	Yes	Yes	Yes, basophilia, many NMY + ve	Yes
P20	*FKRP*	11 years	Yes	No	No	No basophilia, many NMY + ve	Yes
P21	*FKRP*	8 years	N/A	N/A	N/A	Many NMY + ve	N/A
P22	*FKRP*	11 months	Yes	No	Yes	Basophilia, several NMY + ve	No
P23	*FKRP*	13 years	Yes	No	Yes	Basophilia, several NMY + ve	Yes
P24	*FKRP*	10 years	Yes	No	Yes	Basophilia, a few NMY + ve	Yes

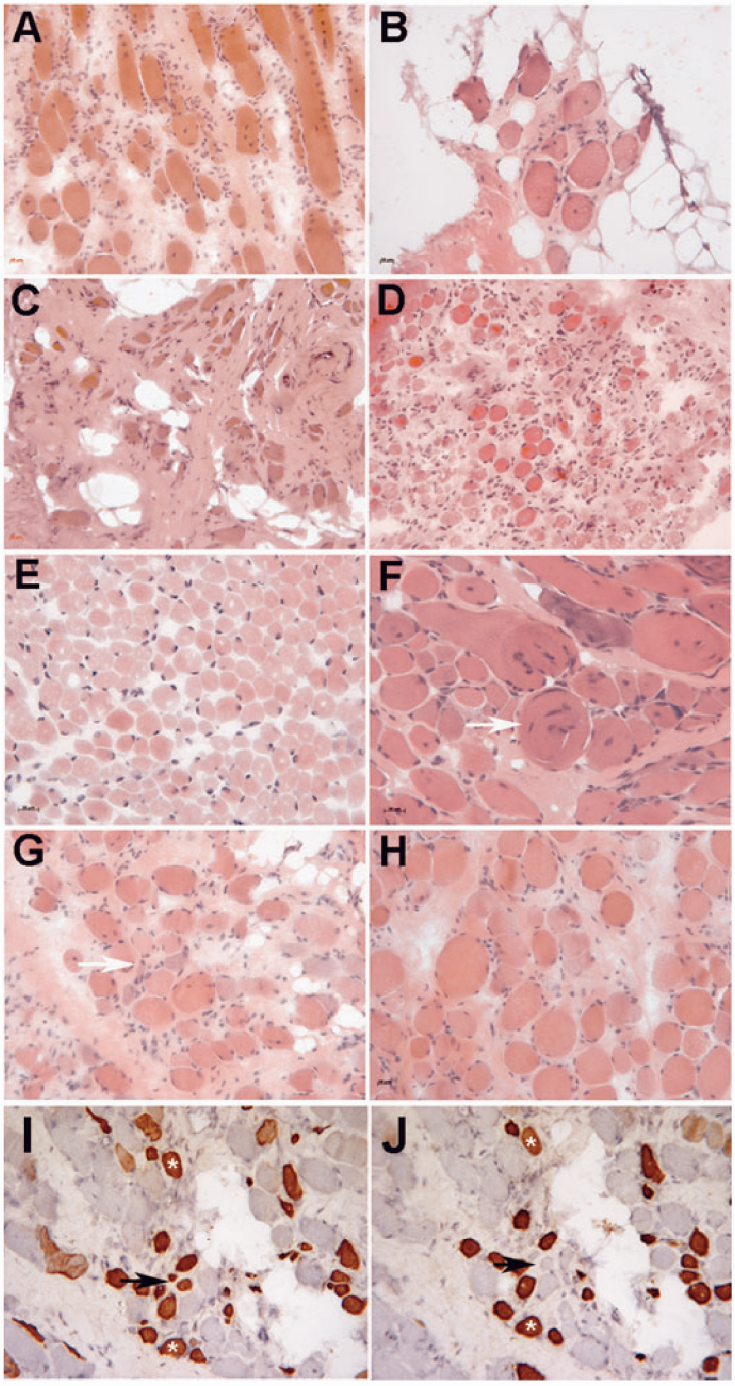

Figure 1. *Illustrative images of the spectrum of pathology seen in this cohort of patients.* Hematoxylin and eosin: **A.** P1. **B.** P2. **C.** P5. **D.** P8. **E.** P10. **F.** P3. **G.** P16. **H.** P9. Immunohistochemistry: **I.** P16, neonatal isoform of myosin heavy chain. **J.** P16, developmental isoform of myosin heavy chain. Scale bars represent 20 μm. White arrows in **F** and **G** point to whorled and basophilic fibers, respectively. Black arrows in **I** and **J** point to fibers that are positive for neonatal myosin but negative for developmental myosin, whereas other fibers are positive for both antibodies (asterisks).

Table 3. Results of immunohistochemistry with dystroglycan and laminin-α2 antibodies. Abbreviations: β-DG = β-dystroglycan; IIH6, GT20ADG, core sheep = α-dystroglycan antibodies (see Materials and Methods); N/A = not available; WWS = Walter–Warburg syndrome; MEB = muscle–eye–brain disease; FCMD = Fukuyama congenital muscular dystrophy; CMD-CRB = congenital muscular dystrophy with cerebellar involvement; CMD-MR = congenital muscular dystrophy with mental retardation; LGMD-MR = limb–girdle muscular dystrophy with mental retardation; LGMD-No MR = limb–girdle muscular dystrophy without mental retardation.

Patient	Gene	Phenotype	β-DG	IIH6	GT20ADG	Core sheep	Laminin-α2
P1	*POMT1*	MEB-FCMD	+++ (small fibers)	0	+++	0	+++
P2	*POMT1*	WWS	+++/++++	0	N/A	0/+	+++
P3	*POMT1*	LGMD-MR	+++/++++	++	+++/++++	+	+++/++++
P4	*POMT1*	CMD MR	++++	+/++	+++ (small fibers)	+	+++/++++
P5	*POMT2*	MEB-FCMD	++	0	++	0/+	++/+++
P6	*POMT2*	MEB-FCMD	+++/++++ (small fibers)	+	++++	++	+++
P7	*POMT2*	MEB-FCMD	+++/++++	0	N/A	0/+	+++
P8	*POMT2*	CMD-CRB	++++	++	++/+++	++	+++/++++
P9	*POMT2*	CMD-MR	++++	++	++++	N/A	+++
P10	*POMGnT1*	MEB-FCMD	+++/++++	0/+	N/A	+/++	++++
P11	*POMGnT1*	LGMD-No MR	+++/++++	+++/++++	++++	+++/++++	++++
P12	*LARGE*	MEB-FCMD	++++	++/+++	++/+++	+++/++++	++++
P13	*fukutin*	LGMD-No MR	++++	0	+++/++++	0/+	+++
P14	*fukutin*	LGMD-No MR	++++	0/+	+++/++++	0/+	+++/++++
P15	*FKRP*	LGMD-No MR	+++/++++	0	+++/++++	+	+++
P16	*FKRP*	CMD-No MR	+++/++++	0	+++	+/++	++++
P17	*FKRP*	CMD-CRB	++++	0	++++	N/A	++/+++
P18	*FKRP*	LGMD-MR (mild)	++++	++	++++	+++	+++
P19	*FKRP*	LGMD-No MR (intermediate)	+++/++++ (small fibers)	++	+++/++++ (small fibers)	+++	+++/++++
P20	*FKRP*	LGMD-No MR (intermediate)	++++	+	++++	N/A	++++
P21	*FKRP*	LGMD-No MR (severe)	++++	+	++++	N/A	++++
P22	*FKRP*	LGMD-No MR (2I-mild)	+++/++++ (small fibers)	+++	N/A	++/+++	++++
P23	*FKRP*	LGMD-No MR (2I-mild)	++++	++/+++	N/A	++	+++/++++
P24	*FKRP*	LGMD-No MR (2I-mild)	++++	+++	N/A	++/+++	+++

Scoring scale: ++++ = normal (based on the control sample in the same sample set); +++/++++ = minimal reduction; +++ = mild reduction; ++ = significant reduction; + = very marked reduction; 0/+ = weak traces; 0 = negative.

markers associated with regeneration such as neonatal and developmental myosins (Figure 1I,J), utrophin and MHC-class I (15). In P10 and P11, the basophilic fibers were often granular in appearance and stained more darkly with NADH-TR, suggesting a possible mitochondrial proliferation in these fibers. Hypercontracted fibers were present but were not as abundant as in other muscular dystrophies such as Duchenne muscular dystrophy (DMD). Other features included split fibers and whorled fibers (Figure 1F). Fiber typing was often indistinct with oxidative enzyme staining. Fibers expressing slow myosin were predominant in most cases, and some fibers coexpressed more than one isoform of myosin (a common myopathic feature).

Glycosylation of α-dystroglycan

The glycosylation of α-dystroglycan was assessed with the monoclonal antibody clone IIH6, which is known to bind to a carbohydrate moiety that mediates and functionally blocks the interaction between α-dystroglycan and laminin-α2 (2, 7, 16). This was evaluated in parallel with β-dystroglycan labeling as previously described (6, 23).

The reduction of IIH6 labeling ranged from an absence on most fibers to a very mild reduction. There was no correlation between the extent of the reduction and the particular gene affected; cases with absent or very weak traces of IIH6 were observed in patients with mutations in *POMT1*, *POMT2*, *POMGnT1*, *fukutin* and *FKRP* (Table 3). An example for each gene group is shown in Figure 2.

Some biopsies showed a marked variability in the labeling of individual fibers across the section, with some fibers appearing negative while others were brightly labeled. The reason for these intensely labeled fibers is unclear but in most cases, these fibers did not express the neonatal isoform of myosin (as shown in the biopsy of P4; asterisks in Figure 3), suggesting that they are unlikely to be regenerating fibers. They also showed good labeling of caveolin-3 and other membrane proteins, including β-dystroglycan (Figure 3), indicating that the sarcolemma was well preserved.

Patients with mutations in either *POMT1* or *POMT2* genes and a relatively milder phenotype (LGMD-MR, CMD-MR) showed more immunolabeling of IIH6 (Table 3; P3 and P9 are shown in Figure 4) than more severe *POMT1* and *POMT2* cases with WWS or MEB-FCMD phenotypes (P1, P2 and P6).

Labeling of glycosylated α-dystroglycan was reduced in all the patients with *FKRP* mutations. The spectrum of IIH6 reduction was very variable and ranged from an absence (P15, P16 and P17; Figure 2B) to a mild reduction (Figure 5, Table 3). Some of these cases showed a mosaic pattern of positive and negative fibers as described previously in other LGMD2I patients (6).

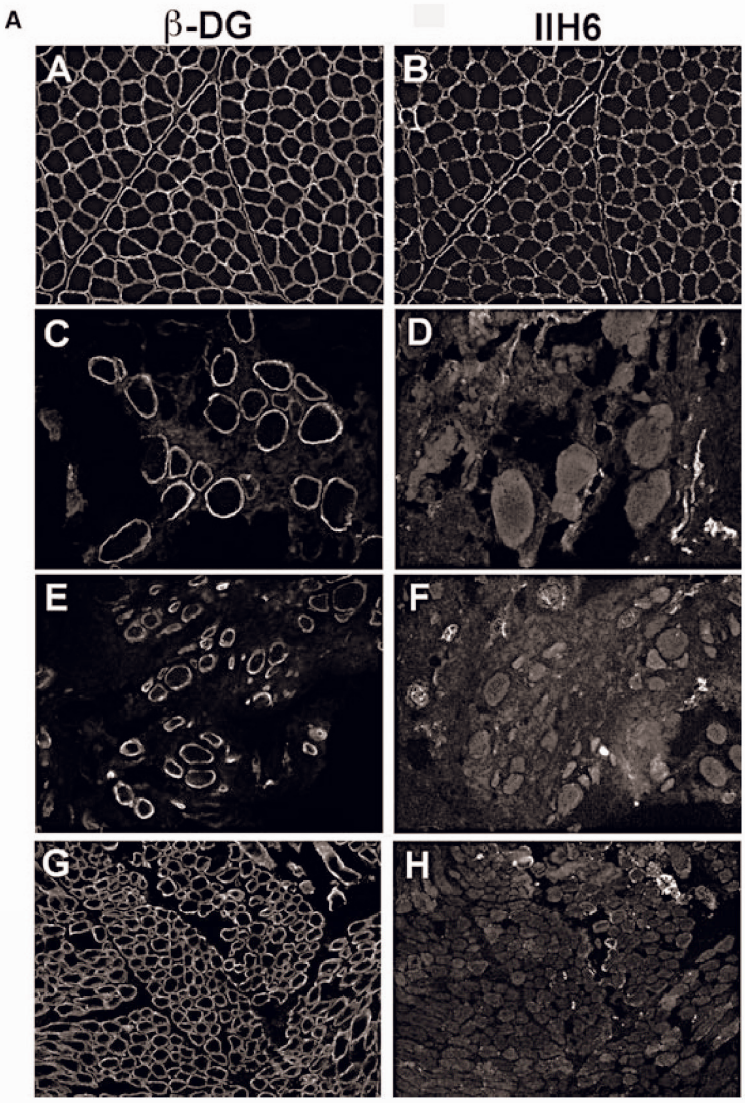

Figure 2. *Representative images of the group of cases with virtually absent or very weak traces of glycosylated α-dystroglycan labeling (0 or 0/+).* Images shown were captured with autoscale to allow visualization of the tissue. **A.** A,C,E,G: β-dystroglycan (β-DG). B,D,F,H: α-dystroglycan using IIH6 antibody. A,B: control; C,D: P2 (*POMT1*); E,F: P5 (*POMT2*); G,H: P10 (*POMGnT1*). **B.** A,C,E: β-DG. B,D,F: α-dystroglycan using IIH6 antibody. A,B: P14 (*fukutin*); C,D: P16 (*FKRP*); E,F: P17 (*FKRP* with cerebellar cysts).

P11 [LGMD-No MR (12)] had a mild phenotype and only very mild reduction of IIH6 labeling, compared with P10 who also had mutations in *POMGnT1* with a more severe phenotype (MEB-FCMD) and a pronounced reduction of IIH6 immunolabeling (Figure 6). In P11, there was a population of fibers with brighter IIH6 and β-dystroglycan on the cell surface and intracellular labeling of caveolin-3 but no neonatal myosin labeling (Figure 6).

Laminin-α2 immunolabeling was also variable between and within cases, and was only reduced in 17 out of 24 cases (Table 3). Even in cases with mutations in the same gene, the degree of reduction varied and there was no correlation with either clinical severity or the degree of reduction of α-dystroglycan labeling. This secondary reduction in laminin-α2 was sometimes subtle and only detectable with the antibody to the 300-kDa fragment, as seen in cases of MDC1A with a partial primary reduction of laminin-α2. However, and in contrast to primary laminin-α2 deficiency, laminin-α2 labeling of peripheral nerves was not affected in the secondary dystroglycanopathies (not shown), suggesting that the secondary reduction in laminin-α2 is a result of the defect in α-dystroglycan glycosylation specific to the muscle fiber basement membrane rather than that of the peripheral nerve.

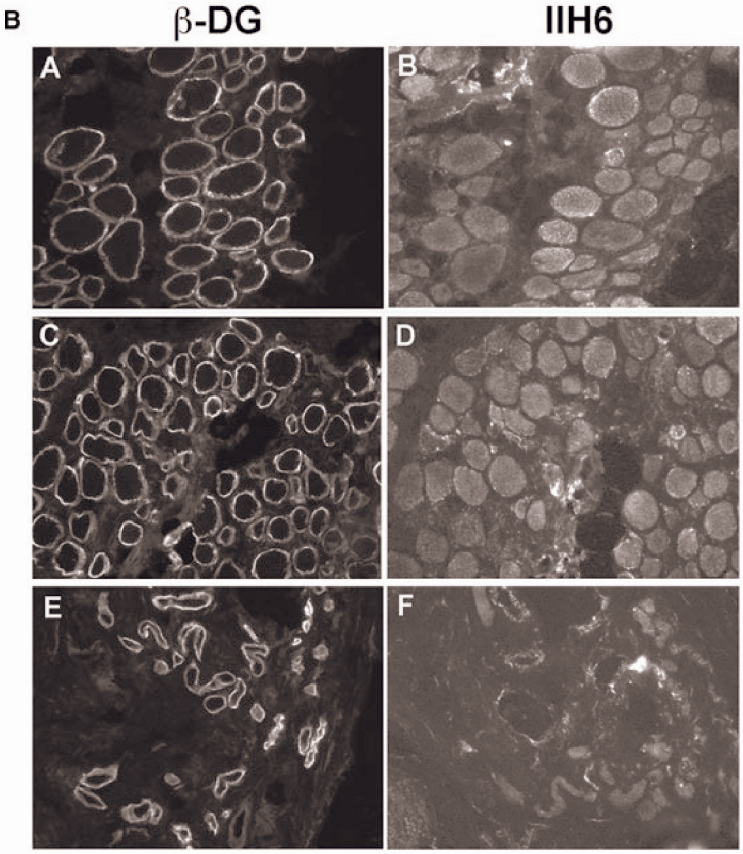

Figure 2. *Continued.*

Antibodies to the core protein of α-dystroglycan

Some of the α-dystroglycan antibodies recognize the primary amino acid sequence in the protein, in theory, independently of whether it is glycosylated or not. Using some of these antibodies [sheep core (20), and IB7 (37)], we and others have previously described a reduction in sarcolemmal labeling that varied from a complete absence to a mild reduction (6, 23, 28, 29).

In the present study, we used a sheep polyclonal antibody raised against the last 20 amino acids of α-dystroglycan (20). In all cases studied, the staining was abnormal, ranging from an absence to a mild reduction (Figures 5 and 7). This reduction often correlated with the level of IIH6 labeling (Table 3). It is not clear if the reduction in labeling with this core antibody is a direct consequence of the hypoglycosylation of α-dystroglycan or the result of the inability of the antibody to bind to the epitope because of masking. A third possibility is that it is a combination of both these possibilities.

In support of the second hypothesis is our observation that studies of cases with either a total or partial primary laminin-α2 deficiency and mutations in the *LAMA2* gene (MDC1A) showed a severe reduction of sarcolemmal labeling with this sheep core antibody (Figure 8). In these MDC1A cases, IIH6 labeling was variable, with only a mild reduction in some fibers but never reduced to the extent observed with the sheep core antibody or to that seen in the dystroglycanopathy cases. Interestingly, in MDC1A patients, the reduction of labeling with the sheep core was independent from the levels of laminin-α2. For example, both the patient shown in Figure 8A–D, who had complete laminin-α2 deficiency, and the patient shown in Figure 8E–H, who had partial laminin-α2 deficiency, had a similar reduction of the sheep core.

In contrast to those findings, the labeling obtained using the core antibody GT20ADG was usually well preserved in dystroglycanopathy patients, compared with IIH6 and sheep core. Only rarely was there some variability with the GT20DAG antibody on fibers with well-preserved β-dystroglycan (Figures 4 and 9). This was most apparent in P8 (*POMT2*; Figure 9A, panel H) and in P12 (*LARGE*; Figure 9B, panel B). In the latter, labeling with GT20DAG was markedly reduced despite preserved β-dystroglycan labeling, suggesting this was not a result of sarcolemmal damage.

Similarly, in the MDC1A cases, the GT20ADG was well preserved, despite the reduction of the sheep core. Unfortunately, we did not have sufficient tissue to perform the wheat germ agglutinin

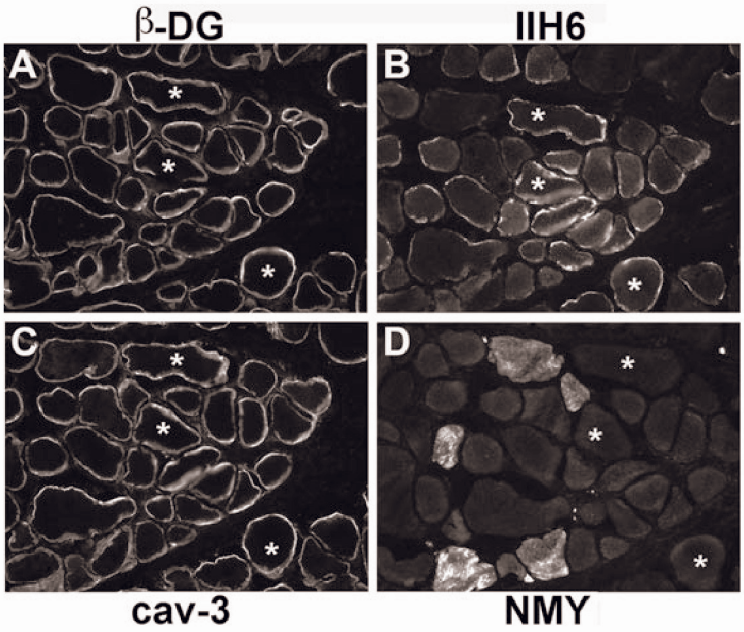

Figure 3. Muscle biopsy from P4 showing that the fibers that are brightly labeled with IIH6 (**B,** asterisks) do not express neonatal myosin (**D**) and their sarcolemma is well preserved [as seen with antibodies to β-dystrolgycan (β-DG) in **A** and caveolin-3 (cav-3) in **C**].

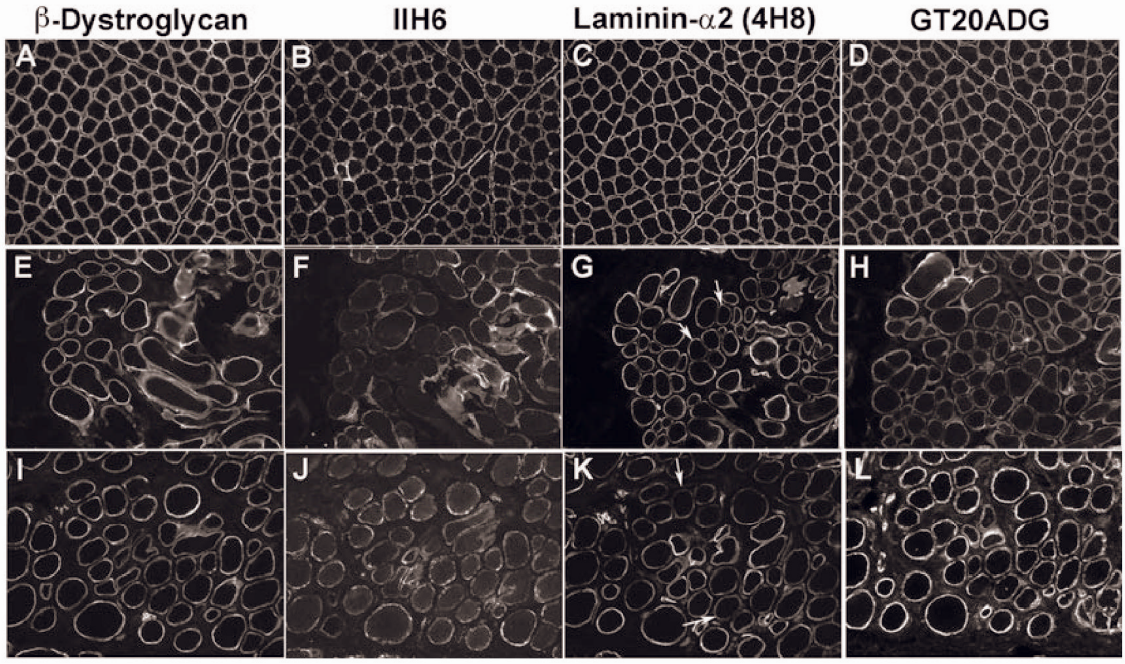

Figure 4. *Muscle biopsy of two patients with mutations in POMT1 and POMT2 with a significant reduction of IIH6 labeling (++).* Laminin-α2 was mildly reduced in some fibers in both patients. **A,E,I.** β-Dystroglycan. **B,F,J.** IIH6. **C,G,K.** Laminin-α2 (4H8 antibody to the N-terminal 300 kDa fragment). **D,H,L.** GT20ADG α-dystroglycan antibody. **A–D:** control; **E–H:** P3; **I–L:** P9. Arrows indicate some of the fibers with reduced laminin-α2 labeling.

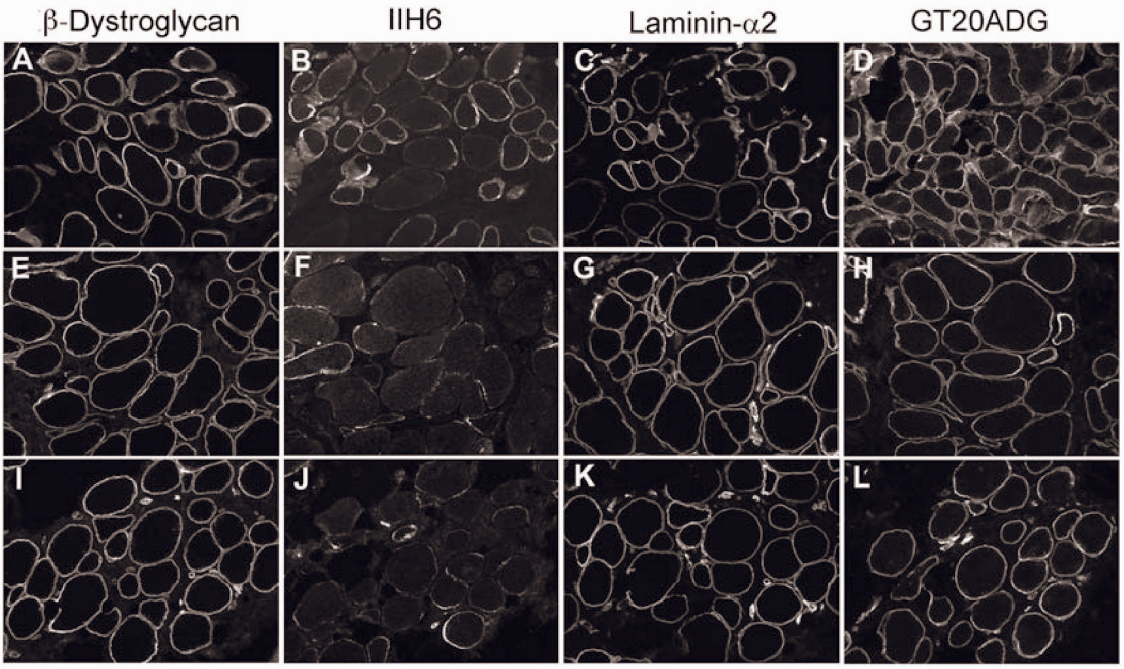

Figure 5. *Muscle biopsy of patients with mutations in FKRP.* **A,E,I.** β-Dystroglycan. **B,F,J.** IIH6. **C,G,K.** Laminin-α2 (4H8 antibody to the N-terminal 300 kDa fragment). **D,H,L.** GT20ADG α-dystroglycan antibody. **A–D:** P18; **E–H:** P20; **I–L:** P21.

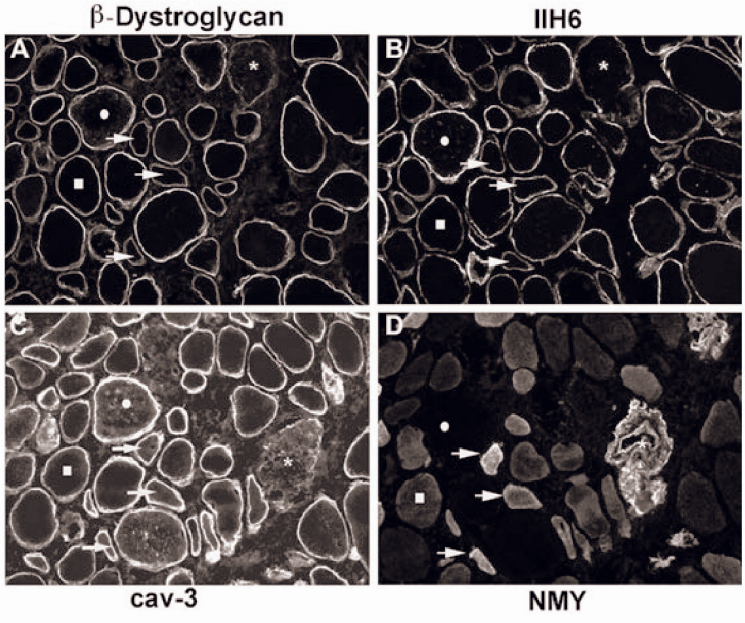

Figure 6. *The biopsy of P11 showed the mildest reduction in IIH6 labeling.* The labeling of individual fibers with antibodies to β-dystroglycan (**A**), IIH6 (**B**), caveolin-3 (cav-3; **C**) and neonatal myosin (NMY; **D**) is compared. A few fibers with reduced IIH6 labeling and normal β-dystroglycan immunoreactivity were seen (squares). Some fibers showed reduced IIH6 and β-dystroglycan and were positive for the neonatal isoform of myosin so they may represent regenerating fibers (arrows). Fibers with low β-dystroglycan, IIH6 and reduced sarcolemmal cav-3 labeling may reflect sarcolemmal damage (asterisks). A population of fibers has marked IIH6 and β-dystroglycan labeling on the cell surface and intracellular labeling of cav-3 but no neonatal myosin labeling (circles).

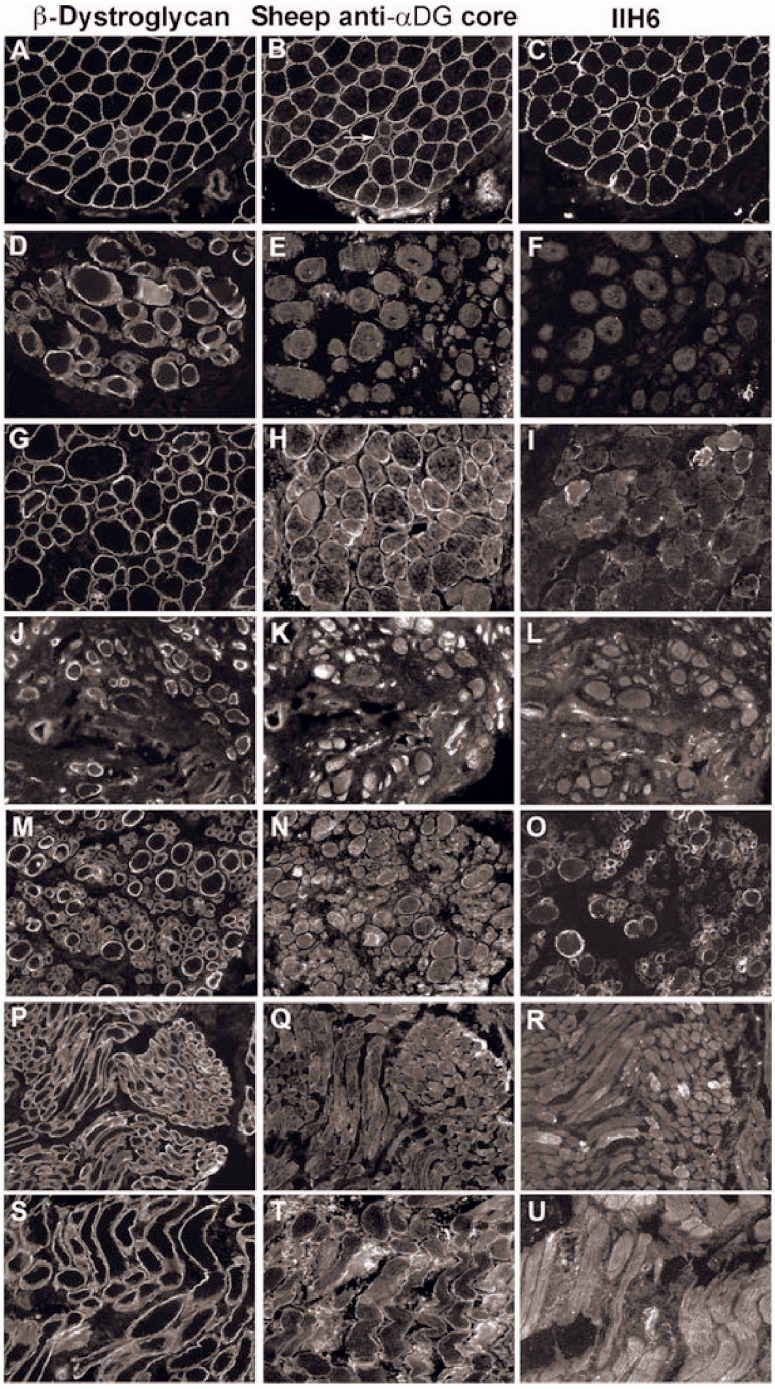

Figure 7. *Spectrum of the reduction in α-dystroglycan labeling using a sheep polyclonal "core" antibody.* **A,D,G,J,M,P,S.** β-Dystroglycan. **B,E,H,K,N,Q,T.** Sheep anti-α-dystroglycan (α-DG) core. **C,F,I,L,O,R,U.** IIH6 antibody. **A–C:** disease control (Becker muscular dystrophy patient showing a group of regenerating fibers with low labeling of both α- and β-dystroglycan; arrow); **D–F:** P1 (*POMT1*); **G–I:** P4 (*POMT1*); **J–L:** P5 (*POMT2*); **M–O:** P8 (*POMT2*); **P–R:** P10 (*POMGnT1*); **S–U:** P15 (*FKRP*).

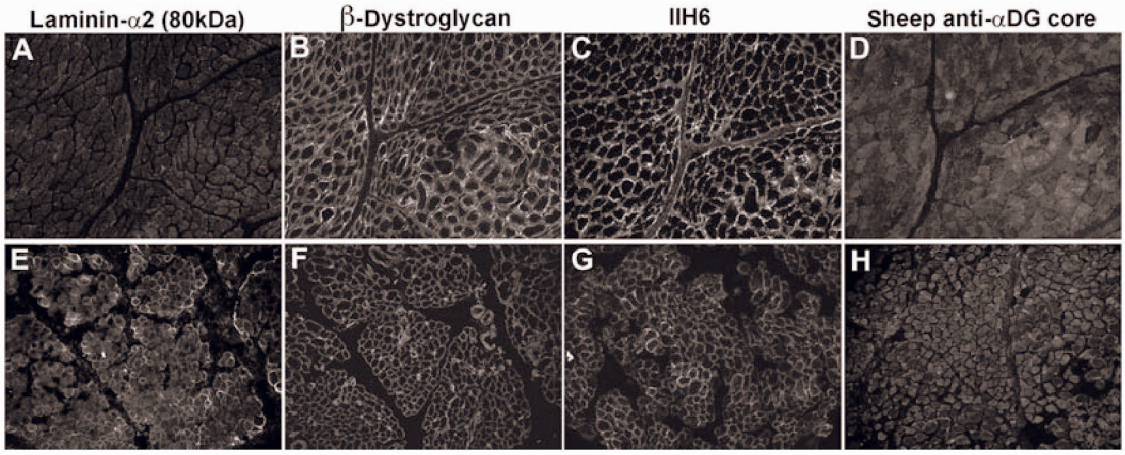

Figure 8. *Cases with confirmed primary laminin-α2-deficient congenital muscular dystrophy.* **A,E.** Laminin-α2 (MAB1922 antibody to the 80 kDa C-terminal fragment). **B,F.** β-Dystroglycan. **C,G.** α-Dystroglycan IIH6. **D,H.** α-Dystroglycan sheep polyclonal core. **A–D:** MDC1A (total absence of laminin-α2); **E–H:** MDC1A (partial laminin-α2 deficiency).

(WGA) purification that is required prior to using this antibody in Western blots.

We found a reduction in β-dystroglycan labeling on the sarcolemma of a proportion of fibers (Table 3). In most cases, these were small and expressed neonatal myosin, suggesting that these were regenerating. It cannot be completely excluded, however, that the whole of the dystrophin-associated glycoprotein complex may be affected in these conditions. As a control for basement membrane preservation, we used antibodies to the laminin-γ1 and laminin-β1 chains. We found that while laminin-γ1 was normal in all cases, laminin-β1 was variably reduced in 10 of the 24 cases. A reduction in laminin-β1 has been reported in other neuromuscular disorders (40).

DISCUSSION

The main conclusions from this study are that irrespective of the primary gene defect, the overall pathology and extent of α-dystroglycan glycosylation in muscle (as determined by the level of IIH6 immunolabeling) is variable. Nevertheless, in this cohort of patients, there was a broad correlation between the amount of glycosylated α-dystroglycan and the severity of the phenotype in patients with mutations in *POMT1*, *POMT2* and *POMGnT1*. The severity of the phenotype in these patients was assigned following the clinical categories described in Godfrey *et al* (19), in which the age of onset of muscle weakness and the presence and severity of brain abnormalities were taken into consideration. It is important to highlight that the limitation of this approach relates to the fact that these clinical categories are based on the combined severity of the skeletal muscle and brain involvement, while in this manuscript we have only studied the glycosylation of α-dystroglycan in the skeletal muscle. In spite of this, there was also a broad correlation between the reduction of glycosylated α-dystroglycan and the maximum motor ability within these gene groups (see Table 1). Patients with mutations in *POMT1*, *POMT2* and *POMGnT1* that achieved independent ambulation showed more α-dystroglycan labeling than those who never walked, while the most severe cases who never acquired the independent sitting position had absent labeling.

In contrast to patients with mutations in *POMT1*, *POMT2* and *POMGnT1*, one patient with *FKRP* mutations (P15) and two patients with mutations in *fukutin* (P13 and P14) and an LGMD phenotype with absent brain involvement, had a complete absence of IIH6 labeling. The mutation in P15 (homozygous p.Pro89Leu) has not previously been reported but it affects a conserved amino acid in *FKRP*, which has been found to be mutated to arginine in a MDC1C patient in combination with a deletion leading to premature termination of translation (31). This patient presented in early infancy following a severe Duchenne-like course. He lost ambulation before 10 years of age. His severity is comparable with that of P21 (*FKRP* mutation; see Table 1), who also lost ambulation at the age of 11. These two patients had, on the whole, a severe depletion of IIH6 immunoreactivity, similar to what we have previously described in nonambulant children with MDC1C (5, 6), despite the fact that they did acquire ambulation. The pattern of IIH6 expression in these two patients and in MDC1C cases is, however, substantially different from the one observed in the majority of the LGMD2I cases who follow a much milder disease course and in whom there appears to be a better correlation between IIH6 expression and clinical severity. For example, P18, P19 and P20, who followed a "typical Becker Muscular Dystrophy (BMD)" course had more IIH6 expression compared with the two DMD-like patients described above but nonetheless showed a significant reduction. Three more LGMD2I patients (P22, P23 and P24), at the milder end of the LGMD phenotype, had well-preserved IIH6 labeling (mosaic pattern) relative to the other LGMD2I cases discussed above (DMD and BMD-like).

We also studied two patients with *fukutin* mutations and an LGMD phenotype. These two patients have been reported previously (18), have no brain involvement and followed a clinical

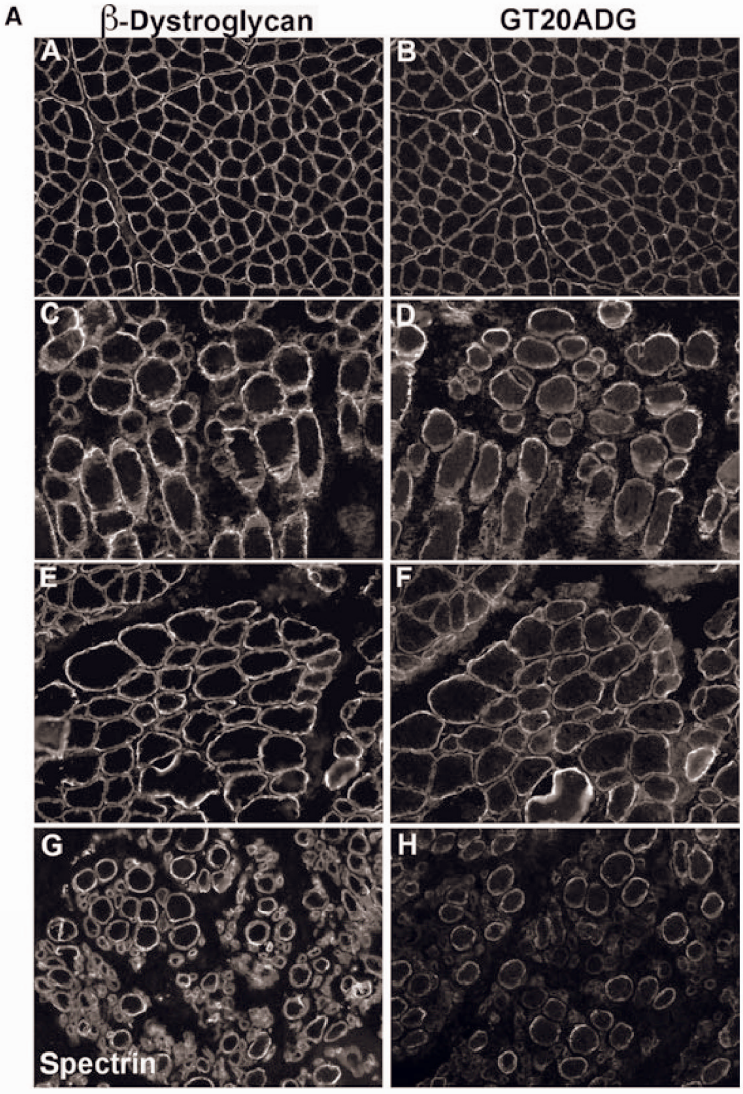

Figure 9. *Immunodetection of α-dystroglycan using GT20ADG antibody.* **A.** A,C,E: β-dystroglycan. G: β-spectrin (as a control of sarcolemma preservation as an adjacent image of β-dystroglycan labeling was not available). B,D,F,H: GT20ADG. A,B: control; C,D: P1 (*POMT1*); E,F: P4 (*POMT1*); G,H: P8 (*POMT2*). **B.** A,C,E,G: β-dystroglycan. B,D,F,H: GT20ADG. A,B: P12 (*LARGE*); C,D: P14 (*fukutin*); E,F: P16 (*FKRP*); G,H: P17 (*FKRP*).

course similar to DMD. As in the *FKRP*-related DMD-like condition, these patients (P14 and P15) had virtual absence of IIH6 labeling. A similar severe depletion of IIH6 has also been observed in other mild *fukutin* patients, as in the cases with dilated cardiomyopathy and minimal muscle weakness described by Murakami *et al* (39). The severity of the IIH6 depletion in these patients contrasts with their disease course. The reason for the relatively limited pathology and the mild phenotypes is unclear but it could relate to the presence of additional laminin-α2-binding epitope(s) on α-dystroglycan, which are not recognized by the IIH6 antibody (32).

Although this cohort of patients encompassed a wide range of phenotypes, it did not include the mildest end of the cases with *POMT2* spectrum, as recently described by Biancheri *et al* (3), who displayed an early-onset LGMD without mental retardation and severely reduced α-dystroglycan labeling with another antibody directed against the glycosylated epitope VIA4-1. Likewise, we have not been able to assess any correlations in cases with mutations in *LARGE* as too few have been identified. The patient described here showed a moderate reduction of IIH6 labeling (28), although we have identified mutations in *LARGE* in a patient with a severe WWS phenotype in whom absence of IIH6 was demonstrated in another center (19). Other cases with mutations in *LARGE* have recently been reported but no immunohistochemical studies were reported (44).

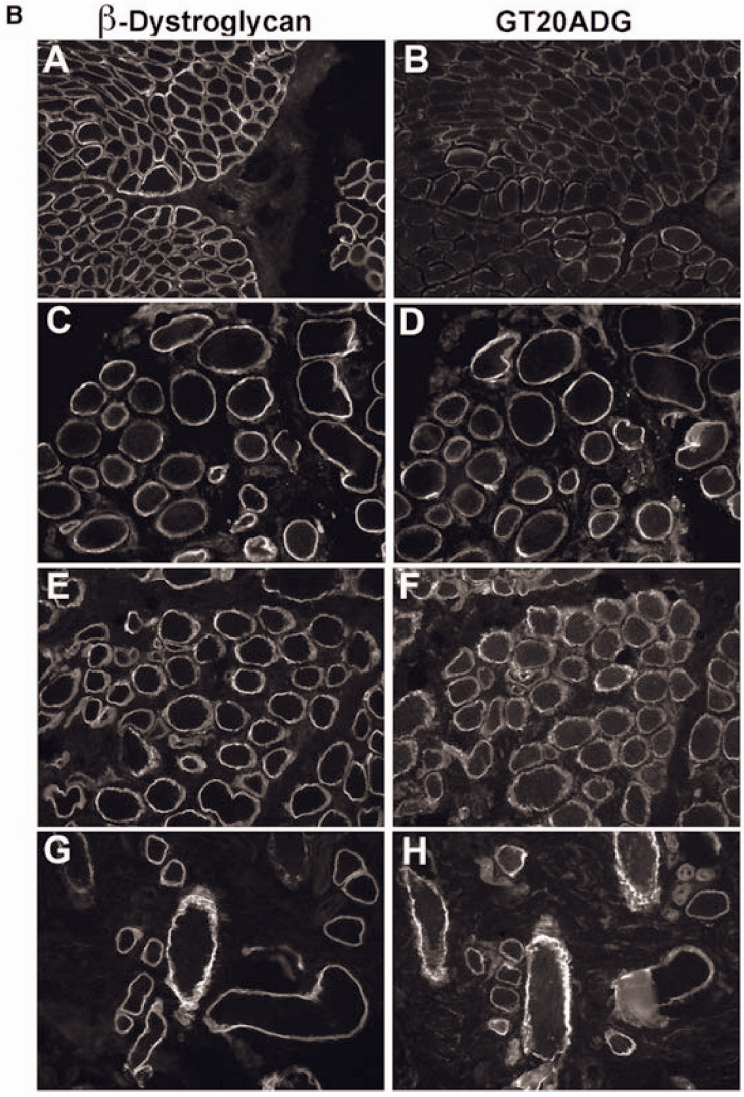

Figure 9. *Continued.*

In P11, the variant p.Asp556Asn was detected in *POMGnT1* along with an altered kinetic profile (12). Very recently, we have become aware that this sequence alteration has been detected in a French family, heterozygously in a patient with MEB yet homozygously in the apparently unaffected sibling. In addition, the variant was detected heterozygously in eight out of 218 alleles from healthy French controls (Céline Bouchet, unpub. obs.). We are carrying out further work to characterize this finding that, however, may point to a secondary reduction in *POMGnT1* activity.

The present studies draw attention to the significantly different patterns of immunolabeling obtained with the so-called "core" α-dystroglycan antibodies and indicate that more studies are needed to understand what they exactly recognize and their significance in the context of dystroglycanopathies. The absence of one of these epitopes in primary laminin-α2 deficiency may provide important clues. As previous work has shown that the glycosylation of α-dystroglycan is extremely complex and that a number of different glycoforms are known to exist in muscle (33), which may be differentially affected by different gene mutations. The generation of new antibodies to known glycosylated epitopes will undoubtedly help clarify some of these issues.

In summary, the present study highlights the limitations of interpreting the extent of α-dystroglycan functionality by evaluating a single epitope, albeit one, that identifies the laminin-binding site. Despite these limitations, we found that α-dystroglycan labeling broadly correlated with clinical severity in cases with

mutations in *POMT1*, *POMT2* and *POMGnT1* mutations and also within each gene group. However, this conclusion could not always be extended to patients with *FKRP* or *fukutin* mutations. Although the function of *FKRP* and *fukutin* are still unknown, our findings indicate that their role in α-dystroglycan glycosylation may be different or broader than that of *POMT1*, *POMT2* and *POMGnT1*, whose enzymatic activity has been demonstrated. The identification of patients with *FKRP* and *fukutin* mutations and a relatively mild muscle phenotype despite absent IIH6 labeling suggests that disruption of the laminin–α-dystroglycan interaction in muscle, as recognized by the IIH6 antibody, might not be the sole pathological mechanism of disease and that in patients with a severe phenotype, other mechanisms may also operate.

ACKNOWLEDGMENTS

We are grateful to the National Commissioning Group (NCG) Department of Health UK for their financial support. C.G. and E.C. are funded by the Muscular Dystrophy Campaign (RA3/734 and PO0916 respectively). B.T. is funded by Hacettepe University Research Grant 02G129.

REFERENCES

1. Balci B, Uyanik G, Dincer P, Gross C, Willer T, Talim B *et al* (2005) An autosomal recessive limb girdle muscular dystrophy (lgmd2) with mild mental retardation is allelic to Walker-Warburg syndrome (WWS) caused by a mutation in the pomt1 gene. *Neuromuscul Disord* **15**:271–275.
2. Barresi R, Campbell KP (2006) Dystroglycan: from biosynthesis to pathogenesis of human disease. *J Cell Sci* **119**:199–207.
3. Biancheri R, Falace A, Tessa A, Pedemonte M, Scapolan S, Cassandrini D *et al* (2007) POMT2 gene mutation in limb-girdle muscular dystrophy with inflammatory changes. *Biochem Biophys Res Commun* **363**:1033–1037.
4. Brockington M, Blake DJ, Prandini P, Brown SC, Torelli S, Benson MA *et al* (2001) Mutations in the fukutin-related protein gene (FKRP) cause a form of congenital muscular dystrophy with secondary laminin alpha2 deficiency and abnormal glycosylation of alpha-dystroglycan. *Am J Hum Genet* **69**:1198–1209.
5. Brockington M, Yuva Y, Prandini P, Brown SC, Torelli S, Benson MA *et al* (2001) Mutations in the fukutin-related protein gene (FKRP) identify limb girdle muscular dystrophy 2I as a milder allelic variant of congenital muscular dystrophy MDC1C. *Hum Mol Genet* **10**:2851–2859.
6. Brown SC, Fassati A, Popplewell L, Page AM, Henry MD, Campbell KP, Dickson G (1999) Dystrophic phenotype induced *in vitro* by antibody blockade of muscle alpha-dystroglycan-laminin interaction. *J Cell Sci* **112**:209–216.
7. Brown SC, Torelli S, Brockington M, Yuva Y, Jimenez C, Feng L *et al* (2004) Abnormalities in alpha-dystroglycan expression in MDC1C and LGMD2I muscular dystrophies. *Am J Pathol* **164**:727–737.
8. Bushby K, Anderson LV, Pollitt C, Naom I, Muntoni F, Bindoff L (1998) Abnormal merosin in adults. A new form of late onset muscular dystrophy not linked to chromosome 6q2. *Brain* **121**:581–588.
9. Chen YJ, Spence HJ, Cameron JM, Jess T, Ilsley JL, Winder SJ (2003) Direct interaction of beta-dystroglycan with F-actin. *Biochem J* **375**:329–337.
10. Chiba A, Matsumura K, Yamada H, Inazu T, Shimizu T, Kusunoki S *et al* (1997) Structures of sialylated O-linked oligosaccharides of bovine peripheral nerve alpha-dystroglycan. The role of a novel O-mannosyl-type oligosaccharide in the binding of alpha-dystroglycan with laminin. *J Biol Chem* **272**: 2156–2162.
11. Chiyonobu T, Sasaki J, Nagai Y, Takeda S, Funakoshi H, Nakamura T *et al* (2005) Effects of fukutin deficiency in the developing mouse brain. *Neuromuscul Disord* **15**:416–426.
12. Clement EM, Godfrey C, Tan J, Brockington M, Torelli S, Feng L *et al* (2008) Mild POMGnT1 mutations underlie a novel limb-girdle muscular dystrophy variant. *Arch Neurol* **65**:137–141.
13. Colognato H, Yurchenco PD (2000) Form and function: the laminin family of heterotrimers. *Dev Dyn* **218**:213–234.
14. D'Amico A, Tessa A, Bruno C, Petrini S, Biancheri R, Pane M *et al* (2006) Expanding the clinical spectrum of POMT1 phenotype. *Neurology* **66**:1564–1567; discussion 461.
15. Dubowitz VSC (2007) *Muscle Biopsy: A Practical Approach*, 3rd edn. Saunders Elsevier: London.
16. Ervasti JM, Campbell KP (1993) A role for the dystrophin-glycoprotein complex as a transmembrane linker between laminin and actin. *J Cell Biol* **122**:809–823.
17. Esapa CT, Bentham GR, Schroder JE, Kroger S, Blake DJ (2003) The effects of post-translational processing on dystroglycan synthesis and trafficking. *FEBS Lett* **555**:209–216.
18. Godfrey C, Escolar D, Brockington M, Clement EM, Mein R, Jimenez-Mallebrera C *et al* (2006) Fukutin gene mutations in steroid-responsive limb girdle muscular dystrophy. *Ann Neurol* **60**:603–610.
19. Godfrey C, Clement E, Mein R, Brockington M, Smith J, Talim B *et al* (2007) Refining genotype phenotype correlations in muscular dystrophies with defective glycosylation of dystroglycan. *Brain* **130**:2725–2735.
20. Herrmann R, Straub V, Blank M, Kutzick C, Franke N, Jacob EN *et al* (2000) Dissociation of the dystroglycan complex in caveolin-3-deficient limb girdle muscular dystrophy. *Hum Mol Genet* **9**:2335–2340.
21. Holt KH, Crosbie RH, Venzke DP, Campbell KP (2000) Biosynthesis of dystroglycan: processing of a precursor propeptide. *FEBS Lett* **468**:79–83.
22. Jayasinha V, Nguyen HH, Xia B, Kammesheidt A, Hoyte K, Martin PT (2003) Inhibition of dystroglycan cleavage causes muscular dystrophy in transgenic mice. *Neuromuscul Disord* **13**:365–375.
23. Jimenez-Mallebrera C, Torelli S, Brown SC, Feng L, Brockington M, Sewry CA *et al* (2003) Profound skeletal muscle depletion of alpha-dystroglycan in Walker-Warburg syndrome. *Eur J Paediatr Neurol* **7**:129–137.
24. Jimenez-Mallebrera C, Brown SC, Sewry CA, Muntoni F (2005) Congenital muscular dystrophy: molecular and cellular aspects. *Cell Mol Life Sci* **62**:809–823.
25. Jung D, Yang B, Meyer J, Chamberlain JS, Campbell KP (1995) Identification and characterization of the dystrophin anchoring site on beta-dystroglycan. *J Biol Chem* **270**:27305–27310.
26. Kondo-Iida E, Kobayashi K, Watanabe M, Sasaki J, Kumagai T, Koide H *et al* (1999) Novel mutations and genotype-phenotype relationships in 107 families with Fukuyama-type congenital muscular dystrophy (FCMD). *Hum Mol Genet* **8**:2303–2309.
27. Kunz S, Sevilla N, McGavern DB, Campbell KP, Oldstone MB (2001) Molecular analysis of the interaction of LCMV with its cellular receptor [alpha]-dystroglycan. *J Cell Biol* **155**:301–310.
28. Longman C, Brockington M, Torelli S, Jimenez-Mallebrera C, Kennedy C, Khalil N *et al* (2003) Mutations in the human LARGE gene cause MDC1D, a novel form of congenital muscular dystrophy

with severe mental retardation and abnormal glycosylation of alpha-dystroglycan. *Hum Mol Genet* **12**:2853–2861.
29. Longman C, Mercuri E, Cowan F, Allsop J, Brockington M, Jimenez-Mallebrera C *et al* (2004) Antenatal and postnatal brain magnetic resonance imaging in muscle-eye-brain disease. *Arch Neurol* **61**:1301–1306.
30. Martin PT (2006) Mechanisms of disease: congenital muscular dystrophies-glycosylation takes center stage. *Nat Clin Pract Neurol* **2**:222–230.
31. Matsumoto H, Hayashi YK, Kim DS, Ogawa M, Murakami T, Noguchi S *et al* (2005) Congenital muscular dystrophy with glycosylation defects of alpha-dystroglycan in Japan. *Neuromuscul Disord* **15**:342–348.
32. McDearmon EL, Combs AC, Ervasti JM (2001) Differential Vicia villosa agglutinin reactivity identifies three distinct dystroglycan complexes in skeletal muscle. *J Biol Chem* **276**:35078–35086.
33. McDearmon EL, Combs AC, Sekiguchi K, Fujiwara H, Ervasti JM (2006) Brain alpha-dystroglycan displays unique glycoepitopes and preferential binding to laminin-10/11. *FEBS Lett* **580**:3381–3385.
34. Mercuri E, D'Amico A, Tessa A, Berardinelli A, Pane M, Messina S *et al* (2006) POMT2 mutation in a patient with "MEB-like" phenotype. *Neuromuscul Disord* **16**:446–448.
35. Michele DE, Barresi R, Kanagawa M, Saito F, Cohn RD, Satz JS *et al* (2002) Post-translational disruption of dystroglycan-ligand interactions in congenital muscular dystrophies. *Nature* **418**:417–422.
36. Moore SA, Saito F, Chen J, Michele DE, Henry MD, Messing A *et al* (2002) Deletion of brain dystroglycan recapitulates aspects of congenital muscular dystrophy. *Nature* **418**:422–425.
37. Moukhles H, Roque R, Carbonetto S (2000) Alpha-dystroglycan isoforms are differentially distributed in adult rat retina. *J Comp Neurol* **420**:182–194.
38. Muntoni F, Brockington M, Blake DJ, Torelli S, Brown SC (2002) Defective glycosylation in muscular dystrophy. *Lancet* **360**:1419–1421.
39. Murakami T, Hayashi YK, Noguchi S, Ogawa M, Nonaka I, Tanabe Y *et al* (2006) Fukutin gene mutations cause dilated cardiomyopathy with minimal muscle weakness. *Ann Neurol* **60**:597–602.
40. Sewry CA, Brown SC, Mercuri E, Bonne G, Feng L, Camici G *et al* (2001) Skeletal muscle pathology in autosomal dominant Emery-Dreifuss muscular dystrophy with lamin A/C mutations. *Neuropathol Appl Neurobiol* **27**:281–290.
41. Talim B, Ferreiro A, Cormand B, Vignier N, Oto A, Gogus S *et al* (2000) Merosin-deficient congenital muscular dystrophy with mental retardation and cerebellar cysts unlinked to the LAMA2, FCMD and MEB loci. *Neuromuscul Disord* **10**:548–552.
42. Toda T, Chiyonobu T, Xiong H, Tachikawa M, Kobayashi K, Manya H *et al* (2005) Fukutin and alpha-dystroglycanopathies. *Acta Myol* **24**:60–63.
43. Topaloglu H, Brockington M, Yuva Y, Talim B, Haliloglu G, Blake D *et al* (2003) FKRP gene mutations cause congenital muscular dystrophy, mental retardation, and cerebellar cysts. *Neurology* **60**:988–992.
44. van Reeuwijk J, Grewal PK, Salih MA, Beltran-Valero de Bernabe D, McLaughlan JM, Michielse CB *et al* (2007) Intragenic deletion in the LARGE gene causes Walker-Warburg syndrome. *Hum Genet* **121**:685–690.
45. Williamson RA, Henry MD, Daniels KJ, Hrstka RF, Lee JC, Sunada Y *et al* (1997) Dystroglycan is essential for early embryonic development: disruption of Reichert's membrane in Dag1-null mice. *Hum Mol Genet* **6**:831–841.
46. Winder SJ (2001) The complexities of dystroglycan. *Trends Biochem Sci* **26**:118–124.
47. Yurchenco PD, Cheng YS, Campbell K, Li S (2004) Loss of basement membrane, receptor and cytoskeletal lattices in a laminin-deficient muscular dystrophy. *J Cell Sci* **117**:735–742.

REFERENCES

Abbott KL, Troupe K, Lee I, Pierce M. Integrin-dependent neuroblastoma cell adhesion and migration on laminin is regulated by expression levels of two enzymes in the O-mannosyl-linked glycosylation pathway, PomGnT1 and GnT-Vb. Exp Cell Res 2006; 312: 2837-50.

Ackroyd MR, Skordis L, Kaluarachchi M, Godwin J, Prior S, Fidanboylu M, et al. Reduced expression of fukutin related protein in mice results in a model for fukutin related protein associated muscular dystrophies. Brain 2009; 132: 439-51.

Aerts S, Lambrechts D, Maity S, Van Loo P, Coessens B, De Smet F, et al. Gene prioritization through genomic data fusion. Nat Biotechnol 2006; 24: 537-44.

Akasaka-Manya K, Manya H, Kobayashi K, Toda T, Endo T. Structure-function analysis of human protein O-linked mannose beta1,2-N-acetylglucosaminyltransferase 1, POMGnT1. Biochem Biophys Res Commun 2004; 320: 39-44.

Akhavan A, Crivelli SN, Singh M, Lingappa VR, Muschler JL. SEA domain proteolysis determines the functional composition of dystroglycan. Faseb J 2008; 22: 612-21.

Aravind L, Koonin EV. The fukutin protein family--predicted enzymes modifying cell-surface molecules. Curr Biol 1999; 9: R836-7.

Ashton EJ, Yau SC, Deans ZC, Abbs SJ. Simultaneous mutation scanning for gross deletions, duplications and point mutations in the DMD gene. Eur J Hum Genet 2008; 16: 53-61.

Attali R, Warwar N, Israel A, Gurt I, McNally E, Puckelwartz M, et al. Mutation of SYNE-1, encoding an essential component of the nuclear lamina, is responsible for autosomal recessive arthrogryposis. Hum Mol Genet 2009; 18: 3462-9.

Balci B, Uyanik G, Dincer P, Gross C, Willer T, Talim B, et al. An autosomal recessive limb girdle muscular dystrophy (LGMD2) with mild mental retardation is allelic to Walker-Warburg syndrome (WWS) caused by a mutation in the POMT1 gene. Neuromuscul Disord 2005; 15: 271-5.

Bao X, Kobayashi M, Hatakeyama S, Angata K, Gullberg D, Nakayama J, et al. Tumor suppressor function of laminin-binding alpha-dystroglycan requires a distinct beta3-N-acetylglucosaminyltransferase. Proc Natl Acad Sci U S A 2009; 106: 12109-14.

Barresi R, Campbell KP. Dystroglycan: from biosynthesis to pathogenesis of human disease. J Cell Sci 2006; 119: 199-207.

Barresi R, Michele DE, Kanagawa M, Harper HA, Dovico SA, Satz JS, et al. LARGE can functionally bypass alpha-dystroglycan glycosylation defects in distinct congenital muscular dystrophies. Nat Med 2004; 10: 696-703.

Beedle AM, Nienaber PM, Campbell KP. Fukutin-related protein associates with the sarcolemmal dystrophin-glycoprotein complex. J Biol Chem 2007; 282: 16713-7.

Beltran-Valero de Bernabe D, Currier S, Steinbrecher A, Celli J, van Beusekom E, van der Zwaag B, et al. Mutations in the O-mannosyltransferase gene POMT1 give rise to the severe neuronal migration disorder Walker-Warburg syndrome. Am J Hum Genet 2002; 71: 1033-43.

Beltran-Valero de Bernabe D, Voit T, Longman C, Steinbrecher A, Straub V, Yuva Y, et al. Mutations in the FKRP gene can cause muscle-eye-brain disease and Walker-Warburg syndrome. J Med Genet 2004; 41: e61.

Berkovic SF, Dibbens LM, Oshlack A, Silver JD, Katerelos M, Vears DF, et al. Array-based gene discovery with three unrelated subjects shows SCARB2/LIMP-2 deficiency causes myoclonus epilepsy and glomerulosclerosis. Am J Hum Genet 2008; 82: 673-84.

Bonne G, Di Barletta MR, Varnous S, Becane HM, Hammouda EH, Merlini L, et al. Mutations in the gene encoding lamin A/C cause autosomal dominant Emery-Dreifuss muscular dystrophy. Nat Genet 1999; 21: 285-8.

Bouchet C, Gonzales M, Vuillaumier-Barrot S, Devisme L, Lebizec C, Alanio E, et al. Molecular heterogeneity in fetal forms of type II lissencephaly. Hum Mutat 2007; 28: 1020-7.

Bowe MA, Mendis DB, Fallon JR. The small leucine-rich repeat proteoglycan biglycan binds to alpha-dystroglycan and is upregulated in dystrophic muscle. J Cell Biol 2000; 148: 801-10.

Brancaccio A, Schulthess T, Gesemann M, Engel J. Electron microscopic evidence for a mucin-like region in chick muscle alpha-dystroglycan. FEBS Lett 1995; 368: 139-42.

Brancaccio A, Schulthess T, Gesemann M, Engel J. The N-terminal region of alpha-dystroglycan is an autonomous globular domain. Eur J Biochem 1997; 246: 166-72.

Breton C, Imberty A. Structure/function studies of glycosyltransferases. Curr Opin Struct Biol 1999; 9: 563-71.

Brockington M, Blake DJ, Prandini P, Brown SC, Torelli S, Benson MA, et al. Mutations in the fukutin-related protein gene (FKRP) cause a form of congenital muscular dystrophy with secondary laminin alpha2 deficiency and abnormal glycosylation of alpha-dystroglycan. Am J Hum Genet 2001a; 69: 1198-209.

Brockington M, Muntoni F. The modulation of skeletal muscle glycosylation as a potential therapeutic intervention in muscular dystrophies. Acta Myol 2005; 24: 217-21.

Brockington M, Sewry CA, Herrmann R, Naom I, Dearlove A, Rhodes M, et al. Assignment of a form of congenital muscular dystrophy with secondary merosin deficiency to chromosome 1q42. Am J Hum Genet 2000; 66: 428-35.

Brockington M, Torelli S, Prandini P, Boito C, Dolatshad NF, Longman C, et al. Localization and functional analysis of the LARGE family of glycosyltransferases: significance for muscular dystrophy. Hum Mol Genet 2005; 14: 657-65.

Brockington M, Yuva Y, Prandini P, Brown SC, Torelli S, Benson MA, et al. Mutations in the fukutin-related protein gene (FKRP) identify limb girdle muscular dystrophy 2I as a milder allelic variant of congenital muscular dystrophy MDC1C. Hum Mol Genet 2001b; 10: 2851-9.

Brown SC, Fassati A, Popplewell L, Page AM, Henry MD, Campbell KP, et al. Dystrophic phenotype induced in vitro by antibody blockade of muscle alpha-dystroglycan-laminin interaction. J Cell Sci 1999; 112 (Pt 2): 209-16.

Brown SC, Piercy RJ, Muntoni F, Sewry CA. Investigating the pathology of Emery-Dreifuss muscular dystrophy. Biochem Soc Trans 2008; 36: 1335-8.

Brown SC, Torelli S, Brockington M, Yuva Y, Jimenez C, Feng L, et al. Abnormalities in alpha-dystroglycan expression in MDC1C and LGMD2I muscular dystrophies. Am J Pathol 2004; 164: 727-37.

Browning CA, Grewal PK, Moore CJ, Hewitt JE. A rapid PCR method for genotyping the Large(myd) mouse, a model of glycosylation-deficient congenital muscular dystrophy. Neuromuscul Disord 2005; 15: 331-5.

Bushby KM, Beckmann JS. The limb-girdle muscular dystrophies--proposal for a new nomenclature. Neuromuscul Disord 1995; 5: 337-43.

Campanelli JT, Roberds SL, Campbell KP, Scheller RH. A role for dystrophin-associated glycoproteins and utrophin in agrin-induced AChR clustering. Cell 1994; 77: 663-74.

Cao W, Henry MD, Borrow P, Yamada H, Elder JH, Ravkov EV, et al. Identification of alpha-dystroglycan as a receptor for lymphocytic choriomeningitis virus and Lassa fever virus. Science 1998; 282: 2079-81.

Capell BC, Collins FS. Human laminopathies: nuclei gone genetically awry. Nat Rev Genet 2006; 7: 940-52.

Cartaud A, Coutant S, Petrucci TC, Cartaud J. Evidence for in situ and in vitro association between beta-dystroglycan and the subsynaptic 43K rapsyn protein. Consequence for acetylcholine receptor clustering at the synapse. J Biol Chem 1998; 273: 11321-6.

Chai W, Yuen CT, Kogelberg H, Carruthers RA, Margolis RU, Feizi T, et al. High prevalence of 2-mono- and 2,6-di-substituted manol-terminating sequences among O-glycans released from brain glycopeptides by reductive alkaline hydrolysis. Eur J Biochem 1999; 263: 879-88.

Chan YM, Bonnemann CG, Lidov HG, Kunkel LM. Molecular organization of sarcoglycan complex in mouse myotubes in culture. J Cell Biol 1998; 143: 2033-44.

Chiba A, Matsumura K, Yamada H, Inazu T, Shimizu T, Kusunoki S, et al. Structures of sialylated O-linked oligosaccharides of bovine peripheral nerve alpha-dystroglycan. The role of a novel O-mannosyl-type oligosaccharide in the binding of alpha-dystroglycan with laminin. J Biol Chem 1997; 272: 2156-62.

Chung W, Campanelli JT. WW and EF hand domains of dystrophin-family proteins mediate dystroglycan binding. Mol Cell Biol Res Commun 1999; 2: 162-71.

Clement E, Mercuri E, Godfrey C, Smith J, Robb S, Kinali M, et al. Brain involvement in muscular dystrophies with defective dystroglycan glycosylation. Ann Neurol 2008a; 64: 573-82.

Clement EM, Godfrey C, Tan J, Brockington M, Torelli S, Feng L, et al. Mild POMGnT1 mutations underlie a novel limb-girdle muscular dystrophy variant. Arch Neurol 2008b; 65: 137-41.

Cohen MW, Jacobson C, Yurchenco PD, Morris GE, Carbonetto S. Laminin-induced clustering of dystroglycan on embryonic muscle cells: comparison with agrin-induced clustering. J Cell Biol 1997; 136: 1047-58.

Cohn RD, Henry MD, Michele DE, Barresi R, Saito F, Moore SA, et al. Disruption of DAG1 in differentiated skeletal muscle reveals a role for dystroglycan in muscle regeneration. Cell 2002; 110: 639-48.

Colombo R, Bignamini AA, Carobene A, Sasaki J, Tachikawa M, Kobayashi K, et al. Age and origin of the FCMD 3'-untranslated-region retrotransposal insertion mutation causing Fukuyama-type congenital muscular dystrophy in the Japanese population. Hum Genet 2000; 107: 559-67.

Cormand B, Pihko H, Bayes M, Valanne L, Santavuori P, Talim B, et al. Clinical and genetic distinction between Walker-Warburg syndrome and muscle-eye-brain disease. Neurology 2001; 56: 1059-69.

Cote PD, Moukhles H, Lindenbaum M, Carbonetto S. Chimaeric mice deficient in dystroglycans develop muscular dystrophy and have disrupted myoneural synapses. Nat Genet 1999; 23: 338-42.

Coutinho PM, Deleury E, Davies GJ, Henrissat B. An evolving hierarchical family classification for glycosyltransferases. J Mol Biol 2003; 328: 307-17.

Crisp M, Liu Q, Roux K, Rattner JB, Shanahan C, Burke B, et al. Coupling of the nucleus and cytoplasm: role of the LINC complex. J Cell Biol 2006; 172: 41-53.

Currier SC, Lee CK, Chang BS, Bodell AL, Pai GS, Job L, et al. Mutations in POMT1 are found in a minority of patients with Walker-Warburg syndrome. Am J Med Genet A 2005; 133A: 53-7.

Davies KE, Nowak KJ. Molecular mechanisms of muscular dystrophies: old and new players. Nat Rev Mol Cell Biol 2006; 7: 762-73.

Davies KE, Pearson PL, Harper PS, Murray JM, O'Brien T, Sarfarazi M, et al. Linkage analysis of two cloned DNA sequences flanking the Duchenne muscular dystrophy locus on the short arm of the human X chromosome. Nucleic Acids Res 1983; 11: 2303-12.

de Bernabe DB, van Bokhoven H, van Beusekom E, Van den Akker W, Kant S, Dobyns WB, et al. A homozygous nonsense mutation in the fukutin gene causes a Walker-Warburg syndrome phenotype. J Med Genet 2003; 40: 845-8.

Dean FB, Hosono S, Fang L, Wu X, Faruqi AF, Bray-Ward P, et al. Comprehensive human genome amplification using multiple displacement amplification. Proc Natl Acad Sci U S A 2002; 99: 5261-6.

Diesen C, Saarinen A, Pihko H, Rosenlew C, Cormand B, Dobyns WB, et al. POMGnT1 mutation and phenotypic spectrum in muscle-eye-brain disease. J Med Genet 2004; 41: e115.

Dubowitz V, Sewry C. Muscle Biopsy: A practical approach: Saunders, 2006.

Dubowitz V, Sewry CA. Muscle Biopsy- A Practical Approach: Saunders, 2007.

Dudanova I, Sedej S, Ahmad M, Masius H, Sargsyan V, Zhang W, et al. Important contribution of alpha-neurexins to Ca2+-triggered exocytosis of secretory granules. J Neurosci 2006; 26: 10599-613.

Endo T. O-mannosyl glycans in mammals. Biochim Biophys Acta 1999; 1473: 237-46.

Ervasti JM, Campbell KP. Membrane organization of the dystrophin-glycoprotein complex. Cell 1991; 66: 1121-31.

Ervasti JM, Campbell KP. A role for the dystrophin-glycoprotein complex as a transmembrane linker between laminin and actin. J Cell Biol 1993; 122: 809-23.

Ervasti JM, Ohlendieck K, Kahl SD, Gaver MG, Campbell KP. Deficiency of a glycoprotein component of the dystrophin complex in dystrophic muscle. Nature 1990; 345: 315-9.

Esapa CT, Benson MA, Schroder JE, Martin-Rendon E, Brockington M, Brown SC, et al. Functional requirements for fukutin-related protein in the Golgi apparatus. Hum Mol Genet 2002; 11: 3319-31.

Evans DM, Cardon LR. Guidelines for genotyping in genomewide linkage studies: single-nucleotide-polymorphism maps versus microsatellite maps. Am J Hum Genet 2004; 75: 687-92.

Freeze HH. Genetic defects in the human glycome. Nat Rev Genet 2006; 7: 537-51.

Frosk P, Greenberg CR, Tennese AA, Lamont R, Nylen E, Hirst C, et al. The most common mutation in FKRP causing limb girdle muscular dystrophy type 2I (LGMD2I) may have occurred only once and is present in Hutterites and other populations. Hum Mutat 2005; 25: 38-44.

Godfrey C, Clement E, Mein R, Brockington M, Smith J, Talim B, et al. Refining genotype phenotype correlations in muscular dystrophies with defective glycosylation of dystroglycan. Brain 2007; 130: 2725-35.

Godfrey C, Escolar D, Brockington M, Clement EM, Mein R, Jimenez-Mallebrera C, et al. Fukutin gene mutations in steroid-responsive limb girdle muscular dystrophy. Ann Neurol 2006; 60: 603-10.

Grewal PK, Holzfeind PJ, Bittner RE, Hewitt JE. Mutant glycosyltransferase and altered glycosylation of alpha-dystroglycan in the myodystrophy mouse. Nat Genet 2001; 28: 151-4.

Grewal PK, McLaughlan JM, Moore CJ, Browning CA, Hewitt JE. Characterization of the LARGE family of putative glycosyltransferases associated with dystroglycanopathies. Glycobiology 2005; 15: 912-23.

Groh S, Zong H, Goddeeris MM, Lebakken CS, Venzke D, Pessin JE, et al. Sarcoglycan complex: implications for metabolic defects in muscular dystrophies. J Biol Chem 2009; 284: 19178-82.

Gros-Louis F, Dupre N, Dion P, Fox MA, Laurent S, Verreault S, et al. Mutations in SYNE1 lead to a newly discovered form of autosomal recessive cerebellar ataxia. Nat Genet 2007; 39: 80-5.

Gruenbaum Y, Margalit A, Goldman RD, Shumaker DK, Wilson KL. The nuclear lamina comes of age. Nat Rev Mol Cell Biol 2005; 6: 21-31.

Guglieri M, Straub V, Bushby K, Lochmuller H. Limb-girdle muscular dystrophies. Curr Opin Neurol 2008; 21: 576-84.

Hammerle MM, Aleksandrov AA, Chang XB, Riordan JR. A novel CFTR disease-associated mutation causes addition of an extra N-linked oligosaccharide. Glycoconj J 2000; 17: 807-13.

Harel T, Goldberg Y, Shalev SA, Chervinski I, Ofir R, Birk OS. Limb-girdle muscular dystrophy 2I: phenotypic variability within a large consanguineous Bedouin family associated with a novel FKRP mutation. Eur J Hum Genet 2004; 12: 38-43.

Hayashi YK, Engvall E, Arikawa-Hirasawa E, Goto K, Koga R, Nonaka I, et al. Abnormal localization of laminin subunits in muscular dystrophies. J Neurol Sci 1993; 119: 53-64.

Hayashi YK, Ogawa M, Tagawa K, Noguchi S, Ishihara T, Nonaka I, et al. Selective deficiency of alpha-dystroglycan in Fukuyama-type congenital muscular dystrophy. Neurology 2001; 57: 115-21.

Henry MD, Campbell KP. Dystroglycan inside and out. Curr Opin Cell Biol 1999; 11: 602-7.

Henry MD, Cohen MB, Campbell KP. Reduced expression of dystroglycan in breast and prostate cancer. Hum Pathol 2001; 32: 791-5.

Henry MD, Williamson RA, Campbell KP. Analysis of the role of dystroglycan in early postimplantation mouse development. Ann N Y Acad Sci 1998; 857: 256-9.

Hirsch C, Gauss R, Horn SC, Neuber O, Sommer T. The ubiquitylation machinery of the endoplasmic reticulum. Nature 2009; 458: 453-60.

Hohenester E, Tisi D, Talts JF, Timpl R. The crystal structure of a laminin G-like module reveals the molecular basis of alpha-dystroglycan binding to laminins, perlecan, and agrin. Mol Cell 1999; 4: 783-92.

Holt KH, Crosbie RH, Venzke DP, Campbell KP. Biosynthesis of dystroglycan: processing of a precursor propeptide. FEBS Lett 2000; 468: 79-83.

Holzfeind PJ, Grewal PK, Reitsamer HA, Kechvar J, Lassmann H, Hoeger H, et al. Skeletal, cardiac and tongue muscle pathology, defective retinal transmission, and neuronal migration defects in the Large(myd) mouse defines a natural model for glycosylation-deficient muscle - eye - brain disorders. Hum Mol Genet 2002; 11: 2673-87.

Hosono S, Faruqi AF, Dean FB, Du Y, Sun Z, Wu X, et al. Unbiased whole-genome amplification directly from clinical samples. Genome Res 2003; 13: 954-64.

Ibraghimov-Beskrovnaya O, Ervasti JM, Leveille CJ, Slaughter CA, Sernett SW, Campbell KP. Primary structure of dystrophin-associated glycoproteins linking dystrophin to the extracellular matrix. Nature 1992; 355: 696-702.

Ibraghimov-Beskrovnaya O, Milatovich A, Ozcelik T, Yang B, Koepnick K, Francke U, et al. Human dystroglycan: skeletal muscle cDNA, genomic structure, origin of tissue specific isoforms and chromosomal localization. Hum Mol Genet 1993; 2: 1651-7.

Ichimiya T, Manya H, Ohmae Y, Yoshida H, Takahashi K, Ueda R, et al. The twisted abdomen phenotype of Drosophila POMT1 and POMT2 mutants coincides with their heterophilic protein O-mannosyltransferase activity. J Biol Chem 2004; 279: 42638-47.

Imperiali M, Thoma C, Pavoni E, Brancaccio A, Callewaert N, Oxenius A. O Mannosylation of alpha-dystroglycan is essential for lymphocytic choriomeningitis virus receptor function. J Virol 2005; 79: 14297-308.

Inamori K, Endo T, Gu J, Matsuo I, Ito Y, Fujii S, et al. N-Acetylglucosaminyltransferase IX acts on the GlcNAc beta 1,2-Man alpha 1-Ser/Thr moiety, forming a 2,6-branched structure in brain O-mannosyl glycan. J Biol Chem 2004; 279: 2337-40.

Inamori K, Endo T, Ide Y, Fujii S, Gu J, Honke K, et al. Molecular cloning and characterization of human GnT-IX, a novel beta1,6-N-acetylglucosaminyltransferase that is specifically expressed in the brain. J Biol Chem 2003; 278: 43102-9.

Inamori K, Mita S, Gu J, Mizuno-Horikawa Y, Miyoshi E, Dennis JW, et al. Demonstration of the expression and the enzymatic activity of N-acetylglucosaminyltransferase IX in the mouse brain. Biochim Biophys Acta 2006; 1760: 678-84.

Ishii H, Hayashi YK, Nonaka I, Arahata K. Electron microscopic examination of basal lamina in Fukuyama congenital muscular dystrophy. Neuromuscul Disord 1997; 7: 191-7.

Jayasinha V, Nguyen HH, Xia B, Kammesheidt A, Hoyte K, Martin PT. Inhibition of dystroglycan cleavage causes muscular dystrophy in transgenic mice. Neuromuscul Disord 2003; 13: 365-75.

Jimenez-Mallebrera C, Torelli S, Brown SC, Feng L, Brockington M, Sewry CA, et al. Profound skeletal muscle depletion of alpha-dystroglycan in Walker-Warburg syndrome. Eur J Paediatr Neurol 2003; 7: 129-37.

Jimenez-Mallebrera C, Torelli S, Feng L, Kim J, Godfrey C, Clement E, et al. A Comparative Study of alpha-Dystroglycan Glycosylation in Dystroglycanopathies Suggests that the Hypoglycosylation of alpha-Dystroglycan Does Not Consistently Correlate with Clinical Severity. Brain Pathol 2008.

Jurado LA, Coloma A, Cruces J. Identification of a human homolog of the Drosophila rotated abdomen gene (POMT1) encoding a putative protein O-mannosyl-transferase, and assignment to human chromosome 9q34.1. Genomics 1999; 58: 171-80.

Kanagawa M, Saito F, Kunz S, Yoshida-Moriguchi T, Barresi R, Kobayashi YM, et al. Molecular recognition by LARGE is essential for expression of functional dystroglycan. Cell 2004; 117: 953-64.

Kaneko M, Alvarez-Manilla G, Kamar M, Lee I, Lee JK, Troupe K, et al. A novel beta(1,6)-N-acetylglucosaminyltransferase V (GnT-VB)(1). FEBS Lett 2003; 554: 515-9.

Kawahara G, Guyon JR, Nakamura Y, Kunkel LM. Zebrafish models for human FKRP muscular dystrophies. Hum Mol Genet 2010; 19: 623-33.

Keramaris-Vrantsis E, Lu PJ, Doran T, Zillmer A, Ashar J, Esapa CT, et al. Fukutin-related protein localizes to the Golgi apparatus and mutations lead to mislocalization in muscle in vivo. Muscle Nerve 2007; 36: 455-65.

Knoll R, Hoshijima M, Hoffman HM, Person V, Lorenzen-Schmidt I, Bang ML, et al. The cardiac mechanical stretch sensor machinery involves a Z disc complex that is defective in a subset of human dilated cardiomyopathy. Cell 2002; 111: 943-55.

Kobayashi K, Nakahori Y, Miyake M, Matsumura K, Kondo-Iida E, Nomura Y, et al. An ancient retrotransposal insertion causes Fukuyama-type congenital muscular dystrophy. Nature 1998; 394: 388-92.

Koenig M, Monaco AP, Kunkel LM. The complete sequence of dystrophin predicts a rod-shaped cytoskeletal protein. Cell 1988; 53: 219-28.

Kunz S, Campbell KP, Oldstone MB. Alpha-dystroglycan can mediate arenavirus infection in the absence of beta-dystroglycan. Virology 2003; 316: 213-20.

Kunz S, Rojek JM, Kanagawa M, Spiropoulou CF, Barresi R, Campbell KP, et al. Posttranslational modification of alpha-dystroglycan, the cellular receptor for arenaviruses, by the glycosyltransferase LARGE is critical for virus binding. J Virol 2005; 79: 14282-96.

Kunz S, Sevilla N, McGavern DB, Campbell KP, Oldstone MB. Molecular analysis of the interaction of LCMV with its cellular receptor [alpha]-dystroglycan. J Cell Biol 2001; 155: 301-10.

Kurahashi H, Taniguchi M, Meno C, Taniguchi Y, Takeda S, Horie M, et al. Basement membrane fragility underlies embryonic lethality in fukutin-null mice. Neurobiol Dis 2005; 19: 208-17.

Lefeber DJ, Schonberger J, Morava E, Guillard M, Huyben KM, Verrijp K, et al. Deficiency of Dol-P-Man synthase subunit DPM3 bridges the congenital disorders of glycosylation with the dystroglycanopathies. Am J Hum Genet 2009; 85: 76-86.

Leschziner A, Moukhles H, Lindenbaum M, Gee SH, Butterworth J, Campbell KP, et al. Neural regulation of alpha-dystroglycan biosynthesis and glycosylation in skeletal muscle. J Neurochem 2000; 74: 70-80.

Levedakou EN, Chen XJ, Soliven B, Popko B. Disruption of the mouse Large gene in the enr and myd mutants results in nerve, muscle, and neuromuscular junction defects. Mol Cell Neurosci 2005; 28: 757-69.

Li H, Coghlan A, Ruan J, Coin LJ, Heriche JK, Osmotherly L, et al. TreeFam: a curated database of phylogenetic trees of animal gene families. Nucleic Acids Res 2006; 34: D572-80.

Lin YC, Murakami T, Hayashi YK, Nishino I, Nonaka I, Yuo CY, et al. A novel FKRP gene mutation in a Taiwanese patient with limb-girdle muscular dystrophy 2I. Brain Dev 2007; 29: 234-8.

Liu J, Ball SL, Yang Y, Mei P, Zhang L, Shi H, et al. A genetic model for muscle-eye-brain disease in mice lacking protein O-mannose 1,2-N-acetylglucosaminyltransferase (POMGnT1). Mech Dev 2006; 123: 228-40.

Lomako J, Lomako WM, Whelan WJ. Glycogenin: the primer for mammalian and yeast glycogen synthesis. Biochim Biophys Acta 2004; 1673: 45-55.

Longman C, Brockington M, Torelli S, Jimenez-Mallebrera C, Kennedy C, Khalil N, et al. Mutations in the human LARGE gene cause MDC1D, a novel form of congenital muscular dystrophy with severe mental retardation and abnormal glycosylation of alpha-dystroglycan. Hum Mol Genet 2003; 12: 2853-61.

Lyalin D, Koles K, Roosendaal SD, Repnikova E, Van Wechel L, Panin VM. The twisted gene encodes Drosophila protein O-mannosyltransferase 2 and genetically interacts with the rotated abdomen gene encoding Drosophila protein O-mannosyltransferase 1. Genetics 2006; 172: 343-53.

Manya H, Chiba A, Yoshida A, Wang X, Chiba Y, Jigami Y, et al. Demonstration of mammalian protein O-mannosyltransferase activity: coexpression of POMT1 and POMT2 required for enzymatic activity. Proc Natl Acad Sci U S A 2004; 101: 500-5.

Manya H, Sakai K, Kobayashi K, Taniguchi K, Kawakita M, Toda T, et al. Loss-of-function of an N-acetylglucosaminyltransferase, POMGnT1, in muscle-eye-brain disease. Biochem Biophys Res Commun 2003; 306: 93-7.

Manzini MC, Gleason D, Chang BS, Hill RS, Barry BJ, Partlow JN, et al. Ethnically diverse causes of Walker-Warburg syndrome (WWS): FCMD mutations are a more common cause of WWS outside of the Middle East. Hum Mutat 2008; 29: E231-41.

Manzur AY, Kinali M, Muntoni F. Update on the management of Duchenne muscular dystrophy. Arch Dis Child 2008; 93: 986-90.

Martin-Blanco E, Garcia-Bellido A. Mutations in the rotated abdomen locus affect muscle development and reveal an intrinsic asymmetry in Drosophila. Proc Natl Acad Sci U S A 1996; 93: 6048-52.

Martin PT. Dystroglycan glycosylation and its role in matrix binding in skeletal muscle. Glycobiology 2003; 13: 55R-66R.

Matsumoto H, Maruse H, Inaba Y, Yoshizawa K, Sasazaki S, Fujiwara A, et al. The ubiquitin ligase gene (WWP1) is responsible for the chicken muscular dystrophy. FEBS Lett 2008; 582: 2212-8.

Matsumoto H MH, Yoshizawa K, Sasazaki S, Fujiwara A, Kikuchi T. Pinpointing the candidate region for muscular dystrophy in chickens with an abnormal muscle gene. Animal Science Journal 2007; 78: 476-483.

Matsumoto H, Noguchi S, Sugie K, Ogawa M, Murayama K, Hayashi YK, et al. Subcellular localization of fukutin and fukutin-related protein in muscle cells. J Biochem 2004; 135: 709-12.

Matsumura K, Chiba A, Yamada H, Fukuta-Ohi H, Fujita S, Endo T, et al. A role of dystroglycan in schwannoma cell adhesion to laminin. J Biol Chem 1997; 272: 13904-10.

Mercuri E, Brockington M, Straub V, Quijano-Roy S, Yuva Y, Herrmann R, et al. Phenotypic spectrum associated with mutations in the fukutin-related protein gene. Ann Neurol 2003; 53: 537-42.

Mercuri E, Messina S, Bruno C, Mora M, Pegoraro E, Comi GP, et al. Congenital muscular dystrophies with defective glycosylation of dystroglycan. A population study. Neurology 2009.

Mercuri E, Sewry C, Brown SC, Muntoni F. Congenital muscular dystrophies. Semin Pediatr Neurol 2002; 9: 120-31.

Mercuri E, Topaloglu H, Brockington M, Berardinelli A, Pichiecchio A, Santorelli F, et al. Spectrum of brain changes in patients with congenital muscular dystrophy and FKRP gene mutations. Arch Neurol 2006; 63: 251-7.

Michele DE, Barresi R, Kanagawa M, Saito F, Cohn RD, Satz JS, et al. Post-translational disruption of dystroglycan-ligand interactions in congenital muscular dystrophies. Nature 2002; 418: 417-22.

Michele DE, Campbell KP. Dystrophin-glycoprotein complex: post-translational processing and dystroglycan function. J Biol Chem 2003; 278: 15457-60.

Middleton FA, Pato MT, Gentile KL, Morley CP, Zhao X, Eisener AF, et al. Genomewide linkage analysis of bipolar disorder by use of a high-density single-nucleotide-polymorphism (SNP) genotyping assay: a comparison with microsatellite marker assays and finding of significant linkage to chromosome 6q22. Am J Hum Genet 2004; 74: 886-97.

Moore CJ, Goh HT, Hewitt JE. Genes required for functional glycosylation of dystroglycan are conserved in zebrafish. Genomics 2008; 92: 159-67.

Moore SA, Saito F, Chen J, Michele DE, Henry MD, Messing A, et al. Deletion of brain dystroglycan recapitulates aspects of congenital muscular dystrophy. Nature 2002; 418: 422-5.

Moreira ES, Wiltshire TJ, Faulkner G, Nilforoushan A, Vainzof M, Suzuki OT, et al. Limb-girdle muscular dystrophy type 2G is caused by mutations in the gene encoding the sarcomeric protein telethonin. Nat Genet 2000; 24: 163-6.

Mu J, Skurat AV, Roach PJ. Glycogenin-2, a novel self-glucosylating protein involved in liver glycogen biosynthesis. J Biol Chem 1997; 272: 27589-97.

Muntoni F, Brockington M, Blake DJ, Torelli S, Brown SC. Defective glycosylation in muscular dystrophy. Lancet 2002; 360: 1419-21.

Muntoni F, Guicheney P, Voit T. 158th ENMC international workshop on congenital muscular dystrophy (Xth international CMD workshop) 8th-10th February 2008 Naarden, The Netherlands. Neuromuscul Disord 2009; 19: 229-34.

Muntoni F, Taylor J, Sewry CA, Naom I, Dubowitz V. An early onset muscular dystrophy with diaphragmatic involvement, early respiratory failure and secondary alpha2 laminin deficiency unlinked to the LAMA2 locus on 6q22. Eur J Paediatr Neurol 1998; 2: 19-26.

Muntoni F, Torelli S, Brockington M. Muscular dystrophies due to glycosylation defects. Neurotherapeutics 2008; 5: 627-32.

Murakami T, Hayashi YK, Noguchi S, Ogawa M, Nonaka I, Tanabe Y, et al. Fukutin gene mutations cause dilated cardiomyopathy with minimal muscle weakness. Ann Neurol 2006; 60: 597-602.

Muschler J, Levy D, Boudreau R, Henry M, Campbell K, Bissell MJ. A role for dystroglycan in epithelial polarization: loss of function in breast tumor cells. Cancer Res 2002; 62: 7102-9.

Ng SB, Buckingham KJ, Lee C, Bigham AW, Tabor HK, Dent KM, et al. Exome sequencing identifies the cause of a mendelian disorder. Nat Genet 2010; 42: 30-5.

Olson EC, Walsh CA. Smooth, rough and upside-down neocortical development. Curr Opin Genet Dev 2002; 12: 320-7.

Parsons MJ, Campos I, Hirst EM, Stemple DL. Removal of dystroglycan causes severe muscular dystrophy in zebrafish embryos. Development 2002; 129: 3505-12.

Patnaik SK, Stanley P. Mouse large can modify complex N- and mucin O-glycans on alpha-dystroglycan to induce laminin binding. J Biol Chem 2005; 280: 20851-9.

Petrof BJ, Shrager JB, Stedman HH, Kelly AM, Sweeney HL. Dystrophin protects the sarcolemma from stresses developed during muscle contraction. Proc Natl Acad Sci U S A 1993; 90: 3710-4.

Peyrard M, Seroussi E, Sandberg-Nordqvist AC, Xie YG, Han FY, Fransson I, et al. The human LARGE gene from 22q12.3-q13.1 is a new, distinct member of the glycosyltransferase gene family. Proc Natl Acad Sci U S A 1999; 96: 598-603.

Puntervoll P, Linding R, Gemund C, Chabanis-Davidson S, Mattingsdal M, Cameron S, et al. ELM server: A new resource for investigating short functional sites in modular eukaryotic proteins. Nucleic Acids Res 2003; 31: 3625-30.

Rambukkana A, Yamada H, Zanazzi G, Mathus T, Salzer JL, Yurchenco PD, et al. Role of alpha-dystroglycan as a Schwann cell receptor for Mycobacterium leprae. Science 1998; 282: 2076-9.

Ruan J, Li H, Chen Z, Coghlan A, Coin LJ, Guo Y, et al. TreeFam: 2008 Update. Nucleic Acids Res 2008; 36: D735-40.

Sabatelli P, Columbaro M, Mura I, Capanni C, Lattanzi G, Maraldi NM, et al. Extracellular matrix and nuclear abnormalities in skeletal muscle of a patient with Walker-Warburg syndrome caused by POMT1 mutation. Biochim Biophys Acta 2003; 1638: 57-62.

Sabeti PC, Schaffner SF, Fry B, Lohmueller J, Varilly P, Shamovsky O, et al. Positive natural selection in the human lineage. Science 2006; 312: 1614-20.

Saito F, Blank M, Schroder J, Manya H, Shimizu T, Campbell KP, et al. Aberrant glycosylation of alpha-dystroglycan causes defective binding of laminin in the muscle of chicken muscular dystrophy. FEBS Lett 2005; 579: 2359-63.

Saito Y, Yamamoto T, Mizuguchi M, Kobayashi M, Saito K, Ohno K, et al. Altered glycosylation of alpha-dystroglycan in neurons of Fukuyama congenital muscular dystrophy brains. Brain Res 2006; 1075: 223-8.

Sasaki K, Kurata-Miura K, Ujita M, Angata K, Nakagawa S, Sekine S, et al. Expression cloning of cDNA encoding a human beta-1,3-N-acetylglucosaminyltransferase that is essential for poly-N-acetyllactosamine synthesis. Proc Natl Acad Sci U S A 1997; 94: 14294-9.

Singh J, Itahana Y, Knight-Krajewski S, Kanagawa M, Campbell KP, Bissell MJ, et al. Proteolytic enzymes and altered glycosylation modulate dystroglycan function in carcinoma cells. Cancer Res 2004; 64: 6152-9.

Smalheiser NR, Kim E. Purification of cranin, a laminin binding membrane protein. Identity with dystroglycan and reassessment of its carbohydrate moieties. J Biol Chem 1995; 270: 15425-33.

Smalheiser NR, Schwartz NB. Cranin: a laminin-binding protein of cell membranes. Proc Natl Acad Sci U S A 1987; 84: 6457-61.

Sotgia F, Lee JK, Das K, Bedford M, Petrucci TC, Macioce P, et al. Caveolin-3 directly interacts with the C-terminal tail of beta -dystroglycan. Identification of a central WW-like domain within caveolin family members. J Biol Chem 2000; 275: 38048-58.

Spence HJ, Dhillon AS, James M, Winder SJ. Dystroglycan, a scaffold for the ERK-MAP kinase cascade. EMBO Rep 2004; 5: 484-9.

Su XZ, Wu Y, Sifri CD, Wellems TE. Reduced extension temperatures required for PCR amplification of extremely A+T-rich DNA. Nucleic Acids Res 1996; 24: 1574-5.

Sudol M, Chen HI, Bougeret C, Einbond A, Bork P. Characterization of a novel protein-binding module--the WW domain. FEBS Lett 1995; 369: 67-71.

Tabuchi K, Sudhof TC. Structure and evolution of neurexin genes: insight into the mechanism of alternative splicing. Genomics 2002; 79: 849-59.

Takeda S, Kondo M, Sasaki J, Kurahashi H, Kano H, Arai K, et al. Fukutin is required for maintenance of muscle integrity, cortical histiogenesis and normal eye development. Hum Mol Genet 2003; 12: 1449-59.

Talts JF, Andac Z, Gohring W, Brancaccio A, Timpl R. Binding of the G domains of laminin alpha1 and alpha2 chains and perlecan to heparin, sulfatides, alpha-dystroglycan and several extracellular matrix proteins. Embo J 1999; 18: 863-70.

Taniguchi K, Kobayashi K, Saito K, Yamanouchi H, Ohnuma A, Hayashi YK, et al. Worldwide distribution and broader clinical spectrum of muscle-eye-brain disease. Hum Mol Genet 2003; 12: 527-34.

Thomas PD, Campbell MJ, Kejariwal A, Mi H, Karlak B, Daverman R, et al. PANTHER: a library of protein families and subfamilies indexed by function. Genome Res 2003; 13: 2129-41.

Thornhill P, Bassett D, Lochmuller H, Bushby K, Straub V. Developmental defects in a zebrafish model for muscular dystrophies associated with the loss of fukutin-related protein (FKRP). Brain 2008; 131: 1551-61.

Tisi D, Talts JF, Timpl R, Hohenester E. Structure of the C-terminal laminin G-like domain pair of the laminin alpha2 chain harbouring binding sites for alpha-dystroglycan and heparin. Embo J 2000; 19: 1432-40.

Toda T, Kobayashi K, Takeda S, Sasaki J, Kurahashi H, Kano H, et al. Fukuyama-type congenital muscular dystrophy (FCMD) and alpha-dystroglycanopathy. Congenit Anom (Kyoto) 2003; 43: 97-104.

Topaloglu H, Brockington M, Yuva Y, Talim B, Haliloglu G, Blake D, et al. FKRP gene mutations cause congenital muscular dystrophy, mental retardation, and cerebellar cysts. Neurology 2003; 60: 988-92.

Torelli S, Brown SC, Brockington M, Dolatshad NF, Jimenez C, Skordis L, et al. Sub-cellular localisation of fukutin related protein in different cell lines and in the muscle of patients with MDC1C and LGMD2I. Neuromuscul Disord 2005; 15: 836-43.

Vajsar J, Zhang W, Dobyns WB, Biggar D, Holden KR, Hawkins C, et al. Carriers and patients with muscle-eye-brain disease can be rapidly diagnosed by enzymatic analysis of fibroblasts and lymphoblasts. Neuromuscul Disord 2006; 16: 132-6.

van Reeuwijk J, Brunner HG, van Bokhoven H. Glyc-O-genetics of Walker-Warburg syndrome. Clin Genet 2005a; 67: 281-9.

van Reeuwijk J, Grewal PK, Salih MA, Beltran-Valero de Bernabe D, McLaughlan JM, Michielse CB, et al. Intragenic deletion in the LARGE gene causes Walker-Warburg syndrome. Hum Genet 2007; 121: 685-90.

van Reeuwijk J, Janssen M, van den Elzen C, Beltran-Valero de Bernabe D, Sabatelli P, Merlini L, et al. POMT2 mutations cause alpha-dystroglycan hypoglycosylation and Walker-Warburg syndrome. J Med Genet 2005b; 42: 907-12.

Varki A. Essentials of Glycobiology: Cold Spring Harbor Laboratory Press, 2008.

Vieira NM, Schlesinger D, de Paula F, Vainzof M, Zatz M. Mutation analysis in the FKRP gene provides an explanation for a rare cause of intrafamilial clinical variability in LGMD2I. Neuromuscul Disord 2006; 16: 870-3.

Vogt G, Chapgier A, Yang K, Chuzhanova N, Feinberg J, Fieschi C, et al. Gains of glycosylation comprise an unexpectedly large group of pathogenic mutations. Nat Genet 2005; 37: 692-700.

Watanabe M, Kobayashi K, Jin F, Park KS, Yamada T, Tokunaga K, et al. Founder SVA retrotransposal insertion in Fukuyama-type congenital muscular dystrophy and its origin in Japanese and Northeast Asian populations. Am J Med Genet A 2005; 138: 344-8.

Willer T, Amselgruber W, Deutzmann R, Strahl S. Characterization of POMT2, a novel member of the PMT protein O-mannosyltransferase family specifically localized to the acrosome of mammalian spermatids. Glycobiology 2002; 12: 771-83.

Willer T, Prados B, Falcon-Perez JM, Renner-Muller I, Przemeck GK, Lommel M, et al. Targeted disruption of the Walker-Warburg syndrome gene Pomt1 in mouse results in embryonic lethality. Proc Natl Acad Sci U S A 2004; 101: 14126-31.

Williamson RA, Henry MD, Daniels KJ, Hrstka RF, Lee JC, Sunada Y, et al. Dystroglycan is essential for early embryonic development: disruption of Reichert's membrane in Dag1-null mice. Hum Mol Genet 1997; 6: 831-41.

Wing DR, Rademacher TW, Schmitz B, Schachner M, Dwek RA. Comparative glycosylation in neural adhesion molecules. Biochem Soc Trans 1992; 20: 386-90.

Wood JD, Yuan J, Margolis RL, Colomer V, Duan K, Kushi J, et al. Atrophin-1, the DRPLA gene product, interacts with two families of WW domain-containing proteins. Mol Cell Neurosci 1998; 11: 149-60.

Xiong H, Kobayashi K, Tachikawa M, Manya H, Takeda S, Chiyonobu T, et al. Molecular interaction between fukutin and POMGnT1 in the glycosylation pathway of alpha-dystroglycan. Biochem Biophys Res Commun 2006; 350: 935-41.

Yaffe D, Saxel O. Serial passaging and differentiation of myogenic cells isolated from dystrophic mouse muscle. Nature 1977; 270: 725-7.

Yamada H, Shimizu T, Tanaka T, Campbell KP, Matsumura K. Dystroglycan is a binding protein of laminin and merosin in peripheral nerve. FEBS Lett 1994; 352: 49-53.

Yanagisawa A, Bouchet C, Van den Bergh PY, Cuisset JM, Viollet L, Leturcq F, et al. New POMT2 mutations causing congenital muscular dystrophy: identification of a founder mutation. Neurology 2007; 69: 1254-60.

Yang B, Jung D, Motto D, Meyer J, Koretzky G, Campbell KP. SH3 domain-mediated interaction of dystroglycan and Grb2. J Biol Chem 1995; 270: 11711-4.

Yoshida-Moriguchi T, Yu L, Stalnaker SH, Davis S, Kunz S, Madson M, et al. O-mannosyl phosphorylation of alpha-dystroglycan is required for laminin binding. Science 2010; 327: 88-92.

Yoshida A, Kobayashi K, Manya H, Taniguchi K, Kano H, Mizuno M, et al. Muscular dystrophy and neuronal migration disorder caused by mutations in a glycosyltransferase, POMGnT1. Dev Cell 2001; 1: 717-24.

Yoshida M, Ozawa E. Glycoprotein complex anchoring dystrophin to sarcolemma. J Biochem 1990; 108: 748-52.

Zhang Q, Bethmann C, Worth NF, Davies JD, Wasner C, Feuer A, et al. Nesprin-1 and -2 are involved in the pathogenesis of Emery Dreifuss muscular dystrophy and are critical for nuclear envelope integrity. Hum Mol Genet 2007; 16: 2816-33.

Zhang W, Betel D, Schachter H. Cloning and expression of a novel UDP-GlcNAc:alpha-D-mannoside beta1,2-N-acetylglucosaminyltransferase homologous to UDP-GlcNAc:alpha-3-D-mannoside beta1,2-N-acetylglucosaminyltransferase I. Biochem J 2002; 361: 153-62.

Zhang W, Vajsar J, Cao P, Breningstall G, Diesen C, Dobyns W, et al. Enzymatic diagnostic test for Muscle-Eye-Brain type congenital muscular dystrophy using commercially available reagents. Clin Biochem 2003; 36: 339-44.